UNIVERSITÀ DEL PIEMONTE ORIENTALE

School of Medicine

Department of Translational Medicine

Ph.D. Program in Medical Sciences and Biotechnology

XXXV cycle

GRADUATION THESIS

"Investigation of diacylglycerol kinase alpha role in lipid signalling during T cell activation"

Supervisor:

Prof. Gianluca Baldanzi

Candidate:

Sara Centonze

Academic years 2019/2022

"*Nothing in life is to be feared, it is only to be understood. Now is the time to understand more, so that we may fear less*."

(Marie Curie)

ABSTRACT

The diacylglycerol kinases (DGKs) are a conserved family of lipid enzymes able to convert diacylglycerol (DAG) into phosphatidic acid (PA). This reaction attenuates DAG intracellular levels, an important second messenger which regulates several signalling proteins. At the same time, also the product of DGK activity, PA, controls different cell functions such as cell growth, differentiation, and migration. Thus, DGK enzymes play a pivotal role within the cells, linking lipid metabolism to signalling functions. In T cells, DGKα and DGKζ isoforms play a major role as negative regulators of DAG-mediated T cell receptor (TCR) signalling, since their activity limits RasGRP1/Ras/MAPK pathway and interleukin 2 (IL-2) production.

The aim of the research efforts described in this thesis is to explore the regulation of DGKα-mediated lipid signalling and the resulting biological effects during T cell activation. The project started from the observation that, upon T-cell receptor stimulation, the adaptor protein SAP mediates DGKα inhibition and this process is essential for a correct restimulation induced cell death (RICD) and cytokines production. However, the molecular pathway that links SAP to DGKα was poorly understood. To clarify the pathway and the mechanisms involved we explored the molecular mechanisms which lead to DGKα inhibition, focusing on the reported SAP interactors and specifically on the Wiskott-Aldrich syndrome protein (WASp). The results obtained demonstrate that WASp interacts with the DGKα recoverin homology domain through its homology 1 domain and this interaction leads to DGKα inhibition. In addition, the role of the adaptor protein NCK-1 and the small G protein CDC42 in this signalling was investigated, indicating an indirect WASp mediated role. A second research topic was the investigation of the DGKα promoted signalling, focusing on lipid binding and regulation by PA and other phospholipids on atypical PKCs, an important class of lipid regulated kinases. Finally, the biological relevance of WASp/DGKα was explored in the context of RICD and cytokine production in primary human T cells. While this pathway does not affect RICD, WASp silencing reduces IL-2 synthesis and DGKα inhibition restores this defect of WASp-deficient lymphocytes.

In conclusion, we discovered a novel signalling pathway composed of SAP/CDC42 and NCK-1/WASp that, downstream to strong TCR stimulation, blocks DGKα activity resulting in a full cytokine response but minimally perturbs RICD. These findings could be relevant for the treatment not only of primary immunodeficiencies but also of other T cell hyporesponsive states such as anergy of tumour infiltrating lymphocytes.

RIASSUNTO

Le diacilglicerolo chinasi (DGK) sono una famiglia conservata di enzimi lipidici in grado di convertire il diacilglicerolo (DAG) in acido fosfatidico (PA). Questa reazione attenua i livelli intracellulari di DAG, un importante secondo messaggero che regola diverse proteine di segnalazione. Allo stesso tempo, anche il prodotto dell'attività DGK, il PA, controlla varie funzioni cellulari come la crescita, il differenziamento e la migrazione. Pertanto, gli enzimi DGK svolgono un ruolo fondamentale nelle cellule, collegando il metabolismo lipidico alle funzioni di segnalazione. Nelle cellule T, le isoforme DGKα e DGKζ svolgono un ruolo importante come regolatori negativi della segnalazione del recettore delle cellule T (TCR) mediata da DAG, poiché la loro attività limita la via di segnale RasGRP1/Ras/MAPK e la produzione di interleuchina 2 (IL-2).
Lo scopo di questa tesi è quello di esplorare la regolazione del segnale lipidico mediato da DGKα e i conseguenti effetti biologici durante l'attivazione delle cellule T. Il progetto è partito dall'osservazione per cui, dopo la stimolazione del TCR, la proteina SAP media l'inibizione della DGKα e questo processo risulta essenziale sia per una corretta morte cellulare indotta da re-stimolazione (RICD) che per la produzione di citochine. Tuttavia, il pathway che collega SAP a DGKα era poco conosciuto. Per chiarire tale pathway abbiamo esplorato i meccanismi che portano all'inibizione della DGKα, concentrandoci sugli interattori noti di SAP e sulla proteina della sindrome di Wiskott-Aldrich (WASp). I dati ottenuti dimostrano che WASp interagisce con il dominio RVH di DGKα attraverso il suo dominio WH1 e questa interazione porta all'inibizione di DGKα. Inoltre, è stato studiato il ruolo delle proteine NCK-1 e CDC42 in questa via di segnalazione, dimostrando un ruolo indiretto mediato da WASp. Un secondo argomento di ricerca è stato lo studio del segnale promosso da DGKα, approfondendo il legame lipidico e la regolazione delle PKC atipiche da parte di PA e altri fosfolipidi. Infine, la rilevanza biologica di WASp/DGKα è stata esplorata nel contesto di RICD e della produzione di citochine: sebbene questo pathway non influenzi la RICD, il silenziamento di WASp riduce la sintesi di IL-2 e l'inibizione di DGKα ripristina questo difetto dei linfociti privi di WASp. In conclusione, abbiamo scoperto una nuova via di segnalazione composta da SAP/CDC42 e NCK-1/WASp che, a valle di una forte stimolazione del TCR, blocca l'attività DGKα portando a una risposta citochinica completa, ma perturba minimamente la RICD. Tali risultati potrebbero essere rilevanti per il trattamento non solo di immunodeficienze primarie ma anche di altri stati di iporeattività delle cellule T come l'anergia dei linfociti infiltranti il tumore.

TABLE OF CONTENTS

1. INTRODUCTION

1.1 Diacylglycerol kinases and signal transduction

Lipids are active components of the signal transduction pathways that regulate cell homeostasis. Thus, addition or removal of phosphate groups in lipid structures represents a critical event for cellular signal transduction. In this context the diacylglycerol kinases (DGKs) family of lipid enzymes plays a relevant role, catalysing the phosphorylation of diacylglycerol (DAG) into phosphatidic acid (PA). Indeed, both these bioactive molecules function as second messengers regulating a wide set of signalling processes such as cell growth, differentiation, motility, membrane trafficking and immune responses [1]. The majority of signalling DAG is generated by the activity of phospholipase C enzyme (PLC) which mediates the hydrolysis of phosphatidylinositol-4,5-bisphosphate (PIP_2). However, DAG can also be produced when phosphatidic acid phosphatases (PAP) remove the phosphate headgroup from PA (Fig. 1).

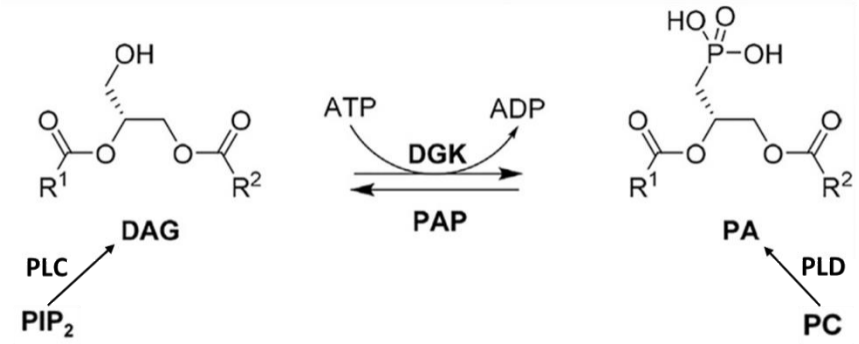

Figure 1. Enzymatic pathways which lead to DAG and PA production

PLC enzymes generate DAG that in turn can be phosphorylated by DGKs producing PA. PA can be generated also by phosphatidylcholine (PC) or phosphatidylethanolamine hydrolysis by phospholipase D (PLD) activity. Furthermore, PA can be further hydrolysed by PAPs to produce DAG. R^1; R^2 = fatty acids (adapted from Velnati et al., 2019).

DAG and PA are not only important precursors for the biosynthesis of all glycerolipids in eukaryotic cells - including membrane phospholipids (PLs) and triglycerides - but also key signalling molecules upstream different intracellular pathways. Both DAG and PA comprise at least 50 distinct molecular species which differ for the acyl chains length and a diverse number of carbon atoms (14-22) and double bonds. Importantly, these lipids are able to alter the physical structure of the cell membranes by introducing negative curvature, and this modification is crucial for the recruitment of signalling

proteins and for fusion and/or fission processes of cell plasma membranes [2]. Indeed, it has been reported that the local DAG and PA pools influence the activity and localization of an increasing number of effectors, demonstrating that DGKs have pleiotropic effects on various signalling pathways [3].
Furthermore, the spatio-temporal regulation of DAG/PA interconversion provides a good level of versatility which is essential for the signal to be dynamic and transient. However, even though DAG- and PA-dependent signalling pathways are closely interconnected, these molecules exhibit distinct mechanisms of interaction with other lipids or proteins.

In contrast to PA, DAG is able to move freely across the bilayer membranes through the so called "flip-flop" mechanism, without any protein assistance [2]. Moreover, DAG regulates the membrane translocation and the activity of numerous signal transduction proteins through its binding to their C1 domains. The main and most characterized DAG targets belongs to serine/threonine protein kinase C family (PKCs), but among the DAG-interacting proteins have been identified also the protein kinase D (PKD), Ras guanyl nucleotide-releasing protein (RAS-GRP), chimaerins (members of Rac-specific GTPase-activating protein family), mammalian uncoordinated 13 (Munc13) protein and the transient receptor potential canonical channels (Ca^{2+}-permeable non-selective cation channels) [3, 4].
In T lymphocytes, the PLC-dependent generation of DAG is essential for a correct immune response. When T cell receptor (TCR) is engaged, PLC enzymes hydrolyse PIP_2 producing DAG and inositol 1,4,5-triphosphate (IP_3): DAG is recognized by C1 domain-containing proteins, whereas IP_3 localizes to the endoplasmic reticulum, where it allows calcium release. In response to increased DAG levels, PKCθ reaches the immune synapse, where it initiates the nuclear factor-κB (NF-κB) cascade whereas RasGRP1 enhances ERK/MAP kinase pathway, promoting T cells activation and proliferation (Fig. 2) [5, 6].

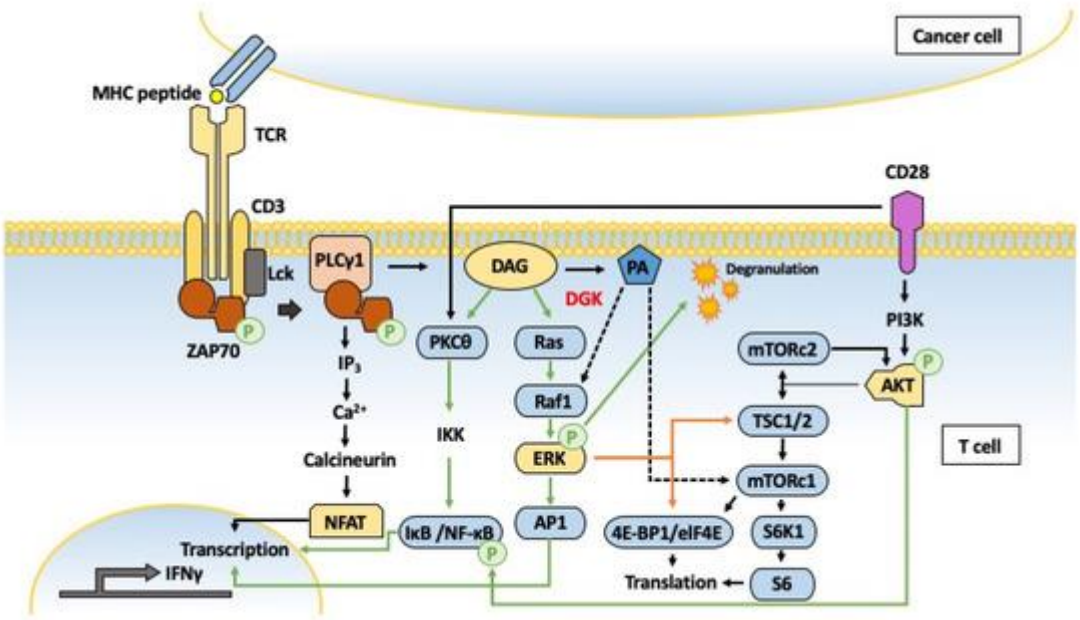

Figure 2. Representative DAG-regulated signalling pathways in activated T cells.

Signals deriving from TCR engagement lead to the recruitment of adaptor molecules and signal transduction, resulting in the lysis of the target cells and secretion of IFNγ (T cell effector function). High DAG levels trigger TCR distal signalling through Ras-MEK-ERK and PKC-NF-κB pathways (green arrows). The biosynthesis of phosphatidic acid (PA) in the T cells is mediated by DGKs and PLD activity (not shown). PA is shown to activate Raf1 and mTORC1 (dotted black arrows) (Sim et al., 2020).

On the other hand, PA signalling has been linked to several intracellular pathways mostly related to survival, proliferation, cytoskeletal organization, and membrane and vesicle trafficking. Interestingly, PA distribution is not limited only to cell membranes, but also to different subcellular compartments, such as mitochondria, Golgi complex, endoplasmic reticulum, and nucleus. It has been reported that PA can bind to putative PA-binding regions of more than 50 distinct proteins (the so called "PA-binding proteins" or PABPs). In particular, it has been demonstrated that PA regulates key signalling protein such as Raf-1 (C-Raf) kinase, mammalian/mechanistic target of rapamycin (mTOR) [7, 8], PKCε, PKCζ, lipid kinases including phosphatidylinositol (PI)-4-phosphate 5-kinase (PIP5K) and sphingosine kinase (SphK) 1, protein phosphatase-1 catalytic subunit (PP1c), Lipin 1β, phospholipase C (PLC) β1 and γ1, G-proteins and G-protein regulators such as RasGAP, and chimaerin, and some phosphodiesterases. However, it is interesting to note that the number of PABPs is much greater than that of DAG-binding proteins and the reason could relies on the fact that there are no common binding motifs like the C1 domain for DAG binding [3, 4].

However, PA is not produced only by DGKs activity: the phospholipase D (PLD) family of enzymes mediate the hydrolysis of phosphatidylcholine or phosphatidylethanolamine [9], whereas lysophosphatidic acid acyltransferase (LPAAT) mediates the PA de novo synthesis via sequential acylation of G3P and lysophosphatidic acid. Conversely, the termination of PA signalling is mediated by lipins through dephosphorylation, in a process that has been shown to regulate mast cell function [10]. Intracellular levels of PA change dynamically in response to environmental stimuli and this is particularly important for the regulation of the immune cell functions. PA role in receptors signalling is still poorly defined, however in a study by Liu et al., 2007 it has been demonstrated that DGK-derived PA can control innate immunological responses, since DGKζ deficiency resulted in impaired interleukin-12 (IL-12) production following Toll-like receptor (TLRs) stimulation both *in vitro* and *in vivo* and PA treatment restored this deficit in DGKζ-deficient macrophages [11]. Furthermore, in a work by Guo et al., the authors provide evidence that loss of both DGKα and ζ (the two mainly expressed DGK isoforms in T lymphocytes) selectively inhibits T cells positive selection in thymus and surprisingly this defect can be rescued by PA treatment [12]. These observations demonstrate that these two structurally distinct DGK isoforms perform synergistic roles in enhancing T cell maturation through PA production. However, the relevance of PA as signalling protein recruiter and/or activator in T cells has not been fully determined and requires further studies.

Based on these premises, the DGK activity is particularly important in lipid signalling regulation, since the efficacy of DAG/PA-mediated signals is intimately interconnected with their metabolism. Indeed, attenuating DAG signalling and producing PA makes these enzymes pivotal regulators of the DAG/PA balance within the cells and, as consequence, of their related signalling processes and cellular functions. Therefore, it is not surprising that alterations in DGKs' activity have been linked to various pathological conditions including, neurological disorders, type 2 diabetes, autoimmune diseases, and cancer.

1.2 The diacylglycerol kinases family

Since DGKs enzymatic activity controls the amount of DAG and PA within the cells, consequently it also modulates all the downstream processes triggered by these bioactive lipids and for this reason DGKs have been defined as "hubs of cell signalling" [1]. To date, 10 mammalian DGK isoforms are known (DGKα, β, γ, δ, ε, ζ, η, θ, ι and κ), mainly expressed in brain tissue (including the regions of cerebellum, hippocampus, and the olfactory bulb) and in hematopoietic organs. However, some DGK isozymes have been found also in retina (ε, γ, and ι), in striated (δ and ζ) and cardiac muscle (β and ε), and in the lungs (α, ε, ζ and η) [13, 14]. Interestingly, it has been reported that different DGK isoforms can be co-expressed in the same tissue and also in the same cell, suggesting that each subtype may have tissue or cell-specific functions [15]. Moreover, different DGK isoforms have been identified in specific subcellular compartments, such as plasma membrane, nucleus, endoplasmic reticulum (ER), Golgi, cytoskeleton, and endosomes. However, the precise functional roles of these DGKs or their spatio-temporal regulation within the cells is not yet fully understood and requires further investigations. DGK isozymes expression pattern and their subcellular localization are extensively described in *Shulga et al., 2011* and *Sim et al., 2020* and summarized in Table 1 [3].

Isoform	Main tissue Expression	Subcellular Localization
α	T cells, brain	Plasma membrane and nucleus, cytoplasm
β	Brain	Cytoskeleton, perisynaptic membrane
γ	Brain	Golgi and nucleus
δ	Ubiquitous	Cytoplasm, endoplasmic reticulum, endosomes, nucleus
η	Ubiquitous	Cytoplasm, endosomes
κ	Reproductive organs	Plasma membrane,
ε	Ubiquitous	Plasma membrane and endoplasmic reticulum
ξ	Ubiquitous	Cytoplasm, plasma membrane and nucleus
ι	Brain, retina	Cytoplasm, nucleus
θ	Brain, smooth muscle, and endothelial cells	Plasma membrane and nucleus, presynaptic vesicles

Table 1. DGK isoforms expression and subcellular distribution (adapted from Sim et al., 2020).

All DGK isoforms share two common structural features: at least two cysteine-rich C1 domains (protein kinase C homologous zinc finger structures) and a catalytic domain (composed of accessory and catalytic subunits). In particular, the catalytic subdomain is characterized by a highly conserved glycine-rich motif which is essential to bind ATP to protein kinases [16].

However, DGKs are grouped into 5 subtypes (type I–V) according to their structural elements (Fig. 3):

- **Type I DGKs** (comprising isoforms **α**, **β** and **γ**) are calcium sensitive and possess two EF-hand motifs and an N-terminal recoverin homology domain (RVH);
- **Type II DGKs** (including isoforms **δ**, **η** and **κ**) contain a pleckstrin homology (PH) domain which mediates protein and lipid interactions and a sterile α motif (SAM) at their carboxy termini region;
- **Type III DGKs** (consisting of the sole DGK**ε**) contain just the C1 tandem and the catalytic domains;
- **Type IV DGKs** (comprising isoforms **ζ** and **ι**) possess a myristoylated alanine-rich C kinase substrate (MARCKS) domain, four ankyrin repeats, and a PDZ-binding domain mediating the protein-protein interactions;
- **Type V DGKs** (including only the **DGKθ** isoform) contain an additional C1 domain (for a total of three instead of two) preceded by a glycine/proline-rich region in the N-terminal portion. Moreover, they present a PH domain-like region overlapping with a Ras-associating domain [16].

Interestingly, the occurrence of alternative splicing has been demonstrated in at least six of these DGK genes (β, γ, δ, η, ζ and ι isozymes) and in most of the cases, it is known to alter both localization and enzyme activity of the DGK variants, even though its biological significance has been not yet fully understood [3].

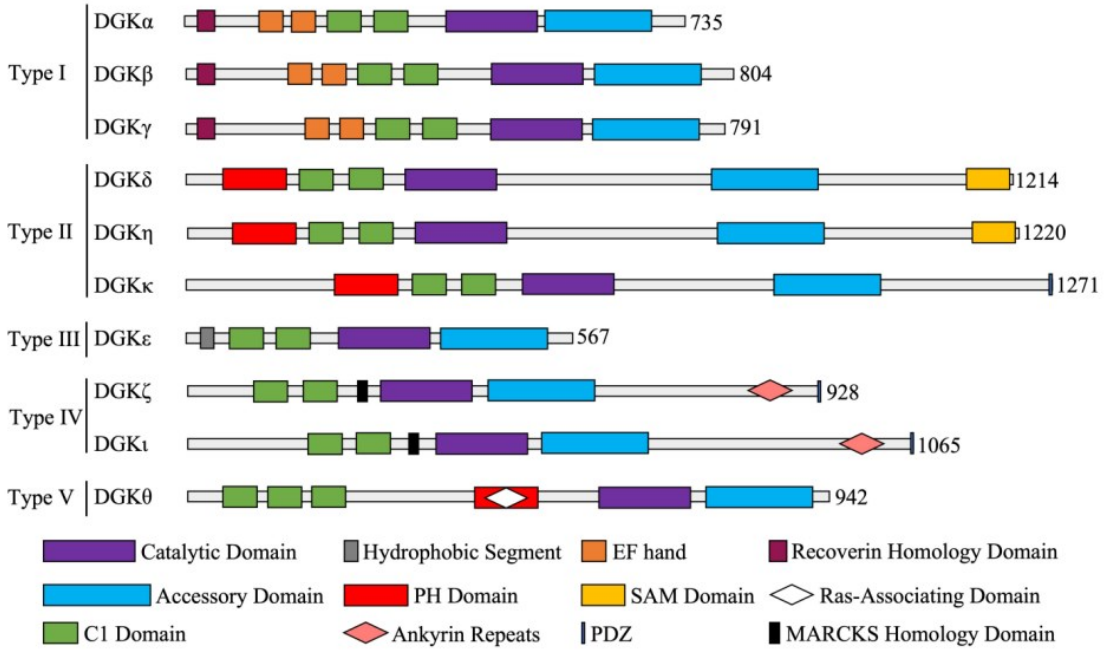

Figure 3. Classification and structure of the 10 mammalian DGK isozymes

Schematic illustration highlighting structural differences between the five DGK sub-types.

PH, pleckstrin homology; MARCKS, myristoylated alanine rich protein kinase C substrate phosphorylation site; SAM, sterile alpha motif (Aulakh et al., 2022).

Even though these structural differences among the DGK enzymes are well known, currently the three-dimensional structures are not resolved for any of the human DGKs, limiting the knowledge of both mechanisms of action and regulation of these lipid kinases. However, in an increasing number of recent studies, artificial intelligence software (i.e., Alphafold 2.0) are emerging as promising tools to obtain a quite accurate protein structure prediction, providing novel insights into the enzyme's structural and functional features [17, 18] . Interestingly, Aulakh and colleagues found that the spatial conformation of DGKs' C1, catalytic and accessory domains is structurally conserved among all the paralogs, indicating its relevance for the enzymatic activity. Moreover, the molecular docking analysis suggested the presence of a conserved ATP binding site located between the catalytic and the accessory subdomains, not necessarily distinct from the glycine-rich region (Fig. 4). Remarkably, their results demonstrate that almost all the DGKs isoforms (excluding DGKβ) show a more energetically favourable interaction with curved membranes [17].

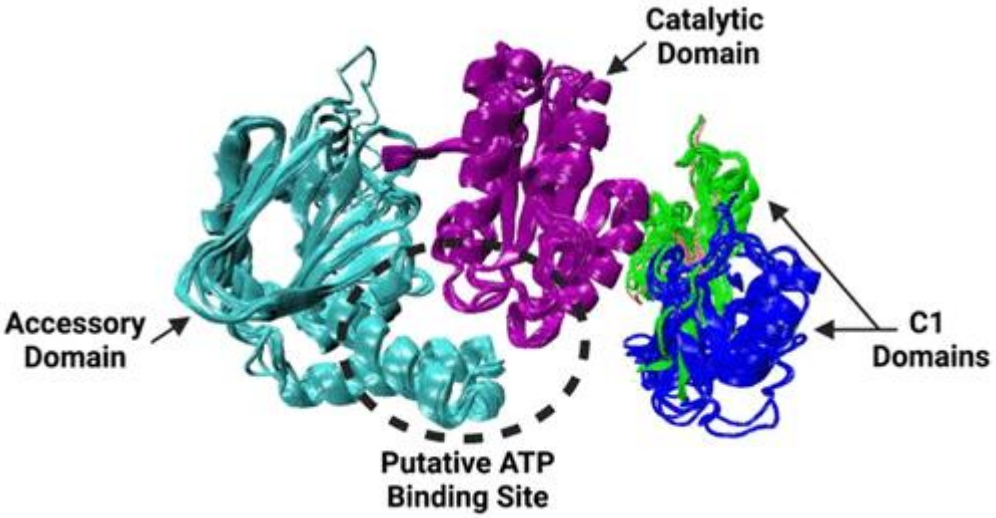

Figure 4. **DGK protein structural prediction by artificial intelligence**

Virtual DGK structure prediction generated by Alphafold 2.0 software. Accessory domain is represented in light blue, catalytic domain in purple, the two C1 domains in green and dark blue respectively. Putative ATP binding pocket is highlighted between the accessory and catalytic domain (Aulakh et al., 2022).

1.3 DGKα and DGKζ in T cell function and activation

DGKα and DGKζ are the main isoforms expressed in T lymphocytes, where their activity downstream from the T cell receptor has been reported to control multiple signalling pathways such as RasGRP1/Ras/Erk1/2 pathway, PKCθ/IKK/NFκB signalling, and mTOR pathway, consequently regulating T cell activation, survival, cytokines secretion and effector function [19].

In brief, TCR engagement leads to the activation of Lck and ZAP70 tyrosin kinases, which in turn mediate the recruitment of a multimolecular signalling complex, comprehending the adaptor protein linker of activated T cells (LAT) and the SH2 domain containing leukocyte protein of 76 kDa (SLP-76). This complex then promotes the activation of PLCγ1 that hydrolyses PIP_2 into DAG and IP_3. The DAG-activated signalling cascade enhances the transcriptional factor activator protein 1 (AP-1) activity, which is crucial for IL-2 production and T cell activation.

Therefore, constraining DAG levels, both DGKα and DGKζ act as negative regulators of TCR signalling, attenuating downstream pathways such as PKCθ and Ras/ERK signalling. ERK is a member of the mitogen-activated protein kinase (MAPK) family which transduces the signal to downstream intracellular targets. The MAPK cascades are central signalling elements where the signal is propagated by progressive phosphorylation and activations of sequential protein kinases, leading to the

phosphorylation of target regulatory proteins. Each cascade consists of three core kinases (MAP3K, MAPKK, and MAPK), and often also additional upstream and downstream components. Receptors membrane activation is transmitted to the small GTPase Ras, which is activated mainly at the plasma membranes. In turn, activated Ras recruits the MAP3K (mostly Raf-1 and B-Raf) promoting their activation. Thereafter, the signal is transmitted to the MAPKKs, MEK1 and MEK2 (MEK1/2), which in turn transmit their signal to ERK1 and ERK2 (ERK1/2). ERKs are generally localised in the cytoplasm of unstimulated cells but, once activated, ERK1/2 are transferred to the nucleus where they regulate the activity of several transcription factors and gene expression, promoting cell proliferation, differentiation, survival and motility [20, 21].
Interestingly, the upregulation of both these DGK isoforms has been linked also to T cell anergy, a hypo-responsive condition often caused by tumours to escape immune response while their inhibition rescues defective anti-tumour killing activity in tumour-specific exhausted T cells [22-24].

Initial studies carried out on human T cell lines and mouse models, suggested redundant roles for DGKα and DGKζ in the DAG-mediated regulation of the Ras-ERK signalling pathway. For instance, experiments conducted in T cells indicate that ectopic DGKα expression constrains the TCR-mediated activation of Ras-ERK pathway and AP-1-dependent transcriptional activity [21]. In addition, following studies demonstrated that DGKα gene (DGKA) shows an increased expression upon cell anergy induction [25] supporting the idea that DGKα-mediated consumption of DAG leads to anergy. Indeed, further experiments conducted in murine primary T cells highlighted a direct correlation between DGKα expression and T cell anergy [26] and conversely, DGKα-deprived mouse models exhibit an anergy-resistant phenotype [27].
On the other hand, similarly to what was observed for DGKα isoform, in T cells also DGKζ overexpression limits Ras signalling and the activation marker CD69 transcription [28]. Vice versa, DGKζ knockout murine cells exhibit an increased Ras-ERK activation, as well as increased CD69 amount upon TCR stimulation. In line with these results, it has been observed that lack of DGKζ leads to T cells hyperproliferation and resistance to anergy [29].
Taken together, these data indicate that these two DGK isoforms have redundant functions in T cells [30], since they both act as DAG consumers and PA producers.

However, the fact that these two kinases belong to two distinct DGK subgroups (type I and type V) suggests that they are not fully redundant, as they have distinct activation mechanisms and/or expression patterns. Therefore, an increasing number of studies started to define more in detail important isoform-related contributions to specific T cell functions.

The regulation of DGKα and DGKζ presents as well as some similarities and differences. It is known that these DGK isoforms are regulated at the transcriptional level, since it has been reported that activation of murine T cells through TCR and co-stimulation causes down-modulation of both DGKα and DGKζ mRNA transcripts [27]. A study by Zheng et al., reported that, among the transcriptional factors upregulated in response to TCR triggering, the early growth responsive gene 2 (Egr2) can bind to DGKα gene promoter, increasing DGKα transcription after TCR engagement [31]. Interestingly, the same authors observed that Egr2 binds also to the regulatory regions of DGKζ and other anergy-associated genes, and deletion of Egr2 prevents their up-regulation after anergy induction [32]. Furthermore, also some members of forkhead box O (FoxO) transcriptional factors family have been found to interact with DGKα gene promoter: in quiescent T lymphocytes, FoxO1 and FoxO3 enhance DGKα transcription binding to the promoter but, after T cell activation, FoxO proteins are phosphorylated and this event correlates with a decreased DGKα transcription. Interestingly, it has been observed that IL-2 binding to IL-2 receptor also promotes the PI3K-AKT pathway and inhibits FoxO-mediated transcription, enhancing T cells differentiation into $CD8^+$ cytotoxic lymphocytes (CTLs). Consequently, IL-2 limits DGKα expression and this explains why IL-2 is able to contrast T cell anergy [33]. As further confirm, it has been demonstrated that CTLs derived from DGKα-deprived mice exhibit increased IL-2 dependent proliferation and enhanced Ras-ERK signalling [33].
In contrast to what observed for the Egr2-mediated transcriptional regulation, this last transcriptional control of DGK activity by the PI3K-AKT-FoxO pathway seems to be specific to the sole DGKα isoform, since the authors report that the inhibition of AKT does not alter the expression of DGKζ. Lastly, in literature have been reported some translational miRNA-mediated mechanisms of genetic DGK regulation. In a study by Shin et al., DGKζ expression is downregulated by microRNA 34a (miR-34a) is an isoform-specific manner during T cell activation [34]. Even though this kind of

miRNA-dependent regulation has not been described for DGKα in T cells, in glioblastoma miR-297 seems to control DGKα expression [35] (Fig. 5).

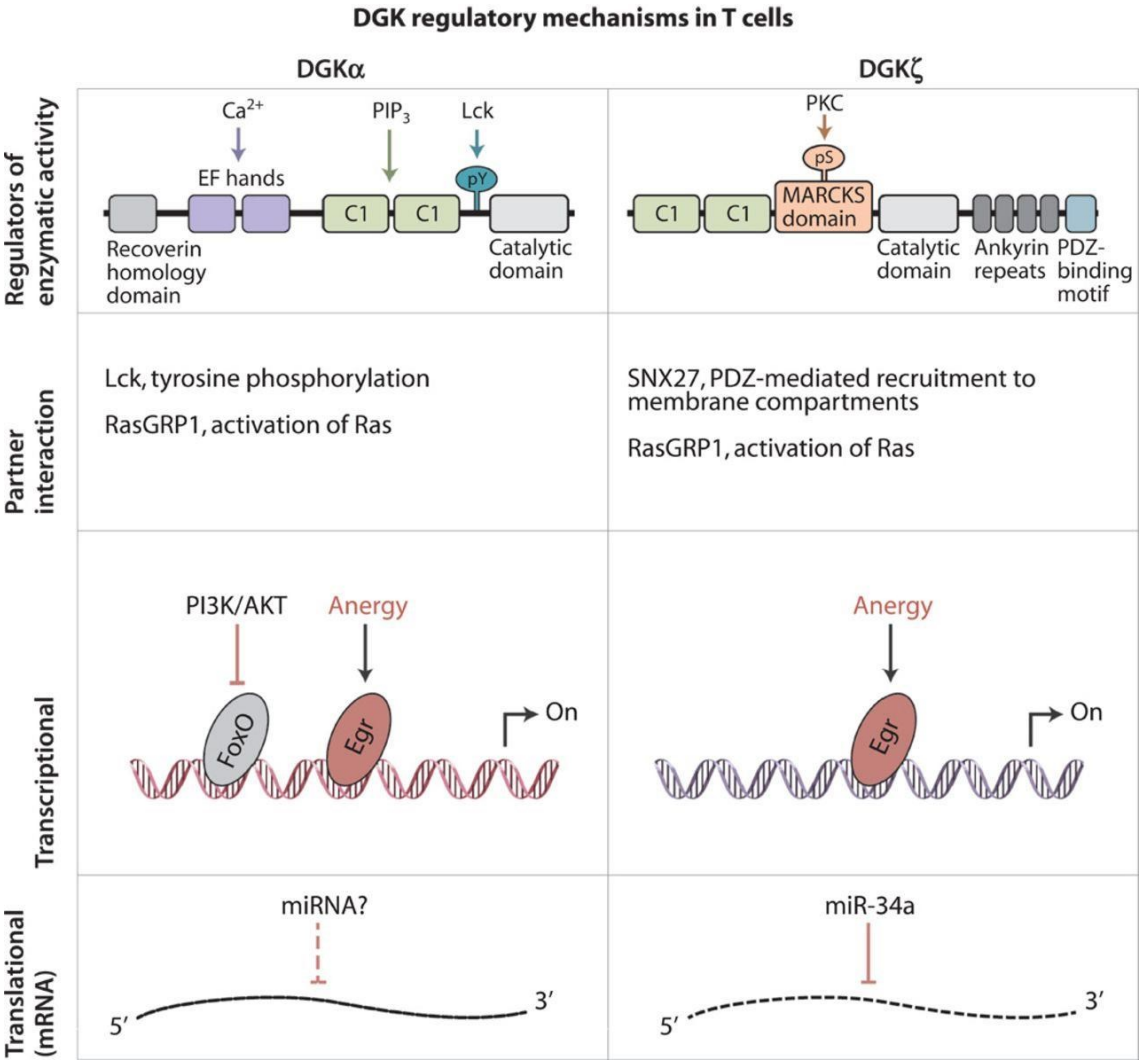

Figure 5. Comparison between DGKα and DGKζ proposed mechanisms of regulation in T cells.
Scheme of regulatory domains of the DGKα (left column) and DGKζ (right column) isoforms. Whereas both isoforms have in common the C1 and the catalytic domains, DGKα possess two EF-hand motifs Ca^{2+}- sensitive, responsible for conformational change and localization at the plasma membrane. Moreover, the DGKα C1 regions bind to PIP_3, and Lck phosphorylates the enzyme at Tyr^{335} (pY). On the other hand, DGKζ contains a MARCKS-like domain that can be phosphorylated by PKC, as well as an ETAV sequence at the C-terminus region, which interacts with PDZ domain containing proteins. In lymphoid cells, binding partners of DGKα include RasGRP1 and Lck, while DGKζ interacts mostly with RasGRP1 and SNX27. The PI3K- and AKT-mediated inactivation of FoxO limits DGKα expression, whereas in anergic condition both DGK isoforms shows an increased expression under the transcriptional regulation by Egr2. Interestingly, miRNAs-mediated mechanisms of genetic control can occur. For instance, DGKζ expression is targeted by miR-34a during T cell activation, whereas no evidence of DGKα miRNA regulation is reported in T cells (Merida et al., 2015).

Interestingly, also the distribution and localization of these two DGK isoforms appears to be differently regulated. DGKα EF-hand domains are Ca^{2+}-sensitive and experiments with GPF tagged DGKα in Jurkat cells demonstrate that, in presence of Ca^{2+}, they mediate the translocation of cytosolic DGKα to plasma membrane along with the activation of tyrosine kinases [36]. A following study by the same group, confirmed *in vivo* that antigenic stimulation leads to rapid DGKα membrane localization. Moreover, using the same transgenic mice, the authors also report that RasGRP1 relocates to the T cell membranes with a kinetic similar to the one observed for DGKα, suggesting a novel mechanism by which DGKα controls Ras attenuation [37]. Further studies focused also on the recruitment of these two DGK isoforms during the immune synapse formation, an event which results in Golgi apparatus, the microtubule organizing center (MTOC), and mitochondria polarization toward the antigen presenting cell. In a study by Gharbi and colleagues, GFP-DGKα and -ζ constructs were used to verify the kinases respective translocation dynamics during IS formation. The authors observed the only GFP-DGKζ translocated rapidly to the plasma membrane at early stages of IS formation following TCR triggering, suggesting that DGKζ is the isoform that mainly controls the overall DAG abundance [38]. In contrast to these data, overexpression experiments in murine primary T cells showed comparable recruitment levels of both GFP-DGKα and GFP-DGKζ to the IS [39]. Another study by Chauveau et al., reported a relevant impairment in MTOC polarization in DGKα$^{-/-}$ T cells during IS formation, whereas this defect was not observed in absence of DGKζ [40]. The authors, using TIRF (total internal reflection fluorescence) microscopy technique demonstrated the localization of GFP-DGKα at the peripheral ring of F-actin suggesting that this isoform phosphorylates DAG at the peripheral supramolecular adhesion complex (pSMAC) (Fig. 6).

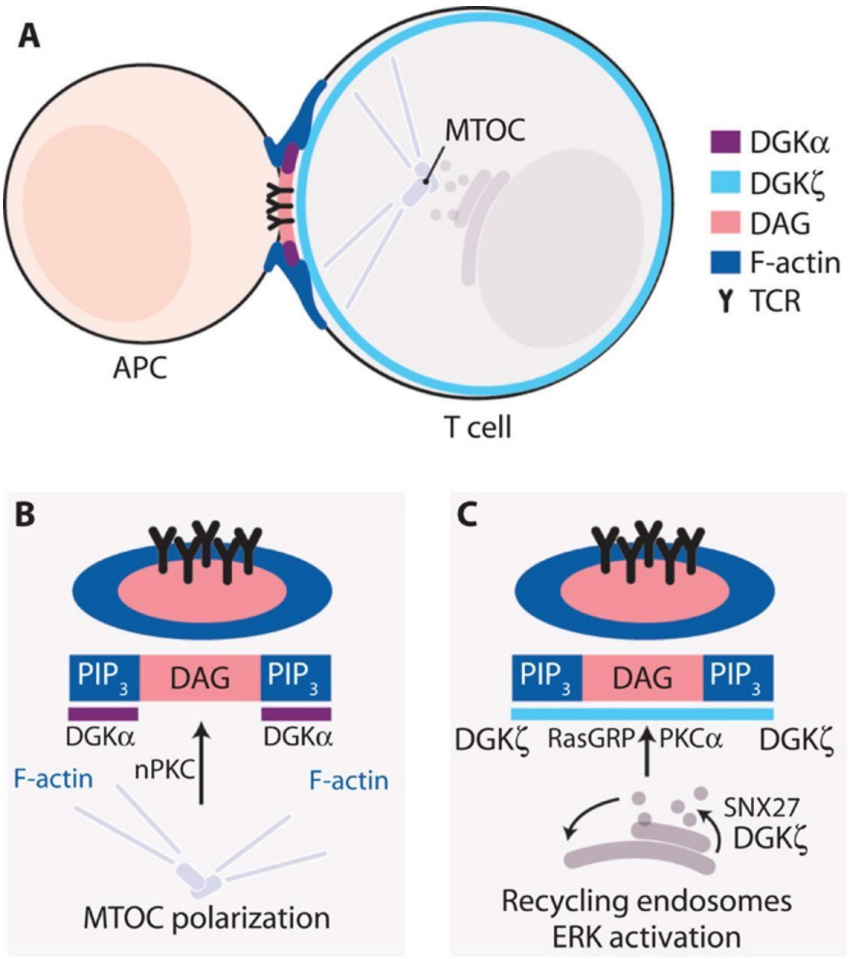

Figure 6. Proposed spatial distribution of DGKα and DGKζ during immunological synapse formation.

(A) The accumulation of DAG during immune synapse formation mediates polarization of the MTOC and the scheme proposes a possible redistribution of DGKα and DGKζ isoforms during IS formation.

(B) The generation of PIP_3 at the peripheral synapse area promotes the recruitment of DGKα that, metabolizing DAG limits the recruitment and activation of nPKCs, which drives MTOC polarization.

(C) The interaction between SNX27 and DGKζ limits the consumption of DAG in recycling compartments, which promotes the localization of RasGRP1 and PKCα to the IS and their activation (Merida et al., 2015).

To better understand the role of these DGK isoforms in T cells several studies have been conducted in murine models, a summary of which is included in the following Table 2, adapted from a work by Zhong et al., 2016 [19] .

		DGKζ$^{-/-}$	DGKα$^{-/-}$	DGKα$^{-/-}$ DGKζ$^{-/-}$	References
T cell development	Positive selection	Not affected	Not affected	Severe decreases of CD4 SP and CD8 SP thymocytes	[29]; [27]; [12]
	Negative selection	Not affected	Not affected	Not affected	[12]
Regulatory T cell	Foxp3^{-}CD25^{+} CD4^{+} SP thymocytes	Increased frequencies	Increased but less obvious than DGKζ$^{-/-}$	Not reported	[39]; [41]
	Foxp3^{+} Treg	Increased in thymus and spleen	Not increased	Not reported	[41]
	Suppressive function (*in vitro*)	Enhanced	Not obviously changed	Not reported	[42]
CD8 T cells	Primary responses to pathogens	Enhanced expansion and cytokine production in response to LCMV	Less obvious expansion than DGKζ$^{-/-}$ but similar enhanced cytokine production in response to LCMV	Severely impaired in migration, expansion, and cytokine production in response to LM-Ova	[29]; [43]; [44]
	Memory responses	Decreased formation; impaired in expansion, enhanced IFNγ and TNFα production in recall responses to LCMV	Decreased formation; impaired in expansion (more severe than DGKζ$^{-/-}$), enhanced IFNγ and TNFα production in recall responses to LCMV	Impaired formation and maintenance; Decreased expansion but enhanced IFNγ and TNFα production in recall response to LM-Ova	[43]; [44]
				Not reported	[45]
	Sensitivity to TGF-β	Decreased	Not reported	Not reported	[46]; [47]
	Anti-tumor immunity-OT1 T cells	Enhanced expansion and effector function; Enhanced tumor control	Not reported		
	Anti-tumor immunity-Meso-CAR T cells	Enhanced effector function	Enhanced effector function	Stronger effector function than DGKα or ζ single deficiency; Better tumor control	[47]

Table 2. Comparison of DGKα−/−, DGKζ−/−, and DGKα−/−ζ−/− mice

(Adapted from Zhong et al., 2016)

1.4 SAP signalling mediates DGKα inhibition

Signalling lymphocyte activation molecule (SLAM)-associated protein (SAP) is a 128 aa adaptor protein encoded by SH2D1A gene, localized to the Xq24-27 interval, on the long arm of X chromosome. SAP mutations are mostly loss of function and their occurrence gives rise to the X-linked lymphoproliferative disease type 1 (XLP-1), a rare immunodeficiency affecting about one-two out of one million males and characterized by an increased vulnerability to the Epstein-Barr virus (EBV) infections. It has been reported that cells derived by SAP-deficient mice exhibit dysregulations in both $CD4^+$ and $CD8^+$ T cell functions, altered IL-4, IL-13, and IL-10 cytokines production, impaired germinal-centre formation, and a decreased TCR-mediated cell activation [48]. In particular, SAP-deficient $CD8^+$ lymphocytes show a defective cytotoxic activity [49] while the $CD4^+$ cells fail in supporting B cell maturation [50].

The SAP adaptor protein consists in a N-terminal region, a central SH2 domain and a C-terminal domain. Upon TCR stimulation, SAP SH2 domain binds to the cytoplasmic portion of the SLAM family of transmembrane receptors, in a specific region containing the conserved Immunoreceptor Tyrosine-based Switch Motif (ITSM). Thus, SAP acts as a regulator for the balance between activating and inhibitory signals downstream SLAM receptors, since its binding to ITSM sequences prevent the recruitment of both SHP1/2 tyrosine phosphatases and SH2 containing inositol phosphatase (SHIP) by competition. Moreover, its binding couples the Src-family kinase Fyn to the SLAM receptors where the activated Fyn kinase phosphorylates further downstream effectors such as Dok1 and Dok2, leading to NFκB signalling activation and IFN- γ production (Fig. 5) [51]. According to Cannons et al., in $CD4^+$ cells this NFκB activation is mediated by PKCθ, which is recruited through the SAP/Fyn pathway [52]. Conversely, it has been reported that, in absence of SAP, the interaction between SHP1/2 with SLAM receptors could have a role in reducing TCR signalling strength [53, 54]. In line with these studies, Proust and colleagues demonstrated that SAP silencing decreases various signalling pathways downstream TCR, such as ERK, Akt and PLCγ1, consequently reducing IL-2 and IL-4 production [55].

Moreover, in SAP-deficient conditions, the $CD8^+$ cells show an impaired restimulation-induced cell death (RICD), a particular kind of apoptosis which prevent excessive lymphoproliferation. Usually, a healthy immune system relies on the ability of T cells to

recognize and respond to system perturbations over a certain background threshold. However, to prevent autoimmune responses, the system also requires a mechanism to control the intensity of the immune responses within the self-tolerance limits. Thus, TCR RICD is a physiological apoptotic program counteracting excessive T cells clonal proliferation [56]. In normal conditions, an optimal T-cell activation occurs via recognition of antigen-loaded MHC complexes through a specific TCR, and concomitant engagement of CD28 and/or other costimulatory molecules on the antigen presenting cell surface. This interaction initiates a rapid production of IL-2, a crucial growth and survival cytokine for activated T cells: its uptake triggers an autocrine signalling loop that drives responding T cells into several cycles of proliferation. Both antigen and IL-2 abundance in the surrounding environment ultimately establishes effector T cells' fate: some will be more prone to apoptosis whereas others will give rise to the "long-lived memory T cells" (Fig. 7).

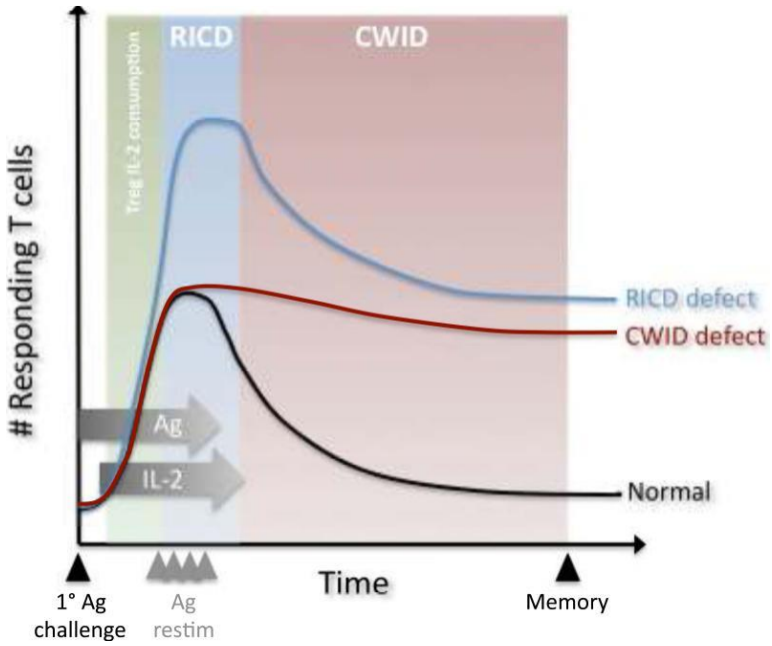

Figure 7. Apoptotic program is used to maintain T cells homeostasis

During immune response, T-cell fate is determined by the relative quantity of Ag and IL-2 (black line) (horizontal grey arrows). TCR restimulation after a secondary Ag encounter (Ag restim, grey arrowheads) can cause RICD in the presence of IL-2 (blue zone), limiting T-cell growth. When Ag is eliminated and IL-2 levels decrease, cytokine withdrawal-induced death (CWID) regulates the constriction of the effector T-cell pool (red zone), reserving a small pool of memory T cells (Snow et al., 2010).

Based on this concept, results obtained by Snow et al., indicate that T cells restimulation triggers apoptosis only when certain threshold is reached and in this context SAP acts as a "signal amplifier", which increases TCR signal intensity allowing the signal to reach the required threshold and leading to an increased expression of pro-apoptotic molecules such as FAS ligand, Bcl-2 Interacting Mediator of cell death (BIM), and nuclear receptor 4A1 (NUR77). Vice versa, in absence of SAP, the strength of TCR signalling is attenuated, the RICD threshold is not reached and consequently lymphocytes gain the ability to escape cell death (Fig. 8) [57].

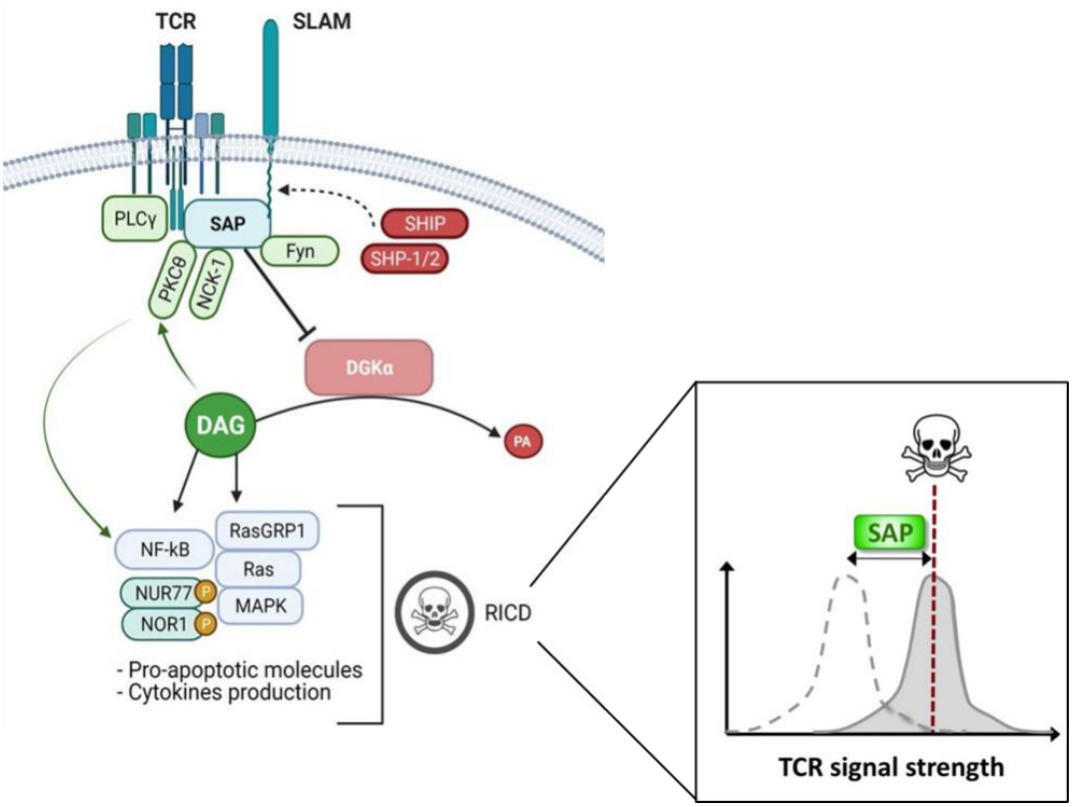

Figure 8. SAP signalling pathway mediates DGKα inhibition

Upon TCR stimulation, the adaptor protein SAP binds to ITSMs sequences of the SLAM-family receptors, competing with SHIP and SHP-1/2 phosphatases and promoting activation signals. Here, SAP interacts with distinct binding partners, such as Fyn, PKCθ and NCK-1, promoting T cell activation. Moreover, SAP mediates the inhibition of DGKα, leading to PLCγ-derived DAG accumulation and resulting in MAPKs activation, pro-apoptotic molecules expression and cytokines production. In antigen-experienced $CD8^+$ cells, these events trigger the RICD program, which promotes effector T cells clearance and prevents excessive lymphoproliferation (Adapted from Velnati et al., 2021 and Snow et al., 2009).

Interestingly, in a work by Ruffo et al., it has been demonstrated that DGKα inhibition or downregulation restores *in vitro* a correct DAG-dependent signal transduction, cytokines production and RICD [58]. In physiological conditions, DGKs activity is constrained during TCR stimulation, allowing DAG accumulation which results in PKCθ and Ras-GRP activation, for a full T cell response. However, the molecular mechanisms underlying DGKs inhibition in T cells are only partially understood.
Notably, our group found that, upon strong TCR/CD28 co-stimulation, the adaptor protein SAP downmodulates DGKα activity and this SAP-mediated DGKα inhibition is required for a full T cell response. As further confirm of this central role of SAP in regulating DGKα function, we demonstrated that DGKα inhibition can be induced either overexpressing SAP or by triggering a recombinant SLAM receptor [59]. Following TCR stimulation, DGKα is recruited to the cell membrane where its catalytic activity is suppressed, and this inhibition is dependent on PLCγ1 activity. SAP knockdown restores DGK enzymatic activity and decreases translocation to the cell membrane following TCR co-stimulation [59]. Since a direct protein contact between SAP and DGKα was not found, we speculate that SAP influences the post-translational regulation of DGKα through an undetermined mechanism, whose investigation will be one of the main topics of this thesis work.

In literature, several and complementary pathways have been linked to SAP functions in T cells, due to its ability to interact with various signalling proteins. For instance, SAP can associate with Lck which plays a critical role in initiating the TCR signalling cascade. Indeed, SAP-Lck complex is reported to interact with the SLAM receptors as well as directly with the CD3 zeta chain [55], suggesting that SAP has a role in physically bridging co-receptors, as well as bringing kinases such as LCK to the immunological synapse, promoting signal transduction [60].
Interestingly, in SAP protein sequence, the R78 residue has been reported to mediate a connection with the SH3 domain of PAK-interacting exchange factor (PIX), facilitating the development of a trimeric complex between SAP, PIX, and the cell division control protein 42 (CDC42), contributing to T cell activation process [61]. Furthermore, Li and colleagues identified NCK Adaptor Protein 1 (NCK-1) as a novel SAP binding partner through a screening of regulatory proteins containing the SH3 domain, observing that SAP knock-down reduced phosphorylation of NCK-1 and other proteins downstream of

TCR signalling, leading to a decreased cell proliferation and ERK pathway activation [62]. Intriguingly, some of these SAP interactors, such as NCK-1, CDC42, Vav1 are also involved in the Wiskott-Aldrich syndrome protein (WASp) recruitment and activation [63, 64]. WASp belongs to the nucleation-promoting factors family and, by activating the actin related protein 2/3 (ARP2/3), participates to both innate and adaptive immunity through the regulation of actin cytoskeleton-dependent cellular processes, including immune synapse formation, cell signalling, migration, and cytokine release [65]. Indeed, inactivating mutations or loss of WASp protein leads to a rare X-linked disorder, the Wiskott-Aldrich syndrome (WAS) described originally by Dr. Alfred Wiskott in 1937 and Dr. Robert Aldrich in 1954 as a familial disease characterized by frequent infections, bleeding tendency, thrombocytopenia, and eczema [66]. WAS condition can lead to autoimmune complications in 40% to 70% patients and it is not surprising that WASp absence has been linked to cellular immune defects also in both WAS and WASp-deficient mice [67, 68]. Among them, it is interesting to note that lymphocytes from WASp knockout mice exhibit an impaired RICD [68] similarly to what was observed in SAP-deficient conditions: these similarities between these two immunodeficiencies prompted us to verify the hypothesis of a SAP-WASp pathway which will be further discussed in the next chapters of this thesis work.

1.5 Lipid signalling effectors: the protein kinase C family

The modulation of DAG and PA concentrations within the cells by DGKs influences downstream signalling proteins which are activated by lipid binding. Among them, the PKC proteins are calcium (Ca^{2+}) and phospholipid-dependent enzymes that catalyse the covalent transfer of phosphate from ATP to protein serine and threonine residues. Phosphorylation of the substrate protein causes a conformational shift and, as a result, a change in its functional characteristics [69].

These kinases phosphorylate many molecules involved in the intracellular signalling network both *in vitro* and *in vivo* and several target proteins exhibit a preferential phosphorylation by distinct PKC isotypes [70]. Thus, the PKC family is essential in cellular signal processing and increasing evidence suggests that distinct PKC isoforms regulate mainly processes related to cell proliferation, differentiation, motility, survival, and death. Indeed, it is not surprising that PKCs absence or functional dysregulations occur in a various malignancies and diseases such as heart failure [71, 72], diabetes [73,

74], Alzheimer and Parkinson diseases [75, 76], inflammatory diseases [77], allergies [78], and a wide range of autoimmune diseases [79-82]. Furthermore, PKC alterations have been linked also to cancer diseases in different organs [83].

Immunological interest in PKC grew in the mid-1980s, when it was observed that antigen receptors in T and B lymphocytes regulate PLC, resulting in the modulation of intracellular concentrations of Ca^{2+} and DAG. In parallel, it was recognized that PKC proteins are key targets for the effects of DAG and its pharmacological mimics, the phorbol esters [84]. Indeed, the action of DAG is direct and the DAG-binding site in PKCs is a highly conserved in C1 domain or cysteine-rich domain.

To date, at least ten to twelve members of the PKC family are known, and they are classified into three different subgroups: classical or conventional PKCs (cPKCs, including α, βI, βII, and γ isoforms), novel PKCs (nPKCs, comprehending δ, ε, η, θ isoforms), and atypical PKCs (aPKCs, including ζ and ι/λ) [69, 70] (Fig. 9).

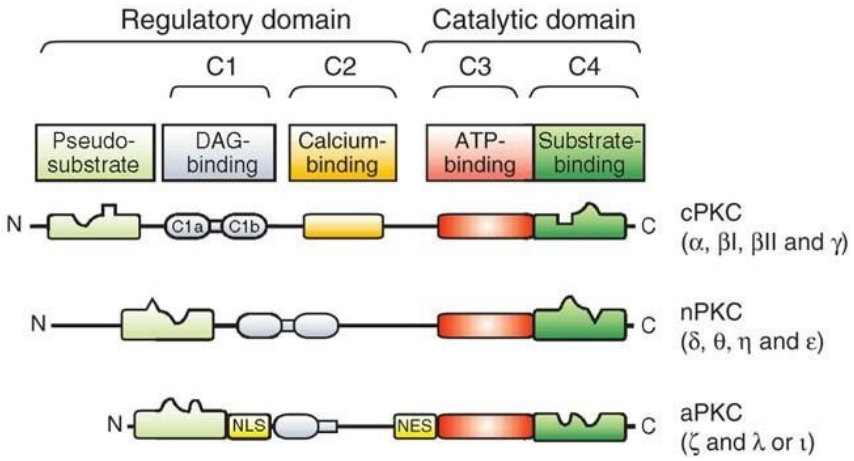

Figure 9. Classification and structural features of PKC isoforms.

The PKC isoforms share a conserved catalytic domain, while their regulatory domain differs among the three subgroups. The classical PKC isoforms (cPKC) possess the autoinhibitory pseudosubstrate region, two DAG-binding C1 domains (named C1a and C1b domains) and the calcium-binding C2 domain. Conversely, novel PKC isoforms (nPKC) do not contain a Ca^{2+}-binding motif but show an extended N-terminal region that is still sensitive to DAG regulatory signals. Finally, the atypical PKC isoforms (aPKC) lack of Ca^{2+}-binding and sensitive DAG-binding domains, thus their catalytic activity is independent of both DAG and calcium. Their regulation appears to be mainly driven by intracellular localization, mediated by interaction between regulatory proteins and nuclear localization signals (NLS) or nuclear export signals (NES) in their regulatory domain (Spitaler and Cantrell, 2004).

All these members of the PKC family possess a common structural backbone that consists mostly of a regulatory domain at the N-terminus and a catalytic domain at the C-terminus. These protein portions are defined as conserved (C1-C4) or variable regions between isoforms. cPKCs isoforms are characterized by a DAG-binding C1 domain and a Ca^{2+}-sensitive C2 domain. Thus, they are activated by anionic phospholipids in a calcium-dependent manner. Conversely, nPKCs are Ca^{2+}-independent but still require DAG or phorbol esters to be activated. In contrast, the aPKCs, do not contain a C2 domain, thus they are Ca^{2+} independent and they possess only a single C1 DAG-insensitive domain. It is interesting to note that all the PKC isoforms exhibit a basic pseudo-substrate region (PSR) region preceding the C1 domain. In absence of second messengers, the PSR motif keeps the kinase in an inactive state interacting with the substrate-binding site and blocking sterically the catalytic domain. Then, binding of lipids to PKC isoforms results in a conformational change that releases the PSR and increases the catalytic activity of the enzymes (Fig. 10).

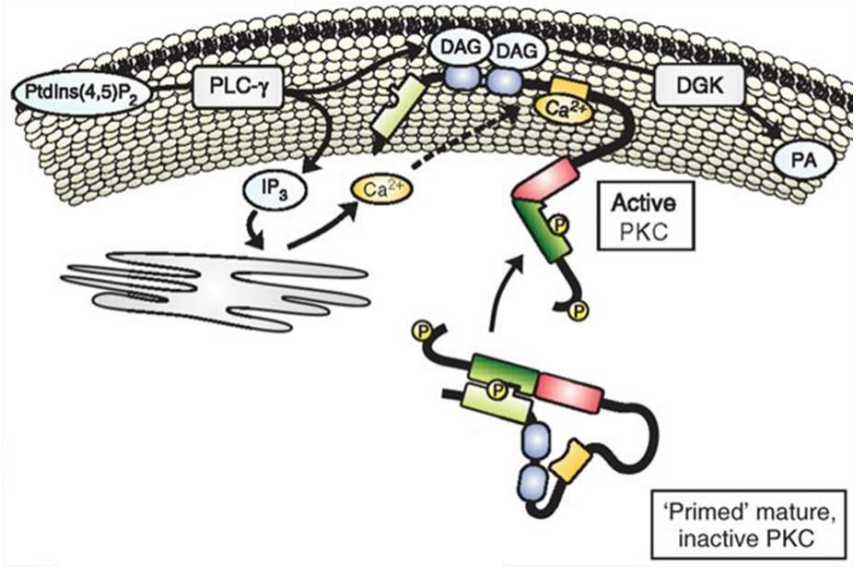

Figure 10. Mechanism of activation for classical and novel PKCs

Second messengers binding is a key event for the release of the PSR from the active site, allowing signalling effectors to interact with the PCKs. The PKC domains are highlighted with different colours: PSR in bright green; C1 domains in blue; calcium-binding domain in orange; ATP-binding subdomain in red; substrate-binding subdomain of the catalytic domain in dark green (Adapted from Spitaler and Cantrell, 2004).

Even though aPKCs are not DAG-sensitive, they are recruited to membranes upon cell stimulation, by lipid-protein and/or protein-protein interactions [85-88]. However, the role of lipid binding in aPKCs localisation is not yet fully understood.

In a work by Limatola et al., using a gel-shift assay the authors demonstrated that PA directly binds and activates PKCζ [89] while in Pu et al., authors observed that, compared with the other PKCs C1 domains, the rim of the binding cleft of the aPKCs C1 domain contains extra positively charged arginine residues (more precisely, at positions 7, 10, 11, and 20) that may be responsible for the PA binding [90].

Moreover, the relevance of PA for aPKC regulation has been highlighted also by our previous work, where we show that DGKα-produced PA at cell-ruffling sites recruits aPKCs promoting protrusions extension and cell migration [85]. Although several works have shown functions for the DGKα/ζ-generated PA, most studies were not performed with T cells. For instance, it has been reported that the mammalian target of rapamycin (mTOR), a well-known regulator of cell growth and proliferation, is a key target of DGKζ-derived PA in HEK293T and skeletal muscle cells [8, 91]. Furthermore, several reports associate the DGK-mediated generation of PA with the control of membrane and protein trafficking [92, 93]. In T lymphocytes, DGKα is critical for the polarization of multivesicular bodies and the release of exosomes toward the immunological synapse [94]. In a similar way, an interaction between DGK-produced PA and aPKCs (although it has not yet been described) could contribute to some effector functions during T cell activation process.

However, the mechanisms behind aPKCs localization and activation in T cells are still obscure and further studies should explore the connection between DGKα/ζ-derived PA and aPKCs in T cell activation.

2. AIM OF THE WORK

2.1 Aim of the thesis project

The diacylglycerol kinases are fascinating enzymes that play a pivotal role within the cells connecting *lipid metabolism* to *signalling functions*.

Therefore, the purpose of the present thesis work is to investigate the regulation of their activity and the resulting lipid signalling modulating T cell survival and cytokines production. Thus, this research thesis is divided into three main topics:

- The study of the regulation of DGKα activity by Wiskott-Aldrich syndrome protein (WASp) downstream T cell receptor (TCR) in activated T lymphocytes;
- The investigation of the interaction between signalling phospholipids and a particular class of DGKα effectors: the atypical protein kinases C (aPKCs);
- Biological role of WASp-DGKα axis in RICD and IL-2 production.

The main findings of the thesis project led to the identification of a novel function of WASp, which downstream TCR signalling modulates the kinase activity resulting in a full cytokines response. Those studies in T cells are complemented in vitro by the study of lipid regulation of aPKCs by PA and other phospholipids.

The data obtained resulted in three scientific papers that were used to prepare this thesis and are attached at the end for your reference, in the section "Publications". Two of them are already published, while a third is under revision:

- Velnati S, **Centonze S**, Girivetto F, Baldanzi G. **Diacylglycerol Kinase alpha in X Linked Lymphoproliferative Disease Type 1.** Int J Mol Sci. 2021 May 29;22(11):5816. doi: 10.3390/ijms22115816. PMID: 34072296; PMCID: PMC8198409.
- Velnati S, **Centonze S**, Girivetto F, Capello D, Biondi RM, Bertoni A, Cantello R, Ragnoli B, Malerba M, Graziani A, Baldanzi G. **Identification of Key Phospholipids That Bind and Activate Atypical PKCs.** Biomedicines. 2021 Jan 6;9(1):45. doi: 10.3390/biomedicines9010045. PMID: 33419210; PMCID: PMC7825596.
- **Centonze S**†, Velnati S†, Giulia Rossino, Beatrice Purghè, Annamaria Antona, Elisa Ruffo, Valeria Malacarne, Mario Malerba, Marcello Manfredi, Andrea Graziani and Gianluca Baldanzi. **Wiskott-Aldrich syndrome protein interacts and inhibits diacylglycerol kinase alpha promoting IL-2 induction.**
  Actually under revision to "*Frontiers in immunology*" Journal.

3. MATERIALS AND METHODS

3.1 Lab reagents

All the chemical reagents used in this work are listed in the following Table 3.

Antibodies			
Antibody	**Clone**	**Cat. number**	**Provider**
Anti-human CD3	UCHT1	MA1-80537	Invitrogen
Anti-human CD3	OKT3	40-0037-U500	Tonbo biosciences
Anti-human CD28	CD28.2	16-0289-85	Invitrogen
Anti-DGKα	-	11547-1-AP	Proteintech
Anti-DGKα	-	AB64845	Abcam
Anti-Phospho-p44/42 MAPK (Erk1/2)	-	9101	Cell Signalling Technology
Anti-p38 MAPK	-	9212S	Cell Signalling Technology
Anti-WASp	D9C8	4271	Cell Signalling Technology
Anti-WASp	-	4860	Cell Signalling Technology
Anti-WASp	--	Sc-13139	Santa Cruz Biotechnology
Anti-CDC42	5B7	Sc-87	Santa Cruz Biotechnology
Anti NCK-1	hVIN-1	12778	Cell Signalling Technology
Anti-Vinculin	8H10D10	V9264	Sigma-Aldrich
Anti-b-actin	9E10	3700	Cell Signalling Technology
Anti- c-myc	9E10	MA1-980-1MG	Invitrogen
Anti- c-myc- AC	-	sc-40 AC	Santa Cruz Biotechnology
Anti-ECS (DDDDK) HRP conjugated	-	A190-101P	Bethyl laboratories
Anti-FLAG HRP conjugated	M2	HRP-66008	Proteintech
Anti-FLAG	FG4R	A2220	Sigma-Aldrich
Anti-DYKDDDDK tag	FG4R-HRP	MA1 91878	Life technologies
Anti-DYKDDDDK tag HRP-Conjugated	Z-5	MA1 91878-HRP	Invitrogen
Anti-GST		sc-459	Santa Cruz Biotechnology
Chemical Compounds			
Name	**Function**	**Cat. number**	**Provider**
rhIL-2	IL-2	200-02	Preprotech
CK-666	ARP2/3 Inhibitor	SML0006-5MG	Sigma Aldrich
AMB639752	DGKα inhibitor		Ambinter
siRNAs (Where not specified, siRNAs are from Thermo Fisher Scientific (Life Technologies))			
Target	**siRNA type**	**siRNA ID & Cat. #**	**Sequence**
SAP	Stealth RNAi™	siRNA ID: Custom	Forward UGUACUGCCUAUGUGUGCUGUAUCA

	siRNA	Cat. # 10620312	Reverse	UGAUACAGCACACAUAGGCAGUACA
WASp	Silencer ™ Select Pre-Designed siRNA	siRNA ID: s14836	Forward	UGAACAACCUCGACCCAGAtt
		Cat. # 4392420	Reverse	ACUGGGUCGAGGUUGUUCAcg
CDC42	Silencer ™ Select Pre-Designed siRNA	siRNA ID: s2765	Forward	UGGUGCUGUUGGUAAAACAtt
		Cat. # 4392420	Reverse	UGUUUUACCAACAGCACCAtc
NCK-1	Silencer ™ Select Pre-Designed siRNA	siRNA ID: s9311	Forward	CCUCAUUCGUGAUAGUGAAtt
		Cat. # 4392421	Reverse	UUCACUAUCACGAAUGAGGaa
DGKα	Stealth RNAi™ siRNA	siRNA ID: Custom	Forward	CGAGGAUGGCGAGAUGGCUAAAUAU
		Cat. # 10620312	Reverse	AUAUUUAGCCAUCUCGCCAUCCUCG

SYBR green Primers (where not specified, SYBR green primers are from Sigma-Aldrich (Merck)).

Gene	Code	Primer	Sequence
DGKA	FH1_DGKA	Forward	AATGTTCCCAGACACCTAAG
	RH1_DGKA	Reverse	AGTAGCAGGAAACATCATTG
SH2D1A	FH1_SH2D1A	Forward	AAGGGATAAGAGAAGATCCTG
	RH1_SH2D1A	Reverse	CATTACAGGACTACAATGGC
WAS	FH1_WAS	Forward	TACTCACAGCTTGTCTACTC
	RH1 WAS	Reverse	TTTTGTATCTTCTCCTGCAC
CDC42	FH1 CDC42	Forward	GAACAAACAGAAGCCTATCAC
	RH1 CDC42	Reverse	TTTAGGCCTTTCTGTGTAAG
NCK-1	FH1_NCK1	Forward	CCAAGTATATTGTGTCTGCC
	RH1_NCK1	Reverse	CTATGTCTCATGTGTCTTGC
GAPDH	FH1_GAPDH	Forward	TTGAGCACAGGGTACTTTA
	RH1_GAPDH	Reverse	ACAGTTGCCATGTAGACC

TaqMan probes (Where not specified, TaqMan probes are from Thermo Fisher Scientific (Life Technologies)).

Gene	Cat. Number
IL-2	Hs00174114_m1
GAPDH	Hs02758991_g1
NR4A1	Hs00374226_m1
FASLG	Hs00181225_m1
FOS	Hs04194186_s1
IFNγ	Hs00989291_m1

Buffers	
Buffer	**Composition**
Lysis buffer	25 mM HEPES, 150 mM NaCl, 5 mM EDTA, 1 mM EGTA, 1% NP40, 10% glycerol, (supplemented with 1 mM sodium orthovanadate along with protease inhibitors before use), pH 8.0
$LiCl_2$ buffer	25 mM Tris, 0.5 M LiCl, pH 8.0
TNE buffer	25 mM Tris, 150 mM NaCl, 1 mM EDTA, pH 8.0
Homogenization buffer	25 mM Hepes (pH 8), 20% glycerol, 135 mM NaCl, 5 mM ethylenediaminetetraacetic acid (EDTA), 1 mM ethylene glycol-bis (beta-aminoethyl ether)-N,N,N′,N′-tetra acetic acid (EGTA), 1 mM sodium orthovanadate and protease inhibitor cocktail
Laemmli sample buffer	187.4 mM Tris HCl, 30% glycerol, 6% SDS, bromophenol blue in sufficient quantity, (supplemented with DTT 150 mM before use), pH 6.8
TBS-T	50 mM Tris, 120 mM NaCl, 0.01% TWEEN20 detergent
PBS	137 mM NaCl, 2.7 mM KCl, 4.3 mM Na_2HPO_4, and 1.5 mM KH_2PO_4, pH 7.4
HEPES-Triton X-100 buffer	HEPES pH 7.4 20 mM, sucrose 300 mM, NaCl 50 mM, MgCl2 3 mM, Triton X-100 0.5%
Elution buffer	100 mM Tris HCl, pH 8.0, 10-mM NaCl, 5% glycerol supplemented with fresh 2-mM DTT, and glutathione 10 mM

Plasmids and mutants		
Plasmid	**Reference**	**Cat. Number**
myc-DGKα	Described in [95]	
GST-DGKα	Described in [96]	
FLAG-WASp		47432
myc-FLAG-N-WASp		RC207967
myc-DGKα L360*	Described in [96]	
FLAG-PKCζ	Kindly provided by Dr Alex Toker (Boston, MA, USA) [90]	
FLAG-PKCι	Origene	TP305379
GST-PKCζ	Described in [97]	
GST-PKCι	Described in [97]	

To create mutant variants of the above-mentioned plasmids we used Phusion™ Site-Directed Mutagenesis Kit (Thermo Fisher Scientific) according to the manufacturer's instructions. Mutagenesis was performed using the following primers:

Mutant		Sequence
DGKα E86*	Forward	TCACTGCTTAAATTAGACAAATGTGACAAA
	Reverse	CCAGTCTCAAAGGATTGAAACAGTGC
WASp K232*	Forward	CTCAGGGAAGAAGTAGATCAGCAAAG
	Reverse	CGTTTCTTATCAGCTGGGCTAGG
WASp Q297*	Forward	TTCATTGAGGACTAGGGTGGGCTGG
	Reverse	GTCGTAGATAAGTTTAGAGGTCTCGGCG

shRNA plasmids			
Target	**Vector plasmid**	**Cat. number**	**Provider**
WASp	MISSIONpLKO.1-puro Empty Vector Plasmid DNA	TRCN0000029819	Sigma-Aldrich
NT (Non targeting)	MISSIONpLKO.1-puro Empty Vector Plasmid DNA	SHC002	Sigma-Aldrich

Table 3. Detailed list of lab reagents used in the present work.

3.2 Cell culturing

Human embryonic kidney 293T cells were cultured in 100 mm plates using DMEM with 10% FBS (Lonza) and 1% penicillin/ streptomycin (Life Technologies).

Jurkat cells were cultured in RPMI-GlutaMAX (Life Technologies) with 10% FBS (Lonza) and 1% penicillin/ streptomycin (Life Technologies).

Peripheral blood mononuclear cells (PBMCs) were isolated from healthy anonymous human buffy coats (provided by the Transfusion Service of Ospedale Maggiore della Carità, Novara, Italy). PBMCs were isolated by Ficoll-Paque PLUS (GE Healthcare) density gradient centrifugation, washed, and resuspended at 2 x 10^6 cells/ml in RPMI-GlutaMAX containing 10% heat-inactivated FBS, 2 mM glutamine, and 100 U/ml of penicillin and streptomycin. T cells were activated with 1 μg/ml anti-CD3 (clone UCHT1) and anti-CD28 (clone CD28.2) antibodies for 72 hours. Activated T cells were then washed and cultured in the complete medium along with 100 IU/ml rhIL-2 (PeproTech) at 1-2 x 10^6 cells/ml for ≥ 7 days by changing media every 2–3 days.

3.3 Generation of Jurkat WASp shRNA and Jurkat control shRNA

To generate stable WASp-silenced Jurkat cells we used MISSIONpLKO.1-puro Empty Vector Plasmid DNA (Sigma-Aldrich) harbouring either the sequence targeting human WASp (WASp shRNA) or a non-targeting short hairpin RNA (shRNA). Jurkat cells were plated and transduced with lentiviral particles in the presence of polybrene (6 μg/ml: Sigma-Aldrich, Saint Louis, MO, USA). Spinoculation protocol was performed as follows: the plate was centrifuged for 30 minutes at 32°C, 800 g. Subsequently, the medium containing viral particles was removed, and cells were resuspended in a fresh medium and incubated for three days (37°C, 5% CO_2). Lastly, 1 μg/ml puromycin (Sigma-Aldrich, Saint Louis, MO, USA) was added for the selection.

3.4 Jurkat cell stimulations and immunoprecipitation for activity assays

Jurkat cells (control shRNA and WASp shRNA) were cultured at a concentration of 1 x 10^6 cells/ml for 3 continuous weeks. 3 x 10^7 cells for each condition were resuspended in RPMI 1640 (preheated at 37°C) and/or pre-treated with DMSO or ARP2/3 inhibitor and/or DGKα inhibitor for 30 minutes. After pre-treatment, cells were stimulated using anti CD3 (UCHT1 clone) at a concentration of 10 µg/ml for 15 minutes and cells were lysed in 1 ml of lysis buffer. An aliquot of 50 µl cell lysates was retained for western blot analysis and the remaining was subjected to immunoprecipitation using 5 µg/ml of anti-DGKα antibodies (Abcam-AB64845) for 4 hours using protein G agarose beads in continuous rotation at 4°C. After immunoprecipitation, beads with DGKα antibody were washed twice with lysis buffer followed by 2 washes in $LiCl_2$ and 2 in TNE buffer. Following, the DGKα immunoprecipitates were subjected to DGK assay to measure DGK activity.

3.5 Preparation of 293T homogenates for activity assays

293T cells were transiently transfected with indicated plasmid DNA using Lipofectamine 3000, Invitrogen (Carlsbad, CA) in 10 cm^2 plates. 48 hours post-transfection, cells were harvested and homogenized by passing them 30 times through a 29G-needle using 500 µl of homogenization buffer for each dish and immediately stored in aliquots at -80°C. Cells transfected with GFP were used as controls.

3.6 DGK activity assay

Fundamentally, the same procedure was followed as reported previously in [98]. In brief, DGK activity was assayed by measuring initial velocities (5 minutes at 27°C) in presence of saturating substrate concentration. Reaction conditions: 0.9 mg/ml 1,2-dioleoyl-sn-glycerol, 5 mM ATP, 0.01 mCi/ml [c^{32}P]-ATP (for homogenates) or 0.04 mCi/ml [c^{32}P]-ATP (for immunoprecipitates), 1 mM sodium orthovanadate, 10 mM $MgCl_2$, 1.2 mM EGTA in 7.5 mM HEPES pH 8. The reaction mixture is assembled by mixing enzyme (25 µl of either cell homogenates or immunoprecipitated endogenous DGKα), 5X ATP solution, and 3X DAG solution. The reaction was terminated after 5 minutes by adding 200 µl of freshly prepared 1 M HCl and lipid was extracted by adding 200 µl of CH_3OH:$CHCl_3$ 1:1 solution and vortexing for 1 minute. The two phases were separated by centrifugation (12,000 RCF for 2 minutes). Either 25 µl (for

homogenates) or 50 µl (for DGKα immunoprecipitates) of the lower organic phase was spotted in small drops on silica TLC plates. TLC was run 10 cm and dried before radioactive signals were detected by GS-250 molecular imager and were quantified by either quantity one 4.01 or image lab 6.0 (Bio-Rad, Hercules, CA) software assuring the absence of saturated spots.

3.7 Lipidomic analysis

Jurkat cells were starved overnight in RPMI 0% FBS at a concentration of 2 x 10^6 cells/ml. The following morning, cells were washed in PBS and stimulated using anti CD3 (OKT3 clone) + CD28 (CD28.2 clone) antibodies at a concentration of 1 µg/ml for 15 minutes at 37°C. Post-stimulation, cells were washed four times in ice-cold PBS by centrifugation (700 g for 5 minutes) and after the last wash, the pellet was dried and subjected to lipidomic analysis.

Cells were extracted using 1 ml of 75:15 IPA/H_2O solution, after the addition of 100 µl of CH_3OH 5% deuterated standard (Splash Lipidomix®). Then the samples were vortexed for 30 seconds, sonicated for 2 minutes, vortexed again for 30 seconds and then they were incubated for 30 minutes at 4°C, under gentle, constant shaking. Subsequently, samples were rested on ice for additional 30 minutes. To remove debris and other impurities, the samples were centrifuged for 10 minutes at 3500 g at 4 °C. 1 ml of supernatant was collected and dried using a SpeedVac centrifuge (Labogene). The dried samples were reconstituted in 100 µl of CH_3OH containing the internal standard CUDA (12.5 ng/ml).

For the analysis of the reconstituted lipids, a UHPLC Vanquish system (Thermo Scientific, Rodano, Italy) coupled with an Orbitrap Q-Exactive Plus (Thermo Scientific) was used. Mass spectrometry analysis was performed in positive ion mode. The source voltage was maintained at 3.5 kV. The capillary temperature, sheath gas flow, and auxiliary gas flow were set at 320 °C, 40 arb, and 3 arb respectively. S-lens was settled at 50 rf. Data were collected in a data-dependent (ddMS2) top 10 scan mode. Survey full-scan MS spectra (mass range m/z 80 to 1200) were acquired with resolution R = 70,000 and AGC target 1e6. MS/MS fragmentation was performed using high-energy c-trap dissociation (HCD) with resolution R = 17,500 and AGC target 1e5. The stepped normalized collision energy (NCE) was set to 15, 30, and 45 respectively. The injection volume was 3 µl. Lockmass and regular inter-run calibrations were used for

accurate mass-based analysis. An exclusion list for background ions was generated by analysing a procedural blank sample. The acquired raw data were processed using MSDIAL software (Yokohama City, Kanagawa, Japan), version 4.24.
A QC-based regression model using linear weighted scatter plot smoothing (LOWESS) was used to adjust real sample signals according to the analytical order. Results are then reported as normalized peak intensity.

3.8 Proximity ligation assay (PLA)

Isolated human PBLs (0.15 x 10^6) were seeded in poly-L-lysine coated glasses in a 24-well plate and treated with the indicated stimuli. The cells were washed with ice-cold PBS, fixed in 3% paraformaldehyde/4% sucrose pH 7.4 for 10 minutes, permeabilized in ice-cold HEPES-Triton X-100 buffer for 5 minutes, washed twice with PBS, and processed according to the PLA (Duolink, Merck, cat. DUO92101) manufacturer's protocol. The samples were imaged with TCS SP5 confocal microscope (Leica Microsystem) as z stack of 1 µm thickness to cover the entire volume of the cells with a Plan Apo 63 X (NA 1.4) oil objective. PLA dots were quantified manually on maximum projection images obtained with Image J software (NIH).

3.9 Complex formation assays

293T cells were plated in 100 mm diameter Petri dishes and allowed to reach 90% confluence. Transfections were performed with the indicated DNA plasmids using Lipofectamine 3000 reagent according to the manufacturer's instructions (Invitrogen by Thermo Fisher). After 48 hours, cells were washed in ice-cold PBS and lysed in 1 ml of lysis buffer. Subsequently, lysates were incubated with 5 µg/ml anti-FLAG antibody (Sigma-Aldrich) or with 5 µg/ml anti-myc antibody agarose conjugated (Santa Cruz Biotechnology) and 20 µl Protein G Sepharose beads Fast Flow (Sigma) at 4 °C. 1 hour post-incubation beads were washed in lysis buffer six times and boiled in Laemmli Sample Buffer for 5 minutes at 95 °C. Thus, obtained immunoprecipitates were loaded on SDS-PAGE and analysed by western blotting using ChemiDocTM Imaging System (Bio-Rad).

3.10 Restimulation-induced cell death (RICD) assays in human PBLs

Activated human PBLs were transfected with 200 pmol of siRNA oligonucleotides specific for the target protein or a non-specific Stealth RNAi Negative Control Duplexes (12935-300) (Stealth Select siRNA; Life Technologies). Transient transfections were performed using Amaxa nucleofector kits for human T cells (Lonza) and either the Amaxa Nucleofector 4D systems (programs E0-115) or the Amaxa Nucleofector II system (program "primary lymphocyte T-020"). Cells were cultured in IL-2 (100 IU/ml) for 4 days to allow target gene knockdown. Knockdown efficiency was periodically evaluated either by Western blotting or by rt-PCR. To test restimulation-induced cell death (RICD), activated T cells (10^5 cells/well in 200 µl) were plated in either triplicates or quadruplicates in 96-well round-bottom plate and treated with increasing concentrations of anti-CD3 (clone OKT3) 0, 10, 100 ng/ml in RPMI-GlutaMAX supplemented with 100 IU/ml rhIL-2 for 24 hours. In these assays, DGK inhibitor AMB639752 (10 µM) was added 30 minutes before the restimulation with OKT3. 24 hours after treatment, cells were stained with 20 ng/ml propidium iodide and collected for a constant volume of 150 µl per sample on Attune Nxt Flow Cytometer (Thermo Fisher Scientific). Cell death is expressed as % cell loss and calculated as:

% Cell loss = (1-(number of viable cells in sample/number of viable cells in control) x 100).

Results were expressed as mean ± standard error mean (SEM). We always compare controls and WASp silenced lymphocytes from the same donors as there is a large individual variability in RICD sensitivity.

3.11 Gene expression assays

Activated human PBLs were transfected as described above and 4 days after transfection, cells were collected, washed, and seeded at the concentration of 1.5 x 10^6 cells in 1 ml of RPMI supplemented with 10% FBS and 100 IU/ml rhIL-2. Subsequently, cells were pre-treated for 30 minutes with the indicated inhibitors or DMSO and stimulated with OKT3 + CD28.2 at the concentration of 1 µg/ml. After 4 hours, cells were collected, washed twice with ice-cold PBS, and subjected to RNA extraction using RNeasy Plus mini kit from Qiagen or Maxwell RSC simply RNA extraction kit (AS1390, Promega Italia), following manufacturer instructions. The RNA

concentration and purity were estimated by a spectrophotometric method using Nanodrop 2000c (Thermo Scientific). The RNA was retrotranscribed with LunaScript RT Supermix kit (NEB) or High-Capacity cDNA Reverse Transcription Kits (Applied Biosystems). The resulting cDNA was quantified by real-time PCR (Luna Universal qPCR Master Mix by NEB or ABI7900 by Applied Biosystems) in either 96 or 384 well plates using GUSB or GAPDH as normalizers.

WASp shRNA transduced Jurkat cells were collected periodically along with control shRNA transduced Jurkat cells to check the efficiency of WASp silencing.

3.12 Western blot analysis

To verify the protein expression in immunoprecipitated Jurkat cells or 293T cells, equal amounts of protein lysates or homogenates were analysed by western blotting as following described. Proteins were separated on SDS–PAGE gels and subsequently transferred to a polyvinylidene fluoride (PVDF) membrane. The membranes were then blocked by incubating with 3% (w/v) dried BSA for 1 hour at room temperature and subjected to overnight incubation with respective primary antibodies at 4 °C with gentle agitation. The following day, membranes were washed 4 times in TBS-T buffer at 15 minutes time intervals. They were then incubated with alkaline HRP-conjugated rabbit or mouse secondary antibody (1:5000, PerkinElmer, USA) diluted in TBS-T, for 1 hour at room temperature with gentle agitation. After four additional 15 minutes washes with TBS-T, the membranes were developed using the Western Chemiluminescence Substrate (PerkinElmer) using the ChemiDoc^{TM} Imaging System (Bio-rad).

3.13 Protein purification

For lipid overlay assays with lipid arrays, recombinant proteins were obtained by transfecting 293T cells (5 × 10 cm dishes) with the corresponding constructs using lipofectamine 3000 (Thermo Fisher Scientific) according to the manufacturer's instruction. After 48 hours, cells in each plate were lysed in 0.5 mL of lysis buffer and clarified after centrifugation for 15 minutes at 12,000 rpm at 4 °C.

FLAG-tagged recombinant proteins were batch-purified by overnight immunoprecipitation with 50-µg antibody against the protein tag and 100 µl protein-agarose beads. After 4 washes in lysis buffer and 2 in phosphate-buffered saline, the immunoprecipitated protein was eluted twice with 100 µL of 0.1-M glycine (pH 3.5)

and immediately neutralised with 10× tris buffer saline (0.5-M tris and 1.2-M NaCl, pH 7.4).

For purification of GST-tagged recombinant proteins, lysis buffer was supplemented with 2-mM dithiothreitol. GST-tagged proteins were batch-purified upon 4 hours of immunoprecipitation with 200 µl glutathione-agarose beads (GE healthcare). After 4 washes in lysis buffer and 2 in PBS, the immunoprecipitated protein was eluted with 200 µl elution buffer. Purified proteins were further subjected to SDS-PAGE for purity evaluation and protein quantification against a BSA calibration curve.

3.14 Lipid overlay assay

PIP Strip (P6001), Membrane Lipid Strip (P6002), Membrane Lipid Array (P6003), PIP Array (P6100), and Sphingo Array (S6001) from Echelon Biosciences were used in this study. Membranes were incubated overnight with the protein of interest diluted in the same solution after saturation (3% bovine serum albumin and 0.1% Tween 20 in TBS buffer) in a final volume of 5mL. After four washes with TBS-T solution, the lipid-bound protein was identified after 1 hour incubation with the corresponding HRP-labeled anti-tag antibody, followed by four additional washes. Western Lightning Chemiluminescence Reagent Plus (Perkin Elmer) and a ChemiDoc imager were used to see and quantify detection antibodies (Bio-Rad). To optimize signal/noise, the instrument automatically evaluates saturation and auto-scaled photos.

3.15 Cova PIP plate (ELISA) Assay

Proteins of interest were diluted in TBS supplemented with 1% BSA (1 µg/mL in a final volume of 100 µL per well) and added to Cova PIP screening plates by Echelon Bioscience (specifically H-6203; H-6204), followed by overnight incubation with gentle agitation at 4°C. After 3 washes with TBS-T buffer, primary antibody anti-GST (1:1000 dilution in TBS + 1% BSA) was added and incubated at room temperature for 1 h with gentle agitation. Post-incubation, 3 washes with TBS-T buffer were performed before adding the secondary antibody (1:5000 dilution in TBS + 1% BSA) for 1 hour at room temperature on a plate shaker. After for 5 additional washes, the peroxidase substrate 3,3′,5,5′-Tetramethylbenzidine liquid substrate (TMB) was added in a volume of 100 µL per well and the reaction was then stopped by adding 50 µL per well of 0.5-M

H_2SO_4 when significant blue colour developed. Immediately after adding the stop solution, the absorbance was read with a Tecan Spark instrument plate reader at 450-nm wavelength.

3.16 aPKC activity assay

Protein kinase assays were performed using the PKCι Kinase Enzyme System, PKCζ Kinase Enzyme System, and ADP-Glo Kinase Assay kit by Promega. The reaction was performed in a final volume of 25 µL containing 5 µL of stock solution reaction buffer A supplemented with 2.5-µL DTT (final concentration 50 µM); 5-µL active full-length PKCι (final concentration 4 nM) and 5-µL active full-length PKCζ (final concentration 1 nM); 5 µL of CREBtide substrate stock solution; 2.5 µL of ATP (final concentration 50 µM); 2.5 µL of DMSO (10%); 2.5 µL of lipid activator (10×); or PS, PA, and PI(4)P (dissolved by sonication in MOPS; final concentration 50 µg/mL).

The assay was carried out in 96-well luminescent white plates by incubating the reaction mixture at 30 °C for 20 minutes. After this incubation period, the ADP-GloTM Reagent was added to simultaneously terminate the kinase reaction and deplete the remaining ATP. The plate was then incubated for 40 minutes at room temperature before adding 50 µL of Kinase Detection Reagent to convert ADP to ATP and incubated again for a further 30 minutes at room temperature. The luminescence of the 96-well reaction plate was finally read using the Tecan Spark 10 M Multimode Plate Reader. Controls were set up including all the assay components by replacing the enzyme with equal volume of water (negative control). Lipids were replaced with equal volume of MOPS (for both positive and negative controls).

3.17 Data processing and statistical analysis

Evaluation of all the in vitro assays across multiple treatments, DGK activity assays, homogenates activity assays, RICD assays, and gene expression assays were analysed by using either one-way ANOVA or two-way ANOVA with multiple comparisons correction using either GraphPad PRISM 9.0 or 9.4 software. Single treatments of lipidomic data were analysed with Student T-test using GraphPad PRISM software. Error bars are described in Figure legends as ± SEM or ± SD where appropriate. A single, double, triple, and four asterisks denote their significance of a p-value ≤ 0.05, ≤ 0.01, ≤ 0.001 and ≤ 0.0001 respectively in all experiments.

The binding spots obtained on membrane strips or arrays were acquired with the ChemiDoc imager and quantified by using Image lab 6.0 software (Bio-Rad). Data obtained from PIP arrays and membrane arrays were collected as Excel files and analysed using GraphPad Prism 9.0 software. We analysed our data using one-way ANOVA analysis with Dunnett's multiple comparisons for ELISA assays, and for kinase activation assays. For the kinase activation assays, we used two-way ANOVA with Dunnett's multiple comparisons.

4. RESULTS

The findings described in this section resulted from a collective effort which involved several researchers working both in University of Eastern Piedmont and University of Turin, and a number of internal collaborators working at the Center of Autoimmune and Allergic Diseases (CAAD) in Novara.

Their personal contribution to this thesis work is here briefly acknowledged:

- Previous results obtained by Dr. Suresh Velnati (post-doc in our biochemistry lab) were a starting point for my following work; specifically, the kinases activity assays and the RICD assays in WASp deprived cells, along with the setting for the investigation of IL-2 defects in WASp silenced cells. Also, his findings from lipid overlay assays during the aPKC study paved the way for the interaction studies and binding site identification that I performed followingly.
- I acknowledge Dr. Annamaria Antona (collaborator from biochemistry lab) for creating and providing us with the WASp shRNA and the control shRNA Jurkat cell lines, which were very useful tools to explore WASp role in the TCR-mediated DGKα inhibition.
- Experiments performed in double silencing to assess the effect of WASp/DGKα on IL-2 induction were complementary to our gene expression assays and were conducted by Prof. Graziani lab group (including Dr. Valeria Malacarne and Dr. Giulia Rossino) in University of Turin. Also, they further confirmed by PLA assays the endogenous WASp-DGKα interaction that I previously observed by immunoprecipitation assays in a different experimental system. Lastly, I want to acknowledge them for the supportive data discussion and suggestions during the paper revisions process.
- I acknowledge Dr. Manfredi and Dr. Beatrice Purghè for carrying out the lipidomic analysis of my samples in an effort to identify the DAG species modulated by WASp.
- Finally, I acknowledge Dr. Federico Girivetto, for performing the luminescent kinase assay in order to investigate the effects of PA and other lipids binding on aPKCs activity.

DGKα activity regulation by Wiskott-Aldrich syndrome protein

4.1 WASp is required for DGKα inhibition upon TCR activation

Previous works from our lab demonstrated that T cell co-stimulation with anti-CD3 and and CD28 antibodies results in a SAP-mediated inhibition of the DGKα activity [59]. However, since a direct SAP-DGKα interaction was not found, we started screening different SAP interacting proteins reported in literature to explore the molecular mechanism involved in SAP-mediated DGKα inhibition. Among them we found that, similarly to SAP, WASp is an adaptor protein tuning the TCR signalling which leads to cytokine production and RICD [67, 99]. Thus, we investigated whether WASp is involved in the signalling pathway triggered by TCR which leads to DGKα inhibition. Moreover, as we observed that TCR triggering with the sole strong agonist UCHT1 (CD3 clone antibody) is sufficient for DGKα inhibition, we used this condition in the following experiments.

Initially, we silenced WASp expression in Jurkat cells by lentiviral-mediated stable expression of a WASp-specific short hairpin RNA (shRNA). The silencing efficiency was verified regularly and we observed a reduced WASp mRNA expression of around 50% when compared to control shRNA (non-targeting shRNA) transduced Jurkat cells (Fig. 11C). After 15 minutes stimulation with UCHT1 antibody (10 μg/ml), we measured the enzymatic activity of immunoprecipitated DGKα in both Jurkat cells transduced with WASp shRNA and control shRNA. In line with our previous results, the enzyme activity was reduced by ~50% upon CD3 stimulation in control shRNA Jurkat cells, but this reduction was not observed in WASp shRNA Jurkat cells (Fig. 11A) indicating that WASp is necessary for the negative regulation of DGKα activity upon TCR stimulation. Moreover, in the same assays, western blot analysis demonstrated that DGKα protein content does not change upon TCR triggering in both Jurkat cell lines (Fig. 11B), showing that this regulation is not due to changes in DGKα protein amount.

To demonstrate that in these experiments DGKα protein is reproducibly immunoprecipitated we repeated the immunoprecipitation twice, in the same conditions. In Fig. 8D we show that DGKα is reproducibly immunoprecipitated independently of the cell type (control shRNA versus WASp shRNA) or stimulation (unstimulated condition versus UCHT1 10 μg/ml).

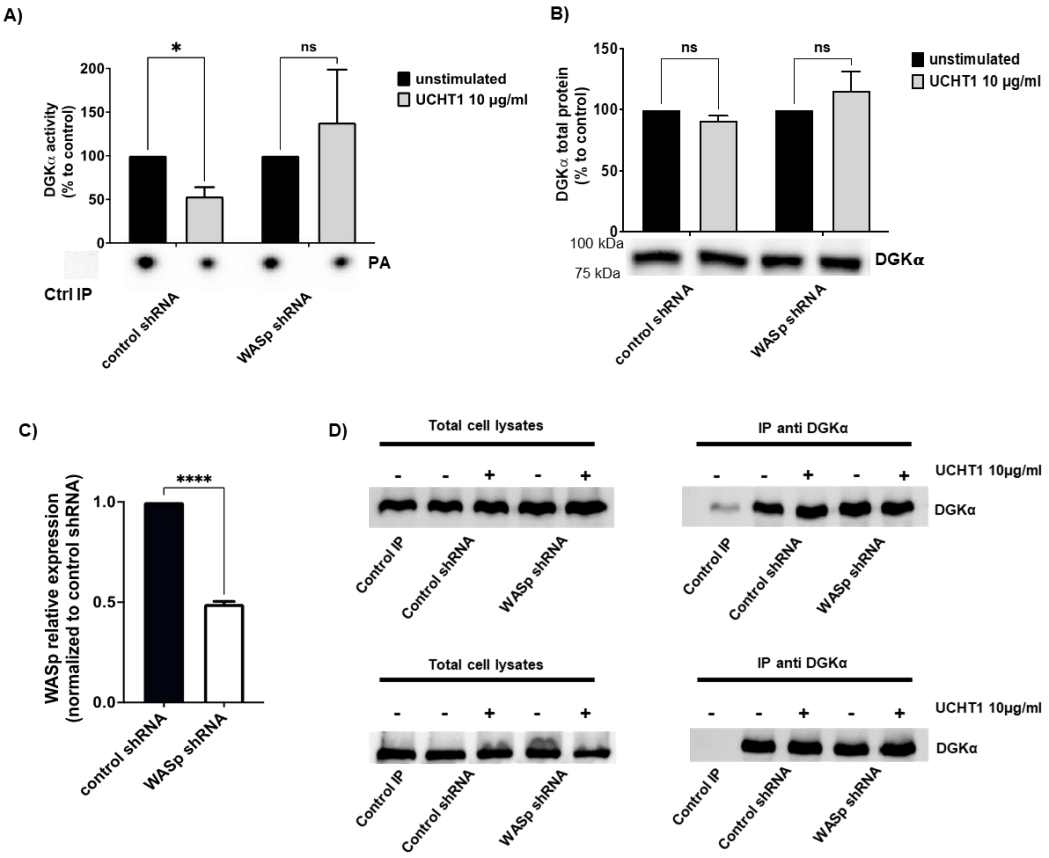

Figure 11: WASp is required for DGKα inhibition upon CD3 stimulation

Control shRNA and WASp shRNA Jurkat cells (3 x 10^7) were stimulated for 15 minutes with UCHT1 (10 µg/ml). Post-stimulation, cells were lysed and:

- **A)** immunoprecipitated with anti-DGKα antibody followed by DGK activity assays, the lower panel is a representative assay, upper panel is the mean ± SEM of 4 experiments normalized as the % of unstimulated cells.
- **B)** total cell lysates were analysed by western blotting with anti DGKα antibodies, the lower panel is a representative blot, upper panel is the mean ± SEM of 4 experiments normalized as the % of unstimulated cells.
- **C)** WASp mRNA levels were measured by qRT-PCR at 3 different timings during the experiments and shown as mean ± SEM using control shRNA as reference.
- **D)** immunoprecipitated with anti-DGKα antibody followed by western blotting with anti DGKα antibodies (left panel). The corresponding total cell lysates were subjected to western blot analysis with the same antibody (right panel). Two independent experiments are shown, indicating that DGKα immunoprecipitation is not affected by stimulation in both control shRNA and WASp shRNA Jurkat cells.

Since these data demonstrated that WASp is involved in the TCR-driven signalling cascade upstream DGKα, we checked whether WASp could promote this newly found DGKα inhibition in a direct manner. To verify this possibility, we co-transfected myc-DGKα with either FLAG-WASp or GFP control vector in 293T cells and measured DGKα activity at 48 hours post transfection using total cell homogenates. In this system, DGKα is overexpressed and the DGK activity was proportional to the amount of transfected DGKα and was distinguishable from the endogenous background (Fig. 12A). Notably, upon co-transfection with FLAG-WASp, the DGKα enzymatic activity was reduced by around 50% without any variation in DGKα protein amount (Fig. 12A and 12B). This observation indicates that WASp overexpression in 293T cells is sufficient to inhibit the DGKα activity without affecting its expression. We also noted that co-transfection with DGKα but not GFP control vector, strongly increases WASp protein levels (Fig. 12C) suggesting that the presence of DGKα may stabilize WASp similarly to what was previously observed for the WASp interacting protein (WIP) [100].

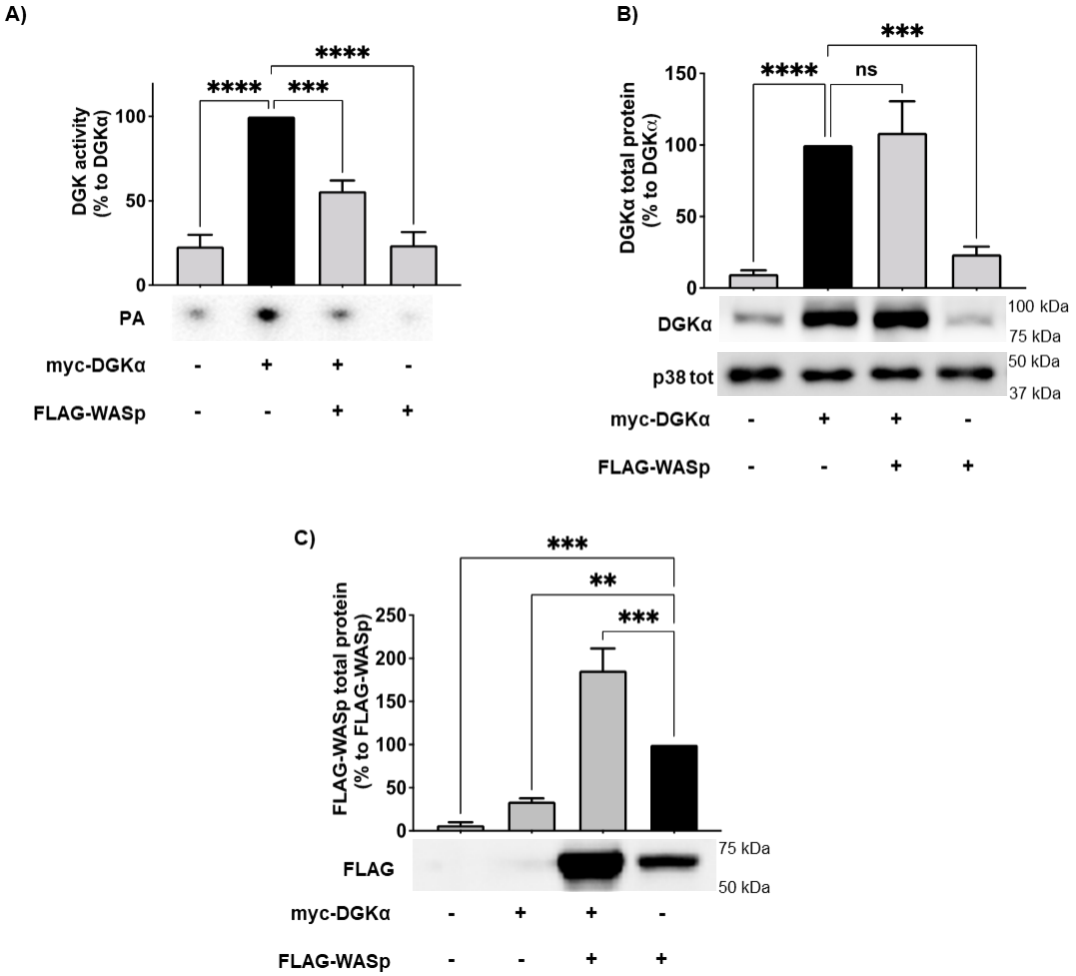

Figure 12: WASp overexpression inhibits DGKα activity

myc-DGKα and FLAG-WASp were transfected together or with GFP control vector in 293T-cells. 48 hours post-transfection, cells were collected, homogenized, and used in:

- **A)** DGK activity assays normalized considering DGKα overexpressed homogenates as control, the lower panel is a representative assay, upper panel is the mean ± SEM of 5 independent experiments.
- **B)** Quantifications of DGKα total protein as % of myc-DGKα transfected cells, the lower panel is a representative assay, upper panel is the mean ± SEM of 5 independent experiments.
- **C)** Quantifications of FLAG-WASp total protein as % of FLAG-WASp transfected cells, the lower panel is a representative assay, upper panel is the mean ± SEM of 5 independent experiments.

4.2 CDC42 does not directly influence DGKα activity

Being an adaptor signalling protein, WASp plays a key role in protein-protein interactions, and it has been reported that active WASp forms a complex with CDC42 protein [101]. Thus, we also explored the possibility of DGKα regulation by this small GTPase. To verify the involvement of CDC42 in DGKα inhibition, we co-transfected

myc-DGKα with the constitutively active myc-CDC42 Q61L. Differently from what was observed upon co-transfection with FLAG-WASp, in WASp absence the presence of active CDC42 did not affect DGKα enzymatic activity or protein level reinforcing its central role in the control of DGKα activity (Fig. 13).

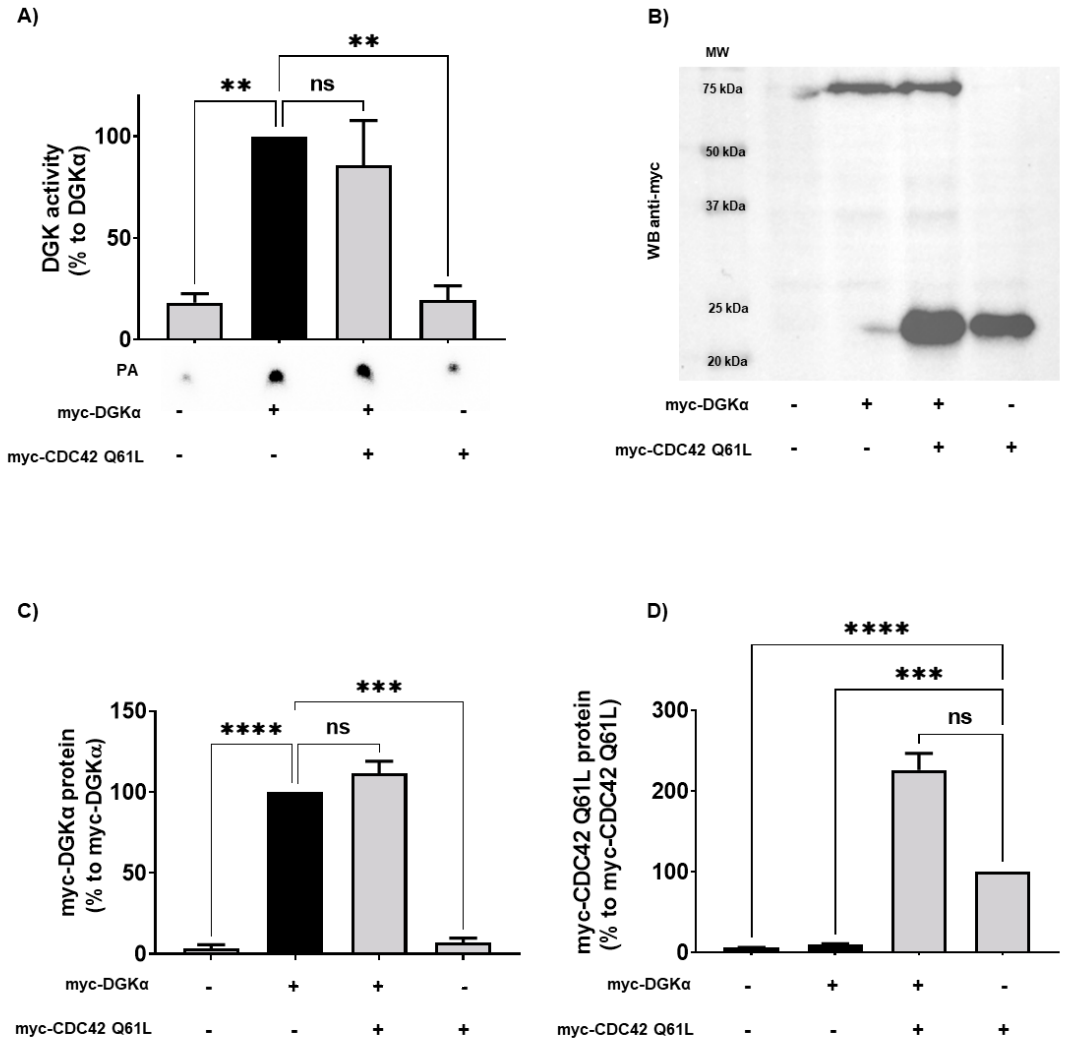

Figure 13: CDC42 Q61L overexpression does not inhibit DGKα

Myc-DGK**α** and myc-CDC42 Q61L were transfected either alone or together in 293T-cells. 48h post-transfection, cells were collected, homogenized and used in:

A) DGKα activity assays. A representative experiment is shown together with the mean ± SEM of 4 independent experiments.

B) A representative western blot using anti-myc antibody.

C) Quantification of myc-DGKα in the corresponding homogenates normalised for myc-DGKα single transfection at 100%

D) Quantification of myc-CDC42 Q61L in the corresponding homogenates normalised for myc-CDC42 Q61L single transfection at 100%.

4.3 WASp is relatively dispensable for ERK pathway activation and does not regulate the global DAG levels

TCR induction of the MAPK pathways is partially dependent on the DAG activation of the RasGRP1 [102]. To evaluate the DAG signalling in the absence of WASp, we assessed the phosphorylation status of ERK1/2 in the same samples analysed in Fig. 11. We observed a threefold increase in ERK1/2 phosphorylation upon UCHT1 treatment, which was not consistently influenced by WASp silencing (Fig. 14). Those data suggest that upon intense CD3 stimulation by UCHT1, WASp is relatively dispensable for TCR signalling on the ERK1/2 pathway. To directly evaluate the influence of WASp on T cell DAG levels, we used a targeted mass spectrometry approach to quantify the DAG species. Jurkat cells were stimulated for 15 minutes with OKT3 (1 μg/ml) and CD28.2 (1 μg/ml) antibodies, and by mass spectrometry analysis we detected a significant increase in selected DAG species (Fig. 15). However, we observed the same species also increased in WASp silenced cells upon CD3 + CD28 co-stimulation, suggesting that the DAG pool regulated by DGKα under WASp modulation is quantitatively small.

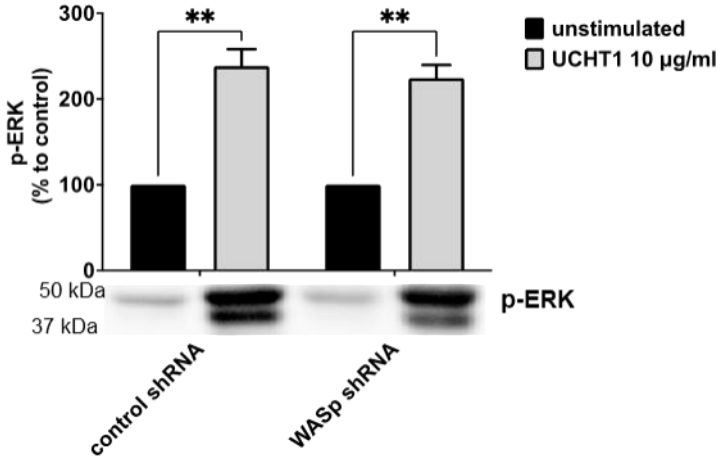

Figure 14: Control shRNA and WASp shRNA Jurkat cells (3 x 10^7) were stimulated with UCHT1 (10 μg/ml) for 15 minutes. Post-stimulation, cells were lysed and total cell lysates were analysed by western blotting with anti-pERK antibodies, the lower panel is a representative blot, upper panel is the mean ± SEM of 4 experiments normalized as the % of unstimulated cells.

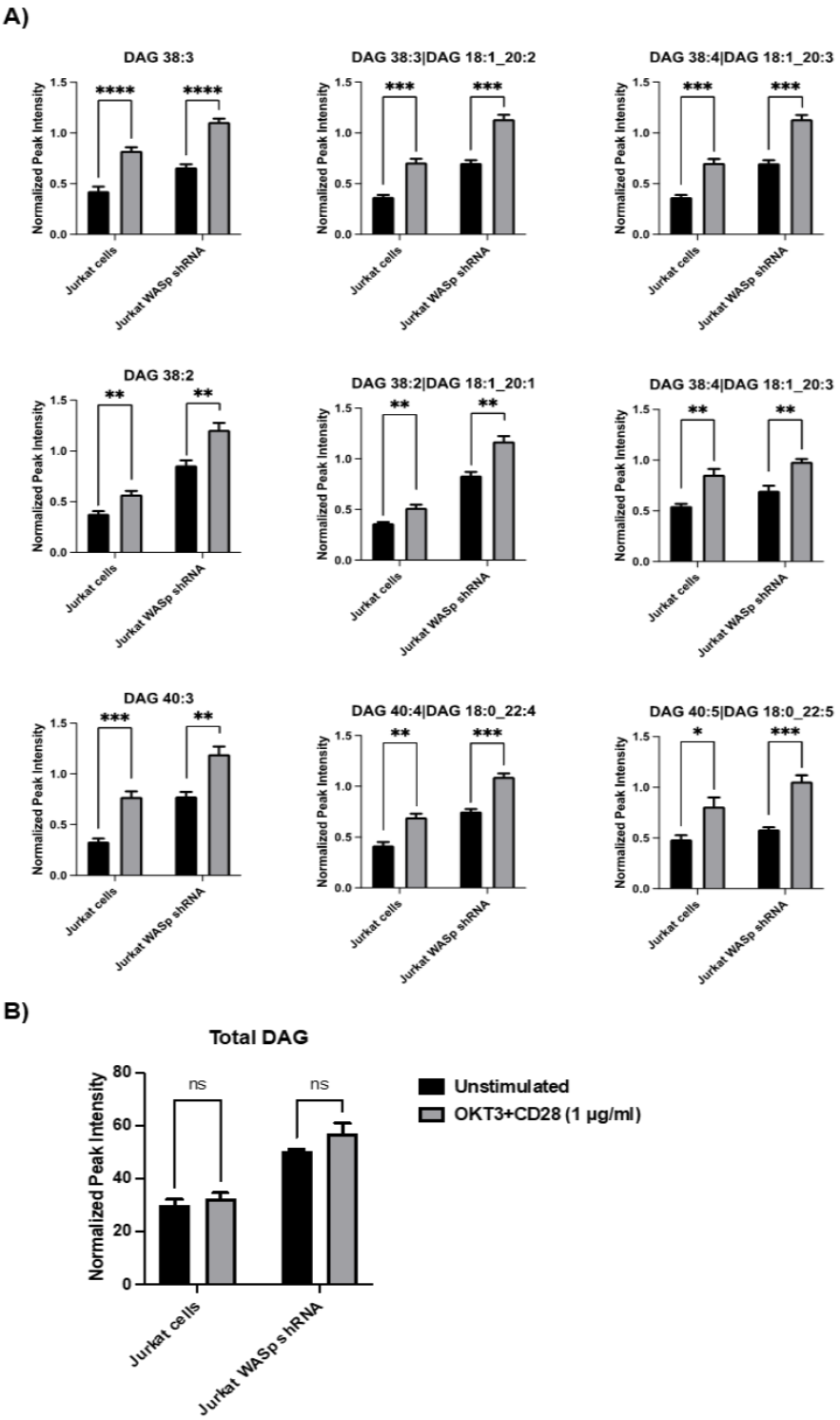

Figure 15: No significant differences were observed in DAG fluctuations between Jurkat cells and Jurkat WASp shRNA cells

A) Single DAG species modulation associated with Jurkat cells unstimulated *vs* stimulated (OKT3 + CD28, 1µg/ml) and Jurkat WASp shRNA unstimulated *vs* stimulated (OKT3 + CD28, 1µg/ml).

B) Total DAG fluctuations in Jurkat cells unstimulated vs stimulated (OKT3 + CD28, 1µg/ml) and Jurkat WASp shRNA unstimulated *vs* stimulated (OKT3 + CD28, 1µg/ml).

4.4 WASp interacts with DGKα associating in a complex

Since we observed a role for WASp in controlling DGKα activity, we set to investigate whether the two proteins may associate. Thus, to verify if the endogenous proteins are in close proximity in primary T cells, we performed a Proximity Ligation Assay (PLA). Several fluorescent spots were detected in both unstimulated and anti-CD3/CD28 stimulated cells; in contrast, no signals were generated where primary antibodies were missing (negative control) (Fig. 16A). Quantification of PLA events highlights the close association between DGKα and WASp, without a significant modulation driven by CD3-CD28 co-stimulation (Fig. 16B).

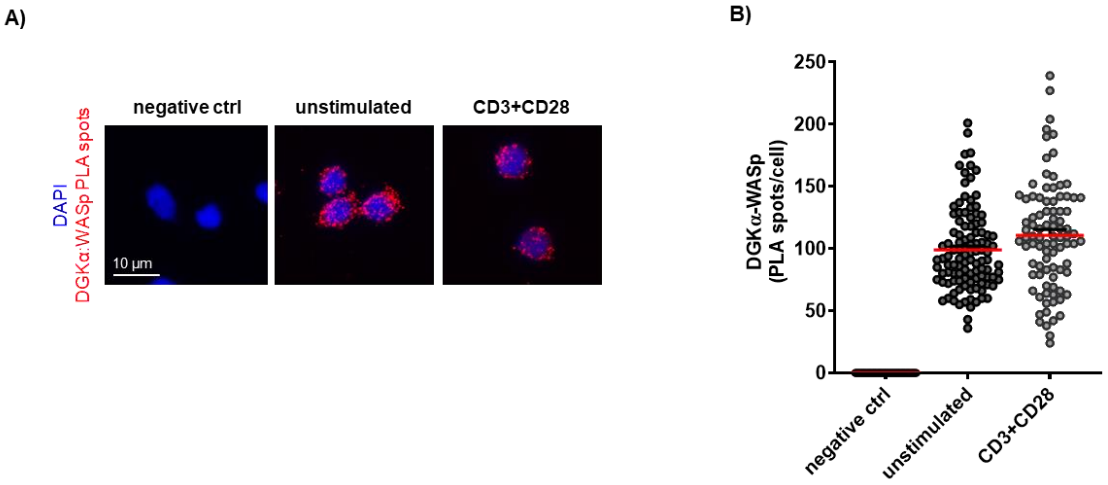

Figure 16: DGKα and WASp are close enough to associate in a complex

A) Isolated human PBLs were seeded on poly-L-lysine coated glasses and stimulated for 15 minutes with anti-CD3 (UCHT1 10 µg/ml) and anti-CD28 (CD28.2, 5 µg/ml) antibodies, fixed and permeabilized. PLA was performed to assess DGKα and WASp proximity, representative images are shown.

B) Quantification of the spots/cell resulting from PLA of two independent experiments are shown with mean ± SEM (n = 60 negative control; n = 109 unstimulated; n = 90 CD3+CD28).

In line with these results, to confirm the formation of a complex between DGKα and WASp, we co-expressed both the proteins in 293T cells and immunoprecipitated myc-DGKα and/or FLAG-WASp. The co-precipitation of the partner protein was verified by western blotting. We observed the presence of myc-DGKα in anti-FLAG immunoprecipitates when the two proteins were co-expressed, indicating the existence of a DGKα-WASp complex (Fig. 17A left side). We also detected FLAG-WASp

protein in the corresponding anti-myc immunoprecipitated lysate, as a further confirmation of this interaction (Fig. 17A right side). The input bands indicating equal transfection efficiency are shown in Fig. 17B.

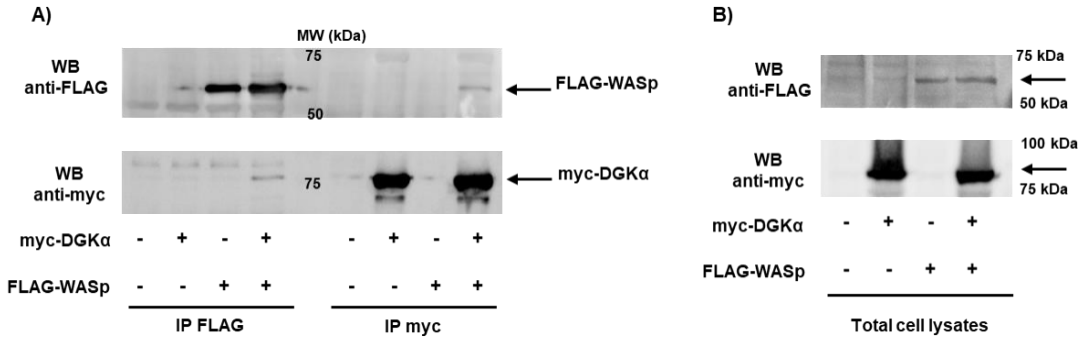

Figure 17: DGKα and WASp co-immunoprecipitate

A) Myc-DGKα and FLAG-WASp were co-expressed in 293T cells. After 48 hours lysates were immunoprecipitated with either anti-FLAG (left side) or anti-myc (right side) antibodies. Immunoprecipitated proteins were analysed by western blotting with anti-FLAG antibody followed by anti-myc antibody after stripping..A representative experiment is shown out of 3.

B) Total cell lysates from experiments shown in C.

Moreover, to explore this DGKα-WASp complex formation and to identify their protein binding site, we performed the same immunoprecipitation assays using a series of DGKα and WASp deletion mutants (Fig. 18A and Fig. 19A). Initially, we used the myc-DGKα-L360* mutant, which lacks the C-terminal catalytic region [96]. Our results (Fig. 18B) demonstrate that this DGKα mutant retains the ability to bind WASp, indicating that WASp-DGKα interaction is mediated by the N-terminal DGKα regulatory domain. Thus, we produced the GST-DGKα E86* mutant maintaining the sole recoverin homology domain of DGKα. As expected, glutathione beads pulled down GST-DGKα wt and the associated FLAG-WASp confirming the interaction between the two. The observation that also the GST-DGKα E86* mutant pulled down FLAG-WASp indicates a role of the N-terminal recoverin homology domain of DGKα in this complex (Fig. 18C). To further verify the specificity of this interaction, we repeated the co-immunoprecipitation assay with the highly homologous HA-DGKγ. We observed that the amount of HA-DGKγ immunoprecipitated by anti-FLAG antibodies depends on its overexpression but not by the presence of FLAG-WASp. Those data suggest that this isoform does not associate with FLAG-WASp (Fig. 18D).

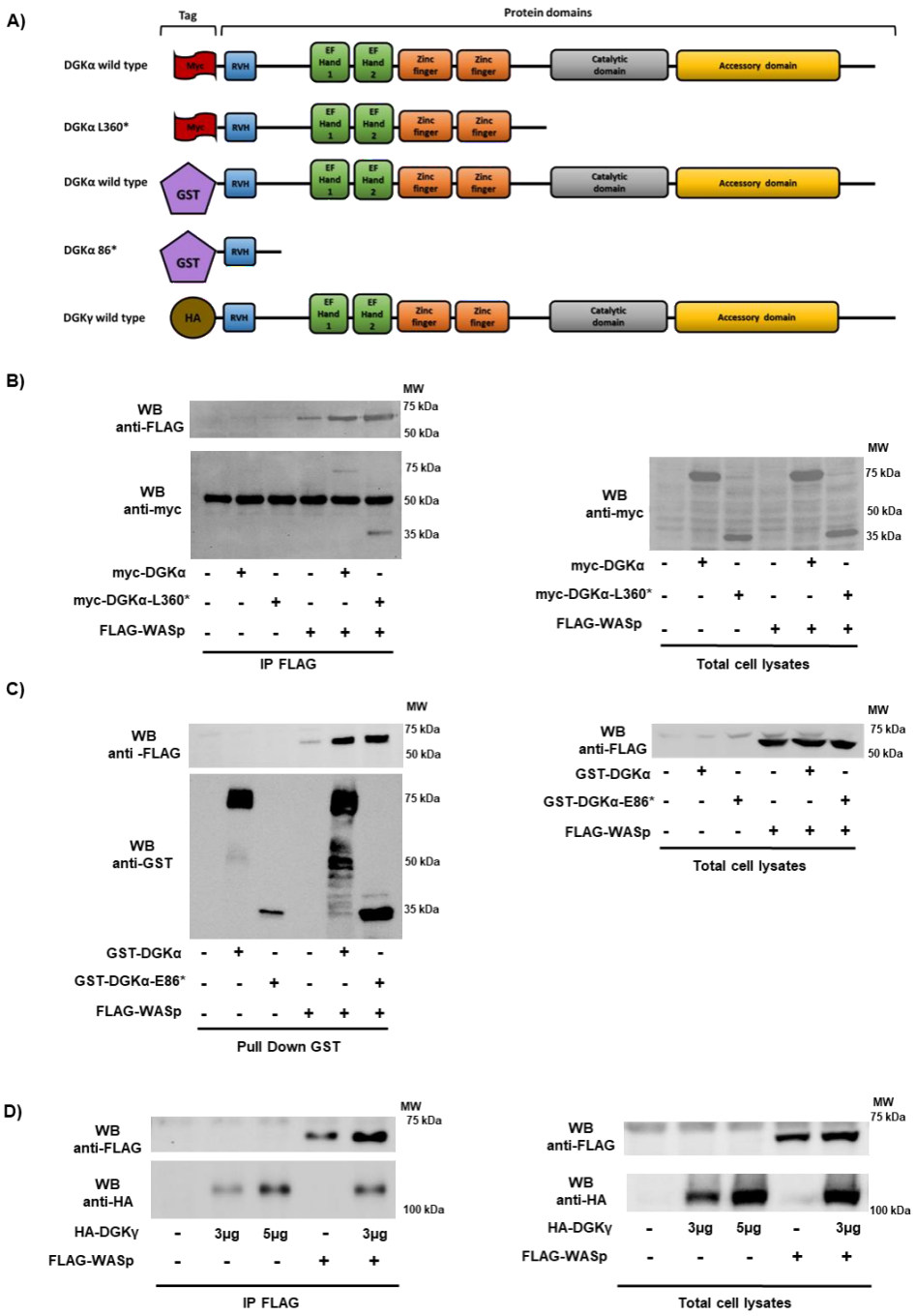

Figure 18: DGKα binds to WASp through the recoverin homology domain

HEK 293-T cells were co-transfected with the indicated plasmids. 48 hours later, proteins were immunoprecipitated with anti-FLAG (B and D) or anti-GST antibody (C) and subsequently analysed by western blotting.

A) DGKα and DGKγ constructs used with domains and tags highlighted.

B) Interaction between FLAG-WASp and myc-DGKα WT or myc-DGKα-L360* deletion mutant and the corresponding total cell lysates.

C) Interaction between FLAG-WASp and GST-DGKα or GST-DGKα-E86* deletion mutant and the corresponding total cell lysates.

D) Interaction between FLAG-WASp and HA-DGKγ and the corresponding total cell lysates.

Conversely, we produced the FLAG-tagged WASp Q297* mutant lacking the C-terminal proline-rich and VCA domains and the WASp K232* mutant retaining the sole WH1 domain. The observation that similar amounts of myc-DGKα wt co-immunoprecipitated with FLAG-WASp wt and the two deletion mutants indicate the role of the WH1 domain in the formation of the complex with DGKα (Fig. 19B).

Lastly, to investigate the specificity of this interaction we tested the interaction between myc-DGKα and myc-FLAG-N-WASp a closely related WASp homologue featuring non-redundant functions. The immunoprecipitation with the anti-FLAG antibody revealed that myc-DGKα co-immunoprecipitates specifically with FLAG-WASp but not with myc-FLAG-N-WASp even if the latter is far more expressed (Fig. 19C). This indicates a selectivity for WASp in the interaction with DGKα.

Taken together these data demonstrate that *in vitro* DGKα and WASp can associate selectively by forming a stable complex mediated by WASp WH1 domain and DGKα recoverin homology domain. Here in, WASp inhibits DGKα enzymatic activity putatively impairing the shift to the active conformation for which the recoverin homology domain is required [103].

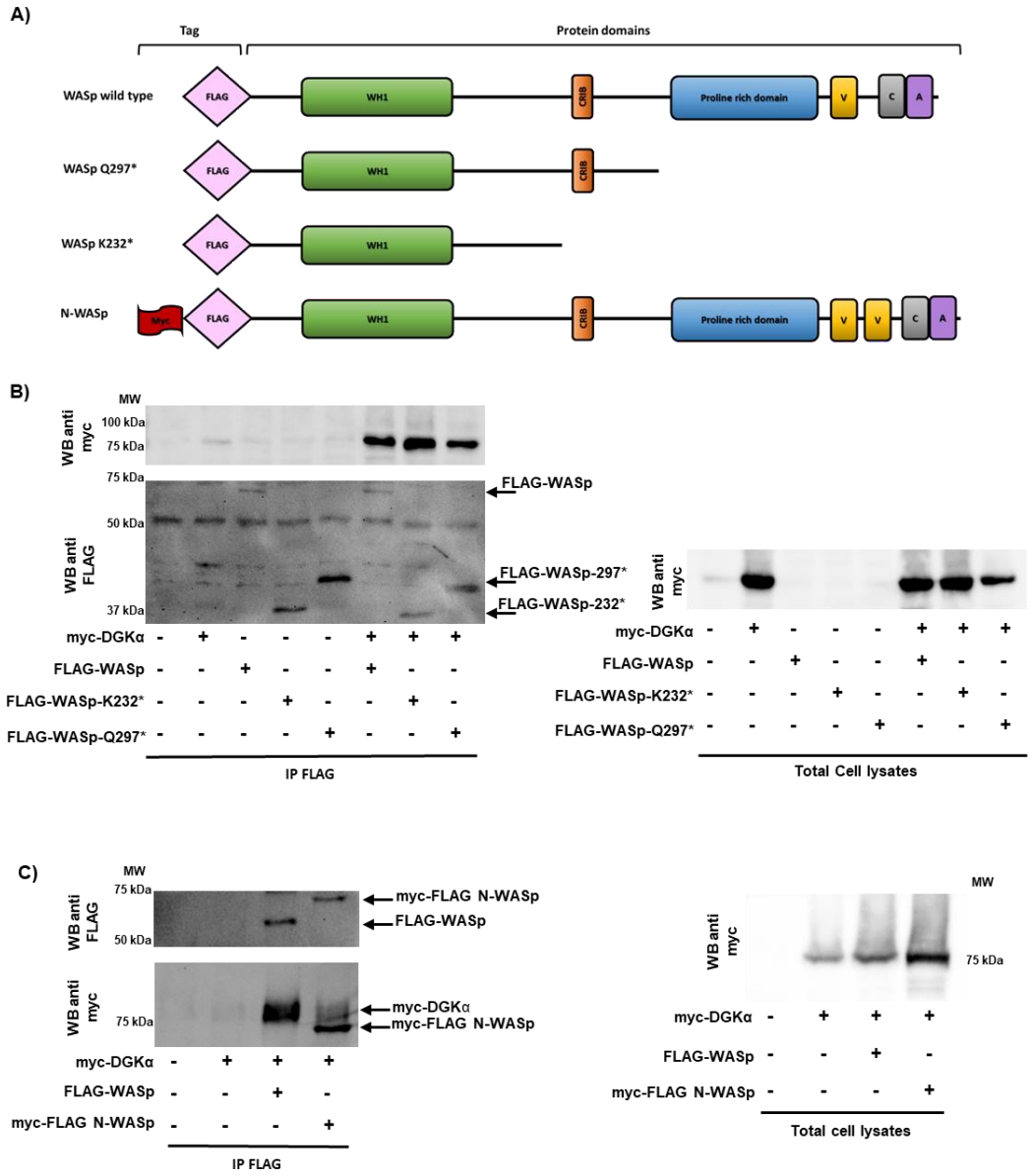

Figure 19: WASp interacts with DGKα through the WH1 domain while N-WASp does not bind.

HEK 293-T cells were co-transfected with the indicated plasmids. 48 hours later, proteins were immunoprecipitated with anti-FLAG antibody and subsequently analysed by western blotting.

A) WASP constructs used with domains and tags highlighted.

B) Interaction between myc-DGKα and FLAG-WASp or FLAG-WASp deletion mutants (FLAG-WASp K232* and FLAG-WASp Q297*) and the corresponding total cell lysates.

C) Interaction between FLAG-WASp or myc-FLAG N-WASp with myc-DGKα WT and the corresponding total cell lysates.

4.5 DGKα silencing or inhibition rescues IL-2 expression in WASp deficient T cells

DGKα inhibition is known to enhance TCR-promoted induction of IL-2 [27]. Moreover, the lack of DGKα inhibition in SAP deficient cells drives defective cytokine induction and RICD, which are rescued by the DGKα inhibition [51, 58]. Since a similar defect in RICD and IL-2 induction is present in murine WASp deficient cells [67, 104] we evaluated the effect of DGKα inhibition on RICD, TCR signalling potency, and IL-2 production in WASp deficient human primary lymphocytes. We silenced WASp in activated primary peripheral blood T lymphocytes (PBLs) using specific siRNA. To assess WASp silencing, WASp mRNA levels were evaluated in all the experiments. At 4 days post silencing, we observed 80% reduction of WASp mRNA (Fig. 21B).

To evaluate the effect on RICD, we re-stimulated control, WASp, and SAP silenced cells with increasing concentrations of anti-CD3 antibody (OKT3 from 0 to 100 ng/ml for 24 hours). We pre-treated all the cells with either vehicle (DMSO) or the DGKα-specific inhibitor AMB639752 (10 μM, 30 minutes). In line with our previous work [105], SAP deficiency reduced RICD, and this defect was partially compensated by AMB639752 treatment, which conversely did not affect RICD in control cells. In those experimental conditions, human PBLs silenced for WASp feature a normal RICD (Fig. 20A). In WASp silenced cells we also evaluated TCR signalling outputs co-stimulating CD3 and CD28, notably NR4A1, FASLG and cFOS were robustly induced but were not affected by either WASp silencing or AMB639752 treatment (Fig. 20B, 20C and 20D). In line with previous results on DAG signalling, those data suggest that WASp is less relevant for TCR signalling potency and RICD onset than SAP and that loss of the WASp inhibitory signalling on DGKα is not sufficient for the onset of apoptosis resistance.

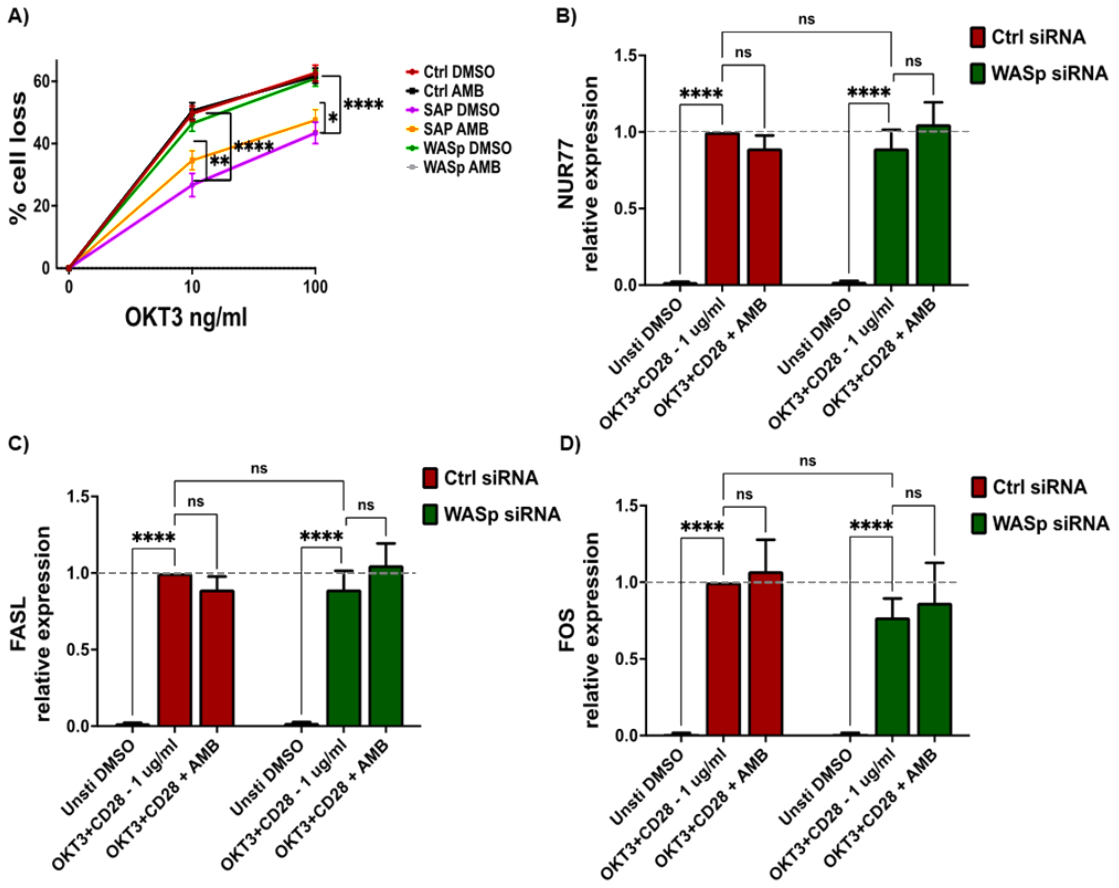

Figure 20: WASp deficiency neither affects RICD nor NUR77, FASLG or FOS expression

Activated lymphocytes from healthy donors were transfected using the indicated siRNA's and after 4 days cells were restimulated with: A) increasing concentrations of OKT3 for 24 hours either in the presence or absence of specific DGKα inhibitor (AMB639752 – 10 µM) and the % of cell loss was evaluated by FACS using PI staining to evaluate RICD. Data are the mean ± SEM of 14 experiments from 9 individual healthy donors. OKT3 (1 µg/ml) and CD28 (1 µg/ml) for 4 hours in the presence or absence of DGKα inhibitor (AMB639752 – 10 µM) followed by quantitative rt-PCR gene expression analysis to verify NUR77 B), FASL C) and FOS D). Data are the mean ± SEM of at least 4 experiments from 4 individual healthy donors.

A different picture emerges when measuring IL-2 mRNA in the same setting. In accordance with previous reports [27, 59], DGKα silencing or inhibition potentiated IL-2 induction upon co-stimulation of CD3 and CD28 of control cells indicating the importance of DGKα enzymatic activity (Fig. 21). siRNA-mediated WASp silencing resulted in a significant decrease in IL-2 induction by TCR, indicating the key role of WASp in regulation IL-2 induction. Moreover, the observation that AMB639752 treatment fully restored IL-2 induction defect (Fig. 21) suggests the relevance of WASp-mediated DGKα activity inhibition in this signalling. Notably, similar results

were obtained in the same experimental setting using a siRNA mediated DGKα silencing instead of pharmacological inhibition (data not shown).

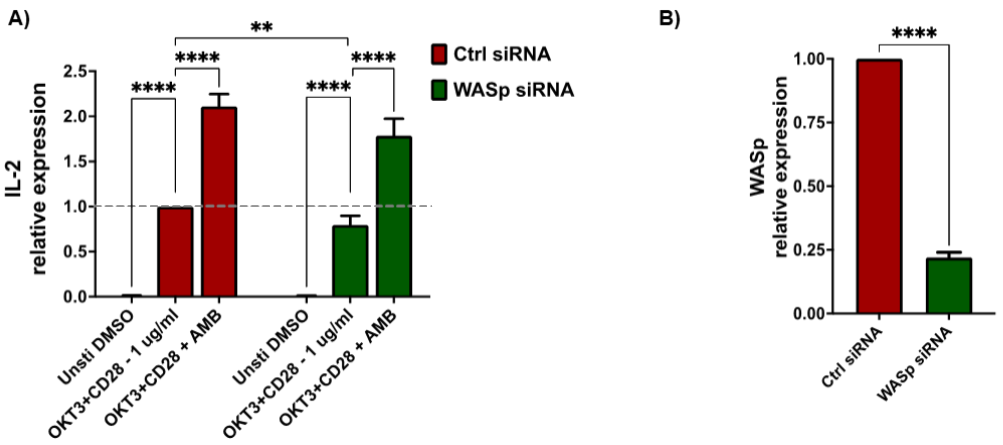

Figure 21: DGKα silencing or pharmacological inhibition rescues IL-2 defects in WASp deficient lymphocytes

A) Activated lymphocytes from healthy donors were transfected using ctrl siRNAs or WASp siRNAs. After 4 days, transfected cells were restimulated using both OKT3 (1 µg/ml) and CD28.2 (1 µg/ml) for 4 hours in the presence or absence of the DGKα specific inhibitor (AMB639752 - 10 µM), followed by quantitative rt-PCR gene expression analysis to verify IL-2 expression. Data are the mean ± SEM of 10 experiments performed in triplicates from 10 individual healthy donors.

B) Quantitative rt-PCR gene expression analysis of WASp mRNA in the experiments shown in A.

These observations imply that WASp-mediated inhibition of DGKα selectively regulates IL-2 gene expression without affecting the TCR signalling potency. In WASp absence DGKα is active, and its activity reduces IL-2 induction while TCR proapoptotic signalling is not influenced. This is different from what was observed with SAP silencing which reduces both IL-2 induction and RICD suggesting that the WASp-DGKα axis is only a branch of the numerous SAP-dependent signalling pathways.

4.6 CDC42 deficiency reduces IL-2 expression in T cells and this defect is rescued by DGKα inhibition

To further investigate the role of SAP signalling in the control of IL-2 induction, we silenced selected SAP effectors and measured IL-2 induction.

CDC42 is not only a key regulator of the WASp activity [101] but also a crucial SAP effector in the T cells [61]. Thus, to verify its involvement in this signalling pathway,

CDC42 was silenced in primary lymphocytes resulting in a 75% reduction of CDC42 mRNA 4 days after electroporation. After 4 days cells were restimulated, and quantitative rt-PCR revealed a consistent reduction of IL-2 induction by CD3 and CD28 co-stimulation in CDC42 silenced cells. When DGKα was inhibited in AMB639752 pre-treated cells, we observed potentiation of IL-2 induction in control cells and a full rescue in CDC42 silenced cells, in line with the major role of CDC42 as a WASp-DGKα pathway regulator (Fig. 22). Moreover, this set of experiments was also replicated replacing the treatment with AMB639752 with a siRNA mediated DGKα silencing, obtaining similar results (data not shown).

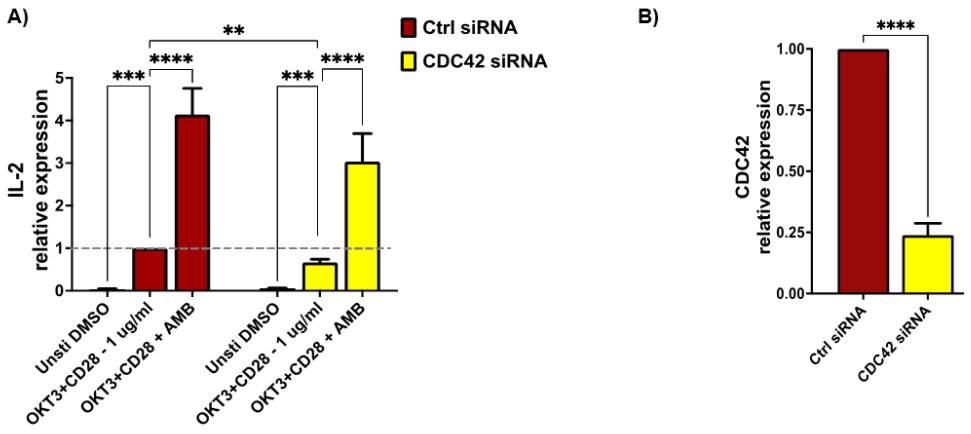

Figure 22: DGKα silencing or pharmacological inhibition rescues IL-2 defects in CDC42 deficient lymphocytes

A) Activated lymphocytes from healthy donors were transfected using ctrl siRNAs or CDC42 siRNAs. After 4 days, transfected cells were restimulated using both OKT3 (1 µg/ml) and CD28.2 (1 µg/ml) for 4 hours in the presence or absence of the DGKα specific inhibitor (AMB639752 - 10 µM), followed by quantitative rt-PCR gene expression analysis to verify IL-2 expression. Data are the mean ± SEM of 8 experiments performed in triplicates from 6 individual healthy donors.

B) Quantitative rt-PCR gene expression analysis of CDC42 mRNA in the experiments shown in A.

4.7 NCK-1 deficiency decreases IL-2 expression in T cells and this defect is compensated by DGKα inhibition

NCK-1 is a binding partner for SAP and a direct regulator of TCR signalling along with the T cell proliferation [62]. Interestingly, NCK-1 is also a WASp interactor, involved in WASp recruitment and activation at the TCR [63]. Thus, we speculated that the NCK-1 adaptor could represent a crucial scaffold protein in this signalling pathway.

To verify this hypothesis, we silenced NCK-1 expression in PBLs resulting in a 50% reduction of NCK-1 mRNA 4 days after electroporation (Fig. 23B). Then, 72 hours post silencing we measured IL-2 induction in presence or absence of AMB639752 and we observed that IL-2 induction was reduced upon NCK-1 silencing and rescued by DGKα inhibition (Fig. 23A). A similar trend was observed with DGKα silencing: the reduction in IL-2 expression was compensated by a strong IL-2 induction upon DGKα silencing (Data not shown). However, in co-silencing experiments, the reduction of IL-2 upon NCK-1 silencing strived to reach statistical significance, this may be due to the residual NCK-1 protein that may still play its function (data not shown). Alternatively, other SAP effectors may participate in this pathway and compensate for NCK-1 absence.
Altogether these experiments indicate that CDC42 and NCK-1 contribute to the SAP signalling network controlling WASp and DGKα activity.

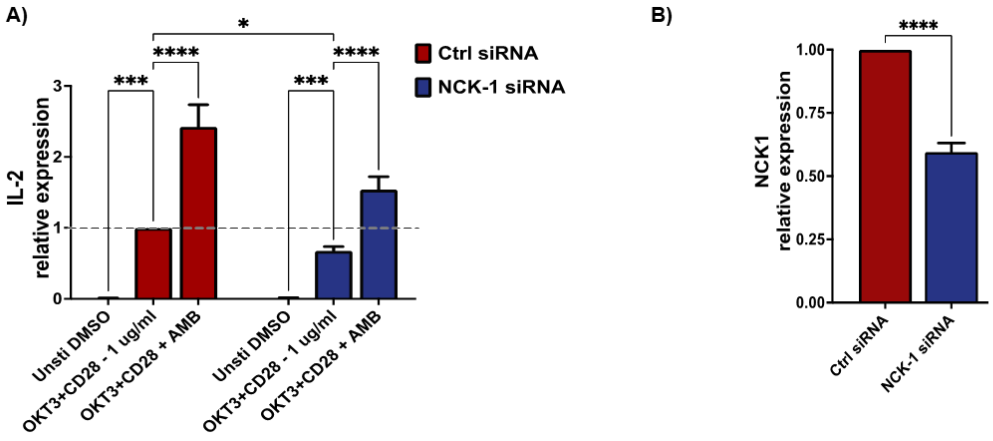

Figure 23: DGKα silencing or pharmacological inhibition potentiates IL-2 expression in NCK-1 deficient lymphocytes

A) Activated lymphocytes from healthy donors were transfected using ctrl siRNAs or NCK-1 siRNAs. After 4 days, transfected cells were restimulated using both OKT3 (1 µg/ml) and CD28.2 (1 µg/ml) for 4 hours in the presence or absence of the DGKα specific inhibitor (AMB639752 - 10 µM), followed by quantitative rt-PCR gene expression analysis to verify IL-2 expression. Data are the mean ± SEM of 6 experiments from 6 individual healthy donors for gene expression analysis and all experiments were performed in triplicates.

B) NCK-1 mRNA in the experiments shown in E was measured by quantitative rt-PCR gene expression analysis.

4.8 ARP2/3 activity is not required for IL-2 regulation by the WASp-DGKα complex

The CDC42-WASp signalling axis is a well-known regulator of actin branching polymerization through the ARP2/3 complex. To explore the role of the ARP2/3 complex in IL-2 induction by the TCR, PBLs were activated, cultured for 3 weeks, and pre-treated with ARP2/3 inhibitor CK666 at a concentration of 60 µM before restimulation (OKT3 1 µg/ml, CD28.2 1 µg/ml, 4 hours). When we measured IL-2 induction we observed a normal induction by the TCR and potentiation by the DGKα inhibitor AMB639752 (10 µM). These results indicate that ARP2/3 is dispensable for the signalling pathway that controls IL-2 induction downstream to CDC42/WASp/DGKα (Fig. 24).

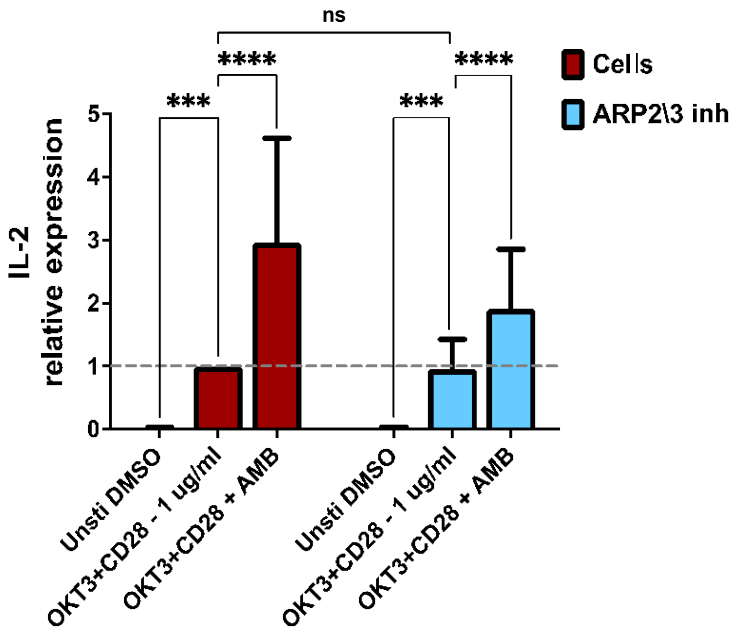

Figure 24: ARP2/3 inhibition has no effect on IL-2 expression

Activated lymphocytes from healthy donors were treated with ARP2/3 inhibitor (CK666 – 60 µM) for 30 minutes and restimulated with OKT3 (1 µg/ml) and CD28 (1 µg/ml) for 4 hours in the presence or absence of DGKα inhibitor (AMB639752 – 10 µM) followed by quantitative rt-PCR gene expression analysis to verify IL-2 expression. Data are the mean ± SEM of 9 experiments from 6 healthy donors.

aPKCs binding and activity regulation by PA and other phospholipids

4.9 Both aPKC isoforms bind to PA and PS, while PKCι binds selectively also to phosphatidylinositol monophosphates

Firstly, we test human FLAG-PKCζ (purified by in-house immunoprecipitation) and highly purified homologous human PKCι (commercial preparation) against the key signaling lipids found in cell membranes. Specifically, 100 pmol of eight phosphoinositides have been spotted on a lipid PIP strip P-6001 (PI, PI(3)P, PI(4)P, PI (5)P, PI(3,4)P2, PI(3,5)P2, PI(4,5)P2, and PI(3,4,5)P3) along with seven other biologically important lipids (lysophosphatidic acid (LPA), lysophosphocoline (LPC), phosphatidylethanolamine (PE), phosphatidylcholine (PC), S1P, PA, and PS).

As expected, the results obtained confirmed the previously described interaction of both aPKC isoforms with PA and PS [89], and interestingly in this assay we found that PKCι also specifically binds to phosphatidylinositol monophosphates (PIPs, e.g., PI(3)P, PI(4)P, and PI(5)P), independently of the phosphorylation position. Surprisingly, PKCι neither binds to the phosphatidylinositol diphosphates nor triphosphates, suggesting a very selective mechanism of interaction (Figure. 25A and 25B).

At this point, to measure the relative affinity for PA and PS, we spotted with DAG, PA, PS, PI, PE, PC, phosphatidylglycerol (PG), and sphingomyelin (SM) the lipid array membrane P-6003 in a concentration gradient (from 100 to 1.56 pmol). As result, we observed the presence of selective and comparable binding to PS and PA in both the aPKCs isoforms (Fig. 25C and Fig. 25D). Interestingly, we found that PKCζ show a very mild interaction also to PG (Figure 25C), while PKCι exhibits a modest binding to sulfatide (SM4), which, however, could be due to its structural similarity in charge and dimensions to PIPs (data not shown).

Furthermore, to investigate more in deep PKCι relative affinity to PIPs, we utilized a PIP array P-6100 by Echelon bioscience previously spotted with all eight phosphoinositides, in a concentration gradient. Specifically, in this study we used i.e., PI, PI(3)P, PI(4)P, PI(5)P, PI(3,4)P2, PI(3,5)P2, PI(4,5)P2, and PI(3,4,5)P3. We confirmed the binding to phosphatidylinositol monophosphates and a lack of selectivity for the phosphate position in the PIPs, since purified FLAG-PKCι binds to PI(3)P, PI(4)P, and PI(5)P in comparable levels (Figure 25E).

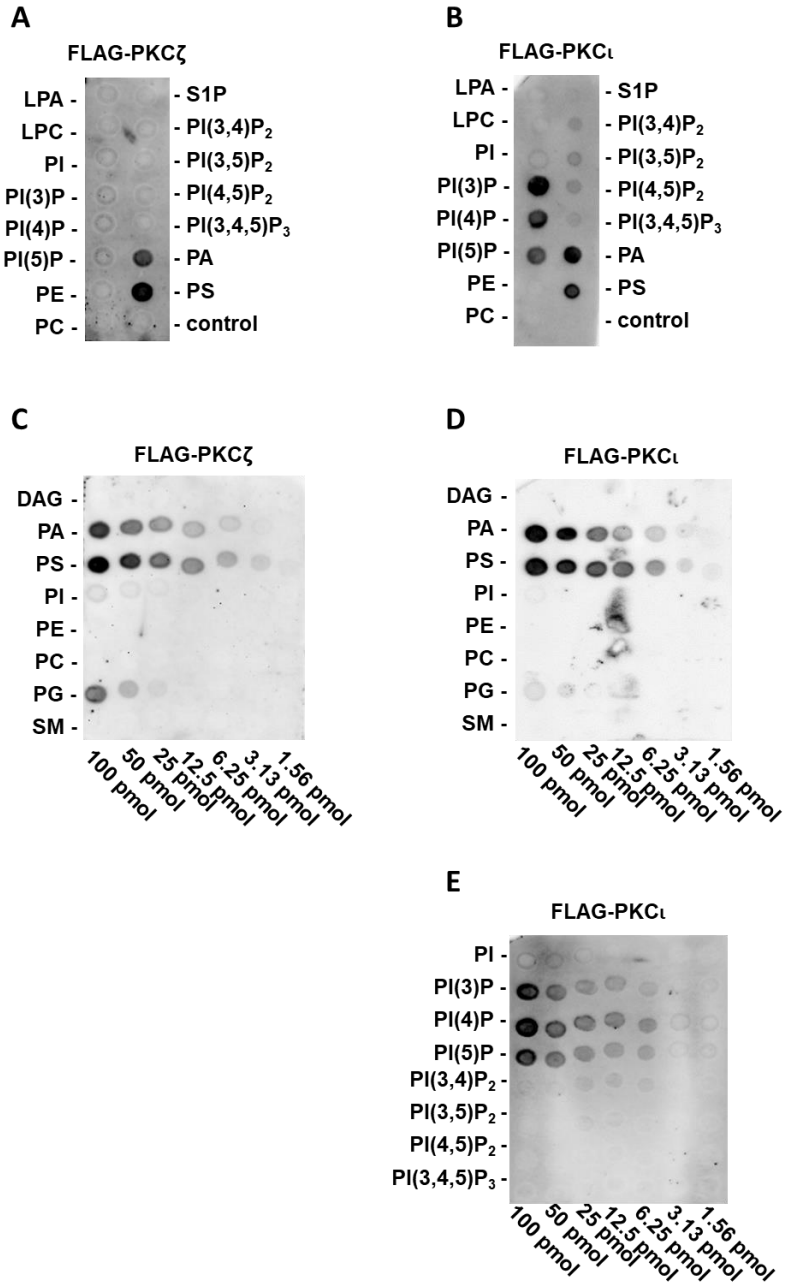

Figure 25: aPKC selectively binds PA and PS, while PKCι binds also to PIPs

(**A**) Batch purified FLAG-PKCζ was incubated with a PIP strip overnight, and after washing detected with anti-FLAG antibody. A representative experiment out of three performed is shown. (**B**) Highly purified FLAG-PKCι was incubated with a PIP strip overnight and, after washing, detected with anti-FLAG antibody. (**C**) Batch purified with FLAG-PKCζ was incubated with a membrane lipid array overnight and, after washing, detected with anti-FLAG antibody. (**D**) Highly purified FLAG-PKCι was incubated with a membrane lipid array overnight and, after washing, detected with anti-FLAG antibody (**E**) Highly purified FLAG-PKCι was incubated with a PIP array overnight and after, washing detected, with anti-FLAG antibody. DAG: diacylglycerol, PE: phosphatidylethanolamine, PC: phosphatidylcholine, SM: sphingomyelin, PKC: protein kinase C, LPA: lysophosphatidic acid, LPC: lysophosphocoline, S: sphingosine, S1P: sphingosine-1-phosphate, PI: phosphatidylinositol, PG: phosphatidylglycerol.

4.10 PKCι binds to PI(3)P and PI(4)P through the catalytic domain

Considering these data from lipid overlay assays, at this point we wanted to identify the specific binding site in the aPKC domains, thus, we performed an enzyme-linked immunosorbent assay (ELISA) using Cova PIP screening plates, previously precoated with 20 nmols of either PI(3)P or PI(4)P per well, pre-blocked and ready for the adding the proteins. On those plates, we tested in-house purified GST-tagged full-length aPKCs and their corresponding deletion mutants. As negative control we used the same concentrations of purified GST. Following, we measured their binding using anti-GST antibodies. A description of the constructs used in this study is reported in Fig. 26A [97]. The GST alone used as negative control shown no detectable binding. Vice versa, the PKCι isoform strongly interact with both PI(3)P and PI(4)P, in line with our previous results. Conversely, PKCζ did not bind either to PI(3)P or PI(4)P (Fig. 26B and 26C). Those data show that, the binding of PKCι to PIPs is isoform-specific and does not require the presence of additional proteins. Furthermore, all the deletion mutant of PKCι gave some detectable binding to both PI(3)P and PI(4)P, suggesting that the lipid binding takes place putatively in the catalytic domain (CD), since it is the only common domain shared in all those truncated proteins. On the other hand, we observed an increased binding signal towards PI(3)P and PI(4)P when using the PKCι PSR. Indeed, the PSR is a polybasic domain, with higher number of Arg and Lys residues, which confers to the protein the ability to bind directly the phosphoinositiede such as PI(4)P but is hidden when the protein is not involved in interactions with PAR-6 [106]. It may be possible that removing the PB1 region makes the PSR domain more available to the electrostatic interactions with the lipids, giving a stronger binding when compared to the full-length protein. Furthermore, we observed a strong interaction with both PI(3)P and PI(4)P to PKCζ CD, a deletion mutant lacking the N-terminal PB1, PSR, and C1 domains. Interestingly, the full-length PKCζ did not bind (Fig. 26D and 26E), indicating that the N-terminal domains inhibited the binding and that the PI(3)P and PI(4)P interacting region is localized within evolutionarily conserved regions in the CD region of PKCζ and PKCι. Overall, these data demonstrate that full-length PKCι readily binds selectively to PI(3)P and PI(4)P, while the CD appears as a primary binding site for phosphatidylinositol monophosphates. In PKCζ, this binding is masked by the presence of N-terminal regulatory domains.

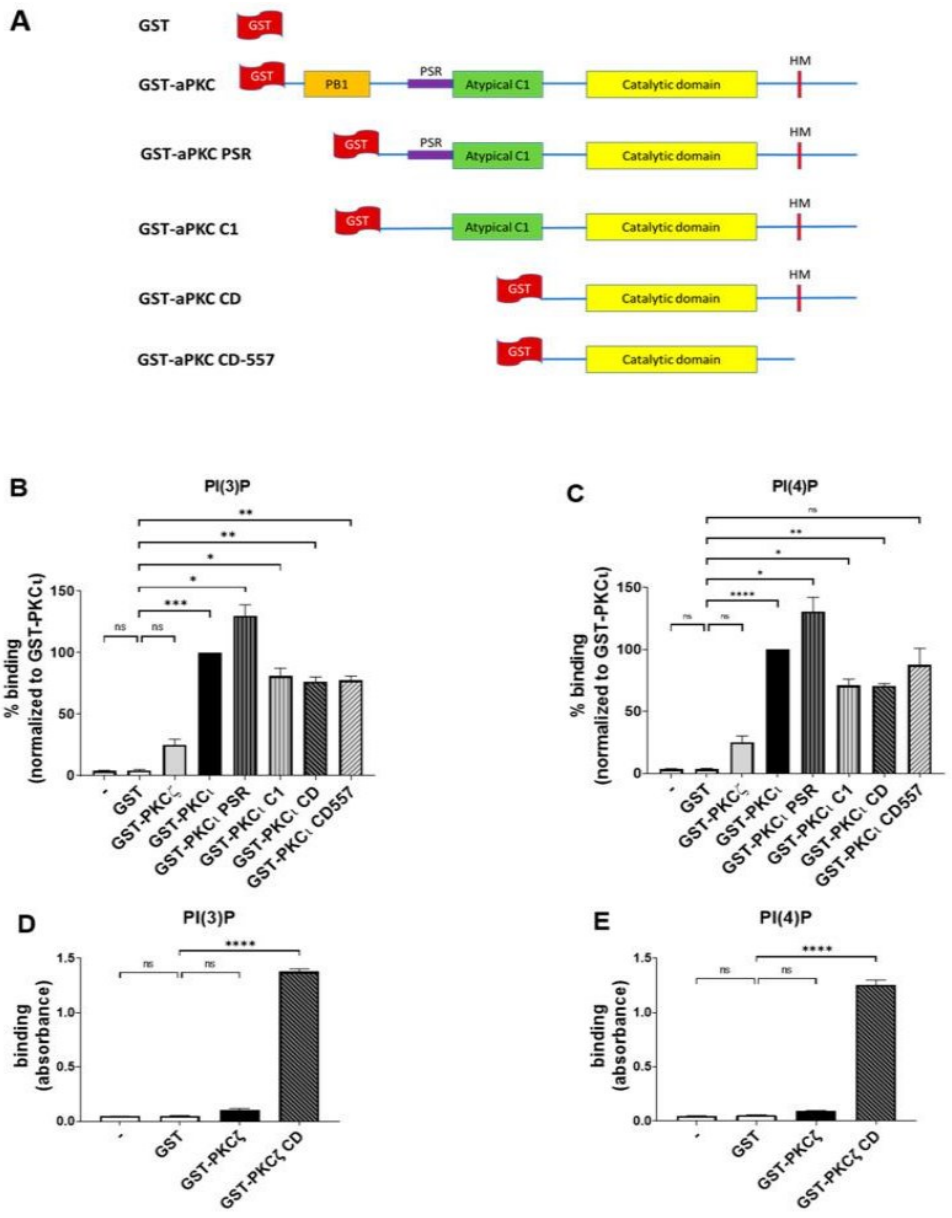

Figure 26: PKCι, but not PKCζ, binds selectively to both PI(3)P and PI(4)P through catalytic domain. (A) Schematic domain structure of GST tagged PKCζ, PKCι, and the deletion mutants used in this study. (B) GST-PKCζ, GST-PKCι, and deletion mutants binding on Cova PIP screening plates coated with PI(3)P. Purified GST was used as a negative control. Data are the mean ± SEM of three independent experiments. (C) GST-PKCζ, GST-PKCι, and deletion mutants binding on Cova PIP screening plates coated with PI(4)P. Purified GST was used as a negative control. Data are the mean ± SEM of three independent experiments. (D) GST-PKCζ and GST-PKCζ CD binding on Cova PIP screening plates coated with PI(3)P. Purified GST was used as a negative control. Data are the mean ± SEM of three independent experiments. (E) GST-PKCζ and GST-PKCζ CD binding on Cova PIP screening plates coated with PI(4)P. Purified GST was used as a negative control. Data are the mean ± SEM of three independent experiments. A single, double, triple and four asterisks denote their significance of *p*-value ≤ 0.05, ≤ 0.01, ≤ 0.001 and ≤ 0.0001 respectively, ns mean No significant.

4.11 PS and PA activates both aPKCs, while PI(4)P activates PKCι selectively

We performed kinase activity assay using highly purified commercial PKCι and in-house purified PKCζ to assess the influence of lipid binding on the catalytic activity of human aPKCs. PS, PA, and PI(4)P were incubated along with the kinases in a final concentration of 50 µg/mL. Subsequently, the ADP produced was measured using the ADP-Glow luminescence kit (Promega). Those assays were run following the pre-optimised conditions suggested by the provider, even though in those conditions the basal PKCζ activity is quite low. This could be due to the low concentrations of the enzyme (0.1 ng/µL of PKCζ) (four times less enzyme when compared to PKCι -0.4 ng/µL). In similar experimental system, the PKCι is clearly more active when compared to the background (data not shown). However, our results confirm the expected activation of PKCζ in the presence of either PA or PS, whereas with PI(4)P is ineffective (Fig. 27A). Those data are in line with previous reports in the literature [89, 106]. Conversely, we can easily measure the basal activity of unstimulated PKCι, since it is at least 10x when compared to the background. We observed that PKCι basal activity is strongly stimulated by PA, followed by PS (Fig. 27B). Interestingly, PI(4)P acts an allosteric activator selective for PKCι, as we observed no activation of highly purified commercial PKCζ by this lipid (Fig. 27A and 27B). These data suggest that the previously reported binding of aPKC to PS, PA, and PIPs enhanced enzyme activity, putatively promoting the switch to the open more active conformation.

To further investigate the domains involved in lipid-mediated PKCι activation, we performed the kinase activity assays by using in-house purified full-length GST-tagged PKCι and its truncated forms (PKCι C1 and PKCι CD) in the presence of PS, PA, or PI(4)P. Similar to what we observed before, full-length GST-PKCι is strongly activated with PA and PI(4)P, whereas PS activation is still significant but less strong (Fig. 27C). The CD is not further activated by lipid mixes *in vitro* [107]. Even though we noticed some binding of PI(4)P to the PKCι CD mutant, no further activation of the CD was detected in kinase activity assays. The PKCι C1 mutant, which lacks the PB1 and PSR, is considerably inhibited by the C1 domain [97]. The PKCι C1 mutant retained the ability to respond to PA and PI(4)P, indicating that the PSR is not required for the activation by these lipids (Fig. 27C). Together, the results indicate that the activation by PA and PI(4) is linked to the release of autoinhibition by the C1 domain.

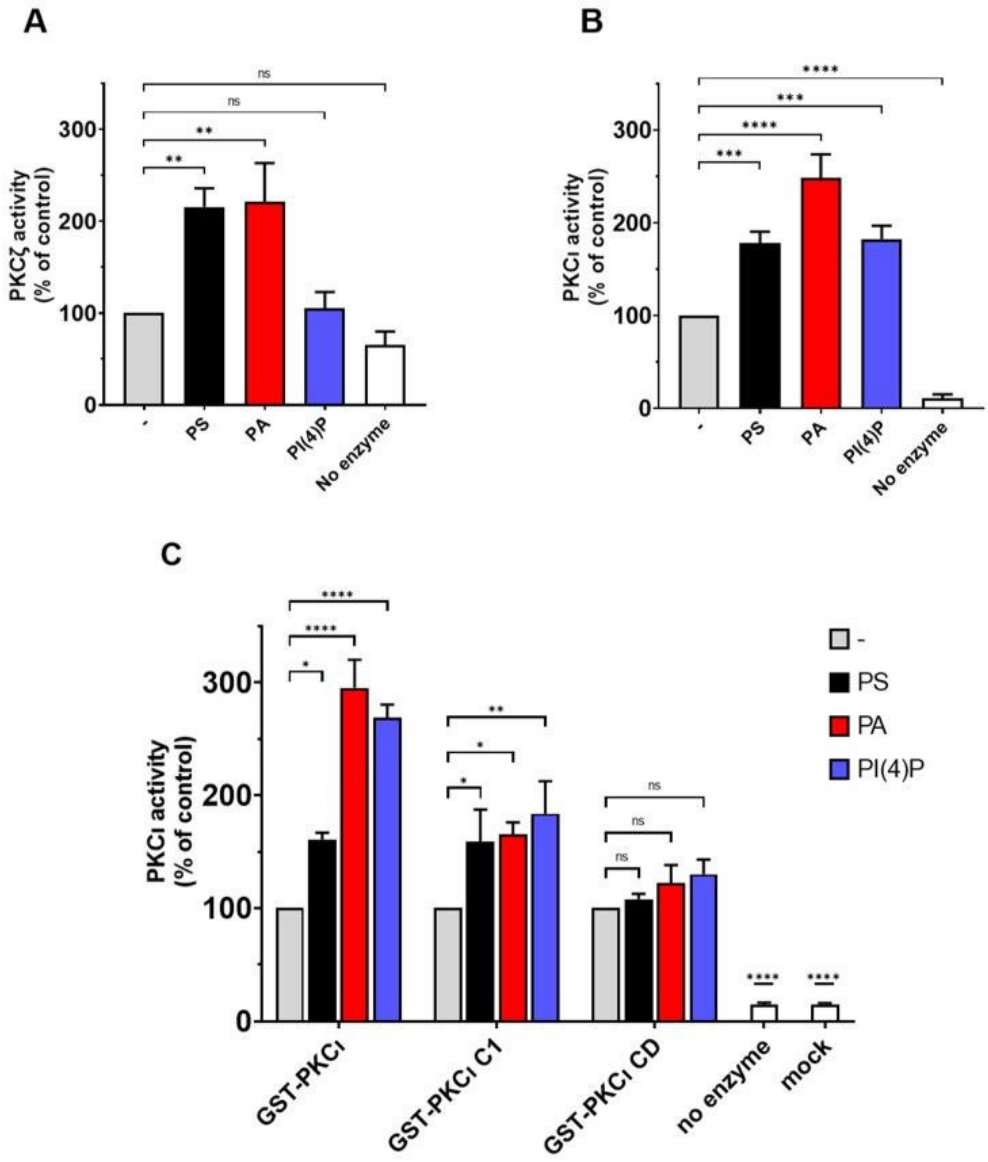

Figure 27: PKCι is activated by PS, PA, and PI(4)P.

(**A**) The activity of commercial purified GST-PKCζ was measured in the presence of 50-µg/mL PS or PA or PI(4)P. A complete reaction without an enzyme is considered as the negative control. (**B**) The activity of commercial purified GST-PKCι was measured in presence of 50-µg/mL PS or PA or PI(4)P. A complete reaction without an enzyme is considered as the negative control. (**C**) The activity of in-house purified GST-PKCι and deletion mutants was measured in presence of 0.5-ng/mL PS or PA or PI(4)P. Mock purification and no enzyme conditions are used as negative controls. Data are the mean ± SEM of at least 4 independent experiments performed in triplicate. A single, double, triple and four asterisks denote their significance of *p*-value ≤ 0.05, ≤ 0.01, ≤ 0.001 and ≤ 0.0001 respectively, ns mean No significant.

5. DISCUSSION

The purpose of the present thesis work is to investigate the molecular mechanisms regulating DGKα and lipid signalling during T cell activation.

Therefore, in this study, we started exploring the *regulatory mechanisms* involved in the control of DGKα activity in T cells.

Considering preliminary screening studies on SAP interacting proteins conducted by Dr. Elisa Ruffo in our biochemistry lab, we focused our attention on WASp, since this protein is known to interact with molecules downstream to SAP such as CDC42 and NCK-1 [61, 108] and interestingly there are some similarities between the XLP-1 (caused by SAP mutations) and the WAS disease (caused by WASp mutations) phenotypes [109]. Our data by proximity ligation assays demonstrate that DGKα and WASp are localized in close proximity in primary T cells. Performing co-immunoprecipitation assays we found that this DGKα interaction with WASp is highly specific and selective, since we did not observe its occurrence either using the highly homologous DGKγ (Fig. 18D) or N-WASp (Fig. 19C). Further investigation by coimmunoprecipitation of selected deletion mutants indicates that they form a complex through the interaction between the DGKα recoverin homology (RVH) domain and the WASp homology 1 (WH1) domain. DGKα RVH domain is a short N-terminal domain which is involved in maintaining a close conformation along with the two Ca^{2+}-binding EF-hands [110]. Following the binding of Ca^{2+} to these EF hand motifs triggers a conformational change in the DGKα N-terminus, which consequently exposes active and hydrophobic sites promoting membrane binding, resulting in a constitutively active and membrane-localized DGKα [111]. On the other hand, the WASp WH1 domain specifically recognizes proline-rich sequences and it associates with the WASp interacting protein (WIP), which is known to stabilize the protein in an auto-inhibited conformation. Interestingly, it has been observed that the WH1 domain also contributes to WASp recruitment at the immune synapse [64, 100]. However, by PLA experiments we did not observe any modulation driven by CD3-CD28 co-stimulation, indicating that the two proteins are already in close proximity in unstimulated cells (Fig. 16).

Furthermore, by kinase activity assays, we observed that WASp is required for DGKα inhibition following the TCR triggering, and co-overexpressing WASp and DGKα in the same system is a sufficient condition to block DGKα activity similarly to what observed with SAP (Fig. 11 and 12). However, since it has been reported that WASp is

activated by CDC42 protein [101] and that CDC42 is activated downstream SAP trough βPIX exchange factor, we also explored the possibility of DGKα regulation by this small GTPase. But, in contrast to what was observed for WASp, the constitutively active form of CDC42 (myc-CDC42 Q61L construct) used in kinase assay was unable to block DGKα activity in absence of WASp (Fig. 13), indicating that among these two signalling proteins WASp appear to be the most relevant regulator of DGKα activity. Taken together these findings suggest that WASp is a key adaptor protein in the regulation of the SAP-mediated pathway which leads to DGKα inhibition.

Since DGKs terminate DAG-regulated signalling phosphorylating DAG to PA, in this thesis work we also explored the *lipid regulation* of the aPKC isozymes by PA and other phospholipids. Indeed, the presence of PA and/or other phospholipids with a conical molecular shape introduce a negative curvature in the cell membranes, which allows recruitment and activation of various signalling effector proteins [18]. Thus, we systematically explored both human PKCζ and PKCι isotype-specific lipid activators, estimating their lipid-binding specificity and their effects on the kinase activation. In line with previous results obtained by others with a lipid motility shift assay [89], we observed through lipid overlay assays that both PKCζ and PKCι bind to PA and PS, but only PKCι also binds to PI(3)P, PI(4)P, and PI(5)P, indicating that even though these two isoforms share a close homology, they may exert different biological roles (Fig. 25-26). Moreover, by kinase assay we show that those lipid interactions result in a selective enhancement of the aPKC activity (Fig. 27).

Based on these observations, we hypothesise that PA along with PS recruits and activates aPKCs to specific membrane compartments, making PA-modulating enzymes such as DGKs and PLD potential regulators of aPKCs localisation and activation.

In a previous work by Chianale et al., our group shown that in epithelial cells DGKα-derived PA is required to localise the aPKCs to the plasma membrane, where their activity results in cytoskeletal reorganisation and membrane ruffling formation [85]. In line with these findings, other works on neuronal and skeletal muscle cells demonstrated that DGKα- and DGKζ-produced PA contributes to Rac-mediated cytoskeletal remodelling [91]. On the other hand, in T lymphocytes, it has been reported that, during immunological synapse formation, PKCζ enhance polarization of MTOC [112]. Thus, we speculate that a functional interaction (although it has not yet been described)

between DGK-produced PA and aPKCs in T cells could contribute to recruit and activate these kinases, promoting events related to immune synapse formation, such as MTOC polarization. Even though some studies report that loss of DGKα leads to some defects in MTOC polarization [40], the role of DGKα-PA-aPKC axis in T lymphocytes still remains unclear, and the function of DGKα- and DGKζ-generated PA during T cell activation would require further investigations.

Lastly, in this thesis work we also evaluated the *biological effects* deriving from this DGKα-mediated lipid signalling regulation.

First, we observed that SAP appears to be more crucial in RICD regulation than WASp (Fig. 20A). In particular, the data obtained indicate that pharmacological DGKα inhibition may compensate quantitatively for alterations of TCR signalosome due to SAP silencing, suggesting a role for DGKα inhibitors for the treatment of XLP-1 disease. Conversely, we did not observe any defect in pro-apoptotic molecules (NUR77 and FASL) induction and in RICD (Fig. 20) using human lymphocytes silenced for WASp in the same assay. This contrasts with data from other works reporting a role for WASp in RICD regulation and autoimmunity [67], but this discrepancy could be due to the different approached used (total genetic ablation in murine lymphocytes versus silencing in humans PBLs). Even if we have not explored this further, our data suggest a possible excessive DGKα activity in WAS patients that decreases the accumulation of selected DAG species. This could contribute to some of the defects in lymphocyte mobility and autoimmunity featured by WAS patients. It is interesting to note that DGKs also negatively regulate megakaryocytes maturation and platelets activation [113] suggesting that DGKα hyperactivity may disturb also the differentiation of platelets and that DGKα inhibitors may have a particularly positive effect on WAS.

Second, we observed that the WASp-mediated inhibition of DGKα activity is relevant for a complete IL-2 induction following TCR stimulation (Fig. 21), and this event appears to be regulated by both SAP and WASp [59, 114]. Nevertheless, in contrast to what was observed with SAP, WASp silencing in our experimental system does not affect the total levels of DAG species produced upon TCR triggering (Fig.15), nor does it alter the ERK signalling pathway (Fig. 14). This suggests that the inhibition of DGKα by WASp affects small pools of DAG which are relevant specifically for IL-2 induction. The observation that the interaction is mediated by the WH1 domain of

WASp, and that ARP2/3 activity appears unessential for IL-2 induction (Fig. 24) suggests that WASp participates to two separate pathways downstream TCR triggering: actin polymerization on one side and regulation of DGKα activity on the other (Fig. 28). To further characterize the SAP-WASp branch signalling which leads to IL-2 induction by modulating DGKα activity, we focused our attention on molecules bridging the two (SAP effectors that are also WASp interactors). Among them we selected the small G protein CDC42 as it is activated downstream SAP trough βPIX exchange factor and its bound to WASp is a key factor for the allosteric release from auto-inhibition. Moreover, we also focused on the SAP interactor protein NCK-1 since it has been reported to regulate WASp function through its SH3 domain both *in vitro* and *in vivo* [115]. Thus, we repeated the same gene expression assays silencing CDC42 and NCK-1 expression in activated human PBLs. We observed that silencing CDC42 and to a minor extent NCK-1, decreases IL-2 induction in a DGKα-dependent manner (Fig. 22 and Fig. 23) as in both cases DGKα inhibition rescues those defects.
This points out that these two proteins participate to this signalling pathway: from one side, NCK-1 can bind both SAP and WASp through its SH3 domains [62, 101] whereas CDC42, which is activated by SAP-βPIX axis, interacts with WASp allowing its activation (Fig. 28).

Overall, our findings demonstrate that upon TCR stimulation the SAP-mediated DGKα inhibition modulates cytokine production and RICD in $CD8^+$ cytotoxic T lymphocytes (CTLs). In this study, we also unveiled a novel branch of this pathway, where WASp is directly involved the regulation of DGKα activity, promoting its inhibition and resulting in a full cytokines induction.
Given that previous studies from our lab and other groups have shown that DGKα inhibition is able to restore T cell responses when the TCR signalling strength is reduced by SAP absence in XLP-1 patients [58] or by anergy [26], our results reinforce the idea that targeting DGKα could represent a promising strategy not only for the treatment of XLP-1 therapy [58] but also for the Wiskott-Aldrich Syndrome.
Intriguingly, it has been reported that SAP is a novel PD-1 signal transducer [116], suggesting that this pathway may be involved also in the regulation of DGKα activity in tumour infiltrating lymphocytes (TILs). Indeed, in these cells DGKα activity is often upregulated, leading the T lymphocytes to a hypo-responsive and anergic state [22].

Interestingly, it has been reported that TILs exhibit also a reduced WASp activation [117] whereas it has been observed that active WASp potentiates T cells and NK lytic function similarly to what was observed with DGKα inhibitors [118]. This paves the way for the use of DGKα inhibitors also in all those T cell hyporesponsive states such as tumour-induced anergy/exhaustion [119, 120].

Concluding, in this present study we explored the signalling pathway that upon strong TCR stimulation promotes SAP-mediated DGKα inhibition. We found that this DGKα inhibition is a novel function of WASp that, independently from ARP2/3 driven actin branching, tunes IL-2 induction during T cell activation (Fig. 28). We also explored the *in vitro* regulation of aPKC by phospholipids highlighting that those kinases are potential DGK's effectors.

Taken together our data suggest that DGKα could represents a promising strategy for the XLP-1 and WAS treatment, as well as for T lymphocytes exhaustion induced by tumours. Those data open new research questions such as the function of DGKα produced PA in T cell signalling and the putative activity of this pathway in different cell lines such as megakaryocytes and platelets.

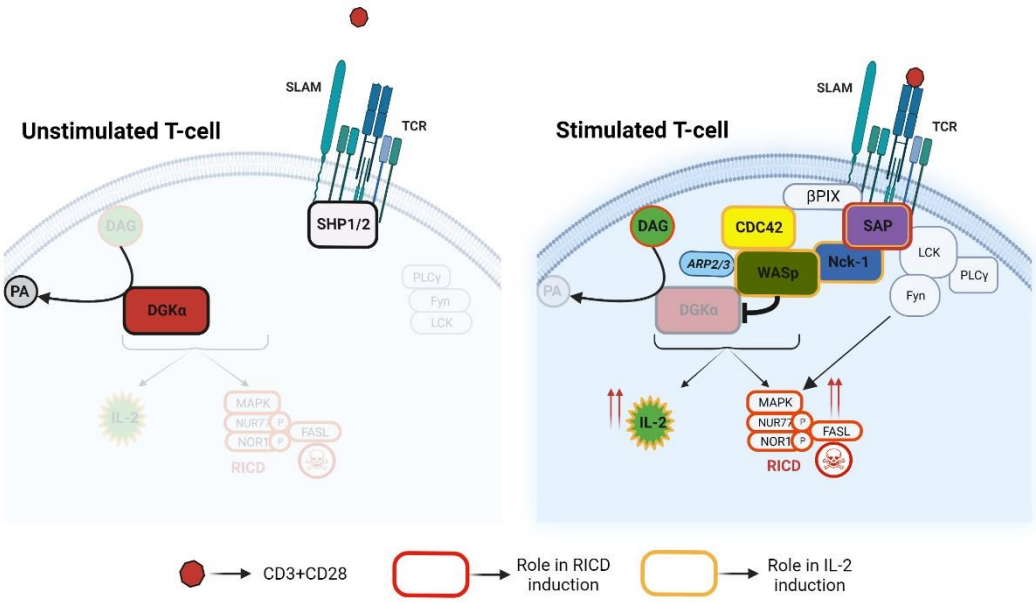

Figure 28. Divergent signalling pathways downstream to SAP

The SAP-NCK-1/CDC42-WASp pathway controls DGKα activity and DAG cellular metabolism. This pathway tunes IL-2 and RICD responses in T cells. Other SAP interactors such as Lck and Fyn are crucial regulators of RICD onset.

6. BIBLIOGRAPHY

References

1. Merida, I., A. Avila-Flores, and E. Merino, *Diacylglycerol kinases: at the hub of cell signalling.* Biochem J, 2008. **409**(1): p. 1-18.
2. Ganesan, S., B.N. Shabits, and V. Zaremberg, *Tracking Diacylglycerol and Phosphatidic Acid Pools in Budding Yeast.* Lipid Insights, 2015. **8**(Suppl 1): p. 75-85.
3. Sim, J.A., J. Kim, and D. Yang, *Beyond Lipid Signaling: Pleiotropic Effects of Diacylglycerol Kinases in Cellular Signaling.* Int J Mol Sci, 2020. **21**(18).
4. Sakane, F., F. Hoshino, and C. Murakami, *New Era of Diacylglycerol Kinase, Phosphatidic Acid and Phosphatidic Acid-Binding Protein.* Int J Mol Sci, 2020. **21**(18).
5. Roose, J.P., et al., *A diacylglycerol-protein kinase C-RasGRP1 pathway directs Ras activation upon antigen receptor stimulation of T cells.* Mol Cell Biol, 2005. **25**(11): p. 4426-41.
6. Carrasco, S. and I. Merida, *Diacylglycerol-dependent binding recruits PKCtheta and RasGRP1 C1 domains to specific subcellular localizations in living T lymphocytes.* Mol Biol Cell, 2004. **15**(6): p. 2932-42.
7. Chen, J. and Y. Fang, *A novel pathway regulating the mammalian target of rapamycin (mTOR) signaling.* Biochem Pharmacol, 2002. **64**(7): p. 1071-7.
8. Avila-Flores, A., et al., *Modulation of the mammalian target of rapamycin pathway by diacylglycerol kinase-produced phosphatidic acid.* J Biol Chem, 2005. **280**(11): p. 10091-9.
9. Jenkins, G.M. and M.A. Frohman, *Phospholipase D: a lipid centric review.* Cell Mol Life Sci, 2005. **62**(19-20): p. 2305-16.
10. Csaki, L.S. and K. Reue, *Lipins: multifunctional lipid metabolism proteins.* Annu Rev Nutr, 2010. **30**: p. 257-72.
11. Liu, C.H., et al., *Diacylglycerol kinase zeta regulates microbial recognition and host resistance to Toxoplasma gondii.* J Exp Med, 2007. **204**(4): p. 781-92.
12. Guo, R., et al., *Synergistic control of T cell development and tumor suppression by diacylglycerol kinase alpha and zeta.* Proc Natl Acad Sci U S A, 2008. **105**(33): p. 11909-14.
13. Topham, M.K. and S.M. Prescott, *Mammalian diacylglycerol kinases, a family of lipid kinases with signaling functions.* J Biol Chem, 1999. **274**(17): p. 11447-50.
14. Fazio, A., et al., *Subcellular Localization Relevance and Cancer-Associated Mechanisms of Diacylglycerol Kinases.* Int J Mol Sci, 2020. **21**(15).

15. Shulga, Y.V., M.K. Topham, and R.M. Epand, *Regulation and functions of diacylglycerol kinases.* Chem Rev, 2011. **111**(10): p. 6186-208.
16. Sakane, F., et al., *Diacylglycerol kinases: why so many of them?* Biochim Biophys Acta, 2007. **1771**(7): p. 793-806.
17. Aulakh, S.S., J.C. Bozelli, Jr., and R.M. Epand, *Exploring the AlphaFold Predicted Conformational Properties of Human Diacylglycerol Kinases.* J Phys Chem B, 2022. **126**(37): p. 7172-7183.
18. Bozelli, J.C., Jr. and R.M. Epand, *DGKalpha, Bridging Membrane Shape Changes with Specific Molecular Species of DAG/PA: Implications in Cancer and Immunosurveillance.* Cancers (Basel), 2022. **14**(21).
19. Chen, S.S., Z. Hu, and X.P. Zhong, *Diacylglycerol Kinases in T Cell Tolerance and Effector Function.* Front Cell Dev Biol, 2016. **4**: p. 130.
20. Guo, Y.J., et al., *ERK/MAPK signalling pathway and tumorigenesis.* Exp Ther Med, 2020. **19**(3): p. 1997-2007.
21. Plotnikov, A., et al., *The MAPK cascades: signaling components, nuclear roles and mechanisms of nuclear translocation.* Biochim Biophys Acta, 2011. **1813**(9): p. 1619-33.
22. Merida, I., et al., *Diacylglycerol kinases in cancer.* Adv Biol Regul, 2017. **63**: p. 22-31.
23. Avila-Flores, A., et al., *Predominant contribution of DGKzeta over DGKalpha in the control of PKC/PDK-1-regulated functions in T cells.* Immunol Cell Biol, 2017. **95**(6): p. 549-563.
24. Arranz-Nicolas, J., et al., *Diacylglycerol kinase zeta limits IL-2-dependent control of PD-1 expression in tumor-infiltrating T lymphocytes.* J Immunother Cancer, 2020. **8**(2).
25. Macian, F., et al., *Transcriptional mechanisms underlying lymphocyte tolerance.* Cell, 2002. **109**(6): p. 719-31.
26. Zha, Y., et al., *T cell anergy is reversed by active Ras and is regulated by diacylglycerol kinase-alpha.* Nat Immunol, 2006. **7**(11): p. 1166-73.
27. Olenchock, B.A., et al., *Disruption of diacylglycerol metabolism impairs the induction of T cell anergy.* Nat Immunol, 2006. **7**(11): p. 1174-81.
28. Zhong, X.P., et al., *Regulation of T cell receptor-induced activation of the Ras-ERK pathway by diacylglycerol kinase zeta.* J Biol Chem, 2002. **277**(34): p. 31089-98.
29. Zhong, X.P., et al., *Enhanced T cell responses due to diacylglycerol kinase zeta deficiency.* Nat Immunol, 2003. **4**(9): p. 882-90.
30. Merida, I., et al., *Redundant and specialized roles for diacylglycerol kinases alpha and zeta in the control of T cell functions.* Sci Signal, 2015. **8**(374): p. re6.

31. Zheng, Y., et al., *Egr2-dependent gene expression profiling and ChIP-Seq reveal novel biologic targets in T cell anergy.* Mol Immunol, 2013. **55**(3-4): p. 283-91.
32. Zheng, Y., et al., *Transcriptional regulator early growth response gene 2 (Egr2) is required for T cell anergy in vitro and in vivo.* J Exp Med, 2012. **209**(12): p. 2157-63.
33. Martinez-Moreno, M., et al., *FoxO-dependent regulation of diacylglycerol kinase alpha gene expression.* Mol Cell Biol, 2012. **32**(20): p. 4168-80.
34. Shin, J., D. Xie, and X.P. Zhong, *MicroRNA-34a enhances T cell activation by targeting diacylglycerol kinase zeta.* PLoS One, 2013. **8**(10): p. e77983.
35. Kefas, B., et al., *A miR-297/hypoxia/DGK-alpha axis regulating glioblastoma survival.* Neuro Oncol, 2013. **15**(12): p. 1652-63.
36. Sanjuan, M.A., et al., *Role of diacylglycerol kinase alpha in the attenuation of receptor signaling.* J Cell Biol, 2001. **153**(1): p. 207-20.
37. Sanjuan, M.A., et al., *T cell activation in vivo targets diacylglycerol kinase alpha to the membrane: a novel mechanism for Ras attenuation.* J Immunol, 2003. **170**(6): p. 2877-83.
38. Gharbi, S.I., et al., *Diacylglycerol kinase zeta controls diacylglycerol metabolism at the immunological synapse.* Mol Biol Cell, 2011. **22**(22): p. 4406-14.
39. Joshi, R.P., et al., *The zeta isoform of diacylglycerol kinase plays a predominant role in regulatory T cell development and TCR-mediated ras signaling.* Sci Signal, 2013. **6**(303): p. ra102.
40. Chauveau, A., et al., *Diacylglycerol kinase alpha establishes T cell polarity by shaping diacylglycerol accumulation at the immunological synapse.* Sci Signal, 2014. **7**(340): p. ra82.
41. Schmidt, A.M., et al., *Diacylglycerol kinase zeta limits the generation of natural regulatory T cells.* Sci Signal, 2013. **6**(303): p. ra101.
42. Schmidt, A.M., et al., *Regulatory T cells require TCR signaling for their suppressive function.* J Immunol, 2015. **194**(9): p. 4362-70.
43. Shin, J., et al., *Differential regulation of primary and memory CD8 T cell immune responses by diacylglycerol kinases.* J Immunol, 2012. **188**(5): p. 2111-7.
44. Yang, J., et al., *Unexpected positive control of NFkappaB and miR-155 by DGKalpha and zeta ensures effector and memory CD8+ T cell differentiation.* Oncotarget, 2016. **7**(23): p. 33744-64.
45. Arumugam, V., et al., *TCR signaling intensity controls CD8+ T cell responsiveness to TGF-beta.* J Leukoc Biol, 2015. **98**(5): p. 703-12.

46. Riese, M.J., et al., *Decreased diacylglycerol metabolism enhances ERK activation and augments CD8+ T cell functional responses.* J Biol Chem, 2011. **286**(7): p. 5254-65.
47. Riese, M.J., et al., *Enhanced effector responses in activated CD8+ T cells deficient in diacylglycerol kinases.* Cancer Res, 2013. **73**(12): p. 3566-77.
48. Cannons, J.L., S.G. Tangye, and P.L. Schwartzberg, *SLAM family receptors and SAP adaptors in immunity.* Annu Rev Immunol, 2011. **29**: p. 665-705.
49. Dupre, L., et al., *SAP controls the cytolytic activity of CD8+ T cells against EBV-infected cells.* Blood, 2005. **105**(11): p. 4383-9.
50. Qi, H., et al., *SAP-controlled T-B cell interactions underlie germinal centre formation.* Nature, 2008. **455**(7214): p. 764-9.
51. Velnati, S., et al., *Diacylglycerol Kinase alpha in X Linked Lymphoproliferative Disease Type 1.* Int J Mol Sci, 2021. **22**(11).
52. Cannons, J.L., et al., *SAP regulates T(H)2 differentiation and PKC-theta-mediated activation of NF-kappaB1.* Immunity, 2004. **21**(5): p. 693-706.
53. Dong, Z., et al., *The adaptor SAP controls NK cell activation by regulating the enzymes Vav-1 and SHIP-1 and by enhancing conjugates with target cells.* Immunity, 2012. **36**(6): p. 974-85.
54. Kageyama, R., et al., *The receptor Ly108 functions as a SAP adaptor-dependent on-off switch for T cell help to B cells and NKT cell development.* Immunity, 2012. **36**(6): p. 986-1002.
55. Proust, R., J. Bertoglio, and F. Gesbert, *The adaptor protein SAP directly associates with CD3zeta chain and regulates T cell receptor signaling.* PLoS One, 2012. **7**(8): p. e43200.
56. Zheng, L., J. Li, and M. Lenardo, *Restimulation-induced cell death: new medical and research perspectives.* Immunol Rev, 2017. **277**(1): p. 44-60.
57. Snow, A.L., et al., *Restimulation-induced apoptosis of T cells is impaired in patients with X-linked lymphoproliferative disease caused by SAP deficiency.* J Clin Invest, 2009. **119**(10): p. 2976-89.
58. Ruffo, E., et al., *Inhibition of diacylglycerol kinase alpha restores restimulation-induced cell death and reduces immunopathology in XLP-1.* Sci Transl Med, 2016. **8**(321): p. 321ra7.
59. Baldanzi, G., et al., *SAP-mediated inhibition of diacylglycerol kinase alpha regulates TCR-induced diacylglycerol signaling.* J Immunol, 2011. **187**(11): p. 5941-51.
60. Gartshteyn, Y., A.D. Askanase, and A. Mor, *SLAM Associated Protein Signaling in T Cells: Tilting the Balance Toward Autoimmunity.* Front Immunol, 2021. **12**: p. 654839.

61. Gu, C., et al., *The X-linked lymphoproliferative disease gene product SAP associates with PAK-interacting exchange factor and participates in T cell activation.* Proc Natl Acad Sci U S A, 2006. **103**(39): p. 14447-52.
62. Li, C., D. Schibli, and S.S. Li, *The XLP syndrome protein SAP interacts with SH3 proteins to regulate T cell signaling and proliferation.* Cell Signal, 2009. **21**(1): p. 111-9.
63. Zeng, R., et al., *SLP-76 coordinates Nck-dependent Wiskott-Aldrich syndrome protein recruitment with Vav-1/Cdc42-dependent Wiskott-Aldrich syndrome protein activation at the T cell-APC contact site.* J Immunol, 2003. **171**(3): p. 1360-8.
64. Sasahara, Y., et al., *Mechanism of recruitment of WASP to the immunological synapse and of its activation following TCR ligation.* Mol Cell, 2002. **10**(6): p. 1269-81.
65. Rivers, E. and A.J. Thrasher, *Wiskott-Aldrich syndrome protein: Emerging mechanisms in immunity.* Eur J Immunol, 2017. **47**(11): p. 1857-1866.
66. Candotti, F., *Clinical Manifestations and Pathophysiological Mechanisms of the Wiskott-Aldrich Syndrome.* J Clin Immunol, 2018. **38**(1): p. 13-27.
67. Nikolov, N.P., et al., *Systemic autoimmunity and defective Fas ligand secretion in the absence of the Wiskott-Aldrich syndrome protein.* Blood, 2010. **116**(5): p. 740-7.
68. Cleland, S.Y. and R.M. Siegel, *Wiskott-Aldrich Syndrome at the nexus of autoimmune and primary immunodeficiency diseases.* FEBS Lett, 2011. **585**(23): p. 3710-4.
69. Breitkreutz, D., et al., *Protein kinase C family: on the crossroads of cell signaling in skin and tumor epithelium.* J Cancer Res Clin Oncol, 2007. **133**(11): p. 793-808.
70. Casabona, G., *Intracellular signal modulation: a pivotal role for protein kinase C.* Prog Neuropsychopharmacol Biol Psychiatry, 1997. **21**(3): p. 407-25.
71. Inagaki, K., E. Churchill, and D. Mochly-Rosen, *Epsilon protein kinase C as a potential therapeutic target for the ischemic heart.* Cardiovasc Res, 2006. **70**(2): p. 222-30.
72. Ferreira, J.C., P.C. Brum, and D. Mochly-Rosen, *betaIIPKC and epsilonPKC isozymes as potential pharmacological targets in cardiac hypertrophy and heart failure.* J Mol Cell Cardiol, 2011. **51**(4): p. 479-84.
73. Geraldes, P. and G.L. King, *Activation of protein kinase C isoforms and its impact on diabetic complications.* Circ Res, 2010. **106**(8): p. 1319-31.
74. Das Evcimen, N. and G.L. King, *The role of protein kinase C activation and the vascular complications of diabetes.* Pharmacol Res, 2007. **55**(6): p. 498-510.
75. Zhang, D., et al., *Neuroprotective effect of protein kinase C delta inhibitor rottlerin in cell culture and animal models of Parkinson's disease.* J Pharmacol Exp Ther, 2007. **322**(3): p. 913-22.

76. Garrido, J.L., et al., *Protein kinase C inhibits amyloid beta peptide neurotoxicity by acting on members of the Wnt pathway.* FASEB J, 2002. **16**(14): p. 1982-4.
77. Anderson, K., et al., *Mice deficient in PKC theta demonstrate impaired in vivo T cell activation and protection from T cell-mediated inflammatory diseases.* Autoimmunity, 2006. **39**(6): p. 469-78.
78. Prescott, S.L., et al., *Protein kinase Czeta: a novel protective neonatal T-cell marker that can be upregulated by allergy prevention strategies.* J Allergy Clin Immunol, 2007. **120**(1): p. 200-6.
79. Miyamoto, A., et al., *Increased proliferation of B cells and auto-immunity in mice lacking protein kinase Cdelta.* Nature, 2002. **416**(6883): p. 865-9.
80. Cirillo, N., A. Lanza, and S.S. Prime, *Induction of hyper-adhesion attenuates autoimmune-induced keratinocyte cell-cell detachment and processing of adhesion molecules via mechanisms that involve PKC.* Exp Cell Res, 2010. **316**(4): p. 580-92.
81. Isakov, N. and A. Altman, *Protein kinase C(theta) in T cell activation.* Annu Rev Immunol, 2002. **20**: p. 761-94.
82. Altman, A. and K.F. Kong, *Protein Kinase C Enzymes in the Hematopoietic and Immune Systems.* Annu Rev Immunol, 2016. **34**: p. 511-38.
83. Isakov, N., *Protein kinase C (PKC) isoforms in cancer, tumor promotion and tumor suppression.* Semin Cancer Biol, 2018. **48**: p. 36-52.
84. Spitaler, M. and D.A. Cantrell, *Protein kinase C and beyond.* Nat Immunol, 2004. **5**(8): p. 785-90.
85. Chianale, F., et al., *Diacylglycerol kinase alpha mediates HGF-induced Rac activation and membrane ruffling by regulating atypical PKC and RhoGDI.* Proc Natl Acad Sci U S A, 2010. **107**(9): p. 4182-7.
86. Rainero, E., et al., *The diacylglycerol kinase alpha/atypical PKC/beta1 integrin pathway in SDF-1alpha mammary carcinoma invasiveness.* PLoS One, 2014. **9**(6): p. e97144.
87. Dang, P.M., et al., *Protein kinase C zeta phosphorylates a subset of selective sites of the NADPH oxidase component p47phox and participates in formyl peptide-mediated neutrophil respiratory burst.* J Immunol, 2001. **166**(2): p. 1206-13.
88. Wang, G., et al., *Direct binding to ceramide activates protein kinase Czeta before the formation of a pro-apoptotic complex with PAR-4 in differentiating stem cells.* J Biol Chem, 2005. **280**(28): p. 26415-24.

89. Limatola, C., et al., *Phosphatidic acid activation of protein kinase C-zeta overexpressed in COS cells: comparison with other protein kinase C isotypes and other acidic lipids.* Biochem J, 1994. **304 (Pt 3)**(Pt 3): p. 1001-8.

90. Pu, Y., et al., *Effects on ligand interaction and membrane translocation of the positively charged arginine residues situated along the C1 domain binding cleft in the atypical protein kinase C isoforms.* J Biol Chem, 2006. **281**(44): p. 33773-88.

91. You, J.S., et al., *The role of diacylglycerol kinase zeta and phosphatidic acid in the mechanical activation of mammalian target of rapamycin (mTOR) signaling and skeletal muscle hypertrophy.* J Biol Chem, 2014. **289**(3): p. 1551-63.

92. Xie, S., N. Naslavsky, and S. Caplan, *Diacylglycerol kinase alpha regulates tubular recycling endosome biogenesis and major histocompatibility complex class I recycling.* J Biol Chem, 2014. **289**(46): p. 31914-31926.

93. Rainero, E., et al., *Diacylglycerol kinase alpha controls RCP-dependent integrin trafficking to promote invasive migration.* J Cell Biol, 2012. **196**(2): p. 277-95.

94. Alonso, R., et al., *Diacylglycerol kinase alpha regulates the formation and polarisation of mature multivesicular bodies involved in the secretion of Fas ligand-containing exosomes in T lymphocytes.* Cell Death Differ, 2011. **18**(7): p. 1161-73.

95. Cutrupi, S., et al., *Src-mediated activation of alpha-diacylglycerol kinase is required for hepatocyte growth factor-induced cell motility.* EMBO J, 2000. **19**(17): p. 4614-22.

96. Baldanzi, G., et al., *Diacylglycerol kinase-alpha phosphorylation by Src on Y335 is required for activation, membrane recruitment and Hgf-induced cell motility.* Oncogene, 2008. **27**(7): p. 942-56.

97. Zhang, H., et al., *Molecular mechanism of regulation of the atypical protein kinase C by N-terminal domains and an allosteric small compound.* Chem Biol, 2014. **21**(6): p. 754-65.

98. Velnati, S., et al., *Structure activity relationship studies on Amb639752: toward the identification of a common pharmacophoric structure for DGKalpha inhibitors.* J Enzyme Inhib Med Chem, 2020. **35**(1): p. 96-108.

99. Kumari, S., et al., *Actin foci facilitate activation of the phospholipase C-gamma in primary T lymphocytes via the WASP pathway.* Elife, 2015. **4**.

100. de la Fuente, M.A., et al., *WIP is a chaperone for Wiskott-Aldrich syndrome protein (WASP).* Proc Natl Acad Sci U S A, 2007. **104**(3): p. 926-31.

101. Tomasevic, N., et al., *Differential regulation of WASP and N-WASP by Cdc42, Rac1, Nck, and PI(4,5)P2.* Biochemistry, 2007. **46**(11): p. 3494-502.

102. Rubio, I., et al., *TCR-induced activation of Ras proceeds at the plasma membrane and requires palmitoylation of N-Ras.* J Immunol, 2010. **185**(6): p. 3536-43.

103. Takahashi, M., et al., *Calcium negatively regulates an intramolecular interaction between the N-terminal recoverin homology and EF-hand motif domains and the C-terminal C1 and catalytic domains of diacylglycerol kinase alpha.* Biochem Biophys Res Commun, 2012. **423**(3): p. 571-6.

104. De Meester, J., et al., *The Wiskott-Aldrich syndrome protein regulates CTL cytotoxicity and is required for efficient killing of B cell lymphoma targets.* J Leukoc Biol, 2010. **88**(5): p. 1031-40.

105. Velnati, S., et al., *Identification of a novel DGKalpha inhibitor for XLP-1 therapy by virtual screening.* Eur J Med Chem, 2019. **164**: p. 378-390.

106. Dong, W., et al., *A polybasic domain in aPKC mediates Par6-dependent control of membrane targeting and kinase activity.* J Cell Biol, 2020. **219**(7).

107. Lopez-Garcia, L.A., et al., *Allosteric regulation of protein kinase PKCzeta by the N-terminal C1 domain and small compounds to the PIF-pocket.* Chem Biol, 2011. **18**(11): p. 1463-73.

108. Sylla, B.S., et al., *The X-linked lymphoproliferative syndrome gene product SH2D1A associates with p62dok (Dok1) and activates NF-kappa B.* Proc Natl Acad Sci U S A, 2000. **97**(13): p. 7470-5.

109. Walter, J.E., I.A. Ayala, and D. Milojevic, *Autoimmunity as a continuum in primary immunodeficiency.* Curr Opin Pediatr, 2019. **31**(6): p. 851-862.

110. Jiang, Y., et al., *A domain with homology to neuronal calcium sensors is required for calcium-dependent activation of diacylglycerol kinase alpha.* J Biol Chem, 2000. **275**(44): p. 34092-9.

111. Yamada, K., et al., *EF-hand motifs of alpha, beta and gamma isoforms of diacylglycerol kinase bind calcium with different affinities and conformational changes.* Biochem J, 1997. **321 (Pt 1)**(Pt 1): p. 59-64.

112. Bertrand, F., et al., *An initial and rapid step of lytic granule secretion precedes microtubule organizing center polarization at the cytotoxic T lymphocyte/target cell synapse.* Proc Natl Acad Sci U S A, 2013. **110**(15): p. 6073-8.

113. Moroi, A.J., et al., *Diacylglycerol kinase zeta is a negative regulator of GPVI-mediated platelet activation.* Blood Adv, 2019. **3**(7): p. 1154-1166.

114. Cianferoni, A., et al., *Defective nuclear translocation of nuclear factor of activated T cells and extracellular signal-regulated kinase underlies deficient IL-2 gene expression in Wiskott-Aldrich syndrome.* J Allergy Clin Immunol, 2005. **116**(6): p. 1364-71.

115. Thrasher, A.J. and S.O. Burns, *WASP: a key immunological multitasker.* Nat Rev Immunol, 2010. **10**(3): p. 182-92.

116. Peled, M., et al., *Affinity purification mass spectrometry analysis of PD-1 uncovers SAP as a new checkpoint inhibitor.* Proc Natl Acad Sci U S A, 2018. **115**(3): p. E468-E477.

117. Koneru, M., et al., *Defective proximal TCR signaling inhibits CD8+ tumor-infiltrating lymphocyte lytic function.* J Immunol, 2005. **174**(4): p. 1830-40.

118. Arranz-Nicolas, J., et al., *Diacylglycerol kinase alpha inhibition cooperates with PD-1-targeted therapies to restore the T cell activation program.* Cancer Immunol Immunother, 2021. **70**(11): p. 3277-3289.

119. Jung, I.Y., et al., *CRISPR/Cas9-Mediated Knockout of DGK Improves Antitumor Activities of Human T Cells.* Cancer Res, 2018. **78**(16): p. 4692-4703.

120. Kritikou, J.S., et al., *Constitutive activation of WASp leads to abnormal cytotoxic cells with increased granzyme B and degranulation response to target cells.* JCI Insight, 2021. **6**(6).

7. PUBLICATIONS

International Journal of
Molecular Sciences

MDPI

Review

Diacylglycerol Kinase alpha in X Linked Lymphoproliferative Disease Type 1

Suresh Velnati [1,2], Sara Centonze [1,2], Federico Girivetto [1,2] and Gianluca Baldanzi [1,2,*]

[1] Department of Translational Medicine, University of Piemonte Orientale, 28100 Novara, Italy; suresh.velnati@med.uniupo.it (S.V.); sara.centonze@uniupo.it (S.C.); 20020549@studenti.uniupo.it (F.G.)
[2] Center for Translational Research on Allergic and Autoimmune Diseases (CAAD), University of Piemonte Orientale, 28100 Novara, Italy
* Correspondence: gianluca.baldanzi@uniupo.it; Tel.: +39-0321-660-527

Abstract: Diacylglycerol kinases are intracellular enzymes that control the balance between the secondary messengers diacylglycerol and phosphatidic acid. DGK and DGK are the prominent isoforms that restrain the intensity of T cell receptor signalling by metabolizing PLC generated diacylglycerol. Thus, their activity must be tightly controlled to grant cellular homeostasis and refine immune responses. DGK is specifically inhibited by strong T cell activating signals to allow for full diacylglycerol signalling which mediates T cell response. In X-linked lymphoproliferative disease 1, deficiency of the adaptor protein SAP results in altered T cell receptor signalling, due in part to persistent DGK activity. This activity constrains diacylglycerol levels, attenuating downstream pathways such as PKC and Ras/MAPK and decreasing T cell restimulation induced cell death. This is a form of apoptosis triggered by prolonged T cell activation that is indeed defective in $CD8^+$ cells of X-linked lymphoproliferative disease type 1 patients. Accordingly, inhibition or downregulation of DGK activity restores in vitro a correct diacylglycerol dependent signal transduction, cytokines production and restimulation induced apoptosis. In animal disease models, DGK inhibitors limit $CD8^+$ expansion and immune-mediated tissue damage, suggesting the possibility of using inhibitors of diacylglycerol kinase as a new therapeutic approach.

Keywords: signal transduction; activation-induced cell death; PKC; ERK; SHP-2; SLAM; SH2D1A

•€••,ƒ„…†
•€•,ƒ„…

Citation: Velnati, S.; Centonze, S.; Girivetto, F.; Baldanzi, G. Diacylglycerol Kinase alpha in X Linked Lymphoproliferative Disease Type 1. Int. J. Mol. Sci. **2021**, 22, 5816. https://doi.org/10.3390/ijms22115816

Academic Editor: Godfrey Getz

Received: 12 May 2021
Accepted: 26 May 2021
Published: 29 May 2021

The investigation of the molecular mechanisms underlying X linked proliferative disease type I (XLP-1) have evidenced a reduced intensity of T cell receptor (TCR) signalling strength [1] and a peculiar defect in diacylglycerol (DAG) mediated signalling [2]. The shreds of evidence indicating an involvement of diacylglycerol kinase (DGK) in this phenotype are presented in here together with a possible implication for the design of targeted XLP-1 therapies.

1. Introduction

DAG is a key second messenger in T cell physiology that promotes membrane recruitment and activation of several effectors. DAG activates conventional and novel protein kinase C (PKC) along with Ras guanine-releasing protein-1 (RasGRP1) and other C1 domain-containing signal transducers [3]. In T cells the majority of receptor-induced DAG is produced by the action of phospholipase C 1 (PLC1) on membrane phosphatidylinos-itol 4,5 bisphosphate. PLC1 is crucial for T cell activation in terms of proliferation and cytokine secretion [4] by acting upstream to kinases such PKC and the mitogen-activated protein kinase cascade (MAPK) and also of key transcription factors such as nuclear factor of activated T-cells (NFAT), nuclear factor-kappa light chain enhancer of activated B cells (NFB) and activator protein 1 (AP1) [5]. In particular, DAG at the plasma membrane starts the MAPK pathway by bringing RasGRP1 close to Ras [6,7] and at the same time it activates conventional and novel PKCs by abrogating the pseudo-substrate binding to the catalytic domain [8]. Both DAG dependent pathways are necessary for immune synapse

organization and full T cell activation [9]. Interestingly, T cell activation in absence of costimulatory signals drives those cells in anergy. This is a hyporesponsive status that contributes to peripheral immunotolerance, characterized by reduced Ras signalling due to DGK overexpression, resulting in defects in lymphocyte proliferation and IL-2 production [10]. In line with a modulatory role of DAG metabolism, DGK inhibitors not only rescue anergic cells but also reinvigorate exhausted tumour infiltrating lymphocytes, suggesting that this isoform plays a key role in the negative regulation of T cell effector functions [11].

The regulation of DAG levels in T cells is the result of a balance between the synthesis by PLC1 and the metabolism mediated by DGK as evidenced by the hyperresponsive phenotypes of DGK and DGK deficient lymphocytes [12,13]. DGK and DGK are both involved in the negative control of TCR signalling with some differences: DGK appears to play a quantitatively predominant role at the plasma membrane, while DGK has a specific role in shaping the DAG gradient at the immune synapse [14]. Blocking DGK or DGK activity potentiates TCR signalling along with the MAPK/AP-1 axis and NFB activity, resulting in enhanced expression of T cells activation markers such as CD69 and Nur77 [15,16].

2. X-Linked Lymphoproliferative Disease Type 1

XLP-1 is a rare form of primary immunodeficiency affecting about one-two out of one million males, resulting in an increased vulnerability to Epstein-Barr viral (EBV) infection. Although the exposure of patients with XLP-1 to EBV induces an uncontrolled immune response including the activation of lymphocytes and monocytes, this response is not able to eradicate the infection [17]. Moreover, EBV persistency may evolve in severe manifestations such as hemophagocytic lymphohistiocytosis (HLH). While HLH is almost always caused by EBV infection, other manifestations are present in XLP-1 EBV^- patients such as malignant lymphoma, hypogammaglobulinemia or dysgammaglobulinemia, bone marrow hypoplasia and lymphocytic vasculitis. This suggests that the exposure to EBV is not responsible for all the clinical features of the disease [18–20].

Mutations in XLP-1 are localized to the SH2D1A gene, a small 4-exon gene located in the long arm of chromosome X (Xq25). SH2D1A encodes for a 128 aa protein named signalling lymphocyte activation molecule (SLAM)–associated protein (SAP). SAP is an adaptor protein consisting of an N-terminal domain of five amino acids, a central SH2 domain of approximately 100 amino acids and a C-terminal region of nearly 20 amino acids [21,22]**.** SAP is expressed in T cells, natural killer (NK), and invariant NKT (iNKT) cells. According to Sayos and colleagues**,** SAP expression is detectable in the majority of human T cells subsets ($CD4^+$, $CD45RO^+$, $CD45RA^+$ and $CD8^+$), in the T-cell tumour cell line Jurkat, and in the Burkitt lymphoma line Raji which is positive in the EBV [22].

The SH2D1A protein product binds to the cytoplasmic portion of the SLAM family of transmembrane receptors. Binding occurs between a conserved Immunoreceptor Tyrosine-based Switch Motif (ITSM) in SLAM and the SAP SH2 domain in which the arginine residue at position 32 has been shown to play a critical role [22]. Studies of crystallographic and nuclear magnetic resonance reported that the interaction between the SAP SH2 domain and its ligand occurs through an atypical binding mode [23,24]. Generally, SH2 domains bind to their ligands by a ‘two-pronged’ mechanism, where they simultaneously interact with the phosphorylated tyrosine and the related C-terminal residue. When it turns to SAP, the interface with its ligand (SLAM) involves an additional interaction between the SH2 domain and residues located N-terminal to the phosphotyrosine, generating a ‘three-pronged’ association. The presence of this third interaction considerably potentiates the affinity of the SH2 domain of SAP for SLAM (K_d120–150 nm; compared to K_d500 nm for traditional SH2 domains) [25]. On the other hand, SAP not only binds to SLAM but also works as an adapter protein by interacting with the protein tyrosine kinase Fyn. The interaction between SAP and Fyn involves the arginine residue in position 78 while SAP– SLAM interaction happens at position 32 (Figure 1A). This allows SAP to simultaneously

bind SLAM and Fyn to form a trimeric complex [26,27]. Fyn contributes both to the phosphorylation of SLAM and to the recruitment of further signalling intermediates leading to the activation of downstream pathways essential for SLAM receptor functions [28–30]. In vivo experiments on both Fyn-silenced and SAP-silenced mice demonstrated that both NK-mediated cytotoxicity and cytokine production were compromised, suggesting that the association between the two proteins is required for NK-cell activation [31].

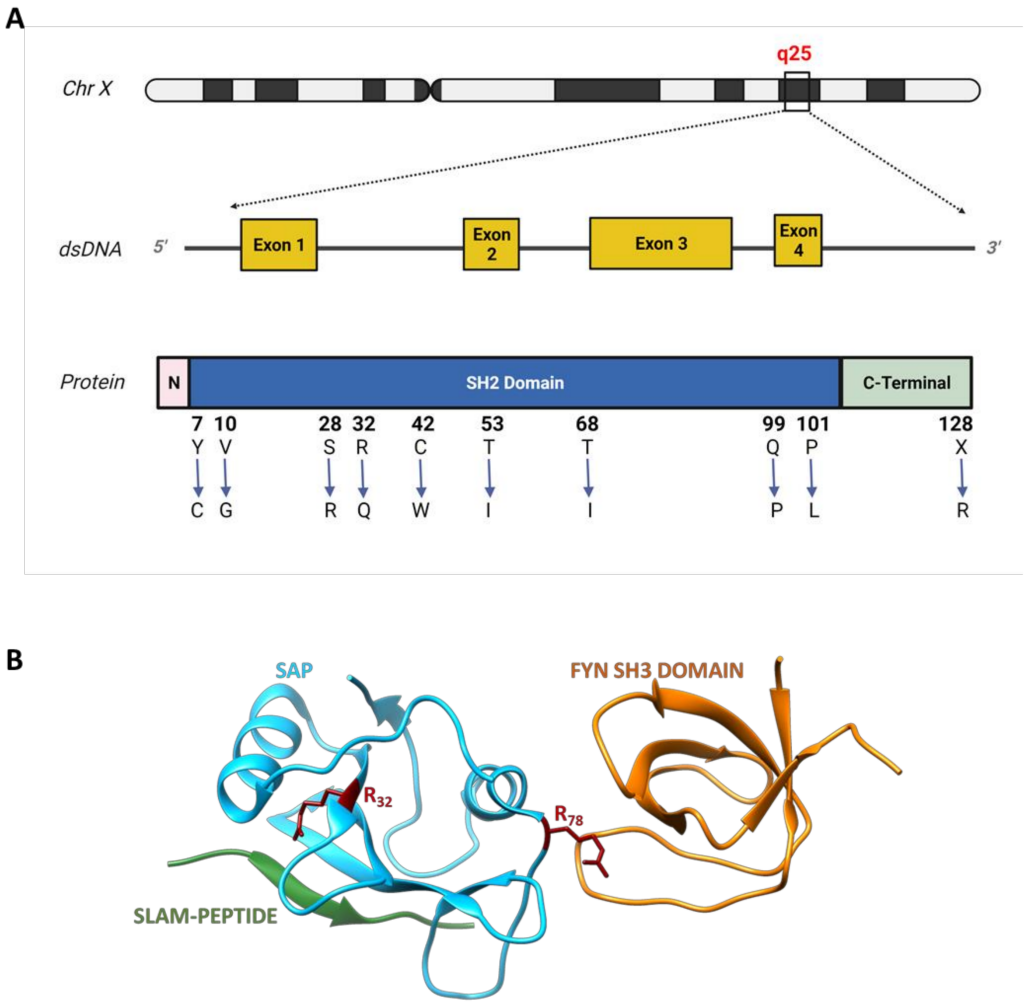

Figure 1. Schematic representation of SH2D1A gene with some missense mutations and the SAP protein structure. (**A**) The SAP gene and the corresponding protein are represented, showing an N-terminal (pink) region encoded by the exon 1, a central SH2 region (blue), encoded by exons 1,2 and 3 and a C-terminal region (light green) encoded both by exon 3 and 4 (exons are represented in yellow and indicated with a number in squares). Ten missense mutations on SAP SH2 and C-terminal domains affecting protein stability (Y_7C, $V_{10}G$, $S_{28}R$, $Q_{99}P$, $P_{101}L$, $X_{128}R$), and binding ability to both phosphorylated ($R_{32}Q$, $C_{42}W$) and unphosphorylated ($R_{32}Q$, $C_{42}W$, $T_{53}I$, $T_{68}I$) forms of SLAM are shown. (**B**) The 3D structure of SAP (light blue), in a trimeric complex with SLAM-PEPTIDE (green) and the SH3 domain of Fyn (orange) is showed [27]. The two arginine residues in positions 32 and 78, are shown (red) which are reported to play a critical role in the binding with SLAM and Fyn, respectively.

More than 50 mutations affecting the SH2D1A gene have been identified in XLP-1 patients, including micro/macro deletions, splice mutations, nonsense mutations and missense mutations, resulting in either partial or complete loss of the genetic product. Several missense mutations have been observed and characterized in vivo and in vitro to assess the mutants' stability as well as their ability in binding SLAM [32]. Therefore,

these mutations can be classified according to their ability to influence protein stability (by decreasing the half-life), or on their ability to impair the binding to the target proteins. Single amino acid substitution such as Y_7C, $V_{10}G$, $S_{28}R$, $Q_{99}P$, $P_{101}L$ and $X_{128}R$ in the SAP SH2 domain (Figure 1B) disrupt hydrophilic bonding resulting in a shorter half-life of the protein. Similarly, the substitution of the proline at the C-terminus of the SH2 domain with a leucine ($P_{101}L$) is responsible for a different protein folding, probably resulting in a less stable product. Conversely, amino acid substitutions like $R_{32}Q$ and $C_{42}W$ (Figure 1B) selectively obstruct the SH2 phosphotyrosine binding pocket, resulting in a lower binding efficiency both to the phosphorylated and unphosphorylated form of SLAM [32]. Indeed, the Y_{32} residue is also highly conserved in other proteins containing the SH2 domain and it is tightly required for phosphotyrosine recognition and binding. Two other important substitutions are $T_{53}I$ and $T_{68}I$ (Figure 1B) which compromise SAP binding abilities to the unphosphorylated form of SLAM, without affecting its half-life. T_{68} is localized close to amino acids involved in residue +3 binding and its substitution with isoleucine drastically affects binding to SLAM [24].

3. Signalling Defects in XLP-1 and Their Biological Effects

The ability of SAP to bind to specific ITMS present in the cytoplasmic portion of SLAM family proteins couples the Src-family kinase Fyn to the SLAM receptors through non-canonical surface-surface interactions between SAP SH2 domain and Fyn SH3 domain [27]. Thus, the activated Fyn kinase phosphorylates several downstream effectors such as Dok1, Dok2 and SH2 containing inositol phosphatase (SHIP), resulting in NFB signalling activation and IFN- production [33,34]. Interestingly, Cannons et al., demonstrated that in $CD4^+$ cells NFB activation is mediated by PKC, which is recruited by the SAP/Fyn pathway (Figure 2). Consequently, in SAP or Fyn deficient conditions this signalling is strongly impaired and IL-4 production is compromised [30] (Figure 3A). In the following studies, by pull-downs and co-immunoprecipitation assays, they demonstrated that SAP constitutively binds to PKC independently by Fyn interaction and that this SAP- PKC association triggers a signal transduction which leads to IL-4 expression upon T-cell stimulation [35]. In particular, the obtained data indicates that R_{78} in SAP sequence plays a key role in the formation of this complex, and interestingly, it has been shown that this residue also mediates an association with the SH3 domain of PAK-interacting exchange factor (PIX), promoting the formation of a trimeric complex SAP-PIX-Cdc42 [36]. Furthermore, through a screening of regulatory proteins containing the SH3 domain, Li and colleagues identified NCK Adaptor Protein 1 (NCK1) as a novel SAP binding partner, observing that the knock-down of SAP reduced phosphorylation of NCK1 and other proteins downstream to TCR signalling, including LAT and SLP-76, resulting in decreased cell proliferation and ERK pathway activation [37].

However, SAP not only acts as an adaptor protein, but also as a key regulator for the balance between activating and inhibitory signals downstream SLAM receptors, as it has been demonstrated that its binding ITSM sequences prevent the recruitment of both SHIP and SHP-2 by competition, blocking the phosphatase's inhibitory functions [34,38] (Figure 2). Interestingly, it has been shown that, in SAP-deficient conditions, the interaction between SHP-1/SHP-2 with SLAM receptors may have a role in reducing TCR signalling intensity [31,39]. Furthermore, SAP has been identified as a direct binding partner of the ITAM sequences of the CD3 chain in the proximal portion of the cell membrane. In line with this, studies by Proust and colleagues indicates that SAP silencing reduces various TCR signalling pathways, such as ERK, Akt and PLC1 and decreases both IL-2 and IL-4 mRNA production [40] (Figure 3A). Interestingly, it has been observed that SAP can also interact with some adhesion molecules such as platelet–endothelial cell adhesion molecule-1 (PECAM-1) through the phosphorylated tyrosine 686, mediating adhesion processes in T cells. CD3 and PECAM-1 binding suggest that SAP is also involved in other signalling pathways not implicated in SLAM-receptor functions [41].

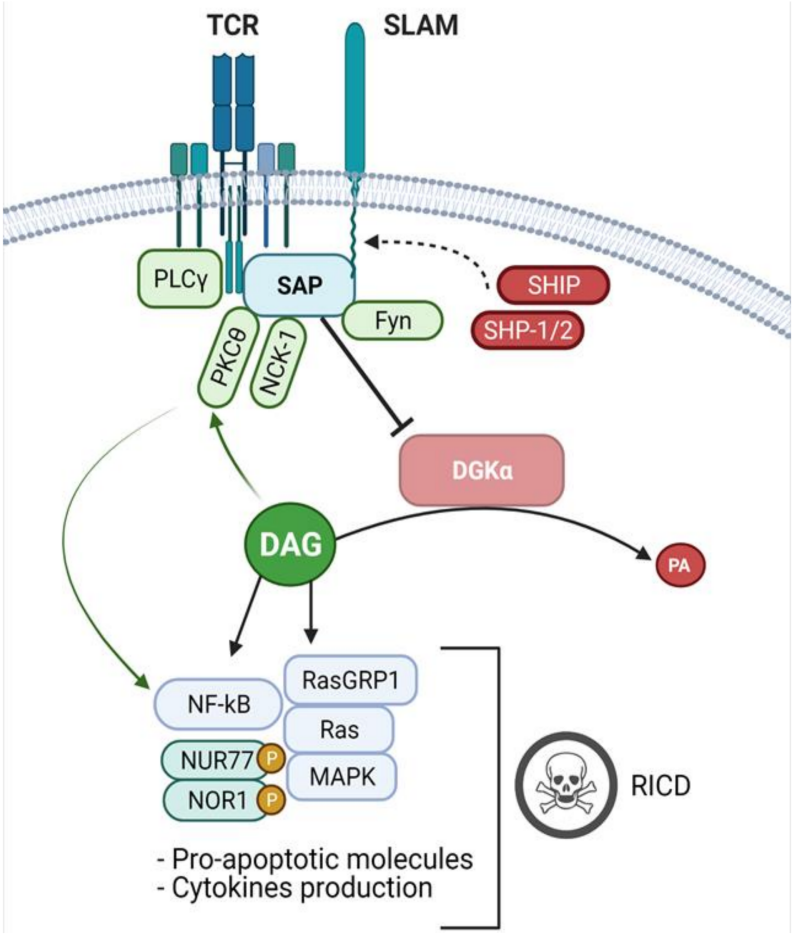

Figure 2. SAP signalling and DGK inhibition. Upon TCR stimulation, the adaptor protein SAP binds to ITSMs sequences on the cytoplasmic tail of the SLAM-family and other receptors, competing with SHIP and SHP-1/2 phosphatases and promoting activator signals. At the membrane, SAP interacts with different binding partners, such as the FYN Kinase, PKC and NCK1, involved in T-cell activation. Moreover, SAP mediates the inhibition of DGK, resulting in an accumulation of PLC-derived DAG, leading to MAPK pathway activation, pro-apoptotic molecules expression and cytokines production. Furthermore, the increased levels of DAG enhance PKC activity re-sulting in signalling which potentiates NFB activation. In antigen-experienced $CD8^+$ cells, these events trigger the RICD program, which promotes effector T-cells clearance and prevents excessive lymphoproliferation.

In line with reduced signalling, in absence of SAP, CTLs also show an impaired restimulation-induced cell death (RICD), a particular kind of apoptosis that constitutes an autoregulatory mechanism to prevent excessive lymphoproliferation and maintain cell homeostasis (Figure 3A). Results obtained by Snow et al. strongly indicate that T cell restimulation triggers apoptosis only when a certain threshold is reached. The authors suggest that SAP may act as a signal amplifier that increases the TCR strength up to the threshold required for RICD, resulting in an increased expression of pro-apoptotic molecules such as FASL and BIM. Conversely, in SAP-deficient conditions, the TCR signal strength is attenuated below the threshold, allowing T-lymphocytes to escape cell death [42] (Figure 3A). Notably, it has been shown that upon TCR stimulation, SAP mediates the association of LCK with the SLAM family receptor NK, T, and B Ag (NTB-A), enhancing pro-apoptotic signals in human T-cells. This signalling complex amplifies the TCR signalling, thereby promoting RICD in SAP dependent manner. Conversely, in SAP deficient conditions, the association between LCK and NTB-A is impaired resulting in reduced TCR strength contributing to RICD resistant cell phenotype [43]. In addition, it has been demonstrated that

SAP can also associate with inhibitory T-cell receptors, such as programmed cell death-1 (PD-1). Through affinity purification and mass spectrometry analysis, Peled and colleagues demonstrated that SAP counteracts PD-1 inhibitory functions in T cells, blocking SHP-2 activation [44]. Thus, in the following study conducted on rheumatoid arthritis patients, the same authors confirm that SAP exerts an inhibitory effect on the PD-1 signalling pathway preventing SHP-2 dephosphorylation on tyrosine 173 of the CD28 receptor. The authors propose a mechanism by which rheumatoid arthritis T cells increase SAP expression or block its degradation in order to avoid PD-1 mediated exhaustion [45].

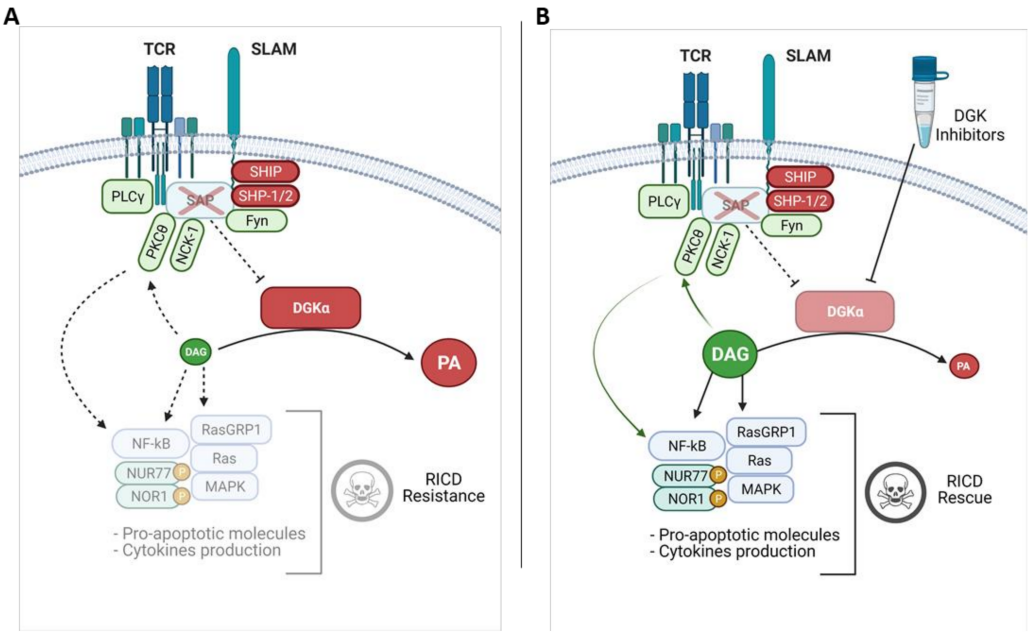

Figure 3. Reduced DAG signalling in XLP-1 and effects of DGK inhibitors. (**A**) In XLP-1 lymphocytes, the absence of SAP allows the binding of SHIP or SHP-1/2 phosphatases to SLAM family receptor ITSMs, promoting the transduction of inhibitory signals which attenuate the TCR signaling strength. In SAP-deficient conditions, DGK shows increased activity and metabolizes DAG, contributing to RICD resistance. (**B**) This defect can be rescued by treating the cells with DGK inhibitors which restore DAG signalling. DAG mediated PKC and MAPK activation leads to NUR77/NOR1 expression and phosphorylation, promoting RICD.

In the XLP syndrome context, SAP mutations are mostly loss of function and the biological effects derived from this immune defect have been investigated in recent years. Cells derived by SAP-deficient murine models exhibit functional dysregulations in both $CD4^+$ and $CD8^+$ T cells, impaired IL-4 IL-13 and IL-10 cytokines production, altered germinal-centre formation and a reduced response to TCR mediated cell activation [46]. Furthermore, XLP patients are characterized by a reduced number of $CD4^+$ T cells displaying a T helper 2 phenotypes, as well as by a loss of circulating memory B cells and iNKT cells [47,48]. SAP-deficient $CD8^+$ T cells show specific defects in their cytotoxic activity [49–51], while $CD4^+$ have reduced activity in supporting B cell maturation [52,53]. Those defects are due to impaired/transient immunological synapse (IS) formation and an inefficient actin clear-ance from the IS central region. Indeed, Zhao et al., demonstrated that SAP is essentially required for effective T-B cell interaction and killing of EBV infected B cell targets. The authors provide evidence that in absence of SAP, the association between SHP-1 and SLAM receptors increases, promoting a negative signal which results in decreased activation of Src family kinases and tyrosine phosphorylation (Figure 3A), both crucial events in early IS formation. Conversely, in the presence of SAP, TCR-mediated positive signals are enhanced and CTL functions are more effective (Figure 2). These data highlight the essential role of SAP and SLAM family proteins in regulating positive and negative signals required for IS organization and CTLs lytic function [48].

Summarizing, SAP is a key multi-functional protein exerting specific roles in different signalling pathways downstream the TCR/SLAM receptors protein family. In absence of SAP, signalling is severely perturbed, impairing T cell and NK homeostasis and function.

4. SAP Controls DGK Activity and DAG Dependent Signalling

Triggering of the TCR promotes a rapid and sustained translocation of DGK and DGK to the plasma membrane [54–56]. While DGK is distributed to all of the cell membrane, DGK is driven at the periphery of the immune synapse [57] by the combined action of calcium binding to the EF-hands motifs, phosphorylation of tyrosine 335 by Lck [54,58] and a still partially characterized interaction with phosphatidylinositol 3 kinase (PI3K) products [57,59]. Despite its abundance and membrane recruitment, DGK plays a quantitatively minor role in DAG metabolism in T cells [60,61] suggesting the existence of some mechanism to finely tune its activity and restricting it at the periphery of IS and some intracellular membranes [57,62]. Indeed, we and others have observed that DGK but not DGK is inhibited upon T cell triggering with strong TCR agonist antibodies or upon TCR/CD28 co-stimulation. This DGK inhibition is required to obtain a full T cell response [2,15,63]. The molecular mechanism involved in negatively regulating DGK activity is still unknown but our observations indicated that it requires PLC activity and calcium, suggesting that this happens at the membrane in proximity of the receptor. Using inhibitors we excluded the involvement of either Src family kinases or PI3K activity [2]. Notably, this inhibition can be induced by triggering a recombinant SLAM receptor or by overexpressing SAP. This observation coupled with the finding that SAP is necessary for DGK inhibition upon TCR/CD28 co-stimulation clearly indicates a central role of SAP in promoting DGK inhibition (Figure 2) [2]. However, a direct SAP-DGK interaction was not observed, as ITMS are not present on DGK. The observation that SAP mutants $R_{55}L$ and $R_{76}A$, defective in respectively phosphotyrosine binding and downstream effector recruitment, are not capable of DGK inhibition, suggests that SAP acts by recruiting further unidentified mediators. The critical effector is not Fyn as Src family activity activates DGK [64] and Src family inhibitor PP2 does not affect DGK inhibition triggered by TCR/CD28, while the effect of PP2 on DGK inhibition induced by SLAM receptors may be due to their intrinsic dependence on Fyn for signal transduction [2].

The observation that, in the absence of SAP, DGK is predominantly active, suggests that the signalling defects observed in T cells from XLP-1 patients are in part due to DAG metabolism by DGK and can be restored by DGK inhibition (Figure 3A,B). Indeed, DGK inhibitors or DGK silencing restore DAG accumulation at the IS and the polariza-tion of T cells toward B cell targets. They also rescue DAG dependent recruitment of PKC and RasGRP1, which drives Ras and the MAPK pathway along with promoting NFAT transcriptional activity and the expression of IL-2 and CD25 (Figure 3B). Intriguingly, the signalling rescue is not total, as BIM and Fas ligand expression remain downregulated in SAP deficient cells despite DGK silencing/inhibition, indicating the existence of TCR signalling pathways that are SAP mediated but DGK independent [2,16].

5. DGK and DGK Inhibitors as Potential XLP-1 Therapies

The rescue of DAG signalling obtained by targeting DGK in SAP deficient cells is sufficient to restore both cytotoxic activity towards B-cell targets and RICD (Figure 3B). The restoring of RICD requires PKC and MAPK pathway activity. Those pathways trigger the intrinsic apoptosis pathway by enhancing DAG-mediated induction of NUR77 (NR4A1) and NOR1 (NR4A3) and their phosphorylation via MAPK-regulated 90-kD ribosomal S6 kinase (RSK) (Figure 3B) [16]. Phosphorylated NUR77 is known to exit from the nucleus and promote transition pore opening [65], thus promoting apoptosis despite the lack of FAS ligand and BIM induction in SAP deficient lymphocytes.

Thus, targeting DGK activity in SAP deficient cells emerged as a promising strat-egy for XLP-1 therapy (an unmet clinical need). However, pharmacological targeting of DGK is quite challenging, as there is no detailed structural information on DGK cat-

alytic domain allowing rational drug design to develop new inhibitors and or refine their specificity against a single isoform. Thus far, a few DGK inhibitors have been discovered, but their limitations, such as off-target effects, lack of selectivity, low potency and poor pharmacokinetic properties, limit their clinical use [66].

The two commercially available allosteric DGK inhibitors, 3-[2-[4-(bis(4-Fluorophenyl) methylene)-1-piperidinyl]ethyl]-2,3-dihydro-2-thioxo-4(1H)-quinazolinone (R59949) [67] and 6-(2-(4-[(4-fluorophenyl)phenylmethylene]-1-piperidinyl)ethyl)-7-methyl-5H-thiazolo (3,2-a)pyrimidin-5-one (R59022) [68] are widely used in vitro. Both these inhibitors can revert the RICD defects in SAP deficient lymphocytes [16]. Furthermore, R59022 also showed beneficial effects in an in vivo model of XLP-1 [16]. In LCMV infected SH2D1A$^{-/-}$ mice, R59022 (2 mg/kg) significantly reduced the activated CD8^{+} T-cells number along with lowering liver lymphocytic infiltrates and reducing serum IFN levels [16]. However, along with their poor pharmacological properties, both R59022 and R59949 exhibits serotonin antagonism which makes their use in human patients unlikely [69].

Ritanserinis a well-known serotonin receptor antagonist with a strong structural similarity with both R59022 and R59949. Indeed, ritanserin and its chemical fragment, RLM001, were reported as DGK inhibitors with high selectivity towards isoform [69,70]. Ritanserin is a very promising compound for drug repurposing or repositioning, as it showed utility in glioblastoma animal models and trough clinical trials for the treatment of psychic disorders like alcohol dependence and schizophrenia, and was proved to be safe for human use [71]. On the other hand, some interesting compounds, CU-3 (5-((2E)-3-(2-furyl)prop-2-enylidene)-3-[(phenylsulfonyl)amino]s-2-thioxo-1,3-thiazolidin-4-one) and compound A were identified which selectively inhibited DGK with very low IC_{50} values [72,73]. Previous studies from our group showed that similar to R59^{6}s, both ritansern and CU-3 rescued the RICD defects in the XLP-1 phenotype [16,74]. However, being a selective 5-HT2A and 5-HT2C serotonin receptor antagonist, ritanserin actions on the central nervous system may limit its use for XLP-1 therapy [69]. Similarly, the structure and high reactivity of CU-3 constrained its utility in in vivo applications [74].

Sequentially, through virtual screening, we identified Amb639752 (1-(2,6-dimethyl-1H-indol-3-yl)-2-[4-(furan-2-ylcarbonyl)piperazin-1-yl]ethenone) as a novel DGK inhibitor [74]. Structure-activity-relationship studies on Amb639752 resulted in compound 11 and 20 which are highly active in inhibiting DGK [75]. Even though they have some 3D structural similarities to R59949, Amb639752 and its analogues do not affect serotonin receptors [74,75]. The high specificity towards DGK isoform and no off-target properties against serotonin receptors makes this molecule an interesting tool in terms of DGK inhibition. Moreover, Amb639752 and its analogues rescued the RICD defects in SAP deficient lymphocytes without affecting RICD sensitivity in control lymphocytes, indicating their potential utility in treating XLP-1 patients [74,75]. Similar to ritanserin and R59s, Amb639752 can promote pro-apoptotic activity through the induction of NUR 77 (NR4A1) and NOR1 (NR4A3), suggesting that this is the main pathway through which DGK inhibition restores RICD defects in XLP-1 [16,74]. However, like other DGK inhibitors, Amb639752 and its daughter molecules have some drawbacks. Even though they have high efficiency in targeting DGK, these molecules proved to be effective only in a micromolar (M) range. In the absence of in vivo and clinical studies, their utility is limited to in vitro experiments. Nevertheless, the pharmacophoric model, resulting from those studies, may be of great help in identifying novel DGK inhibitors that might be suitable for clinical use [76,77].

Notably, Ruffo et.al., reported that along with DGK, silencing DGK also restores the RICD defects in SAP deficient lymphocytes even if DGK is not regulated by SAP [16]. Lack of specific DGK inhibitors never allowed us to test the hypothesis of pharmacological inhibition of DGK in rescuing RICD defects. Recently, substituted naphthyridinone derivatives have been patented as novel T cell activators that can inhibit both DGK and DGK simultaneously with low toxicity in vitro, and in stability and bioavailability profiles [78]. Even though those patented molecules target both and DGK isoforms

with very attractive IC_{50} values, the lack of in vivo and pharmacological studies constrains their utility in clinics.

Conversely, other reports suggested the utility of SHP-2 inhibitors in XLP-1 conditions to restore the SAP deficiency defects. In XLP-1 patients where SAP is not expressed, the tyrosines on SLAM family members bind to several strong inhibitory molecules, especially SHP-1 and SHP-2 [31,48,79,80] which essentially block activation, development and function of T and NK cells [34]. Notably, in vitro targeting of SHP-1/SHP-2 rescued the cytolytic activity of SAP deficient cells against murine B-cells [48]. Several chemical small molecules have been identified as SHP-2 inhibitors in recent times and are reported to have positive effects in cancer cell lines in vitro. In particular, the SHP-2 inhibitors, SHP099 (100 mg/kg), and FGF401 (30 mg/kg) are used in vivo in FGFR-driven cancer mice mod-els [81]. Furthermore, TNO155, RMC-4630, JAB-3312 and JAB-3068 are other available validated SHP-2 inhibitors that are in advanced clinical trials for the treatment of various cancers [76,77]. To our knowledge, none of those inhibitors was tested in XLP-1 models until now.

6. Discussion

The current treatments of choice for XLP-1 aim to contain the life-threatening development of EBV-induced HLH and the frequently arising lymphomas. Patients surviving HLH as well as asymptomatic ones are candidates for allogeneic hematopoietic stem cell transplant that has a consistent percentage of failures [82]. To face the unmet clinical needs of XLP-1 patients, several researchers aim for gene therapy/gene editing approaches that are still in the preclinical phase [83].

The idea of using small molecules to correct the signalling defects of SAP deficient cells was never translated in the clinic. Preclinical studies by our and other groups have developed DGK, DGK and SHP-2 inhibitors that are, in principle, suitable for human use, but there are no registered trials with small molecules in XLP-1. This may be due to the incomplete knowledge of disease pathogenetic mechanisms but also the typical problems of translational research on rare diseases surely contribute. Indeed, XLP-1 patients are, by definition, rare and referred to several centres randomly. At diagnosis patients with HLH are typically very severe, requiring intensive treatment regimens followed by bone marrow transplant, while the treatment of asymptomatic brothers requires careful evaluation from an ethical point of view. Moreover, the efforts to develop patients' registries to track disease natural history and eventually verify treatment efficacy are still really fragmented.

It is interesting to speculate that the role played by DGK activity in rising TCR signalling threshold and promoting RICD resistance may not be unique for XLP-1. Indeed, similar TCR signalling defects give rise to immunodeficiencies with or without EBV-induced HLH [84]. Some monogenic diseases are expected to present reduced TCR-induced DAG signalling such as Zap-70 deficiency, interleukin-2-inducible T-cell kinase (ITK) deficiency, X-linked immunodeficiency with magnesium defect (XMEN) or Wiskott Aldrich syndrome (WAS), and thus may be in principle compensated by DGK targeting. The clarification of the signalling mechanisms that lead to inhibition of DGK would allow this lipid kinase to be positioned better in the TCR signalosome and to identify the primary immunodeficiencies that apart from SAP are characterized by excessive DGK activity and thus potentially targeted by the DGK inhibitors currently under development.

Author Contributions: G.B. conceived the study and raised funds, S.V., S.C., F.G. and G.B. wrote the article, All authors have read and agreed to the published version of the manuscript.

Funding: This research was funded by the Italian Ministry of Education, University and Research program PRIN 2017 (grant 201799WCRH), Telethon Foundation [Grant GGP16252], AGING Project Department Translational Medicine University Piemonte Orientale FAR-2017, and by Consorzio Interuniversitario di Biotecnologie (CIB).

Institutional Review Board Statement: Not applicable.

Informed Consent Statement: Not applicable.

Data Availability Statement: Data sharing not applicable.

Acknowledgments: We thanks Andrea Graziani for the helpful discussion and BioRender software for the scientific graphic illustrations.

Conflicts of Interest: The authors declare no conflict of interest. The funders had no role in the design of the study; in the collection, analyses, or interpretation of data; in the writing of the manuscript, or in the decision to publish the results.

References

1. Snow, A.L.; Pandiyan, P.; Zheng, L.; Krummey, S.M.; Lenardo, M.J. The power and the promise of restimulation-induced cell death in human immune diseases. Immunol. Rev. **2010**, 236, 68–82. [CrossRef]
2. Baldanzi, G.; Pighini, A.; Bettio, V.; Rainero, E.; Traini, S.; Chianale, F.; Porporato, P.E.; Filigheddu, N.; Mesturini, R.; Song, S.; et al. SAP-mediated inhibition of diacylglycerol kinase regulates TCR-induced diacylglycerol signaling. J. Immunol. **2011**, 187, 5941–5951. [CrossRef]
3. Carrasco, S.; Mérida, I. Diacylglycerol, when simplicity becomes complex. Trends Biochem. Sci. **2007**, 32, 27–36. [CrossRef]
4. Fu, G.; Chen, Y.; Yu, M.; Podd, A.; Schuman, J.; He, Y.; Di, L.; Yassai, M.; Haribhai, D.; North, P.E.; et al. Phospholipase C{gamma}1 is essential for T cell development, activation, and tolerance. J. Exp. Med. **2010**, 207, 309–318. [CrossRef]
5. Huang, Y.H.; Sauer, K. Lipid signaling in T-cell development and function. Cold Spring Harb. Perspect. Biol. **2010**, 2, a002428. [CrossRef]
6. Augsten, M.; Pusch, R.; Biskup, C.; Rennert, K.; Wittig, U.; Beyer, K.; Blume, A.; Wetzker, R.; Friedrich, K.; Rubio, I. Live-cell imaging of endogenous Ras-GTP illustrates predominant Ras activation at the plasma membrane. EMBO Rep. **2006**, 7, 46–51. [CrossRef] [PubMed]
7. Ebinu, J.O.; Stang, S.L.; Teixeira, C.; Bottorff, D.A.; Hooton, J.; Blumberg, P.M.; Barry, M.; Bleakley, R.C.; Ostergaard, H.L.; Stone, J.C. RasGRP links T-cell receptor signaling to Ras. Blood **2000**, 95, 3199–3203. [CrossRef] [PubMed]
8. Newton, A.C. Protein kinase C: Perfectly balanced. Crit. Rev. Biochem. Mol. Biol. **2018**, 53, 208–230. [CrossRef]
9. Krishna, S.; Zhong, X. Role of diacylglycerol kinases in T cell development and function. Crit. Rev. Immunol. **2013**, 33, 97–118. [CrossRef] [PubMed]
10. Zha, Y.; Marks, R.; Ho, A.W.; Peterson, A.C.; Janardhan, S.; Brown, I.; Praveen, K.; Stang, S.; Stone, J.C.; Gajewski, T.F. T cell anergy is reversed by active Ras and is regulated by diacylglycerol kinase-alpha. Nat. Immunol. **2006**, 7, 1166–1173. [CrossRef]
11. Arranz-Nicolás, J.; Martin-Salgado, M.; Adán-Barrientos, I.; Liébana, R.; Del Carmen Moreno-Ortíz, M.; Leitner, J.; Steinberger, P.; Ávila-Flores, A.; Merida, I. Diacylglycerol kinase inhibition cooperates with PD-1-targeted therapies to restore the T cell activation program. Cancer Immunol. Immunother. **2021**. [CrossRef]
12. Olenchock, B.A.; Guo, R.; Carpenter, J.H.; Jordan, M.; Topham, M.K.; Koretzky, G.A.; Zhong, X.P. Disruption of diacylglycerol metabolism impairs the induction of T cell anergy. Nat. Immunol. **2006**, 7, 1174–1181. [CrossRef]
13. Zhong, X.P.; Hainey, E.A.; Olenchock, B.A.; Jordan, M.S.; Maltzman, J.S.; Nichols, K.E.; Shen, H.; Koretzky, G.A. Enhanced T cell responses due to diacylglycerol kinase zeta deficiency. Nat. Immunol. **2003**, 4, 882–890. [CrossRef]
14. Baldanzi, G.; Ragnoli, B.; Malerba, M. Potential role of diacylglycerol kinases in immune-mediated diseases. Clin. Sci. **2020**, 134, 1637–1658. [CrossRef] [PubMed]
15. Arranz-Nicolás, J.; Ogando, J.; Soutar, D.; Arcos-Pérez, R.; Meraviglia-Crivelli, D.; Mañes, S.; Mérida, I.; Ávila-Flores, A. Diacylglycerol kinase inactivation is an integral component of the costimulatory pathway that amplifies TCR signals. Cancer Immunol. Immunother. **2018**, 67, 965–980. [CrossRef] [PubMed]
16. Ruffo, E.; Malacarne, V.; Larsen, S.E.; Das, R.; Patrussi, L.; Wülfing, C.; Biskup, C.; Kapnick, S.M.; Verbist, K.; Tedrick, P.; et al. Inhibition of diacylglycerol kinase restores restimulation-induced cell death and reduces immunopathology in XLP-1. Sci Transl Med. **2016**, 8, 321ra7. [CrossRef] [PubMed]
17. Tangye, S.G. XLP: Clinical features and molecular etiology due to mutations in SH2D1A encoding SAP. J. Clin. Immunol. **2014**, 34, 772–779. [CrossRef] [PubMed]
18. Purtilo, D.T.; Cassel, C.K.; Yang, J.P.; Harper, R. X-linked recessive progressive combined variable immunodeficiency (Duncan's disease). Lancet **1975**, 1, 935–940. [CrossRef]
19. Gaspar, H.B.; Sharifi, R.; Gilmour, K.C.; Thrasher, A.J. X-linked lymphoproliferative disease: Clinical, diagnostic and molecular perspective. Br. J. Haematol. **2002**, 119, 585–595. [CrossRef] [PubMed]
20. Nichols, K.E.; Ma, C.S.; Cannons, J.L.; Schwartzberg, P.L.; Tangye, S.G. Molecular and cellular pathogenesis of X-linked lymphoproliferative disease. Immunol. Rev. **2005**, 203, 180–199. [CrossRef]
21. Coffey, A.J.; Brooksbank, R.A.; Brandau, O.; Oohashi, T.; Howell, G.R.; Bye, J.M.; Cahn, A.P.; Durham, J.; Heath, P.; Wray, P.; et al. Host response to EBV infection in X-linked lymphoproliferative disease results from mutations in an SH2-domain encoding gene. Nat. Genet. **1998**, 20, 129–135. [CrossRef]
22. Sayos, J.; Wu, C.; Morra, M.; Wang, N.; Zhang, X.; Allen, D.; van Schaik, S.; Notarangelo, L.; Geha, R.; Roncarolo, M.G.; et al. The X-linked lymphoproliferative-disease gene product SAP regulates signals induced through the co-receptor SLAM. Nature **1998**, 395, 462–469. [CrossRef]

23. Li, S.C.; Gish, G.; Yang, D.; Coffey, A.J.; Forman-Kay, J.D.; Ernberg, I.; Kay, L.E.; Pawson, T. Novel mode of ligand binding by the SH2 domain of the human XLP disease gene product SAP/SH2D1A. Curr. Biol. **1999**, 9, 1355–1362. [CrossRef]
24. Poy, F.; Yaffe, M.B.; Sayos, J.; Saxena, K.; Morra, M.; Sumegi, J.; Cantley, L.C.; Terhorst, C.; Eck, M.J. Crystal structures of the XLP protein SAP reveal a class of SH2 domains with extended, phosphotyrosine-independent sequence recognition. Mol. Cell **1999**, 4, 555–561. [CrossRef]
25. Latour, S.; Veillette, A. Molecular and immunological basis of X-linked lymphoproliferative disease. Immunol. Rev. **2003**, 192, 212–224. [CrossRef] [PubMed]
26. Latour, S.; Gish, G.; Helgason, C.D.; Humphries, R.K.; Pawson, T.; Veillette, A. Regulation of SLAM-mediated signal transduction by SAP, the X-linked lymphoproliferative gene product. Nat. Immunol. **2001**, 2, 681–690. [CrossRef] [PubMed]
27. Chan, B.; Lanyi, A.; Song, H.K.; Griesbach, J.; Simarro-Grande, M.; Poy, F.; Howie, D.; Sumegi, J.; Terhorst, C.; Eck, M.J. SAP couples Fyn to SLAM immune receptors. Nat. Cell Biol. **2003**, 5, 155–160. [CrossRef] [PubMed]
28. Dragovich, M.A.; Mor, A. The SLAM family receptors: Potential therapeutic targets for inflammatory and autoimmune diseases. Autoimmun. Rev. **2018**, 17, 674–682. [CrossRef]
29. Davidson, D.; Shi, X.; Zhang, S.; Wang, H.; Nemer, M.; Ono, N.; Ohno, S.; Yanagi, Y.; Veillette, A. Genetic evidence linking SAP, the X-linked lymphoproliferative gene product, to Src-related kinase FynT in T(H)2 cytokine regulation. Immunity **2004**, 21, 707–717. [CrossRef]
30. Cannons, J.L.; Yu, L.J.; Hill, B.; Mijares, L.A.; Dombroski, D.; Nichols, K.E.; Antonellis, A.; Koretzky, G.A.; Gardner, K.; Schwartzberg, P.L. SAP regulates T(H)2 differentiation and PKC-theta-mediated activation of NF-kappaB1. Immunity **2004**, 21, 693–706. [CrossRef]
31. Dong, Z.; Davidson, D.; Pérez-Quintero, L.A.; Kurosaki, T.; Swat, W.; Veillette, A. The adaptor SAP controls NK cell activation by regulating the enzymes Vav-1 and SHIP-1 and by enhancing conjugates with target cells. Immunity **2012**, 36, 974–985. [CrossRef]
32. Morra, M.; Simarro-Grande, M.; Martin, M.; Chen, A.S.; Lanyi, A.; Silander, O.; Calpe, S.; Davis, J.; Pawson, T.; Eck, M.J.; et al. Characterization of SH2D1A missense mutations identified in X-linked lymphoproliferative disease patients. J. Biol. Chem. **2001**, 276, 36809–36816. [CrossRef]
33. Sylla, B.S.; Murphy, K.; Cahir-McFarland, E.; Lane, W.S.; Mosialos, G.; Kieff, E. The X-linked lymphoproliferative syndrome gene product SH2D1A associates with p62dok (Dok1) and activates NF-kappa B. Proc. Natl. Acad. Sci. USA **2000**, 97, 7470–7475. [CrossRef] [PubMed]
34. Shlapatska, L.M.; Mikhalap, S.V.; Berdova, A.G.; Zelensky, O.M.; Yun, T.J.; Nichols, K.E.; Clark, E.A.; Sidorenko, S.P. CD150 association with either the SH2-containing inositol phosphatase or the SH2-containing protein tyrosine phosphatase is regulated by the adaptor protein SH2D1A. J. Immunol. **2001**, 166, 5480–5487. [CrossRef]
35. Cannons, J.L.; Wu, J.Z.; Gomez-Rodriguez, J.; Zhang, J.; Dong, B.; Liu, Y.; Shaw, S.; Siminovitch, K.A.; Schwartzberg, P.L. Biochemical and genetic evidence for a SAP-PKC-theta interaction contributing to IL-4 regulation. J. Immunol. **2010**, 185, 2819–2827. [CrossRef] [PubMed]
36. Gu, C.; Tangye, S.G.; Sun, X.; Luo, Y.; Lin, Z.; Wu, J. The X-linked lymphoproliferative disease gene product SAP associates with PAK-interacting exchange factor and participates in T cell activation. Proc. Natl. Acad. Sci. USA **2006**, 103, 14447–14452. [CrossRef] [PubMed]
37. Li, C.; Schibli, D.; Li, S.S. The XLP syndrome protein SAP interacts with SH3 proteins to regulate T cell signaling and proliferation. Cell Signal. **2009**, 21, 111–119. [CrossRef]
38. Wilson, T.J.; Garner, L.I.; Metcalfe, C.; King, E.; Margraf, S.; Brown, M.H. Fine specificity and molecular competition in SLAM family receptor signalling. PLoS ONE **2014**, 9, e92184. [CrossRef] [PubMed]
39. Kageyama, R.; Cannons, J.L.; Zhao, F.; Yusuf, I.; Lao, C.; Locci, M.; Schwartzberg, P.L.; Crotty, S. The receptor Ly108 functions as a SAP adaptor-dependent on-off switch for T cell help to B cells and NKT cell development. Immunity **2012**, 36, 986–1002. [CrossRef] [PubMed]
40. Proust, R.; Bertoglio, J.; Gesbert, F. The adaptor protein SAP directly associates with CD3 chain and regulates T cell receptor signaling. PLoS ONE **2012**, 7, e43200. [CrossRef] [PubMed]
41. Proust, R.; Crouin, C.; Gandji, L.Y.; Bertoglio, J.; Gesbert, F. The adaptor protein SAP directly associates with PECAM-1 and regulates PECAM-1-mediated-cell adhesion in T-like cell lines. Mol. Immunol **2014**, 58, 206–213. [CrossRef] [PubMed]
42. Snow, A.L.; Marsh, R.A.; Krummey, S.M.; Roehrs, P.; Young, L.R.; Zhang, K.; van Hoff, J.; Dhar, D.; Nichols, K.E.; Filipovich, A.H.; et al. Restimulation-induced apoptosis of T cells is impaired in patients with X-linked lymphoproliferative disease caused by SAP deficiency. J. Clin. Invest. **2009**, 119, 2976–2989. [CrossRef]
43. Katz, G.; Krummey, S.M.; Larsen, S.E.; Stinson, J.R.; Snow, A.L. SAP facilitates recruitment and activation of LCK at NTB-A receptors during restimulation-induced cell death. J. Immunol **2014**, 192, 4202–4209. [CrossRef]
44. Peled, M.; Tocheva, A.S.; Sandigursky, S.; Nayak, S.; Philips, E.A.; Nichols, K.E.; Strazza, M.; Azoulay-Alfaguter, I.; Askenazi, M.; Neel, B.G.; et al. Affinity purification mass spectrometry analysis of PD-1 uncovers SAP as a new checkpoint inhibitor. Proc. Natl. Acad. Sci. USA **2018**, 115, E468–E477. [CrossRef]
45. Sandigursky, S.; Philips, M.R.; Mor, A. SAP interacts with CD28 to inhibit PD-1 signaling in T lymphocytes. Clin. Immunol. **2020**, 217, 108485. [CrossRef] [PubMed]
46. Cannons, J.L.; Tangye, S.G.; Schwartzberg, P.L. SLAM family receptors and SAP adaptors in immunity. Annu. Rev. Immunol. **2011**, 29, 665–705. [CrossRef] [PubMed]

47. Veillette, A. Immune regulation by SLAM family receptors and SAP-related adaptors. Nat. Rev. Immunol. **2006**, 6, 56–66. [CrossRef] [PubMed]
48. Zhao, F.; Cannons, J.L.; Dutta, M.; Griffiths, G.M.; Schwartzberg, P.L. Positive and negative signaling through SLAM receptors regulate synapse organization and thresholds of cytolysis. Immunity **2012**, 36, 1003–1016. [CrossRef]
49. Dupré, L.; Andolfi, G.; Tangye, S.G.; Clementi, R.; Locatelli, F.; Aricò, M.; Aiuti, A.; Roncarolo, M.G. SAP controls the cytolytic activity of CD8+ T cells against EBV-infected cells. Blood **2005**, 105, 4383–4389. [CrossRef] [PubMed]
50. Hislop, A.D.; Palendira, U.; Leese, A.M.; Arkwright, P.D.; Rohrlich, P.S.; Tangye, S.G.; Gaspar, H.B.; Lankester, A.C.; Moretta, A.; Rickinson, A.B. Impaired Epstein-Barr virus-specific CD8+ T-cell function in X-linked lymphoproliferative disease is restricted to SLAM family-positive B-cell targets. Blood **2010**, 116, 3249–3257. [CrossRef]
51. Palendira, U.; Low, C.; Chan, A.; Hislop, A.D.; Ho, E.; Phan, T.G.; Deenick, E.; Cook, M.C.; Riminton, D.S.; Choo, S.; et al. Molecular pathogenesis of EBV susceptibility in XLP as revealed by analysis of female carriers with heterozygous expression of SAP. PLoS Biol. **2011**, 9, e1001187. [CrossRef] [PubMed]
52. Cannons, J.L.; Qi, H.; Lu, K.T.; Dutta, M.; Gomez-Rodriguez, J.; Cheng, J.; Wakeland, E.K.; Germain, R.N.; Schwartzberg, P.L. Optimal germinal center responses require a multistage T cell:B cell adhesion process involving integrins, SLAM-associated protein, and CD84. Immunity **2010**, 32, 253–265. [CrossRef] [PubMed]
53. Qi, H.; Cannons, J.L.; Klauschen, F.; Schwartzberg, P.L.; Germain, R.N. SAP-controlled T-B cell interactions underlie germinal centre formation. Nature **2008**, 455, 764–769. [CrossRef]
54. Merino, E.; Sanjuán, M.A.; Moraga, I.; Ciprés, A.; Mérida, I. Role of the diacylglycerol kinase alpha-conserved domains in membrane targeting in intact T cells. J. Biol. Chem. **2007**, 282, 35396–35404. [CrossRef] [PubMed]
55. Sanjuán, M.A.; Pradet-Balade, B.; Jones, D.R.; Martínez, A.C.; Stone, J.C.; Garcia-Sanz, J.A.; Mérida, I. T cell activation in vivo targets diacylglycerol kinase alpha to the membrane: A novel mechanism for Ras attenuation. J. Immunol. **2003**, 170, 2877–2883. [CrossRef] [PubMed]
56. Gharbi, S.I.; Rincón, E.; Avila-Flores, A.; Torres-Ayuso, P.; Almena, M.; Cobos, M.A.; Albar, J.P.; Mérida, I. Diacylglycerol kinase controls diacylglycerol metabolism at the immunological synapse. Mol. Biol. Cell **2011**, 22, 4406–4414. [CrossRef] [PubMed]
57. Chauveau, A.; Le Floc'h, A.; Bantilan, N.S.; Koretzky, G.A.; Huse, M. Diacylglycerol kinase establishes T cell polarity by shaping diacylglycerol accumulation at the immunological synapse. Sci. Signal. **2014**, 7, ra82. [CrossRef]
58. Merino, E.; Avila-Flores, A.; Shirai, Y.; Moraga, I.; Saito, N.; Mérida, I. Lck-dependent tyrosine phosphorylation of diacylglycerol kinase alpha regulates its membrane association in T cells. J. Immunol. **2008**, 180, 5805–5815. [CrossRef]
59. Ciprés, A.; Carrasco, S.; Merino, E.; Díaz, E.; Krishna, U.M.; Falck, J.R.; Martínez, A.C.; Mérida, I. Regulation of diacylglycerol kinase alpha by phosphoinositide 3-kinase lipid products. J. Biol. Chem. **2003**, 278, 35629–35635. [CrossRef]
60. Ávila-Flores, A.; Arranz-Nicolás, J.; Andrada, E.; Soutar, D.; Mérida, I. Predominant contribution of DGK over DGK in the control of PKC/PDK-1-regulated functions in T cells. Immunol. Cell Biol. **2017**, 95, 549–563. [CrossRef]
61. Joshi, R.P.; Schmidt, A.M.; Das, J.; Pytel, D.; Riese, M.J.; Lester, M.; Diehl, J.A.; Behrens, E.M.; Kambayashi, T.; Koretzky, G.A. The isoform of diacylglycerol kinase plays a predominant role in regulatory T cell development and TCR-mediated ras signaling. Sci. Signal. **2013**, 6, ra102. [CrossRef] [PubMed]
62. Alonso, R.; Mazzeo, C.; Rodriguez, M.C.; Marsh, M.; Fraile-Ramos, A.; Calvo, V.; Avila-Flores, A.; Merida, I.; Izquierdo, M. Diacylglycerol kinase regulates the formation and polarisation of mature multivesicular bodies involved in the secretion of Fas ligand-containing exosomes in T lymphocytes. Cell Death Differ. **2011**, 18, 1161–1173. [CrossRef]
63. Hurttia, H.; Leino, L. Subcellular localization of diacylglycerol kinase activity in stimulated and unstimulated human peripheral blood lymphocytes and neutrophils. Biochem. Mol. Biol. Int. **1996**, 40, 579–585. [CrossRef] [PubMed]
64. Baldanzi, G.; Cutrupi, S.; Chianale, F.; Gnocchi, V.; Rainero, E.; Porporato, P.; Filigheddu, N.; van Blitterswijk, W.J.; Parolini, O.; Bussolino, F.; et al. Diacylglycerol kinase-alpha phosphorylation by Src on Y335 is required for activation, membrane recruitment and Hgf-induced cell motility. Oncogene **2008**, 27, 942–956. [CrossRef] [PubMed]
65. Wang, A.; Rud, J.; Olson, C.M.; Anguita, J.; Osborne, B.A. Phosphorylation of Nur77 by the MEK-ERK-RSK cascade induces mitochondrial translocation and apoptosis in T cells. J. Immunol. **2009**, 183, 3268–3277. [CrossRef]
66. Merida, I.; Arranz-Nicolás, J.; Torres-Ayuso, P.; Ávila-Flores, A. Diacylglycerol Kinase Malfunction in Human Disease and the Search for Specific Inhibitors. Handb. Exp. Pharmacol. **2020**, 259, 133–162. [CrossRef]
67. Jiang, Y.; Sakane, F.; Kanoh, H.; Walsh, J.P. Selectivity of the diacylglycerol kinase inhibitor 3-[2-(4-[bis-(4-fluorophenyl)methylene]-1-piperidinyl)ethyl]-2, 3-dihydro-2-thioxo-4(1H)quinazolinone (R59949) among diacylglycerol kinase subtypes. Biochem. Pharma-col. **2000**, 59, 763–772. [CrossRef]
68. Sato, M.; Liu, K.; Sasaki, S.; Kunii, N.; Sakai, H.; Mizuno, H.; Saga, H.; Sakane, F. Evaluations of the selectivities of the diacylglycerol kinase inhibitors r59022 and r59949 among diacylglycerol kinase isozymes using a new non-radioactive assay method. Pharmacology **2013**, 92, 99–107. [CrossRef]
69. Boroda, S.; Niccum, M.; Raje, V.; Purow, B.W.; Harris, T.E. Dual activities of ritanserin and R59022 as DGK inhibitors and serotonin receptor antagonists. Biochem. Pharmacol. **2017**, 123, 29–39. [CrossRef] [PubMed]
70. McCloud, R.L.; Franks, C.E.; Campbell, S.T.; Purow, B.W.; Harris, T.E.; Hsu, K.L. Deconstructing Lipid Kinase Inhibitors by Chemical Proteomics. Biochemistry **2018**, 57, 231–236. [CrossRef]
71. Audia, A.; Bhat, K.P. Ritanserin, a novel agent targeting the mesenchymal subtype of glioblastomas. Neuro Oncol. **2018**, 20, 151–152. [CrossRef]

72. Liu, K.; Kunii, N.; Sakuma, M.; Yamaki, A.; Mizuno, S.; Sato, M.; Sakai, H.; Kado, S.; Kumagai, K.; Kojima, H.; et al. A novel diacylglycerol kinase -selective inhibitor, CU-3, induces cancer cell apoptosis and enhances immune response. J. Lipid Res. **2016**, 57, 368–379. [CrossRef] [PubMed]
73. Yamaki, A.; Akiyama, R.; Murakami, C.; Takao, S.; Murakami, Y.; Mizuno, S.; Takahashi, D.; Kado, S.; Taketomi, A.; Shirai, Y.; et al. Diacylglycerol kinase -selective inhibitors induce apoptosis and reduce viability of melanoma and several other cancer cell lines. J. Cell Biochem. **2019**, 120, 10043–10056. [CrossRef] [PubMed]
74. Velnati, S.; Ruffo, E.; Massarotti, A.; Talmon, M.; Varma, K.S.S.; Gesu, A.; Fresu, L.G.; Snow, A.L.; Bertoni, A.; Capello, D.; et al. Identification of a novel DGK inhibitor for XLP-1 therapy by virtual screening. Eur. J. Med. Chem. **2019**, 164, 378–390. [CrossRef] [PubMed]
75. Velnati, S.; Massarotti, A.; Antona, A.; Talmon, M.; Fresu, L.G.; Galetto, A.S.; Capello, D.; Bertoni, A.; Mercalli, V.; Graziani, A.; et al. Structure activity relationship studies on Amb639752: Toward the identification of a common pharmacophoric structure for DGK inhibitors. J. Enzym. Inhib. Med. Chem. **2020**, 35, 96–108. [CrossRef]
76. Song, Z.; Wang, M.; Ge, Y.; Chen, X.P.; Xu, Z.; Sun, Y.; Xiong, X.F. Tyrosine phosphatase SHP2 inhibitors in tumor-targeted therapies. Acta Pharm. Sin. B **2021**, 11, 13–29. [CrossRef] [PubMed]
77. LaMarche, M.J.; Acker, M.; Argintaru, A.; Bauer, D.; Boisclair, J.; Chan, H.; Chen, C.H.; Chen, Y.N.; Chen, Z.; Deng, Z.; et al. Identification of TNO155, an Allosteric SHP2 Inhibitor for the Treatment of Cancer. J. Med. Chem. **2020**, 63, 13578–13594. [CrossRef]
78. Abdel-Magid, A.F. Cancer Immunotherapy through the Inhibition of Diacylglycerol Kinases Alpha and Zeta. ACS Med. Chem. Lett. **2020**, 11, 1083–1085. [CrossRef]
79. Tangye, S.G.; Lazetic, S.; Woollatt, E.; Sutherland, G.R.; Lanier, L.L.; Phillips, J.H. Cutting edge: Human 2B4, an activating NK cell receptor, recruits the protein tyrosine phosphatase SHP-2 and the adaptor signaling protein SAP. J. Immunol. **1999**, 162, 6981–6985.
80. Li, C.; Iosef, C.; Jia, C.Y.; Han, V.K.; Li, S.S. Dual functional roles for the X-linked lymphoproliferative syndrome gene product SAP/SH2D1A in signaling through the signaling lymphocyte activation molecule (SLAM) family of immune receptors. J. Biol. Chem. **2003**, 278, 3852–3859. [CrossRef]
81. Lu, H.; Liu, C.; Huynh, H.; Le, T.B.U.; LaMarche, M.J.; Mohseni, M.; Engelman, J.A.; Hammerman, P.S.; Caponigro, G.; Hao, H.X. Resistance to allosteric SHP2 inhibition in FGFR-driven cancers through rapid feedback activation of FGFR. Oncotarget **2020**, 11, 265–281. [CrossRef] [PubMed]
82. Panchal, N.; Booth, C.; Cannons, J.L.; Schwartzberg, P.L. X-Linked Lymphoproliferative Disease Type 1: A Clinical and Molecular Perspective. Front. Immunol. **2018**, 9, 666. [CrossRef] [PubMed]
83. Rivat, C.; Booth, C.; Alonso-Ferrero, M.; Blundell, M.; Sebire, N.J.; Thrasher, A.J.; Gaspar, H.B. SAP gene transfer restores cellular and humoral immune function in a murine model of X-linked lymphoproliferative disease. Blood **2013**, 121, 1073–1076. [CrossRef]
84. Shabani, M.; Nichols, K.E.; Rezaei, N. Primary immunodeficiencies associated with EBV-Induced lymphoproliferative disorders. Crit. Rev. Oncol. Hematol. **2016**, 108, 109–127. [CrossRef] [PubMed]

biomedicines

MDPI

Article

Identification of Key Phospholipids That Bind and Activate Atypical PKCs

Suresh Velnati [1,2,*], Sara Centonze [1,2], Federico Girivetto [1,2], Daniela Capello [1,3], Ricardo M. Biondi [4,5], Alessandra Bertoni [1], Roberto Cantello [1], Beatrice Ragnoli [6], Mario Malerba [1,6], Andrea Graziani [7,8] and Gianluca Baldanzi [1,2]

1 Department of Translational Medicine, University of Piemonte Orientale, 28100 Novara, Italy; sara.centonze@uniupo.it (S.C.); 20020549@studenti.uniupo.it (F.G.); daniela.capello@uniupo.it (D.C.); alessandra.bertoni@med.uniupo.it (A.B.); roberto.cantello@med.uniupo.it (R.C.); mario.malerba@uniupo.it (M.M.); gianluca.baldanzi@med.uniupo.it (G.B.)
2 Center for Translational Research on Allergic and Autoimmune Diseases (CAAD), University of Piemonte Orientale, 28100 Novara, Italy
3 UPO Biobank, University of Piemonte Orientale, 28100 Novara, Italy
4 Department of Internal Medicine 1, Goethe University Hospital Frankfurt, 60590 Frankfurt, Germany; dabiondi@yahoo.co.uk
5 Biomedicine Research Institute of Buenos Aires—CONICET—Partner Institute of the Max Planck Society, Buenos Aires C1425FQD, Argentina
6 Respiratory Unit, Sant'Andrea Hospital, 13100 Vercelli, Italy; beatrice.ragnoli@hotmail.it
7 Molecular Biotechnology Center, Department of Molecular Biotechnology and Health Sciences, University of Torino, 10126 Turin, Italy; andrea.graziani@unito.it
8 Division of Oncology, Università Vita-Salute San Raffaele, 20132 Milan, Italy
* Correspondence: suresh.velnati@med.uniupo.it

Abstract: PKC and PKC/ form the atypical protein kinase C subgroup, characterised by a lack of regulation by calcium and the neutral lipid diacylglycerol. To better understand the regulation of these kinases, we systematically explored their interactions with various purified phospholipids using the lipid overlay assays, followed by kinase activity assays to evaluate the lipid effects on their enzymatic activity. We observed that both PKC and PKC interact with phosphatidic acid and phosphatidylserine. Conversely, PKC is unique in binding also to phosphatidylinositol-monophosphates (e.g., phosphatidylinositol 3-phosphate, 4-phosphate, and 5-phosphate). Moreover, we observed that phosphatidylinositol 4-phosphate specifically activates PKC, while both isoforms are responsive to phosphatidic acid and phosphatidylserine. Overall, our results suggest that atypical Protein kinase C (PKC) localisation and activity are regulated by membrane lipids distinct from those involved in conventional PKCs and unveil a specific regulation of PKC by phosphatidylinositol-monophosphates.

Keywords: membrane; lipid-protein interaction; lipid signalling; kinase regulation; phosphatidylinositols

•€••,ƒ„…†
•€•,ƒ„…

Citation: Velnati, S.; Centonze, S.; Girivetto, F.; Capello, D.; Biondi, R.M.; Bertoni, A.; Cantello, R.; Ragnoli, B.; Malerba, M.; Graziani, A.; et al. Identification of Key Phospholipids That Bind and Activate Atypical PKCs. Biomedicines **2021**, 9, 45. https://doi.org/10.3390/biomedicines9010045

Received: 30 November 2020
Accepted: 1 January 2021
Published: 6 January 2021

1. Introduction

Protein kinase C (PKC) is a family of multidomain Ser/Thr kinases that regulate cell growth, differentiation, apoptosis, and motility. Considering their protein structure and their biochemical characteristics, these kinases are classified into the classical or conventional PKCs (, , and isoforms; cPKCs); the novel PKCs (, , ", and isoforms; nPKCs); and the atypical PKCs (and (mouse)/ (human) isoforms; aPKCs). In physiological conditions, both atypical PKCs play a vital role in cell polarity and signalling. Indeed, these kinases regulate the subcellular localisation of a wide range of polarity proteins by phosphorylating them [1,2]. The PAR6-PAR3-aPKCs trimeric complex is fundamental to modulate the polarity of the epithelial cells and to determinate the cell fate through the orientation of the apical/basal cell asymmetric division [3–5]. Both the aPKCs are also known to enhance the cell migration, invasion, and epithelial–mesenchymal transition in

multiple cancer cell types [6–8]. However, it is fascinating to observe that the two aPKCs isotypes may have specific functions in different cancer cell types. For instance, the PKC/ isoform promotes cancer growth and metastasis in triple-negative breast cancers [9], while PKC is the isoform required for the head and neck squamous cell carcinoma growth and development [10]. Nevertheless, establishing a specific isoform contribution in tumour development is made difficult by the high degree of homology between the PKC and PKC sequences and the lack of specific tools to evaluate a distinct isotype activation.

All these PKC enzymes are characterised by the presence of a kinase domain in the C-terminal region and a regulatory domain placed in the N-terminal region. cPKC regulatory domains also contain a C2 domain that binds anionic phospholipids in a calcium-dependent manner. Conversely, the nPKCs C2 domain is Ca2+-independent but still diacylglycerol (DAG)-sensitive. aPKCs do not possess a C2 domain, whereas they contain a single DAG-insensitive C1 domain. Interestingly, the aPKCs C1 domain (C1 A in cPKCs and nPKCs) is preceded by a basic pseudosubstrate region (PSR) [11]. The PSR binds at the substrate-binding site in an inactive conformation and participates in keeping the kinase inactive in the absence of second messengers. In aPKCs, the C1 domain also participates in the inhibition of the catalytic domain by interactions with the small lobe [12]. In the process of activation, the PSR and the C1 domain must be released from their interactions with the catalytic domain. aPKCs further contain a Phox and Bem1 (PB1) domain located in the N-terminus. This domain extends about 85 amino acids and binds to other PB1 domain-containing proteins, such as zeta-PKC-interacting protein (ZIP/p62), Partitioning-defective Protein 6 (PAR-6) or Mitogen-Activated Protein Kinase 5 (MAPK5) through a homologous PB1–PB1 domain interaction [13].

Although not DAG-sensitive, aPKCs are recruited to membranes upon cell stimulation through protein–protein and protein–lipid interactions [14–18]. The contribution of lipid binding to aPKC localisation is still obscure. Limatola et al. reported that phosphatidic acid (PA), but not other anionic phospholipids, directly binds and activates PKC using a gel-shift assay [19]. Building upon this, Pu et al. noted that, compared with the DAG/phorbol ester-sensitive C1 domains, the rim of the binding cleft of the aPKCs C1 domains possesses four additional positively charged arginine residues (at positions 7, 10, 11, and 20) that may be responsible for PA binding. Indeed, mutations of those residues to the corresponding residues in the PKC C1b domain conferred a response to phorbol ester [20]. The importance of PA for aPKC regulation is underscored by our previous findings that PA production by diacylglycerol kinase alpha (DGK) at cell-ruffling sites recruits aPKCs at the plasma membrane where their activity is necessary for protrusion extension and cell migration [14,15,21]. PKC is also reported to interact with ceramide (CE), which specifically binds to and regulates its kinase activity in a biphasic manner with high- and low-affinity binding sites characterised by Bmax values of 60 and 600 nM and Kd values of 7.5 and 320 nM, respectively [22]. Using CE overlay assays with proteolytic fragments of PKC and vesicle-binding assays with ectopically expressed protein, Wang et al. 2009 showed that a protein fragment comprising the carboxyl-terminal 20-kDa sequence of PKC (amino acids 405–592, distinct from the C1 domain) bound to C16:0 ceramide [23]. This interaction with CE activates PKC and promotes the local proapoptotic complex formation with PAR-4 [18]. Moreover, an analogous interaction was observed also between sphingosine-1-phosphate (S1P) and PKC. Indeed, S1P is suggested to bind the kinase domain of PKC constituted by R_{375} and K_{399} and reliving an autoinhibitory constrain [24]. While the PSR and C1 domain participates in the autoinhibition of catalytic activity, the PSR was found to be key for the activation by a lipid mix [11]. NMR studies suggested that phosphatidylinositol-3,4,5-trisphosphate (PI(3,4,5)P_3) binds directly to the basic residues in the pseudosubstrate sequence of PKC, displacing it from the substrate-binding site during kinase activation [25]. This finding is controversial, as later studies indicated that PI(3,4,5)P_3 does not directly regulate PKC activity [26]. More recently, an interesting work by Dong and colleagues suggested a membrane-targeting mechanism based on electrostatic binding between the PI(4)P, PI(4,5)P_2, and aPKCs PSR polybasic domains. In PKC, this

binding requires the formation of a complex with PAR-6 through the PB1 domain and regulates localisation but not activity [27].

Although phosphorylation by phosphoinositide-dependent kinase-1 (PDK1) [28] and by mTORC2 (target of rapamycin complex 2) [29] are required for aPKC activity, it is widely considered that, upon phosphorylation (maturation), the aPKCs remain in an inactive conformation stabilised by the PSR and the C1 domain. Signalling lipids activate in vitro its kinase activity, reminiscent of conventional PKC. Activators include acidic phospholipids such PA and phosphatidylserine (PS) [19], PI(3,4,5)P_3 [30], S1P [24], and CE [22,31]. Altogether, these shreds of evidence support the possibility of the direct regulation of PKC by lipids, while no information is available for PKC, which is generally assumed to share regulatory models based on high homology with PKC. However, a full understanding of how lipid signalling contributes to the control of aPKC localisation and activity is made difficult by the presence of heterogeneous results obtained with different assays. In here, we used a lipid overlay assay and ELISA technique by using Cova phosphatidylinositol monophosphate (PIP) screening plates to evaluate systematically the lipid-binding specificity and luminescent kinase activity assays to assess the activation of purified human PKC and PKC in the presence of various lipids. We observed that both aPKC isoforms bind to PS and PA. Conversely, only PKC specifically associates with phosphatidylinositol monophosphates. Likewise, we found that PA and PS activate both aPKCs, while only PKC is PI(4)P-sensitive.

2. Results

To explore systematically the lipid-binding properties of aPKCs, initially, we decided to perform lipid overlay assays that probe highly purified lipids spotted on solid supports to screen for lipid binding in a stable way to recombinant tagged aPKC. The lipid overlay assay technique allows to assay in parallel several lipid species and has been used extensively to study the specificity of lipid-binding domains [32].

2.1. PKC*z* Selectively Binds to PA and PS

At first, we tested human FLAG-PKC purified by immunoprecipitation, against the main signalling lipids present in the cell membrane. Specifically, on a lipid PIP strip P-6001, that has been spotted with 100 pmol of all eight phosphoinositides (PI, PI(3)P, PI(4)P, PI (5)P, PI(3,4)P_2, PI(3,5)P_2, PI(4,5)P_2, and PI(3,4,5)P_3) and seven other biological important lipids (lysophosphatidic acid (LPA), lysophosphocoline (LPC), phosphatidylethanolamine (PE), phosphatidylcholine (PC), S1P, PA, and PS). Interestingly, we can confirm the reported interaction of PKC with PA and PS [19], but no direct binding to PI(3,4,5)P_3 or other phosphatidylinositols was detected (Figure. 1A).

Following, to establish the relative affinity for PA and PS, we used the membrane lipid array P-6003 that has been spotted with DAG, PA, PS, PI, PE, PC, phosphatidylglycerol (PG), and sphingomyelin (SM) in a concentration gradient (100–1.56 pmol). We provided evidence of selective and comparable binding to PS and PA and a very modest binding to PG (Figure 1C,D). As ceramide and S1P were reported to interact with the PKC C-terminal region [18], using FLAG-PKC, we also probed a sphingolipid array S-6001 that has been spotted with a concentration gradient of eight different sphingolipids, but we observed no specific association to any of them (Figure 1B).

To summarise, among all the lipids tested in our assay, full-length PKC binds selectively to PA and PS (Figure 1 and Table 1). Conversely, we did not observe binding to any phosphatidylinositol or sphingolipids.

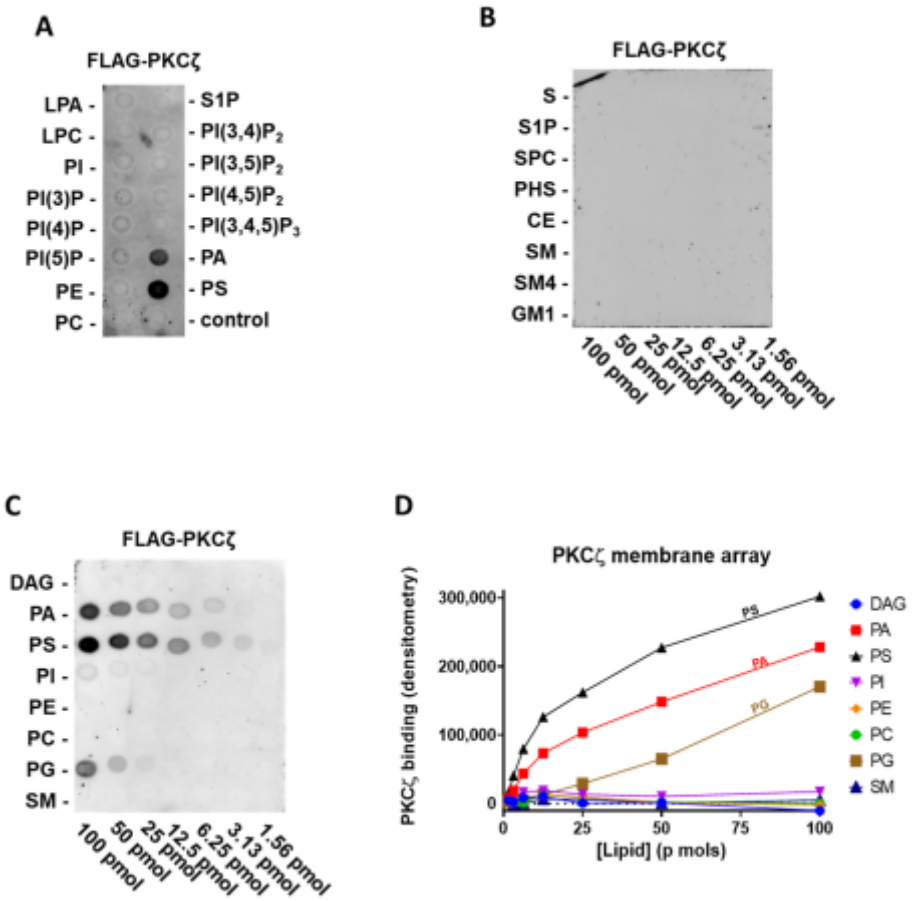

Figure 1. PKC selectively binds phosphatidic acid (PA) and phosphatidylserine (PS) and weakly to phosphatidylglycerol (PG) (**A**) Batch purified FLAG-PKC was incubated with a phosphatidylinositol monophosphate (PIP) strip overnight, and after washing detected with anti-FLAG antibody, a representative experiment out of three performed is shown. (**B**) Batch purified FLAG-PKC was incubated with a sphingo array overnight and, after washing, detected with anti-FLAG antibody. (**C**) Batch purified with FLAG-PKC was incubated with a membrane lipid array overnight and, after washing, detected with anti-FLAG antibody (left). (**D**) Quantification by densitometry of (**C**). DAG: diacylglycerol, PE: phosphatidylethanolamine, PC: phosphatidylcholine, SM: sphingomyelin, PKC: protein kinase C, LPA: lysophosphatidic acid, LPC: lysophosphocoline, S: sphingosine, S1P: sphingosine-1-phosphate, SPC: sphingosylphosphorycholine, PHS: phytosphingosine, CE: ceramide, SM4: sulfatide, and GM1: monosialoganglioside.

2.2. PKC*i* Binds to Phosphatidylinositol Monophosphates, along with PA and PS

To explore the lipid-binding specificity of the highly homologous human PKC, we used a highly purified commercial preparation of FLAG-PKC in the same assay. Like PKC, we tested purified FLAG-PKC on the previously described PIP strip P-6001, representing the main signalling lipids present in the cell membrane. We observed that PKC also interacts with PA and PS but not with PI (Figure 2A). Surprisingly, PKC also selectively binds to phosphatidylinositol monophosphates (PIPs, e.g., PI(3)P, PI(4)P, and PI(5)P), regardless of the phosphorylation position. Interestingly, PKC neither binds to the phosphatidylinositol diphosphates nor triphosphates, which was already indicative of a very selective interaction mechanism.

Table 1. Protein/lipid interactions detected by the lipid overlay assay.

	PKCZ	PKC
PI		
PI(3)P		++
PI(4)P		++
PI(5)P		++
PI(3,4)P_2		
PI(3,5)P_2		
PI(4,5)P_2		
PI(3,4,5)P_3		
PA	++	++
LPA		
PC		
LPC		
PS	++	++
PE		
PG	+	+
DAG		
S		
S1P		
SPC		
PHS		
CE		
SM		
SM4		+
GM1		

++ strong signal, + weak signal, and no signal. PKC: protein kinase C, PIP: phosphatidylinositol monophosphate, PA: phosphatidic acid, LPA: lysophosphatidic acid, PC: phosphatidylcholine, LPC: lysophosphocoline, PS: phosphatidylserine, PE: phosphatidylethanolamine, PG: phosphatidylglycerol, DAG: diacylglycerol, S: sphingosine, S1P: sphingosine-1-phosphate, SPC: sphingosylphosphorycholine, PHS: phytosphingosine, CE: ceramide, SM: sphingomyelin, SM4: sulfatide, and GM1: monosialoganglioside.

Using the membrane lipid array P-6003 that has been spotted with DAG, PA, PS, PI, PE, PC, PG, and SM in a concentration gradient, we can confirm that also PKC binds to PS and PA with a comparable affinity (Figure 2C,D). Moreover, to further investigate the relative affinity in PIP binding, we used a PIP array P-6100 that has been spotted with a concentration gradient of all eight phosphoinositides, i.e., PI, PI(3)P, PI(4)P, PI(5)P, PI(3,4)P_2, PI(3,5)P_2, PI(4,5)P_2, and PI(3,4,5)P_3. We confirmed the binding to phosphatidylinositol monophosphates and a lack of selectivity for the phosphate position in the PIPs (Figure 2E,F) since purified FLAG-PKC binds to PI(3)P, PI(4)P, and PI(5)P to a similar extent. Similar to FLAG-PKC, we did not observe any interaction between purified FLAG-PKC and sphingolipids, apart from a weak binding to sulfatide (SM4), which, however, could be due to its structural similarity in charge and dimensions to PIPs (Figure 2B).

To conclude, PKC also binds to PA and PS. Furthermore, unlike PKC, PKC selectively binds to PIPs without any specificity for the phosphate position (Figure 2 and Table 1).

2.3. PKC*i* Binds to PI(3)P and PI(4)P through the Catalytic Domain

To further confirm the data obtained through lipid overlay assays and to identify the aPKC domains responsible for binding, we performed the ELISA technique using Cova PIP screening plates that were precoated with 20 nmols of either PI(3)P or PI(4)P per well, preblocked and ready for the addition of the proteins. On those plates, we used in-house purified GST-tagged full-length aPKCs and their deletion mutants and detected their binding using anti-GST antibodies. The constructs used are described in Figure 3A [12]. We used the same concentrations of purified GST as in the negative control.

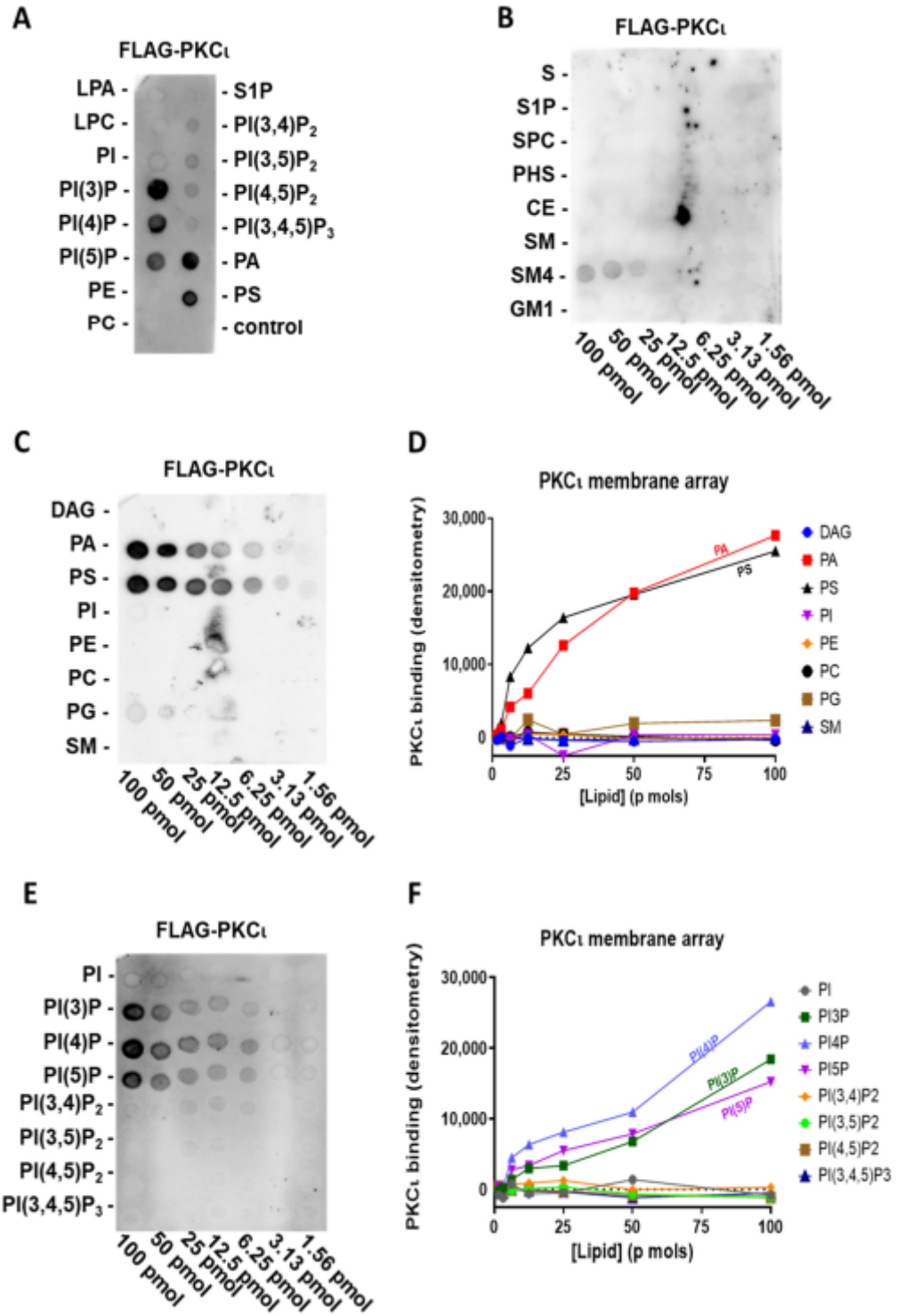

Figure 2. PKC binds PIPs, PA, and PS (**A**) Highly purified FLAG-PKC was incubated with a PIP strip overnight and, after washing, detected with anti-FLAG antibody. (**B**) Highly purified FLAG-PKC was incubated with sphingolipid array overnight and, after washing, detected with anti-FLAG antibody. (**C**) Highly purified FLAG-PKC was incubated with a membrane lipid array overnight and, after washing, detected with anti-FLAG antibody (left). (**D**) Quantification by densitometry of (**C**). (**E**) Highly purified FLAG-PKC was incubated with a PIP array overnight and after, washing detected, with anti-FLAG antibody (left). (**F**) Quantification by densitometry of (**E**).

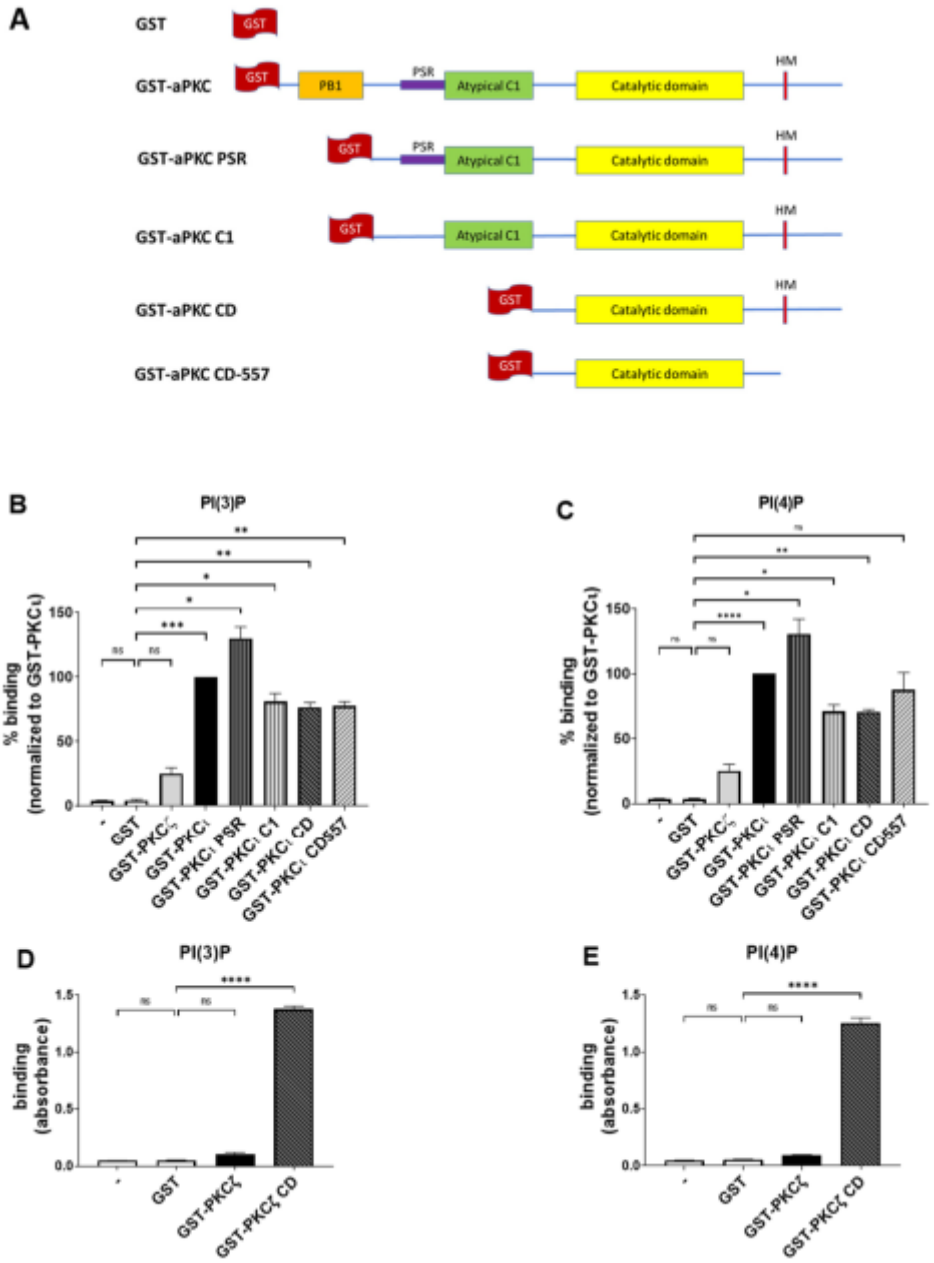

Figure 3. PKC, but not PKC, binds selectively to both PI(3)P and PI(4)P. (**A**) Schematic domain structure of GST tagged PKC, PKC, and the deletion mutants used in this study. (**B**) GST-PKC, GST-PKC, and deletion mutants binding on Cova PIP screening plates coated with PI(3)P. Purified GST was used as a negative control. Data are the mean SEM of three independent experiments. (**C**) GST-PKC, GST-PKC, and deletion mutants binding on Cova PIP screening plates coated with PI(4)P. Purified GST was used as a negative control. Data are the mean SEM of three independent experiments. (**D**) GST-PKC and GST-PKC CD binding on Cova PIP screening plates coated with PI(3)P. Purified GST was used as a negative control. Data are the mean SEM of three independent experiments. (**E**) GST-PKC and GST-PKC CD binding on Cova PIP screening plates coated with PI(4)P. Purified GST was used as a negative control. Data are the mean SEM of three independent experiments. A single, double, triple and four asterisks denote their significance of p-value 0.05, 0.01, 0.001 and 0.0001 respectively, ns mean No significant.

While the GST alone gave no detectable binding, as expected, the PKC isoform strongly bound to both PI(3)P and PI(4)P (Figure 3B,C), in line with our previous findings. Conversely, PKC neither bound to PI(3)P nor PI(4)P (Figure 3B,C). Those data indicate

that, similar to what we observed in the lipid overlay assays, the binding of PKC to PIPs is isoform-specific and does not require the presence of additional proteins.

Besides, all the truncated forms of PKC resulted in some binding to both PI(3)P and PI(4)P, suggesting that a relevant lipid binding takes place in the catalytic domain (CD), as it is the only domain common to all those truncated proteins. On the other hand, we observed an increased binding signal towards PI(3)P and PI(4)P when testing the PKC PSR. Indeed, the PSR is a polybasic domain, enriched with Arg and Lys residues, which confers to the protein the ability to bind directly the phosphoinositides such as PI(4)P but is masked when the protein is not involved in interactions with PAR-6 [27]. It may be possible that removing the PB1 region makes the PSR domain more accessible to the electrostatic binding to the lipids, resulting in a stronger signal when compared to the full-length protein.

Moreover, we observed a strong binding of both PI(3)P and PI(4)P to PKC CD, a truncated mutant lacking the N-terminal PB1, PSR, and C1 domains. Interestingly, the full-length PKC remained unbound (Figure 3D,E), indicating that the N-terminal domains inhibited the interaction and that the PI(3)P and PI(4)P interacting region is located within evolutionarily conserved regions in the CD region of PKC and PKC.

Overall, these data indicate that full-length PKC readily binds selectively to PI(3)P and PI(4)P, while the CD appears as a primary binding site for phosphatidylinositol monophosphates. In PKC, this binding is masked by the presence of N-terminal regulatory domains.

2.4. PS and PA Activates Both aPKCs, While PI(4)P Activates PKC*i* Selectively

To evaluate the effect of lipid binding on the catalytic activity of human aPKC, we performed kinase activity assays using highly purified commercial PKC and PKC, incubated with PS, PA, and PI(4)P at a final concentration of 50 g/mL. Following, the ADP produced was detected using the ADP-Glow luminescence kit. Those assays were run following the preoptimised conditions suggested by the provider; in those conditions, the basal PKC activity is quite low. This might be due to the low concentrations of the enzyme (0.1 ng/L of PKC) (four times less enzyme when compared to PKC—0.4 ng/L). In similar experimental conditions, the PKC activity is evidently higher compared to the background (Supplementary Figure S1). However, we can easily observe the expected stimulation of PKC in the presence of either PA or PS, while PI4P is ineffective (Figure 4A). Those data are in line with previous reports in the literature [19,27].

Conversely, we can easily measure the basal activity of unstimulated PKC, which is at least 10x when compared to the background. The PKC basal activity is strongly stimulated by PA, followed by PS (Figure 4B). Interestingly, PI(4)P acts an allosteric activator selective for PKC, as we observed no activation of highly purified commercial PKC by this lipid (Figure 4A,B). These data suggest that the previously reported binding of aPKC to PS, PA, and PIPs enhanced enzyme activity putatively, promoting the switch to the open more active conformation.

To further investigate the domains involved in lipid-mediated PKC activation, we performed the kinase activity assays by using in-house purified full-length GST-tagged PKC and its truncated forms (PKC C1 and PKC CD) in the presence of PS, PA, or PI(4)P. Similar to what we observed before, full-length GST-PKC is strongly activated with PA and PI(4)P, whereas PS activation is still significant but less strong (Figure 4C). The CD is not further activated by lipid mixes in vitro [11]. Even though we noticed some binding of PI(4)P to the PKC CD mutant, no further activation of the CD was detected in kinase activity assays. The PKC C1 mutant, which lacks the PB1 and PSR, is considerably inhibited by the C1 domain [12]. The PKC C1 mutant retained the ability to respond to PA and PI(4P), indicating that the PSR is not required for the activation by these lipids (Figure 4C). Together, the results indicate that the activation by PA and PI(4) is linked to the release of autoinhibition by the C1 domain.

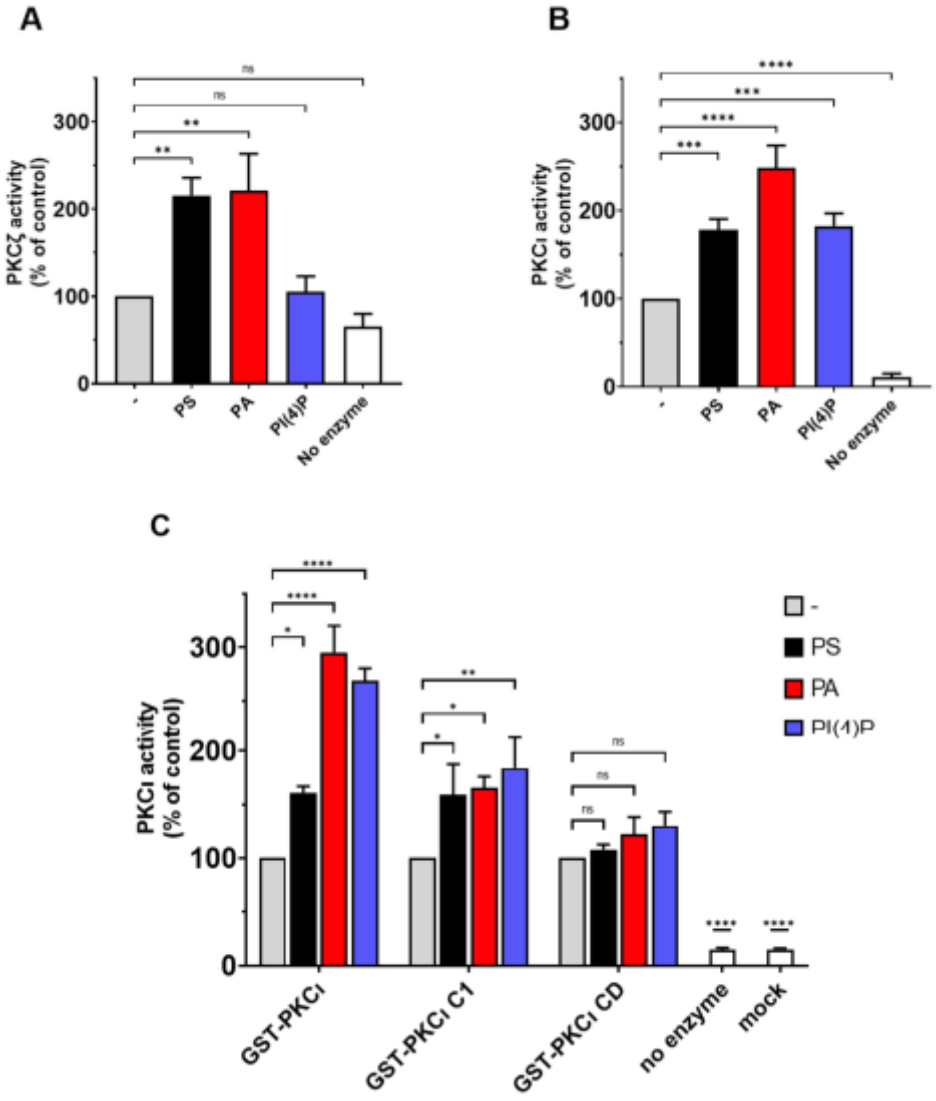

Figure 4. PKC is activated by PS, PA, and PI(4)P. (**A**) The activity of commercial purified GST-PKC was measured in the presence of 50-g/mL PS or PA or PI(4)P. A complete reaction without an enzyme is considered as the negative control. (**B**) The activity of commercial purified GST-PKC was measured in presence of 50-g/mL PS or PA or PI(4)P. A complete reaction without an enzyme is considered as the negative control. (**C**) The activity of in-house purified GST-PKC and deletion mutants was measured in presence of 0.5-ng/mL PS or PA or PI(4)P. Mock purification and no enzyme conditions are used as negative controls. Data are the mean SEM of at least 4 independent experiments performed in triplicate. A single, double, triple and four asterisks denote their significance of p-value 0.05, 0.01, 0.001 and 0.0001 respectively, ns mean No significant.

3. Discussion

Among the three PKCs subfamilies, the aPKCs (PKC and PKC/) do require neither calcium nor DAG for their activation, but many shreds of evidence indicate that their interactions with lipids may contribute to the control of aPKCs localisation and activity. In order to further understand their mechanisms of regulation and explore their isotype-specific lipid activators, the present work aims to estimate the lipid-binding specificity and activation of the human aPKCs isozymes through a systematic approach.

By performing lipid overlay assays, we observed that aPKCs can selectively bind PA and PS, and this binding results in a relevant increase in aPKCs activity. Those findings are in line with previous results obtained with a lipid motility shift assay [19]. Previously, our group demonstrated that DGK-produced PA is required to localise the aPKCs to the

plasma membrane, where their activity leads to cytoskeletal remodelling and membrane ruffles formation, two essential processes required for cell migration [14,15,21]. These findings indicate that PA provides a key signal to recruit and activate aPKCs at specific membrane compartments. This PA can be derived from DAG through DGK activity or else from PC through phospholipase D (PLD) hydrolysing activity. Indeed, through PA-mediated mechanisms, PLD modulates small GTPases, playing an essential role in membrane homeostasis and cytoskeletal remodelling [33], such as antigen-stimulated membrane ruffling [34]. Interestingly, PLD-generated PA is required for sorbitol-induced activation of aPKCs and GLUT4 translocation/glucose transport [35]. Besides PA, we identified binding to PS, a lipid constitutively present at membranes. We hypothesise that PA, together with PS, recruits and activates aPKC to specific membrane domains. In this manner, DGK and PLD, modulating PA availability, may be potential regulators of aPKCs localisation and activation. However, the information regarding the spatial and temporal PA distribution in subcellular compartments is still limited. Nishioka et al., using a Phosphatidic Acid indicator (Pii) biosensor based on the FRET technique, observed a divergence in PA content among various cell types and an individual heterogeneity within the same cell line [36]. The authors reported that, upon EGF stimulation, PA level increases rapidly at the plasma membrane, and it seems that this PA production is due mostly to PLD rather than DGK [36]. Similar results were obtained by Zhang and colleagues using a Phosphatidic Acid biosensor with Superior Sensitivity (PASS), and interestingly, their data seem to suggest that EGF triggers a sequential activation of PLD and DGK in distinct membrane nanodomains [37].

Interestingly, our findings demonstrated that, unlike PKC, PKC interacts directly with phosphatidylinositol monophosphates (PI(3)P, PI(4)P, and PI(5)P) in a specific and dose-dependent manner. This binding is, at least in part, mediated by the PKC catalytic domain and results in enzyme activation. Polyphosphoinositides derivatives represent a crucial membrane-localised signal in the control of essential cellular processes by driving the subcellular localisation and activation of specific effector proteins [38]. Indeed, they feature specific subcellular localisation with PI(4)P mainly at the plasma membrane and Golgi apparatus; PI(3)P at the plasma membrane, early endosomal surface and autophagosome; and PI(5)P in very low concentrations at the plasma membrane, the nucleus, Golgi complex, and sarco/endoplasmic reticulum [39,40]. They also feature specific biologic functions: PI(3)P induces autophagy [41], whereas PI(4)P is associated with endosomal trafficking, endoplasmic reticulum (ER) export, autophagy, signalling at the plasma membrane, cytokinesis, and actin dynamics [39,42]. The role of PI(5)P is not completely understood, despite many pieces of evidence suggesting its involvement in the cell cycle, stress response, T-cell activation, and chromatin remodelling [43].

The biological significance of this differential lipid regulation between these two highly homologous isoforms relies on their distinct functions. Even if PKC and PKC display 72% amino acid sequence homology, several reports demonstrated functional differences among them. PKC is more efficiently involved in the NF-B activation pathway when compared to PKC/ [44,45]. Interestingly, PKC is frequently overexpressed and mislocalised in human tumours when compared to PKC. This involvement results in a consequent loss of cell polarity, which represents the first crucial step towards cell motility and invasiveness [45,46]. In particular, it has been reported that PKC is often mislocalised to the cytoplasm and the nucleus of the transformed cancer cells [47–50], but fascinatingly, despite the loss of its restricted localisation within the membrane, PKC seems to remain in complex with PAR-6 in tumour cells [51–53], indicating that this association, along with the PKC activity, is somehow important for the maintenance of the cancer cell phenotypes [51,54–56].

While this work was in preparation, Dong et al. demonstrated that PKC is capable of PI(4)P binding only when engaged in a complex with PAR-6, which unmasks the polybasic PSR. This PKC-PI(4)P binding is important for the localisation of the complex but not for enzyme activity [27]. Remarkably, our results suggest the existence of a further binding

site in the PKC catalytic domain that is not affected by the phosphorylation position on the inositol ring. While full-length PKC readily interacted with phosphatidylinositol monophosphates, only the construct comprising the isolated CD of PKC showed an interaction with phosphatidylinositol monophosphates. This finding suggests that the CD of both isoforms possess the ability to bind phosphatidylinositol monophosphates but that differences at the N-terminal region hinder the interaction of full-length PKC with the phosphatidylinositol monophosphates. In line with this hypothesis, the removal of N-terminal regulatory domains enables PI(4)P and PI(3)P binding to the PKC catalytic domain (Figure 3D,E). The small differences in the ability to interact with phosphatidylinositol monophosphates suggest that PKC would require binding to PS or PA to "open" the structure of the kinase and expose the catalytic domain that holds the binding site to phosphatidylinositol monophosphates. In a physiological context, those binding sites could be exposed upon PB1 binding to proteins as PAR-6. However, a constitutively active truncated version of PKC consisting of the catalytic domain is normally expressed in neuronal cells and is potentially localised by PIPs [57].

Though further studies are yet to be conducted regarding this binding, we can speculate that PI(3)P and PI(4)P binding may contribute to the reported recruitment of PKC at specific membrane compartments, such as the reported localisations at lysosomes [58] or the apical domains of epithelial cells [50]. In the case of PKC, it may require recruitment by other lipids, and the binding to phosphatidylinositol monophosphates may support the activity once the protein is recruited to the specific membrane location.

The lipid overlay assay used in our work is a very stringent assay in which the protein must remain bound for the relatively long period of washings; therefore, it detects only high-affinity interactions with relatively low off rates. Indeed, even if PI(3,4,5)P_3 has been reported as a PKC activator [25,59], we and others were unable to detect any binding suggesting an indirect interaction between a PKC and PI(3,4,5)P_3 [26]. We also observed no direct binding of a PKC to CE, which was reported to bind PKC [22], resulting in recruitment to lipid raft and enzyme activation [60,61]. Recently, by using CE-binding assays and lipid vesicle-binding assays, Wang and colleagues demonstrated that PKC can bind to C16:0 CE in a specific manner [18,23]. Similarly, recent studies highlighted a specific interaction between a PKCs and S1P, which is a bioactive lipid obtained by the deacylation of ceramide [24]. In contrast with these data, our approach by lipid overlay assay did not reveal any binding between PKC or PKC and CE or S1P. The discrepancies between our data and those of others could be due to the higher off rates of the interactions with CE or S1P. Alternatively, it is possible that our solid-phase/overlay binding assays may not be suitable to identify proteins that bind to ceramide [62], possibly due to the different conformations of ceramide integrated into a lipid membrane compared to a solid phase. Moreover, to perform the overlay assay, Wang et al. used PKC proteolytic fragments, while we used full-length proteins where the CE-binding site may be hidden, as shown for the PI(4)P-binding site. All in vitro studies have limitations, because it is not easy to recapitulate all lipid components and other protein interacting partners in the test tube. Therefore, the study may miss some relevant lipids and protein partners that may be physiologically significant. On the other hand, the assays reported here in two different binding formats and in activity assays were a strong indication that the a PKCs can bind with high affinity and high selectivity to the identified lipids and that they can regulate the activity of PKC.

Whereas PS is considered to bind to the C1 domain, S1P [24] and PIPs bind to the catalytic domain. The binding of lipids at two different sites on a PKCs provides a means for synergistic binding when two lipids are present. The binding site for PIPs on the catalytic domain has not been determined. However, we can exclude the substrate/pseudosubstrate-binding site as a possible interaction site for PIPs, because the binding there would compete with substrate binding and would be inhibitory. We can speculate that S1P and PIPs could bind at the same region on the small lobe of the catalytic domain where the C1 domain

binds. In such a scenario, the activation would be promoted by lipids competing for the two sites of the inhibitory interaction of the C1 domain onto the catalytic domain.

Finally, in the overlay assay, we report the interaction of PKC to sulfatide. The interaction was comparably lower, and we did not validate the binding using a second methodology. However, we would like to note that human and yeast PDK1 bind sulfatide as well [63], and PDK1 has also been described to bind to PS [64]. The simultaneous binding of upstream kinase PDK1 and its aPKC substrate to sulfatide and PS could potentially be relevant for the phosphorylation of aPKCs at the activation loop during the maturation stage or as a regulatory event.

In brief, through lipid overlay assays and kinase assays, we observed that both PKC and PKC bind to PA and PS, and the sole PKC also binds to PI(3)P, PI(4)P, and PI(5)P. Moreover, those interactions result in a selective enhancement of aPKC activity. These data suggest a differential regulation of these two highly homologous isoforms by membrane lipids in line with the reported overlapping but different biological roles.

4. Materials and Methods

4.1. Reagents

Anti-FLAG M2 for immunoprecipitation is from Sigma Aldrich, St. Louis, MO, USA (A2220). Horseradish peroxidase-labelled anti-DDK (FLAG) tag is from Origene, Rockville, MD, USA (A190-101P). Secondary antibodies HRP-mouse and HRP-rabbit were from Perkin Elmer.

Unless specified, all chemical reagents, including protease inhibitors mix and protein G agarose are from Sigma Aldrich.

4.2. Constructs

The FLAG-PKC construct used in Figure 1 was kindly provided by Dr Alex Toker (Boston, MA, USA) [20].

Recombinant human PKC with C-terminal DDK (FLAG) tag purified 80% from human HEK293 cells used in Figure 2 is from Origene, Rockville, USA (TP305379).

GST-PKC, GST-PKC, and their truncated forms were previously described in Zang H et al. [12].

4.3. Protein Purification

For lipid overlay assays with lipid arrays, recombinant proteins were obtained by transfecting 293T cells (5 10 cm dishes) with the corresponding constructs using lipofectamine 3000 (Thermo Fisher Scientific, Waltham, MA, USA) according to the manufacturer's instruction. After 48 h, cells in each plate were lysed in 0.5 mL of lysis buffer (25-mM HEPES, pH 8, 150-mM NaCl, 1% Nonidet P-40, 5-mM EDTA, 2-mM EGTA, 50-mM NaF, 10% glycerol supplemented with fresh 1-mM Na_3VO_4, and protease inhibitors) and clarified after centrifugation for 15 min at 12,000 rpm at 4 C.

FLAG-tagged recombinant proteins were batch-purified by overnight immunoprecipitation with 50-g antibody against the protein tag and 100-L protein-agarose beads. After 4 washes in lysis buffer and 2 in phosphate-buffered saline (PBS—137-mM NaCl, 2.68-mM KCl, 4.3-mM Na_2HPO_4, and 1.47-mM KH_2PO_4, pH 7.3), the immunoprecipitated protein was eluted twice with 100 L of 0.1-M glycine (pH 3.5) and immediately neutralised with 10 tris buffer saline (0.5-M tris and 1.2-M NaCl, pH 7.4).

For purification of GST-tagged recombinant proteins, lysis buffer was supplemented with 2-mM dithiothreitol. GST-tagged proteins were batch-purified upon 4 h of immunoprecipitation with 200-L glutathione-agarose beads (GE healthcare). After 4 washes in lysis buffer and 2 in phosphate-buffered saline (PBS), the immunoprecipitated protein was eluted with 200-L elution buffer (100-mM Tris HCl, pH 8.0, 10-mM NaCl, 5% glycerol supplemented with fresh 2-mM DTT, and glutathione 10 mM).

Purified proteins were further subjected to SDS-PAGE for purity evaluation and protein quantification against a BSA calibration curve.

4.4. Lipid Overlay Assay

Lipid arrays (Echelon Biosciences, Salt Lake City, UT, USA) used in this work are PIP Strip (P6001), Membrane Lipid Strip (P6002), Membrane Lipid Array (P6003), PIP Array (P6100), and Sphingo Array (S6001). After saturation (3% bovine serum albumin and 0.1% Tween 20 in TBS buffer), membranes were incubated overnight with 5 mL of the protein of interest dissolved in the same buffer. After 4 washes with 0.1% Tween 20 in TBS buffer, the lipid-bound protein was detected upon 1-h incubation with the relevant HRP-labelled anti-tag antibody, followed by a further 4 washes. Detection antibodies were visualised and quantified using Western Lightning Chemiluminescence Reagent Plus (Perkin Elmer, Waltham, MA, USA) and a ChemiDoc imager (Bio-Rad, Hercules, CA, USA). The software automatically checks saturation and auto-scaled images to optimise signal/noise.

4.5. Cova PIP ELISA Assay

Proteins of interest were diluted in TBS supplemented with 1% BSA (1 g/mL in a final volume of 100 L per well) and added to Cova PIP screening plates (provided by Echelon Bioscience, H-6203; H-6204), followed by overnight incubation with gentle agitation at 4C.

After 3 washes using 0.1% Tween 20 in TBS buffer, primary antibody anti-GST (Santa Cruz Biotechnology cat # SC-459, 1:1000 dilution in TBS + 1% BSA) was added and incubated at room temperature for 1 h with gentle agitation. Post-incubation, 3 washes with 0.1% Tween 20 in TBS buffer were performed before adding the secondary antibody diluted 1:5000 in TBS + 1% BSA for 1 h at room temperature on a plate shaker. Later, the plates were washed for 5 additional times before adding 100 L/well of peroxidase substrate: $3,3^0,5,5^0$-Tetramethylbenzidine liquid substrate (TMB) and stopped the reaction by adding 50 L/well of 0.5-M H_2SO_4 when significant blue colour developed. The absorbance was read with a Tecan Spark instrument plate reader at 450-nm wavelength immediately after adding the stop solution.

4.6. aPKC Activity Assay

Protein kinase assays were performed using the PKC Kinase Enzyme System (Promega; Catalogue #: V3751) and PKC Kinase Enzyme System (Promega; Catalogue #: V2781) and ADP-Glo Kinase Assay kit (Promega; Catalogue #: V9101). The reaction was performed in a final volume of 25 L containing 5 L of stock solution reaction buffer A supplemented with 2.5-L DTT (final concentration 50 M); 5-L active full-length PKC (final concentra-tion 4 nM) and 5-L active full-length PKC (final concentration 1 nM); 5 L of CREBtide substrate stock solution; 2.5 L of ATP (final concentration 50 M); 2.5 L of DMSO (10%); 2.5 L of lipid activator (10); or PS, PA, and PI(4)P (dissolved by sonication in MOPS; final concentration 50 g/mL).

The assay was carried out in 96-well luminescent white plates by incubating the reaction mixture at 30 C for 20 min. After this incubation period, the ADP-Glo^{TM} Reagent was added to simultaneously terminate the kinase reaction and deplete the remaining ATP. The plate was then incubated for 40 min at room temperature before adding 50 L of Kinase Detection Reagent to convert ADP to ATP and incubated again for a further 30 min at room temperature. The luminescence of the 96-well reaction plate was finally read using the Tecan Spark 10 M Multimode Plate Reader.

Controls were set up including all the assay components by replacing the enzyme with equal volume of water (negative control). Lipids were replaced with equal volume of MOPS (for both positive and negative controls).

4.7. Data Processing and Statistical Analysis

The binding spots obtained on membrane strips or arrays were acquired with the ChemiDoc imager and quantified by using Image lab 6.0 software (Bio-Rad). Data obtained from PIP arrays and membrane arrays were collected as Excel files and analysed using

GraphPad Prism 9.0 software. We analysed our data using one-way ANOVA analysis with Dunnett's multiple comparisons for ELISA assays (Figure 3B,C), and for kinase activation assays (Figure 4A,B). For Figure 4C of the kinase activation assays, we used two-way ANOVA with Dunnett's multiple comparisons.

Supplementary Materials: The following are available online at https://www.mdpi.com/2227-9059/9/1/45/s1.

Author Contributions: A.B., R.C., M.M., D.C., B.R., A.G., R.M.B. and G.B.: study design and funding and S.V., S.C. and F.G.: performed experiments. All authors contributed to the manuscript preparation and data analysis under SV and GB coordination. All authors have read and agreed to the published version of the manuscript.

Funding: This study was funded by the National Ministry of University and research PRIN 2017 (grant 201799WCRH to GB) by the Italian Ministry of Education, University and Research (MIUR) program "Departments of Excellence 2018–2022", AGING Project—Department of Translational Medicine, Università del Piemonte Orientale (DC), FAR-2017 (DC and GB), and by Consorzio Interuniversitario di Biotecnologie (CIB) call "Network-CIB: Catalisi dell'Innovazione nelle Biotecnologie" (GB).

Institutional Review Board Statement: Not applicable.

Informed Consent Statement: Not applicable.

Data Availability Statement: The data presented in this study are available by the authors. For any further request contact the corresponding author.

Conflicts of Interest: The authors declare no conflicts of interest. The funders had no role in the design of the study; in the collection, analyses, or interpretation of data; in the writing of the manuscript, or in the decision to publish the results.

Abbreviations

LPA	lysophosphatidic acid
LPC	lysophosphocoline
PI	phosphatidylinositol
PI(3)P	phosphatidylinositol 3-phosphate
PI(4)P	phosphatidylinositol 4-phosphate
PI(5)P	phosphatidylinositol 5-phosphate
$PI(3,4)P_2$	phosphatidylinositol 3,4-bisphosphate
$PI(3,5)P_2$	phosphatidylinositol 3,5-bisphosphate
$PI(4,5)P_2$	phosphatidylinositol 4,5-bisphosphate
$PI(3,4,5)P_3$	phosphatidylinositol 3,4,5-trisphosphate
DAG	diacylglycerol
PA	phosphatidic acid
PS	phosphatidylserine
PE	phosphatidylethanolamine
PC	phosphatidylcholine
PG	phosphatidylglycerol
S	sphingosine
S1P	sphingosine-1-phosphate
SM	sphingomyelin
SPC	sphingosylphosphorycholine
PHS	phytosphingosine
CE	ceramide
SM4	sulfatide
GM1	monosialoganglioside
TAG	triacylglycerol
CL	cardiolipin
CH	Cholesterol

References

1. Hong, Y. aPKC: The Kinase that Phosphorylates Cell Polarity. F1000Research **2018**, 7, 903. [CrossRef] [PubMed]
2. Xiao, H.; Liu, M. Atypical protein kinase C in cell motility. Cell. Mol. Life Sci. **2012**, 70, 3057–3066. [CrossRef] [PubMed]
3. Chen, J.; Zhang, M. The Par3/Par6/aPKC complex and epithelial cell polarity. Exp. Cell Res. **2013**, 319, 1357–1364. [CrossRef]
4. Vorhagen, S.; Niessen, C.M. Mammalian aPKC/Par polarity complex mediated regulation of epithelial division orientation and cell fate. Exp. Cell Res. **2014**, 328, 296–302. [CrossRef] [PubMed]
5. Drummond, M.L.; Prehoda, K.E. Molecular Control of Atypical Protein Kinase C: Tipping the Balance between Self-Renewal and Differentiation. J. Mol. Biol. **2016**, 428, 1455–1464. [CrossRef]
6. Reina-Campos, M.; Diaz-Meco, M.T.; Moscat, J. The Dual Roles of the Atypical Protein Kinase Cs in Cancer. Cancer Cell **2019**, 36, 218–235. [CrossRef]
7. Du, G.-S.; Qiu, Y.; Wang, W.-S.; Peng, K.; Zhang, Z.-C.; Li, X.-S.; Xiao, W.; Yang, H. Knockdown on aPKC- inhibits epithelial-mesenchymal transition, migration and invasion of colorectal cancer cells through Rac1-JNK pathway. Exp. Mol. Pathol. **2019**, 107, 57–67. [CrossRef]
8. Qian, Y.; Yao, W.; Yang, T.; Yang, Y.; Liu, Y.; Shen, Q.; Zhang, J.; Qi, W.; Wang, J. aPKC-/P-Sp1/Snail signaling induces epithelial-mesenchymal transition and immunosuppression in cholangiocarcinoma. Hepatology **2017**, 66, 1165–1182. [CrossRef]
9. Paul, A.; Gunewardena, S.; Stecklein, S.R.; Saha, B.; Parelkar, N.; Danley, M.; Rajendran, G.; Home, P.; Ray, S.; Jokar, I.; et al. PKC/ signaling promotes triple-negative breast cancer growth and metastasis. Cell Death Differ. **2014**, 21, 1469–1481. [CrossRef]
10. Cohen, E.E.W.; Lingen, M.W.; Zhu, B.; Zhu, H.; Straza, M.W.; Pierce, C.; Martin, L.E.; Rosner, M.R. Protein Kinase C Mediates Epidermal Growth Factor–Induced Growth of Head and Neck Tumor Cells by Regulating Mitogen-Activated Protein Kinase. Cancer Res. **2006**, 66, 6296–6303. [CrossRef]
11. Lopez-Garcia, L.A.; Schulze, J.O.; Fröhner, W.; Zhang, H.; Süss, E.; Weber, N.; Navratil, J.; Amon, S.; Hindie, V.; Zeuzem, S.; et al. Allosteric Regulation of Protein Kinase PKC by the N-Terminal C1 Domain and Small Compounds to the PIF-Pocket. Chem. Biol. **2011**, 18, 1463–1473. [CrossRef] [PubMed]
12. Zhang, H.; Neimanis, S.; Lopez-Garcia, L.A.; Arencibia, J.M.; Amon, S.; Stroba, A.; Zeuzem, S.; Proschak, E.; Stark, H.; Bauer, A.F.; et al. Molecular Mechanism of Regulation of the Atypical Protein Kinase C by N-terminal Domains and an Allosteric Small Compound. Chem. Biol. **2014**, 21, 754–765. [CrossRef] [PubMed]
13. Corbalán-García, S.; Gómez-Fernández, J.C. Protein kinase C regulatory domains: The art of decoding many different signals in membranes. Biochim. Biophys. ActaMol. Cell Biol. Lipids **2006**, 1761, 633–654. [CrossRef] [PubMed]
14. Chianale, F.; Rainero, E.; Cianflone, C.; Bettio, V.; Pighini, A.; Porporato, P.E.; Filigheddu, N.; Serini, G.; Sinigaglia, F.; Baldanzi, G.; et al. Diacylglycerol kinase mediates HGF-induced Rac activation and membrane ruffling by regulating atypical PKC and RhoGDI. Proc. Natl. Acad. Sci. USA **2010**, 107, 4182–4187. [CrossRef] [PubMed]
15. Rainero, E.; Cianflone, C.; Porporato, P.E.; Chianale, F.; Malacarne, V.; Bettio, V.; Ruffo, E.; Ferrara, M.; Benecchia, F.; Capello, D.; et al. The Diacylglycerol Kinase /Atypical PKC/1 Integrin Pathway in SDF-1 Mammary Carcinoma Invasiveness. PLoS ONE **2014**, 9, e97144. [CrossRef]
16. Dang, P.M.-C.; Fontayne, A.; Hakim, J.; El Benna, J.; Périanin, A. Protein Kinase C Phosphorylates a Subset of Selective Sites of the NADPH Oxidase Component p47phoxand Participates in Formyl Peptide-Mediated Neutrophil Respiratory Burst. J. Immunol. **2001**, 166, 1206–1213. [CrossRef]
17. Akimoto, K.; Takahashi, R.; Moriya, S.; Nishioka, N.; Takayanagi, J.; Kimura, K.; Fukui, Y.; Osada, S.-I.; Mizuno, K.; Hirai, S.-I.; et al. EGF or PDGF receptors activate atypical PKClambda through phosphatidylinositol 3-kinase. EMBO J. **1996**, 15, 788–798. [CrossRef]
18. Wang, G.; Silva, J.; Krishnamurthy, K.; Tran, E.; Condie, B.G.; Bieberich, E. Direct Binding to Ceramide Activates Protein Kinase C before the Formation of a Pro-apoptotic Complex with PAR-4 in Differentiating Stem Cells. J. Biol. Chem. **2005**, 280, 26415–26424. [CrossRef] [PubMed]
19. Limatola, C.; Schaap, D.; Moolenaar, W.H.; Van Blitterswijk, W.J. Phosphatidic acid activation of protein kinase C- overexpressed in COS cells: Comparison with other protein kinase C isotypes and other acidic lipids. Biochem. J. **1994**, 304, 1001–1008. [CrossRef]
20. Pu, Y.; Peach, M.L.; Garfield, S.H.; Wincovitch, S.; Marquez, V.E.; Blumberg, P.M. Effects on Ligand Interaction and Membrane Translocation of the Positively Charged Arginine Residues Situated along the C1 Domain Binding Cleft in the Atypical Protein Kinase C Isoforms. J. Biol. Chem. **2006**, 281, 33773–33788. [CrossRef]
21. Chianale, F.; Cutrupi, S.; Rainero, E.; Baldanzi, G.; Porporato, P.E.; Traini, S.; Filigheddu, N.; Gnocchi, V.F.; Santoro, M.M.; Parolini, O.; et al. Diacylglycerol Kinase- Mediates Hepatocyte Growth Factor-induced Epithelial Cell Scatter by Regulating Rac Activation and Membrane Ruffling. Mol. Biol. Cell **2007**, 18, 4859–4871. [CrossRef] [PubMed]
22. Müller, G.; Ayoub, M.; Storz, P.; Rennecke, J.; Fabbro, D.; Pfizenmaier, K. PKC zeta is a molecular switch in signal transduction of TNF-alpha, bifunctionally regulated by ceramide and arachidonic acid. EMBO J. **1995**, 14, 1961–1969. [CrossRef]
23. Wang, G.; Krishnamurthy, K.; Umapathy, N.S.; Verin, A.D.; Bieberich, E. The Carboxyl-terminal Domain of Atypical Protein Kinase C Binds to Ceramide and Regulates Junction Formation in Epithelial Cells. J. Biol. Chem. **2009**, 284, 14469–14475. [CrossRef] [PubMed]
24. Kajimoto, T.; Caliman, A.D.; Tobias, I.S.; Okada, T.; Pilo, C.A.; Van, A.-A.N.; McCammon, J.A.; Nakamura, S.-I.; Newton, A.C. Activation of atypical protein kinase C by sphingosine 1-phosphate revealed by an aPKC-specific activity reporter. Sci. Signal. **2019**, 12, eaat6662. [CrossRef] [PubMed]

25. Ivey, R.A.; Sajan, M.P.; Farese, R.V. Requirements for Pseudosubstrate Arginine Residues during Autoinhibition and Phosphatidylinositol 3,4,5-(PO4)3-dependent Activation of Atypical PKC. J. Biol. Chem. **2014**, 289, 25021–25030. [CrossRef] [PubMed]
26. Tobias, I.S.; Kaulich, M.; Kim, P.K.; Simon, N.; Jacinto, E.; Dowdy, S.F.; King, C.C.; Newton, A.C. Protein kinase C exhibits constitutive phosphorylation and phosphatidylinositol-3,4,5-triphosphate-independent regulation. Biochem. J. **2016**, 473, 509–523. [CrossRef] [PubMed]
27. Dong, W.; Lu, J.; Zhang, X.; Wu, Y.; Lettieri, K.; Hammond, G.R.; Hong, Y. A polybasic domain in aPKC mediates Par6-dependent control of membrane targeting and kinase activity. J. Cell Biol. **2020**, 219. [CrossRef]
28. Chou, M.M.; Hou, W.; Johnson, J.; Graham, L.K.; Lee, M.H.; Chen, C.-S.; Newton, A.C.; Schaffhausen, B.S.; Toker, A. Regulation of protein kinase C by PI 3-kinase and PDK-1. Curr. Biol. **1998**, 8, 1069–1078. [CrossRef]
29. Li, X.; Gao, T. mTORC 2 phosphorylates protein kinase C to regulate its stability and activity. EMBO Rep. **2014**, 15, 191–198. [CrossRef]
30. Nakanishi, H.; Brewer, K.; Exton, J.H. Activation of the zeta isozyme of protein kinase C by phosphatidylinositol 3,4,5-trisphosphate. J. Biol. Chem. **1993**, 268, 13–16. [CrossRef]
31. Wang, Y.M.; Seibenhener, M.L.; Vandenplas, M.L.; Wooten, M.W. Atypical PKC zeta is activated by ceramide, resulting in coactivation of NF-kappaB/JNK kinase and cell survival. J. Neurosci. Res. **1999**, 55, 293–302. [CrossRef]
32. Dowler, S.; Kular, G.; Alessi, D.R. Protein Lipid Overlay Assay. Sci. Signal. **2002**, 2002, pl6. [CrossRef] [PubMed]
33. Gomez-Cambronero, J.; Morris, A.; Henkels, K. PLD Protein–Protein Interactions With Signaling Molecules and Modulation by PA. In Methods in Enzymology; Academic Press: Cambridge, MA, USA, 2017; Volume 583, pp. 327–357. [CrossRef]
34. O'Luanaigh, N.; Pardo, R.; Fensome, A.; Allen-Baume, V.; Jones, D.; Holt, M.R.; Cockcroft, S. Continual Production of Phosphatidic Acid by Phospholipase D Is Essential for Antigen-stimulated Membrane Ruffling in Cultured Mast Cells. Mol. Biol. Cell **2002**, 13, 3730–3746. [CrossRef] [PubMed]
35. Sajan, M.P.; Bandyopadhyay, G.; Kanoh, Y.; Standaert, M.L.; Quon, M.J.; Reed, B.C.; Dikic, I.; Farese, R.V. Sorbitol activates atypical protein kinase C and GLUT4 glucose transporter translocation/glucose transport through proline-rich tyrosine kinase-2, the extracellular signal-regulated kinase pathway and phospholipase D. Biochem. J. **2002**, 362, 665–674. [CrossRef] [PubMed]
36. Nishioka, T.; Frohman, M.A.; Matsuda, M.; Kiyokawa, E. Heterogeneity of Phosphatidic Acid Levels and Distribution at the Plasma Membrane in Living Cells as Visualized by a Förster Resonance Energy Transfer (FRET) Biosensor. J. Biol. Chem. **2010**, 285, 35979–35987. [CrossRef] [PubMed]
37. Zhang, F.; Wang, Z.; Lu, M.; Yonekubo, Y.; Liang, X.; Zhang, Y.; Wu, P.; Zhou, Y.; Grinstein, S.; Hancock, J.F.; et al. Temporal Production of the Signaling Lipid Phosphatidic Acid by Phospholipase D2 Determines the Output of Extracellular Signal-Regulated Kinase Signaling in Cancer Cells. Mol. Cell. Biol. **2014**, 34, 84–95. [CrossRef]
38. De Matteis, M.A.; Di Campli, A.; Godi, A. The role of the phosphoinositides at the Golgi complex. Biochim. Biophys. Acta Bioenergy **2005**, 1744, 396–405. [CrossRef]
39. De Craene, J.-O.; Bertazzi, D.L.; Bär, S.; Friant, S. Phosphoinositides, Major Actors in Membrane Trafficking and Lipid Signaling Pathways. Int. J. Mol. Sci. **2017**, 18, 634. [CrossRef]
40. Phan, T.K.; Williams, S.; Bindra, G.K.; Lay, F.T.; Poon, I.K.H.; Hulett, M.D. Phosphoinositides: Multipurpose cellular lipids with emerging roles in cell death. Cell Death Differ. **2019**, 26, 781–793. [CrossRef]
41. Nascimbeni, A.C.; Codogno, P.; Morel, E. Phosphatidylinositol-3-phosphate in the regulation of autophagy membrane dynamics. FEBS J. **2017**, 284, 1267–1278. [CrossRef]
42. De Matteis, M.A.; Wilson, C.; D'Angelo, G. Phosphatidylinositol-4-phosphate: The Golgi and beyond. BioEssays **2013**, 35, 612–622. [CrossRef] [PubMed]
43. Poli, A.; Zaurito, A.E.; Abdul, S.; Fiume, R.; Faenza, I.; Divecha, N. Phosphatidylinositol 5 Phosphate (PI5P): From Behind the Scenes to the Front (Nuclear) Stage. Int. J. Mol. Sci. **2019**, 20, 2080. [CrossRef] [PubMed]
44. Soloff, R.S.; Katayama, C.; Lin, M.Y.; Feramisco, J.R.; Hedrick, S.M. Targeted Deletion of Protein Kinase C Reveals a Distribution of Functions between the Two Atypical Protein Kinase C Isoforms. J. Immunol. **2004**, 173, 3250–3260. [CrossRef] [PubMed]
45. Murray, N.R.; Kalari, K.R.; Fields, A.P. Protein kinase C expression and oncogenic signaling mechanisms in cancer. J. Cell. Physiol. **2010**, 226, 879–887. [CrossRef] [PubMed]
46. Parker, P.J.; Justilien, V.; Riou, P.; Linch, M.; Fields, A.P. Atypical Protein Kinase C as a human oncogene and therapeutic target. Biochem. Pharmacol. **2014**, 88, 1–11. [CrossRef]
47. Regala, R.P.; Weems, C.; Jamieson, L.; Khoor, A.; Edell, E.S.; Lohse, C.M.; Fields, A.P. Atypical Protein Kinase C Is an Oncogene in Human Non–Small Cell Lung Cancer. Cancer Res. **2005**, 65, 8905–8911. [CrossRef]
48. Eder, A.M.; Sui, X.; Rosen, D.G.; Nolden, L.K.; Cheng, K.W.; Lahad, J.P.; Kango-Singh, M.; Lu, K.H.; Warneke, C.L.; Atkinson, E.N.; et al. Atypical PKC contributes to poor prognosis through loss of apical-basal polarity and Cyclin E overexpression in ovarian cancer. Proc. Natl. Acad. Sci. USA **2005**, 102, 12519–12524. [CrossRef]
49. Du, G.; Wang, J.-M.; Lu, J.-X.; Li, Q.; Ma, C.-Q.; Du, J.-T.; Zou, S.-Q. Expression of P-aPKC-, E-Cadherin, and -Catenin Related to Invasion and Metastasis in Hepatocellular Carcinoma. Ann. Surg. Oncol. **2009**, 16, 1578–1586. [CrossRef]
50. Kojima, Y.; Akimoto, K.; Nagashima, Y.; Ishiguro, H.; Shirai, S.; Chishima, T.; Ichikawa, Y.; Ishikawa, T.; Sasaki, T.; Kubota, Y.; et al. The overexpression and altered localization of the atypical protein kinase C / in breast cancer correlates with the pathologic type of these tumors. Hum. Pathol. **2008**, 39, 824–831. [CrossRef]

51. Justilien, V.; Fields, A.P. Ect2 links the PKC–Par6 complex to Rac1 activation and cellular transformation. Oncogene **2009**, 28, 3597–3607. [CrossRef]
52. Regala, R.P.; Weems, C.; Jamieson, L.; Copland, J.A.; Thompson, E.A.; Fields, A.P. Atypical Protein Kinase C Plays a Critical Role in Human Lung Cancer Cell Growth and Tumorigenicity. J. Biol. Chem. **2005**, 280, 31109–31115. [CrossRef] [PubMed]
53. Erdogan, E.; Lamark, T.; Stallings-Mann, M.; Jamieson, L.; Pellechia, M.; Thompson, E.A.; Johansen, T.; Fields, A.P. Aurothiomalate Inhibits Transformed Growth by Targeting the PB1 Domain of Protein Kinase C. J. Biol. Chem. **2006**, 281, 28450–28459. [CrossRef] [PubMed]
54. Frederick, L.; Matthews, J.; Jamieson, L.; Justilien, V.; Thompson, E.; Radisky, D.C.; Fields, A.P. Matrix metalloproteinase-10 is a critical effector of protein kinase C-Par6-mediated lung cancer. Oncogene **2008**, 27, 4841–4853. [CrossRef] [PubMed]
55. Justilien, V.; Jameison, L.; Der, C.J.; Rossman, K.L.; Fields, A.P. Oncogenic Activity of Ect2 Is Regulated through Protein Kinase C-mediated Phosphorylation. J. Biol. Chem. **2010**, 286, 8149–8157. [CrossRef]
56. Aranda, V.; Haire, T.; Nolan, M.E.; Calarco, J.P.; Rosenberg, A.Z.; Fawcett, J.P.; Pawson, T.; Muthuswamy, S.K. Par6–aPKC uncouples ErbB2 induced disruption of polarized epithelial organization from proliferation control. Nat. Cell Biol. **2006**, 8, 1235–1245. [CrossRef]
57. Hernández, A.I.; Blace, N.; Crary, J.F.; Serrano, P.A.; Leitges, M.; Libien, J.M.; Weinstein, G.; Tcherapanov, A.; Sacktor, T.C. Protein Kinase M Synthesis from a Brain mRNA Encoding an Independent Protein Kinase C Catalytic Domain. J. Biol. Chem. **2003**, 278, 40305–40316. [CrossRef]
58. Sánchez-Gómez, P.; De Cárcer, G.; Sandoval, I.V.; Moscat, J.; Diaz-Meco, M.T. Localization of Atypical Protein Kinase C Isoforms into Lysosome-Targeted Endosomes through Interaction with p62. Mol. Cell. Biol. **1998**, 18, 3069–3080. [CrossRef]
59. Standaert, M.L.; Bandyopadhyay, G.; Kanoh, Y.; Sajan, M.P.; Farese, R.V. Insulin and PIP3Activate PKC- by Mechanisms That Are Both Dependent and Independent of Phosphorylation of Activation Loop (T410) and Autophosphorylation (T560) Sites. Biochemistry **2001**, 40, 249–255. [CrossRef]
60. Fox, T.E.; Houck, K.L.; Oneill, S.M.; Nagarajan, M.; Stover, T.C.; Pomianowski, P.T.; Unal, O.; Yun, J.K.; Naides, S.J.; Kester, M. Ceramide Recruits and Activates Protein Kinase C (PKC) within Structured Membrane Microdomains. J. Biol. Chem. **2007**, 282, 12450–12457. [CrossRef]
61. Bourbon, N.A.; Yun, J.K.; Kester, M. Ceramide Directly Activates Protein Kinase C to Regulate a Stress-activated Protein Kinase Signaling Complex. J. Biol. Chem. **2000**, 275, 35617–35623. [CrossRef]
62. Chalfant, C.E.; Szulc, Z.; Roddy, P.; Bielawska, A.; Hannun, Y.A. The structural requirements for ceramide activation of serine-threonine protein phosphatases. J. Lipid Res. **2003**, 45, 496–506. [CrossRef] [PubMed]
63. Pastor-Flores, D.; Schulze, J.O.; Bahí, A.; Süß, E.; Casamayor, A.; Biondi, R.M. Lipid regulators of Pkh2 in Candida albicans, the protein kinase ortholog of mammalian PDK1. Biochim. Biophys. Acta Mol. Cell Biol. Lipids **2016**, 1861, 249–259. [CrossRef] [PubMed]
64. Heras-Martínez, G.D.L.; Calleja, V.; Bailly, R.; Dessolin, J.; Larijani, B.; Requejo-Isidro, J. A Complex Interplay of Anionic Phospholipid Binding Regulates 3^0-Phosphoinositide-Dependent-Kinase-1 Homodimer Activation. Sci. Rep. **2019**, 9, 1–18. [CrossRef] [PubMed]

Wiskott-Aldrich syndrome protein interacts and inhibits diacylglycerol kinase alpha promoting IL-2 induction

Suresh Velnati[1,2,†$], Sara Centonze[1,2†*], Giulia Rossino[3], Beatrice Purghè[2], Annamaria Antona[1], Elisa Ruffo[4], Valeria Malacarne[3], Mario Malerba[1,5], Marcello Manfredi[2], Andrea Graziani[3] and Gianluca Baldanzi[1,2]

[1]Università del Piemonte Orientale, Department of Translational Medicine, Novara, Italy

[2]Università del Piemonte Orientale, Center for Translational Research on Allergic and Autoimmune Diseases (CAAD), Novara, Italy

[3]University of Turin, Department of Molecular Biotechnology and Health Sciences, Molecular Biotechnology Center (MBC), Turin, Italy

[4]University of Pittsburgh, Department of Surgery and Immunology, Pittsburgh, USA

[5]Respiratory Unit, Sant'Andrea Hospital, Vercelli, Italy

*** Correspondence:**
Sara Centonze
sara.centonze@uniupo.it

† Equal contributions: These authors contributed equally to this work and share the first authorship.

$ Current address: University of Trieste, Department of Life Sciences, Trieste, Italy

Keywords: WAS, DGK, T cell receptor signalling, SLAM-associated protein, restimulation-induced cell death, X-linked lymphoproliferative disease.

Language style: The present article is formatted in British English

Number of words: 7802

Number of figures: 10 Figures, 2 Tables

1 Abstract

Phosphorylation of diacylglycerol by diacylglycerol-kinases represents a major inhibitory event constraining T cell activation upon antigen engagement. Efficient TCR signalling requires the inhibition of the alpha isoform of diacylglycerol kinase, DGKα, by an unidentified signalling pathway triggered by the protein adaptor SAP. We previously demonstrated that, in SAP absence, excessive DGKα activity makes the T cells resistant to restimulation induced cell death (RICD), an apoptotic program counteracting excessive T cells clonal proliferation.

Inhere, we report that DGKα inhibition is mediated by a specific interaction of the DGKα recoverin homology domain with the WH1 domain of the Wiskott-Aldrich syndrome protein (WASp). Indeed, WASp is necessary and sufficient for DGKα inhibition, and this WASp function is independent of ARP2/3 activity. The adaptor protein NCK-1 and the small G protein CDC42 connect WASp-mediated DGKα inhibition to SAP and the TCR signalosome. In primary human T cells, this new signalling pathway is necessary for a full response in terms of IL-2 induction, while minimally affecting TCR signalling and restimulation-induced cell death. Conversely, in T cells made resistant to RICD by SAP silencing, the enhanced DAG signalling due to DGKα inhibition is sufficient to restore apoptosis sensitivity.

Concluding, we discover a novel signalling pathway where WASp triggered by strong TCR agonists, blocks DGKα activity for a full cytokine response.

2 Introduction

Diacylglycerol kinases (DGK) tune lipid signalling by metabolizing diacylglycerol (DAG) to phosphatidic acid. Two isoforms, namely DGKα and DGKζ, play a major role as negative regulators of DAG-mediated TCR signalling. This signalling includes the Ras guanyl nucleotide-releasing protein 1 (RasGRP1)/Ras/mitogen-activated protein kinases (MAPKs) pathway, the activator protein 1 (AP1) transcription factor activity, and the interleukin 2 (IL-2) induction (1). The activity of both isoforms promotes T cells anergy, a tolerance condition characterized by the uncoupling of ligand-induced TCR activation from downstream signalling, while their inhibition potentiates T cell activation and IL-2 synthesis (2, 3). In addition, DGKα and DGKζ contribute to tumour cell immune escape, and their inhibition rescues defective anti-tumour killing activity in tumour-specific exhausted T cells (4, 5). Quantitative studies indicate that DGKζ is responsible for the metabolism of most of the DAG generated by phosphatidylinositol 4,5-bisphosphate (PIP_2) hydrolysis and controls the activation of DAG-effectors such as protein kinase C theta (PKCθ) and RasGRP1 (6, 7). Conversely, DGKα activity is rapidly recruited in a phosphatidylinositol (3,4,5)-trisphosphate (PIP_3)-dependent manner to phosphorylate a minor pool of DAG at the periphery of the immune synapse playing a key function in shaping immune synapse and cell polarization (8).

Consistently with their role as negative regulators, the expression of both DGKα and DGKζ is downregulated 3-5-fold upon antigen-induced T cell differentiation into effector cells through the PIP_3 signalling pathways (9, 10). The simultaneous triggering of CD3 and CD28 causes also a specific and rapid downmodulation of DGKα enzymatic activity. This downmodulation requires PLC activity and the small SH2-containing adaptor protein SAP (SLAM associated protein) (11). Loss of function mutations of the SAP encoding gene SH2D1A causes X-linked lymphoproliferative disease type 1 (XLP-1), a primary immunodeficiency characterized by multiple defects in the T and NK cell compartments leading to EBV-triggered hemophagocytic lymphohistiocytosis (HLH), hypogammaglobulinemia and predisposition to lymphomas (12). In T cells from XLP-1 patients, SAP absence abolishes the costimulatory function of the signalling lymphocytic activation molecule (SLAM) family of membrane receptors and facilitates the recruitment of the inhibitory tyrosine

phosphatases Src homology phosphatase 1 and 2 (SHP-1 and SHP-2). This reduces TCR signalling strength to nuclear factor of activated T-cells (NF-AT) and the induction of interleukins such as IL-2 and IL-10 along with proapoptotic mediators like FAS ligand, Bcl-2 Interacting Mediator of cell death (BIM), and nuclear receptor 4A1 (NUR77). The typical predisposition to HLH of XLP-1 patients is due to two factors: i) decreased signalling strength and modified assembly of the TCR signalosome, which leads to lymphocyte accumulation due to defective restimulation-induced cell death (RICD), and ii) altered immune synapse morphology which decreases cytotoxic T cells (CTL) efficiency in removing Epstein-Barr virus (EBV) infected B cells (13). Those functional defects in T cells are in part due to excessive DGKα activity that, in absence of SAP, blunts T cell signalling. Although the molecular mechanisms connecting SAP and DGKα are uncharacterized, inhibition or silencing of DGKα in SAP-deficient T cells rescues immune synapse morphology and DAG signalling strength along the Ras/MAPK, PKCθ, and NF-AT signalling pathways. Moreover, DGKα inhibitors are effective also in rescuing some aspects of the immunopathology of XLP-1 murine models, indicating a crucial role of DGKα in the XLP-1 pathology onset (14). Interestingly, while knockdown of DGKα in SAP deficient cells rescues the signalling machinery necessary for RICD and IL-2 expression, other crucial effectors such as FASL remain downregulated, indicating the existence of diverging SAP-90 dependent signal pathways (14, 15). Indeed, SAP participates in multiple crucial interactions in T cells such as the recruitment of Fyn and Lck tyrosine kinases to SLAM receptors (16, 17), the recruitment of other SH3-containing adaptors such as NCK adaptor protein 1 (NCK-1) (18) and the activation of Rac/ cell division control protein 42 (CDC42) small G proteins through the pak interacting exchange factor (βPIX) which in turn drives NF-AT activation (19).

To better understand the signalling mechanism by which SAP negatively regulates DGKα activity, we focused on the Wiskott–Aldrich syndrome protein (WASp) as this protein is regulated by NCK-1 binding to the WASp proline-rich region mediating its localization, and CDC42 binding to CRIB domain of WASp promoting its activation (20, 21). Moreover, it was already reported that lymphocytes from WASp deficient mice have defective RICD, reinforcing the notion of the existence of a SAP-WASp signalling pathway (22). WASp belongs to the nucleation-promoting factors (NPFs) family and by activating the actin-related protein 2/3 (ARP2/3) complex, it facilitates actin polymerization at the T cell immune synapse (23, 24) but also NF-AT nuclear translocation for IL-2 induction (25). Loss of function mutations in WASp gives rise to the Wiskott–Aldrich syndrome, which is characterized by bleeding, thrombocytopenia, eczema, frequent infections, and susceptibility to the development of autoimmune diseases and lymphomas (26). Thus, the signalling connections and some similarities between those two primary immunodeficiencies (27) prompted us to explore a role for WASp and CDC42 in regulating DGKα activity and DAG-dependent T cell activation.

3 Materials and Methods

All the chemical reagents used in this study are listed in Table 1.

3.1 Cell culturing

Human embryonic kidney 293T cells were cultured in 100 mm plates using DMEM with 10% FBS (Lonza) and 1% penicillin/ streptomycin (Life Technologies).

Jurkat cells were cultured in RPMI-GlutaMAX (Life Technologies) with 10% FBS (Lonza) and 1% penicillin/ streptomycin (Life Technologies).

Peripheral blood mononuclear cells (PBMCs) were isolated from healthy anonymous human buffy coats (provided by the Transfusion Service of Ospedale Maggiore della Carità, Novara, Italy). PBMCs were isolated by Ficoll-Paque PLUS (GE Healthcare) density gradient centrifugation, washed, and

resuspended at 2 x 10^6 cells/ml in RPMI-GlutaMAX containing 10% heat-inactivated FBS (Lonza), 2 mM glutamine, and 100 U/ml of penicillin and streptomycin (Life Technologies). T cells were activated with 1 µg/ml anti-CD3 (clone UCHT1) and anti-CD28 (clone CD28.2) antibodies for 72 hours. Activated T cells were then washed and cultured in the complete medium along with 100 IU/ml rhIL-2 (PeproTech) at 1-2 x 10^6 cells/ml for ≥ 7 days by changing media every 2–3 days.

3.2 Generation of Jurkat WASp shRNA and the Jurkat control shRNA

To generate stable WASp-silenced Jurkat cells we used MISSIONpLKO.1-puro Empty Vector Plasmid DNA (Sigma-Aldrich) harbouring either the sequence targeting human WASp (WASp *shRNA*) or a non-targeting short hairpin RNA (*shRNA*). Jurkat cells were plated and transduced with lentiviral particles in the presence of polybrene (6 µg/ml: Sigma-Aldrich, Saint Louis, MO, USA). Spinoculation protocol was performed as follows: the plate was centrifuged for 30 minutes at 32°C, 800 g. Subsequently, the medium containing viral particles was removed, and cells were resuspended in a fresh medium and incubated for three days (37°C, 5% CO_2). Lastly, 1 µg/ml puromycin (Sigma-134 Aldrich, Saint Louis, MO, USA) was added for the selection.

3.3 Jurkat cell stimulations and Immunoprecipitation for activity assays

Jurkat cells (Control *shRNA* and WASp *shRNA*) were cultured at a concentration of 1 x 10^6 cells/ml for 3 continuous weeks. 3 x 10^7 cells for each condition were resuspended in RPMI 1640 (preheated at 37°C) and/or pre-treated with DMSO or ARP2/3 inhibitor and/or DGKα inhibitor for 30 minutes. After pre-treatment, cells were stimulated using anti CD3 (UCHT1 clone) at a concentration of 10 µg/ml for 15 minutes and cells were lysed in 1 ml of lysis buffer. An aliquot of 50 µl cell lysates was retained for western blot analysis and the remaining was subjected to immunoprecipitation using 5 µg/ml of anti-DGKα antibodies (Abcam-AB64845) for 4 hours using protein G agarose beads in continuous rotation at 4°C. After immunoprecipitation, beads with DGKα antibody were washed twice with lysis buffer followed by 2 washes in $LiCl_2$ and 2 in TNE buffer. Following, the DGKα immunoprecipitates were subjected to DGK assay to measure DGK activity.

3.4 Preparation of 293T homogenates for activity assays

293T cells were transiently transfected with indicated plasmid DNA using Lipofectamine 3000, Invitrogen (Carlsbad, CA) in 10 cm^2 plates. 48 hours post-transfection, cells were harvested and homogenized by passing them 30 times through a 29G-needle using 500 µl of homogenization buffer for each dish and immediately stored in aliquots at -80°C. Cells transfected with GFP were used as controls.

3.5 DGK activity assay

Fundamentally, the same procedure was followed as reported previously in (11). In brief, DGK activity was assayed by measuring initial velocities (5 minutes at 27°C) in presence of saturating substrate concentration. Reaction conditions: 0.9 mg/ml 1,2-dioleoyl-sn-glycerol, 5 mM ATP, 0.01 mCi/ml [c^{32}P]-ATP (for homogenates) or 0.04 mCi/ml [c^{32}P]-ATP (for immunoprecipitates), 1 mM sodium orthovanadate, 10 mM $MgCl_2$, 1.2 mM EGTA in 7.5 mM HEPES pH 8. The reaction mixture is assembled by mixing enzyme (25 µl of either cell homogenates or immunoprecipitated endogenous DGKα), 5X ATP solution, and 3X DAG solution. The reaction was terminated after 5 minutes by adding 200 µl of freshly prepared 1 M HCl and lipid was extracted by adding 200 µl of CH_3OH:$CHCl_3$ 1:1 solution and vortexing for 1 minute. The two phases were separated by centrifugation (12,000 RCF

for 2 minutes). Either 25 µl (for homogenates) or 50 µl (for DGKα immunoprecipitates) of the lower organic phase was spotted in small drops on silica TLC plates. TLC was run 10 cm and dried before radioactive signals were detected by GS-250 molecular imager and were quantified by either quantity one 4.01 or image lab 6.0 (Bio-Rad, Hercules, CA) software assuring the absence of saturated spots.

3.6 Lipidomic analysis

Jurkat cells were starved overnight in RPMI 0% FBS at a concentration of 2 x 10^6 cells/ml. The following morning, cells were washed in PBS and stimulated using anti CD3 (OKT3 clone) + CD28.2 antibodies at a concentration of 1 µg/ml for 15 minutes at 37°C. Post-stimulation, cells were washed four times in ice-cold PBS by centrifugation (700 g for 5 minutes) and after the last wash, the pellet was dried and subjected to lipidomic analysis.

Cells were extracted using 1 ml of 75:15 IPA/H_2O solution, after the addition of 100 µl of CH_3OH 5% deuterated standard (Splash Lipidomix®). Then the samples were vortexed for 30 seconds, sonicated for 2 minutes, vortexed again for 30 seconds and then they were incubated for 30 minutes at 4°C, under gentle, constant shaking. Subsequently, samples were rested on ice for additional 30 minutes. To remove debris and other impurities, the samples were centrifuged for 10 min at 3500 g at 4 °C. 1 ml of supernatant was collected and dried using a SpeedVac centrifuge (Labogene). The dried samples were reconstituted in 100 µl of CH_3OH containing the internal standard CUDA (12.5 ng/ml).

For the analysis of the reconstituted lipids, a UHPLC Vanquish system (Thermo Scientific, Rodano, Italy) coupled with an Orbitrap Q-Exactive Plus (Thermo Scientific) was used.

Mass spectrometry analysis was performed in positive ion mode. The source voltage was maintained at 3.5 kV. The capillary temperature, sheath gas flow, and auxiliary gas flow were set at 320 °C, 40 arb, and 3 arb respectively. S-lens was settled at 50 rf. Data were collected in a data-dependent (ddMS2) top 10 scan mode. Survey full-scan MS spectra (mass range m/z 80 to 1200) were acquired with resolution R = 70,000 and AGC target 1e6. MS/MS fragmentation was performed using high-energy c-trap dissociation (HCD) with resolution R = 17,500 and AGC target 1e5. The stepped normalized collision energy (NCE) was set to 15, 30, and 45 respectively. The injection volume was 3 µl. Lockmass and regular inter-run calibrations were used for accurate mass-based analysis. An exclusion list for background ions was generated by analysing a procedural blank sample. The acquired raw data were processed using MSDIAL software (Yokohama City, Kanagawa, Japan), version 4.24.

A QC-based regression model using linear weighted scatter plot smoothing (LOWESS) was used to adjust real sample signals according to the analytical order. Results are then reported as normalized peak intensity.

3.7 Proximity Ligation Assay (PLA)

Isolated human PBLs (0.15 x 10^6) were seeded in poly-L-lysine coated glasses in a 24-well plate and treated with the indicated stimuli. The cells were washed with ice-cold PBS, fixed in 3% paraformaldehyde/4% sucrose pH 7.4 for 10 minutes, permeabilized in ice-cold HEPES-Triton X-100 buffer (HEPES pH 7.4 20 mM, sucrose 300 mM, NaCl 50 mM, $MgCl_2$ 3 mM, Triton X-100 0.5%) for 5 minutes, washed twice with PBS, and processed according to the PLA (Duolink, Merck, cat. DUO92101) manufacturer's protocol. The samples were imaged with TCS SP5 confocal microscope (Leica Microsystem) as z stack of 1 µm thickness to cover the entire volume of the cells with a Plan Apo 63 X (NA 1.4) oil objective. PLA dots were quantified manually on maximum projection images obtained with Image J software (NIH).

3.8 Complex formation assays

293T cells were plated in 100 mm diameter Petri dishes and allowed to reach 90% confluence. Transfections were performed with the indicated DNA plasmids using Lipofectamine 3000 reagent according to the manufacturer's instructions (Invitrogen by Thermo Fisher). After 48 hours, cells were washed in ice-cold PBS and lysed in 1 ml of lysis buffer. Subsequently, lysates were incubated with 5 µg/ml anti-FLAG antibody (Sigma-Aldrich) or with 5 µg/ml anti-myc antibody agarose conjugated (Santa Cruz Biotechnology) and 20 µl Protein G Sepharose beads Fast Flow (Sigma) at 4 °C. 1 hour post-incubation beads were washed in lysis buffer six times and boiled in Laemmli Sample Buffer for 5 minutes at 95 °C. Thus, obtained immunoprecipitates were loaded on SDS-PAGE and analysed by western blotting using ChemiDoc™ Imaging System (Bio-Rad).

3.9 Restimulation-induced cell death (RICD) assays in human peripheral T cells

Activated human PBLs were transfected with 200 pmol of siRNA oligonucleotides specific for the target protein or a non-specific Stealth RNAi Negative Control Duplexes (12935-300) (Stealth Select siRNA; Life Technologies). Transient transfections were performed using Amaxa nucleofector kits for human T cells (Lonza) and either the Amaxa Nucleofector 4D systems (programs E0-115) or the Amaxa Nucleofector II system (program "primary lymphocyte T-020"). Cells were cultured in IL-2 (100 IU/ml) for 4 days to allow target gene knockdown. Knockdown efficiency was periodically evaluated either by Western blotting or by rt-PCR.

To test restimulation-induced cell death (RICD), activated T cells (10^5 cells/well in 200 µl) were plated in either triplicates or quadruplicates in 96-well round-bottom plate and treated with increasing concentrations of anti-CD3 (clone OKT3) 0, 10, 100 ng/ml in RPMI-GlutaMAX supplemented with 100 IU/ml rhIL-2 for 24 hours. In these assays, DGK inhibitor AMB639752 (10 µM) was added 30 minutes before the restimulation with OKT3. 24 hours after treatment, cells were stained with 20 ng/ml propidium iodide and collected for a constant volume of 150 µl per sample on Attune Nxt Flow Cytometer (Thermo Fisher Scientific). Cell death is expressed as % cell loss and calculated as

% Cell loss = (1-(number of viable cells in sample/number of viable cells in control) x 100)

Results were expressed as mean ± standard error mean (SEM). We always compare controls and WASp silenced lymphocytes from the same donors as there is a large individual variability in RICD sensitivity.

3.10 Gene expression assays

Activated human PBLs were transfected as described above and 4 days after transfection, cells were collected, washed, and seeded at the concentration of 1.5 x 10^6 cells in 1 ml of RPMI supplemented with 10% FBS and 100 IU/ml rhIL-2. Subsequently, cells were pre-treated for 30 minutes with the indicated inhibitors or DMSO and stimulated with OKT3 + CD28.2 at the concentration of 1 µg/ml. After 4 hours, cells were collected, washed twice with ice-cold PBS, and subjected to RNA extraction using RNeasy Plus mini kit from Qiagen or Maxwell RSC simply RNA extraction kit (AS1390, Promega Italia), following manufacturer instructions. The RNA concentration and purity were estimated by a spectrophotometric method using Nanodrop 2000c (Thermo Scientific). The RNA was retrotranscribed with LunaScript RT Supermix kit (NEB) or High-Capacity cDNA Reverse Transcription Kits (Applied Biosystems). The resulting cDNA was quantified by real-time PCR (Luna Universal qPCR Master Mix by NEB or ABI7900 by Applied Biosystems) in either 96 or 384 well plates using GUSB or GAPDH as normalizers.
WASp shRNA transduced Jurkat cells were collected periodically along with control shRNA transduced Jurkat cells to check the efficiency of WASp silencing.

3.11 Western blot analysis

To verify the protein expression in immunoprecipitated Jurkat cells or 293T cells, equal amounts of protein lysates or homogenates were analysed by western blotting as following described. Proteins were separated on SDS–PAGE gels and subsequently transferred to a polyvinylidene fluoride (PVDF) membrane. The membranes were then blocked by incubating with 3% (w/v) dried BSA for 1 hour at room temperature and subjected to overnight incubation with respective primary antibodies at 4 °C with gentle agitation. The following day, membranes were washed 4 times in TBS-T buffer at 15 minutes time intervals. They were then incubated with alkaline HRP-conjugated rabbit or mouse secondary antibody (1:5000, PerkinElmer, USA) diluted in TBS-T, for 1 hour at room temperature with gentle agitation. After four additional 15 minutes washes with TBS-T, the membranes were developed using the Western Chemiluminescence Substrate (PerkinElmer, USA) using the ChemiDoc™ Imaging System (Bio-rad).

3.12 Statistical analysis

Evaluation of all the *in vitro* assays across multiple treatments, DGK activity assays, homogenates activity assays, RICD assays, and gene expression assays were analysed by using either one-way ANOVA or two-way ANOVA with multiple comparisons correction using either GraphPad PRISM 9.0 or 9.4 software. Single treatments of lipidomic data were analysed with Student T-test using GraphPad PRISM software. Error bars are described in Figure legends as ± SEM or ± SD where appropriate. A single, double, triple, and four asterisks denote their significance of a p-value ≤ 0.05, ≤ 0.01, ≤ 0.001 and ≤ 0.0001 respectively in all experiments.

4 Results

4.1 WASp is necessary for DGKα inhibition upon TCR activation

We have previously reported that T cell co-stimulation with OKT3 and CD28.2 results in a SAP-282 mediated inhibition of the DGKα activity (11). Similarly to SAP, WASp is an adaptor protein tuning the TCR signalling which leads to cytokine expression and RICD (22, 24). Thus, we investigated whether WASp is involved in the signalling pathway triggered by TCR which leads to DGKα inhibition. As we observed that the sole triggering of the TCR with the strong agonist antibody UCHT1 is sufficient for DGKα inhibition, we used this condition in the following experiments.

Initially, WASp expression was downregulated in Jurkat cells by lentiviral-mediated stable expression of a WASp-specific short hairpin RNA (*shRNA).* WASp silencing was monitored regularly to verify the efficiency of WASp knockdown and we observed a decrease of mRNA of around 50%, considering control *shRNA* (non-targeting *shRNA)* transduced Jurkat cells as a suitable control (Fig. 1D). Following 15 minutes of stimulation with CD3 agonist antibody (UCHT1 – 10 µg/ml), the enzymatic activity of immunoprecipitated DGKα was measured in Jurkat cells transduced with WASp *shRNA* or control *shRNA*. Consistently with previous results, the DGKα enzymatic activity was reduced by ∼50% upon CD3 stimulation in control *shRNA* Jurkat cells. Conversely, DGKα activity was not reduced upon stimulation in WASp *shRNA* Jurkat cells (Fig. 1A), indicating that WASp is required for the negative regulation of DGKα activity upon TCR stimulation. In the same assays, western blot analysis confirmed that DGKα protein content does not change upon TCR triggering in both Jurkat cell lines (Fig. 1B), indicating that this regulation is not due to changes in protein expression levels. We also verified that DGKα protein is reproducibly immunoprecipitated independently of the cell type (control shRNA versus WASp shRNA) or stimulation (UCHT1 10 µg/ml) (Supp. Mat. 1).

TCR induction of the MAPK pathways is partially dependent on the DAG activation of the RasGRP1 (28). To evaluate the DAG signalling in the absence of WASp, we assessed the phosphorylation status of ERK1/2 in the same samples. We observed a threefold increase in ERK1/2 phosphorylation upon UCHT1 treatment, which was not consistently influenced by WASp silencing (Fig. 1C). Those data suggest that upon intense CD3 stimulation by UCHT1, WASp is relatively dispensable for TCR signalling on the ERK1/2 pathway. Moreover, the finding that ERK1/2 activation is normal in WASp-silenced cells despite high DGKα activity indicates that the DAG pool phosphorylated by DGKα is relatively dispensable for TCR signalling in those conditions. To directly evaluate the influence of WASp on T-cell DAG levels, we used a targeted mass spectrometry approach to quantify the DAG species. When Jurkat cells were stimulated with OKT3 (1 µg/ml) and CD28.2 (1 µg/ml) for 15 minutes, we observed a significant increase in selected DAG species (Supp. Mat. 2 and Supp. Table S1). The same species also increase in WASp silenced cells upon TCR + CD28 co-stimulation, confirming that the DAG pool regulated by DGKα under the control of WASp is quantitatively small. Upon TCR triggering, WASp regulates actin dynamics at the immune synapse by recruiting and activating the ARP2/3 complex (23). Thus, we verified if either ARP2/3 activity or actin polymerization is required for TCR-promoted inhibition of DGKα activity by using the ARP2/3 inhibitor CK666 or the actin polymerization inducer jasplakinolide. Jurkat cells were pre-treated for 30 minutes with either CK666 (60 µM) or jasplakinolide (0.5 µg/ml) before stimulation with anti-CD3 (UCHT1 10 µg/ml, 15 minutes) and quantification of DGKα enzymatic activity. As expected DGKα activity was reduced by 50% upon TCR stimulation with no change in DGKα protein. Conversely, treatment with ARP2/3 inhibitor had a very mild effect on basal or TCR inhibited DGKα activity and jasplakinolide showed no effect on basal condition (Fig. 2A and 2B). As a readout of DAG signalling, we also assessed the phosphorylation of ERK1/2 using western blot analysis. Both the ARP2/3 inhibitor and jasplakinolide did not show any effects on ERK1/2 phosphorylation (Fig. 2C), suggesting that ARP2/3 or actin polymerization does not participate in the control of DGKα and ERK1/2 activity. Overall, DGKα inhibition upon TCR stimulation is mediated by WASp independently from ARP2/3 activity. In presence of SAP, this modulation of DGKα activity does not affect TCR signalling potency on the ERK1/2 pathway.

4.2 WASp binds and inhibits DGKα

Based on the discovery of the involvement of WASp in the TCR-driven signalling cascade and promoting DGKα inhibition, we checked whether WASp could bind DGKα and promote its inhibition. To verify this possibility, we co-transfected myc-DGKα with either FLAG-WASp or GFP control vector in 293T cells and measured DGKα activity at 48 hours using total cell homogenates. In this system, DGKα is overexpressed and the DGK activity was proportional to the amount of transfected DGKα and was distinguishable from the endogenous background (Fig. 3A). Notably, upon co-transfection with FLAG-WASp, the DGKα enzymatic activity was reduced by around 50% without any reduction of DGKα protein (Fig. 3A and 3B). This observation indicates that WASp overexpression in 293T cells is sufficient to inhibit the DGKα activity without affecting its expression. We also noted that co-transfection with DGKα but not GFP control vector strongly enhances WASp protein levels (Fig. 3) suggesting that the presence of DGKα promotes WASp stabilization similarly to what was previously reported for the WIP (29).

WASp is a hub for protein-protein interactions, active WASp is known to form a complex with CDC42 (20). Thus, we explored the possibility of DGKα regulation by this small GTPase. To verify this possibility, we co-transfected myc-DGKα with the constitutively active myc-CDC42 Q61L. Differently from what was observed upon co-transfection with FLAG-WASp, the presence of active CDC42 did not affect DGKα enzymatic activity or protein level in WASp absence reinforcing its central role in the control of DGKα activity (Supp. Mat. 3).

Since we observed a role for WASp in controlling DGKα activity, we set to investigate whether the two proteins may associate. To verify if the endogenous proteins are in close proximity in primary T cells, we performed a Proximity Ligation Assay (PLA). Several fluorescent spots were detected in both unstimulated and anti-CD3/CD28 stimulated cells; in contrast no signals were generated where primary antibodies were missing (negative control) (Fig. 4A). Quantification of PLA events highlights the close association between DGKα and WASp, without a significant modulation driven by CD3-CD28 co-stimulation (Fig. 4B).

To confirm the formation of a complex between DGKα and WASp, we co-expressed both the proteins in 293T cells and immunoprecipitated myc-DGKα and/or FLAG-WASp. The co-precipitation of the partner protein was verified by western blotting. We observed the presence of myc-DGKα in anti-FLAG immunoprecipitates when the two proteins were co-expressed, indicating the existence of a DGKα-WASp complex (Fig. 4C left side). We also detected FLAG-WASp protein in the corresponding anti-myc immunoprecipitated lysate, as a further confirmation of this interaction (Fig. 4C right side). The input bands indicating equal transfection efficiency are shown in Fig. 4D.

Moreover, to explore this DGKα-WASp complex formation and to identify their protein binding site, we performed the same immunoprecipitation assays using a series of DGKα and WASp deletion mutants. Initially, we used the myc-DGKα-L360* mutant, which lacks the C-terminal catalytic region (30). Our results (Fig. 5B) demonstrate that this DGKα mutant retains the ability to bind WASp, indicating that WASp-DGKα interaction is mediated by the N-terminal DGKα regulatory domain. Thus, we produced the GST-DGKα E86* mutant maintaining the sole recoverin homology domain of DGKα, GST tag was used for this mutant as the corresponding myc tagged version is not sufficiently stable putatively due to the small size. As expected, glutathione beads pulled down GST-DGKα wt and the associated FLAG-WASp confirming the interaction between the two. The observation that also the GST-DGKα E86* mutant pulled down FLAG-WASp indicates a role of the N-terminal recoverin homology domain of DGKα in this complex (Fig. 5C). To further verify the specificity of this interaction, we repeated the co-immunoprecipitation assay with the highly homologous HA-DGKγ. We observed that the amount of HA-DGKγ immunoprecipitated by anti-FLAG antibodies depends on its overexpression but not by the presence of FLAG-WASp. Those data suggest that this isoform does not associate with FLAG-WASp (Fig. 5D).

Conversely, we produced the FLAG-tagged WASp Q297* mutant lacking the C-terminal proline-rich and VCA domains and the WASp K232* mutant retaining the sole WH1 domain. The observation that similar amounts of myc-DGKα wt co-immunoprecipitated with FLAG-WASp wt and the two deletion mutants indicate the role of the WH1 domain in the formation of the complex with DGKα (Fig. 6B).

Lastly, to investigate the specificity of this interaction we tested the interaction between myc-DGKα and myc-FLAG-N-WASp a closely related WASp homologue featuring non-redundant functions. The immunoprecipitation with the anti-FLAG antibody revealed that myc-DGKα coimmunoprecipitates specifically with FLAG-WASp but not with myc-FLAG-N-WASp even if the latter is far more expressed (Fig. 6C). This indicates a selectivity for WASp in the interaction with DGKα.

Taken together these data demonstrate that *in vitro* DGKα and WASp can associate selectively by forming a stable complex mediated by WASp WH1 domain and DGKα recoverin homology domain. Here in, WASp inhibits DGKα enzymatic activity putatively impairing the shift to the active conformation for which the recoverin homology domain is required (31).

4.3 DGKα silencing or inhibition rescues IL-2 expression in WASp deficient T cells

DGKα inhibition is known to enhance TCR-promoted induction of IL-2 (32). Moreover, the lack of DGKα inhibition in SAP deficient cells drives defective cytokine induction and RICD, which are rescued by the DGKα inhibition (14, 15). Since a similar defect in RICD and IL-2 induction is present in murine WASp deficient cells (22, 33) we evaluated the effect of DGKα inhibition on RICD, TCR

signalling potency, and IL-2 production in WASp deficient human lymphocytes. We silenced WASp in activated primary peripheral blood T lymphocytes (PBLs) using specific siRNA. To assess WASp silencing, WASp mRNA or protein levels were evaluated in all the experiments. At 4 days post silencing, we observed 80% reduction of WASp mRNA and 70% decrease in WASp protein compared to control siRNA transfected cells (Fig. 7F and 7C respectively).

To evaluate the effect on RICD, we re-stimulated control, WASp, and SAP silenced cells with increasing concentrations of anti-CD3 antibody (OKT3 from 0 to 100 ng/ml for 24 hours). We pre-treated all the cells with either vehicle (DMSO) or the DGKα-specific inhibitor AMB639752 (10 μM, 30 minutes). In line with our previous work (34), SAP deficiency reduced RICD, and this defect was partially compensated by AMB639752 treatment, which conversely did not affect RICD in control cells. In those experimental conditions, human PBLs silenced for WASp feature a normal RICD (Supp. Mat. 5A). In WASp silenced cells we also evaluated TCR signalling outputs co-stimulating CD3 and CD28, notably cFOS, NR4A1 and FASLG were robustly induced but were not affected by either WASp silencing or AMB639752 treatment (Supp. Mat. 4B, 4C and 4D). In line with previous results on DAG signalling, those data suggest that WASp is less relevant for TCR signalling potency and RICD onset than SAP and that loss of the WASp inhibitory signalling on DGKα is not sufficient for the onset of apoptosis resistance. A different picture emerges when measuring IL-2 mRNA in the same setting. In accordance with previous reports (11, 32), DGKα silencing or inhibition potentiated IL-2 induction upon co-stimulation of CD3 and CD28 of control cells indicating the importance of DGKα enzymatic activity (Fig. 7). siRNA-mediated WASp silencing resulted in a significant decrease in IL-2 induction by TCR, indicating the key role of WASp in IL-2 induction. The observation that both siRNA-mediated DGKα silencing or AMB639752 treatment fully restored IL-2 induction (Fig. 7), suggests the relevance of WASp-mediated DGKα activity inhibition in this signaling. To verify if CD28 triggering is a requirement for this effect we triggered the sole CD3 with higher doses (OKT3 10 μg/ml) and observed a similar potentiation of IL-2 expression by AMB639752 (10 μM) in control siRNA transfected cells and a reduction in WASp silenced cells which is rescued by the DGKα inhibitor (Supp. Mat. 5).

These observations imply that WASp-mediated inhibition of DGKα selectively regulates IL-2 gene expression without affecting the TCR signalling potency. In WASp absence DGKα is active, and its activity reduces IL-2 induction while TCR proapoptotic signalling is not influenced. This is different from what was observed with SAP silencing which reduces both IL-2 induction and RICD suggesting that the WASp-DGKα axis is only a branch of the numerous SAP-dependent signalling pathways.

4.4 CDC42 and NCK-1 deficiencies reduce IL-2 expression, and this defect is rescued by DGKα inhibition

To characterize the role of SAP signalling in the control of IL-2 induction, we silenced selected SAP effectors and measured IL-2 induction.

CDC42 is not only a key regulator of the WASp activity (20) but also a crucial SAP effector in the T cells (19). Thus, to verify its involvement in this signalling pathway, CDC42 was silenced in primary lymphocytes resulting in a 75% reduction of CDC42 mRNA 4 days after electroporation. After 4 days cells were restimulated, and quantitative rt-PCR revealed a consistent reduction of IL-2 induction by CD3 and CD28 co-stimulation in CDC42 silenced cells. When DGKα was silenced or inhibited in AMB639752 pre-treated cells, we observed potentiation of IL-2 induction in control cells and a full rescue in CDC42 silenced cells, in line with the major role of CDC42 as a WASp-DGKα pathway regulator (Fig. 8).

NCK-1 is a binding partner for SAP and a direct regulator of TCR signalling along with the T cell proliferation (18). Interestingly, NCK-1 is also a WASp interactor, involved in WASp recruitment and activation at the TCR (21). Thus, we speculated that the NCK-1 adaptor could represent a crucial

scaffold protein in this signalling pathway. To verify this hypothesis, we silenced NCK-1 expression in PBLs resulting in a 50% reduction of NCK-1 mRNA 4 days after electroporation (Fig. 9F). When we measured RICD induction and TCR-driven gene expression in the presence or absence of AMB639752 we observed a similar picture to what was obtained upon WASp silencing. We did not detect any alteration of either RICD, NUR77 or FASL induction in NCK-1 silenced cells co-stimulated with anti-CD3 and CD28 antibodies (Supp. Mat. 6). Also, in this case, IL-2 induction differed as it was reduced upon NCK-1 silencing and rescued by DGKα inhibition (Fig. 9E). A similar trend was observed with DGKα silencing: a reduction in IL-2 induction that was compensated by a strong induction upon DGKα silencing (Fig. 9A). However, in co-silencing experiments, the reduction of IL-2 upon NCK-1 silencing strived to reach statistical significance, this may be due to the residual NCK-1 protein that may still play its function (Fig. 9A-D). Alternatively, other SAP effectors may participate in this pathway and compensate for NCK-1 absence.
Altogether these experiments indicate that CDC42 and NCK-1 contribute to the SAP signalling network controlling WASp and DGKα activity.

4.5 ARP2/3 activity is not required for IL-2 regulation by the WASp-DGKα complex

The CDC42-WASp signalling axis is a well-known regulator of actin branching polymerization through the ARP2/3 complex. To explore the role of the ARP2/3 complex in IL-2 induction by the TCR, PBLs were activated, cultured for 3 weeks, and pre-treated with ARP2/3 inhibitor CK666 at a concentration of 60 μM before restimulation (OKT3 1 μg/ml, CD28.2 1 μg/ml, 4 hours). When we measured IL-2 induction we observed a normal induction by the TCR and potentiation by the DGKα inhibitor AMB639752 (10 μM). These results indicate that ARP2/3 is dispensable for the signalling pathway that controls IL-2 induction downstream to CDC42/WASp/DGKα (Supp. Mat. 7).

5 Discussion

In this present study, we explored the signalling pathways that mediate TCR-induced DGKα inhibition through the SAP adaptor protein. This pathway tunes cytokine induction and RICD in $CD8^+$ cells (Fig. 10) and thus represents a target for the XLP-1 therapy (14).

We focused our attention on WASp as this protein is known to interact with molecules downstream to SAP such as CDC42 and NCK-1 (19, 35) and there are some similarities in the XLP-1 and WAS disease phenotypes (27). Our data demonstrate that DGKα and WASp are in close proximity in T cells and form a complex through the interaction between the DGKα recoverin homology domain with the WASp WH1 domain. This association is highly selective since it is not shared by the homologous DGKγ and N-WASp (Fig. 4-6). The recoverin homology domain of DGKα is a short N-terminal domain that is involved in the maintenance of the autoinhibited conformation along with the two calcium-binding EF-hands (36). Indeed those domains bind to the catalytic one inhibiting its activity and their removal results in a constitutively active, membrane-localized DGKα (31). The WH1 domain is a protein-protein interaction domain able to bind the WIP chaperone and participate in WASp recruitment at the immune synapse (23, 29). Interestingly, we did not observe a modulation of PLA signal by CD3-CD28 co-stimulation, indicating that the two proteins are already in close proximity in non-stimulated cells (Fig. 4). Forcing DGKα/WASp complex formation by overexpression of both proteins inhibits DGKα (Fig. 3A). Moreover, WASp is required for DGKα inhibition by the TCR triggering while ARP2/3 activity is dispensable (Fig. 1 and 2). Those data suggest that DGKα is a novel WASp effector, and that the WASp function is independent of actin branching. Our results indicate that this interaction is specific for WASp, which is mainly expressed in hematopoietic cells, but not for its close homologue N-WASp. This observation could explain the peculiarity of T-cells where, upon

TCR triggering, DGKα is inhibited. Conversely, in epithelial and endothelial cells we and others observed DGKs activation upon membrane receptors triggering (30, 37, 38).

We observed that this WASp-mediated inhibition of DGKα activity is selectively important for a complete IL-2 induction upon TCR stimulation (Fig. 7), an event that is tuned by both SAP and WASp (11, 25). Differently from what was observed with SAP, WASp silencing in our experimental system does not alter the global profile of DAG species produced upon TCR triggering, nor does it affect the MAPK cascade, NUR77 and FASL induction and RICD (Supp. Mat. 2 and 4). This suggests that the inhibition of DGKα by WASp affects small pools of DAG relevant specifically for IL-2 induction. The observation that the interaction is mediated by the WH1 domain of WASp, and that ARP2/3 activity appears unessential for IL-2 induction reinforces the idea of WASp playing two separate functions in TCR signalling: actin branching morphogenesis on one side and modulation of DGKα activity on the other. This is in line with reports indicating that the defect of IL-2 synthesis in WASp deficient cells is not due to decreased TCR signalling strength but to lack of ERK and nuclear factor of activated T cells (NF-AT) translocation into the nucleus and the consequent poor induction of the FOS transcription factor (25). However, in our experimental system cFOS induction is nearly normal upon WASp silencing indicating that this is not the major transcription factor involved in IL-2 induction upon DGKα silencing/inhibition (Supp. Mat. 4).

The absence of effect of DGKα silencing/inhibition on cells with normal RICD is in line with previous reports of a quantitatively minor role of DGKα compared to DGKζ in the T cell (6, 7). This minor role is indeed the effect of a TCR-driven inhibitory signal (2, 11) reducing DGKα activity at spatially selected DAG pools at the immune synapse (39). Indeed, we and others have observed that loss of DGKα activity in normal fully stimulated T cells has a very moderate effect on TCR signalling apart from a strong IL-2 induction and does not influence apoptosis sensitivity (14, 32). Conversely, previous studies from our lab and other groups evidenced that DGKα inhibition is an efficient way to restore T cell responses when the TCR signalling strength is reduced by anergy (40) or SAP absence in XLP-1 patients (14). A role for WASp in the control of RICD and autoimmunity was observed in lymphocytes from WASp KO mice (22) but not by us in human lymphocytes silenced for WASp, this discrepancy is putatively due to the experimental systems used (total genetic ablation in murine lymphocytes vs silencing in humans PBLs). Even if we have not explored this further, our data suggest a possible excessive DGKα activity in WAS patients that decreases the accumulation of selected DAG species. This could contribute to some of the defects in lymphocyte mobility and autoimmunity featured by WAS patients. It is interesting to note that DGKs also negatively regulate megakaryocytes maturation and platelets activation (41) suggesting that DGKα inhibitors may have a particularly positive effect on WAS.

In the effort to characterize the branch of SAP-mediated TCR signalling controlling DGKα activity we observed that NCK-1 and CDC42 emerge among SAP effectors. Indeed, silencing CDC42 and to a minor extent NCK-1, decreases IL-2 induction in a DGKα-dependent manner (Fig. 8 and Fig. 9). This points out that these two proteins act as putative participants to this signalling pathway as NCK-1 can bind both SAP and WASp with its SH3 domains (20, 42) while CDC42 is activated by SAP trough βPIX exchange factor and is a major WASp regulator (19). However, the crucial DGKα regulator appears to be WASp as active CDC42 is not able to inhibit DGKα in absence of WASp (Supp. Mat. 3).

Conversely, other SAP effectors such as Lyn and Fyn, although important for TCR signalling and RICD, appear to be dispensable for the DGKα regulation (11) and justify the lack of full signalling rescue by the DGKα inhibition (14). Recent data also demonstrate that in SAP's absence excessive SHP2 phosphatase activity contributes to XLP-1 phenotypes such as RICD (43). Those qualitative differences between SAP and WASp signalling render SAP more crucial for the control of RICD than

538 WASp. However, our data indicate that the increase of DAG signalling due to pharmacological DGKα
539 inhibition may compensate quantitatively for alterations of TCR signalosome due to SAP silencing.
540 Intriguingly, SAP is a novel PD-1 signal transducer (44) suggesting that this pathway may be involved
541 also in the control of DGKα activity of tumour infiltrating lymphocytes. This paves the way for the use
542 of DGKα inhibitors not only in primary immunodeficiencies but also in other T cell hyporesponsive
543 states such as tumour-induced anergy/exhaustion (45). Indeed, tumour infiltrating lymphocytes
544 features reduced WASp activation (46) while active WASp potentiates T cells and NK lytic function
545 similarly to what was observed with DGKα inhibitors (4, 47).

546 WASp plays a primary role in the organization of actin dynamics at the immune synapse (24, 48) as
547 the actin organization is not involved in the control of DGKα activity and IL-2 induction we have not
548 explored this issue further. However, the regulation of DGKα activity may represent an actin-549
independent function of WASp at the immune synapse as precise localization of DGKα activity is
550 crucial for IS organization (8).

551 Concluding, we observed that DGKα inhibition is a novel function of WASp independently from
552 ARP2/3 driven actin branching. This regulation allows WASp to tune IL-2 induction by TCR. Those
553 data suggest a potential utility of DGK inhibitors in WAS.
554

6 Figures

7 Tables

Table 1. Detailed list of lab reagents used in the present work.

Antibodies			
Antibody	**Clone**	**Cat. number**	**Provider**
Anti-human CD3	UCHT1	MA1-80537	Invitrogen
Anti-human CD3	OKT3	40-0037-U500	Tonbo biosciences
Anti-human CD28	CD28.2	16-0289-85	Invitrogen
Anti-DGKα	-	11547-1-AP	Proteintech
Anti-DGKα	-	AB64845	Abcam
Anti-Phospho-p44/42 MAPK (Erk1/2)	-	9101	Cell Signalling Technology
Anti-p38 MAPK	-	9212S	Cell Signalling Technology
Anti-WASp	D9C8	4271	Cell Signalling Technology
Anti-WASp	-	4860	Cell Signalling Technology
Anti-WASp	-	Sc-13139	Santa Cruz Biotechnology
Anti-CDC42	-	Sc-87	Santa Cruz Biotechnology
Anti NCK-1	5B7	12778	Cell Signalling Technology
Anti-Vinculin	hVIN-1	V9264	Sigma-Aldrich
Anti-b-actin	8H10D10	3700	Cell Signalling Technology
Anti- c-myc	9E10	MA1-980-1MG	Invitrogen
Anti- c-myc- AC	9E10	sc-40 AC	Santa Cruz Biotechnology
Anti-ECS (DDDDK) HRP conjugated	-	A190-101P	Bethyl laboratories
Anti-FLAG HRP conjugated	-	HRP-66008	Proteintech
Anti-FLAG	M2	A2220	Sigma-Aldrich

Anti-DYKDDDDK tag	FG4R	MA1 91878	Life technologies
Anti-DYKDDDDK tag HRP-Conjugated	FG4R-HRP	MA1 91878-HRP	Invitrogen
Anti-GST	Z-5	sc-459	Santa Cruz Biotechnology
Chemical Compounds			
Name	**Function**	**Cat. number**	**Provider**
rhIL-2	**IL-2**	**200-02**	**Preprotech**
CK-666	ARP2/3 Inhibitor	SML0006-5MG	Sigma Aldrich
AMB639752	DGKα inhibitor		Ambinter
Jasplakinolide	Actin stabilizer	AG-CN2-0037-C100	Vinci Biochem

siRNAs (Where not specified, siRNAs are from Thermo Fisher Scientific (Life Technologies))

Target	Technology	siRNA ID & Cat. #	Sequence	
SAP	Stealth RNAi™ siRNA	siRNA ID: Custom	Forward	UGUACUGCCUAUGUGUGCUGUAUCA
		Cat. # 10620312	Reverse	UGAUACAGCACACAUAGGCAGUACA
WASp	Silencer™ Select Pre-Designed siRNA	siRNA ID: s14836	Forward	UGAACAACCUCGACCCAGAtt
		Cat. # 4392420	Reverse	ACUGGGUCGAGGUUGUUCAcg
CDC42	Silencer™ Select Pre-Designed siRNA	siRNA ID: s2765	Forward	UGGUGCUGUUGGUAAAACAtt
		Cat. # 4392420	Reverse	UGUUUUACCAACAGCACCAtc
NCK-1	Silencer™ Select Pre-Designed siRNA	siRNA ID: s9311	Forward	CCUCAUUCGUGAUAGUGAAtt
		Cat. # 4392421	Reverse	UUCACUAUCACGAAUGAGGaa
DGKα	Stealth RNAi™ siRNA	siRNA ID: Custom	Forward	CGAGGAUGGCGAGAUGGCUAAAUAU
		Cat. # 10620312	Reverse	AUAUUUAGCCAUCUCGCCAUCCUCG

SYBR green Primers (where not specified, SYBR green primers are from Sigma-Aldrich (Merck)).

Gene	Code	Primer	Sequence
DGKA	FH1_DGKA	Forward	AATGTTCCCAGACACCTAAG
	RH1_DGKA	Reverse	AGTAGCAGGAAACATCATTG
SH2D1A	FH1_SH2D1A	Forward	AAGGGATAAGAGAAGATCCTG
	RH1_SH2D1A	Reverse	CATTACAGGACTACAATGGC
WAS	FH1_WAS	Forward	TACTCACAGCTTGTCTACTC
	RH1 WAS	Reverse	TTTTGTATCTTCTCCTGCAC
CDC42	FH1 CDC42	Forward	GAACAAACAGAAGCCTATCAC
	RH1 CDC42	Reverse	TTTAGGCCTTTCTGTGTAAG

NCK-1	FH1_NCK1	Forward	CCAAGTATATTGTGTCTGCC
	RH1_NCK1	Reverse	CTATGTCTCATGTGTCTTGC
GAPDH	FH1_GAPDH	Forward	TTGAGCACAGGGTACTTTA
	RH1_GAPDH	Reverse	ACAGTTGCCATGTAGACC

TaqMan probes (Where not specified, TaqMan probes are from Thermo Fisher Scientific (Life Technologies)).

Gene	Cat. number
IL-2	Hs00174114_m1
GAPDH	Hs02758991_g1
NR4A1	Hs00374226_m1
FASLG	Hs00181225_m1
FOS	Hs04194186_s1
IFNγ	Hs00989291_m1

Buffers

Buffer	Composition
Lysis buffer	25 mM HEPES, 150 mM NaCl, 5 mM EDTA, 1 mM EGTA, 1% NP40, 10% glycerol, (supplemented with 1 mM orthovanadate along with protease inhibitors before use), pH 8.0
$LiCl_2$ buffer	25 mM Tris, 0.5 M LiCl, pH 8.0
TNE buffer	25 mM Tris, 150 mM NaCl, 1 mM EDTA, pH 8.0
Homogenization buffer	25 mM Hepes (pH 8), 20% glycerol, 135 mM NaCl, 5 mM ethylenediaminetetraacetic acid (EDTA), 1 mM ethylene glycol-bis (beta-aminoethyl ether)-N,N,N′,N′-tetra acetic acid (EGTA), 1 mM sodium orthovanadate and protease inhibitor cocktail
Laemmli sample buffer	187.4 mM Tris HCl, 30% glycerol, 6% SDS, bromophenol blue in sufficient quantity, (supplemented with DTT 150 mM before use), pH 6.8
TBS-T	50 mM Tris, 120 mM NaCl, 0.01% TWEEN20 detergent
PBS	137 mM NaCl, 2.7 mM KCl, 4.3 mM Na_2HPO_4, and 1.5 mM KH_2PO_4, pH 7.4

Plasmids and mutants

Plasmid	Reference	Cat. number
myc-DGKα	Cutrupi et al., 2000	
GST-DGKα	Baldanzi et al., 2008	
FLAG-WASp		47432
myc-FLAG-N-WASp		RC207967
myc-DGKα L360*	Baldanzi et al., 2008	

To create mutant variants of the above-mentioned plasmids we used Phusion™ Site-Directed Mutagenesis Kit (Thermo Fisher Scientific) according to the manufacturer's instructions. Mutagenesis was performed using the following primers:

Mutant		Sequence
DGKα E86*	Forward	TCACTGCTTAAATTAGACAAATGTGACAAA
	Reverse	CCAGTCTCAAAGGATTGAAACAGTGC

WASp K232*	Forward	CTCAGGGAAGAAGTAGATCAGCAAAG
	Reverse	CGTTTCTTATCAGCTGGGCTAGG
WASp Q297*	Forward	TTCATTGAGGACTAGGGTGGGCTGG
	Reverse	GTCGTAGATAAGTTTAGAGGTCTCGGCG

shRNA plasmids			
Target	**Vector plasmid**	**Cat. number**	**Provider**
WASp	MISSIONpLKO.1-puro Empty Vector Plasmid DNA	TRCN0000029819	Sigma-Aldrich
NT (Non targeting)	MISSIONpLKO.1-puro Empty Vector Plasmid DNA	SHC002	Sigma-Aldrich

571

572 **Table 2.** Abbreviations list.

Abbreviations	
DGKα	diacylglycerol kinase alpha
DGKζ	diacylglycerol kinase zeta
DAG	Diacylglycerol
WASp	Wiskott-Aldrich syndrome protein
WAS	Wiskott-Aldrich syndrome
NPFs	nucleation-promoting factors
SHP-1	Src homology phosphatase 1
SHP-2	Src homology phosphatase 2
βPIX	Pak interacting exchange factor
TCR	T cell receptor
ARP2/3	actin-related protein 2/3
CDC42	cell division control protein 42
NCK-1	NCK adaptor protein 1
SAP	SLAM-associated protein
SLAM	signalling lymphocyte activation molecule
RICD	restimulation-induced cell death
XLP-1	X-linked lymphoproliferative disease 1
IL-2	interleukin 2
NF-AT	nuclear factor of activated T cells
ERK1/2	extracellular signal-regulated kinase 1 and 2

WIP	WASp interacting protein
FASL	FAS ligand
NUR77	nuclear receptor 4A1
FOS	Finkel-Biskis-Jinkis osteosarcoma gene
IFNγ	Interferon gamma
PBLs	peripheral blood lymphocytes

8 Conflict of Interest

The authors have no relevant financial or non-financial interests to disclose.

9 Author Contributions

Conceptualization and study design: GB, AG, SV, ER and VM; Methodology and investigation: Biochemical assays - SV, SC and GB; Lipidomic experiments - BP, MM (M Manfredi); Biological assays - SV, SC, GR and VM; Formal analysis: SV, SC, GB, BP and MM (M Malerba); Resources: AA, MM (M Manfredi) and MM (M Malerba); Writing - original draft: GB, SV and SC; Writing -582 review and editing: GB, SV, SC, AA, BP, MM (M Manfredi), GR, VM and AG; Funding acquisition: GB and AG; Supervision: GB, AG and MM (M Manfredi); All authors read and approved the final version of the manuscript.

10 Funding

This work was supported by the Italian Ministry of Education, University and Research Program PRIN 2017 (grant 201799WCRH to GB), AGING Project Department Translational Medicine University Piemonte Orientale (FAR-2017 to GB), Telethon Foundation [Grant GGP16252 to AG and GB].

11 Acknowledgements

We thank BioRender software for the scientific graphic illustrations.

12 Data Availability Statement

All data and materials are included in the present paper. The datasets generated and/or analysed during the current study are available from the corresponding author upon reasonable request.

13 References

1. Baldanzi G, Ragnoli B, Malerba M. Potential role of diacylglycerol kinases in immune-mediated diseases. Clin Sci (Lond). 2020;134(13):1637-58.
2. Arranz-Nicolás J, Ogando J, Soutar D, Arcos-Pérez R, Meraviglia-Crivelli D, Mañes S, et al. Diacylglycerol kinase α inactivation is an integral component of the costimulatory pathway that amplifies TCR signals. Cancer Immunol Immunother. 2018;67(6):965-80.
3. Takao S, Akiyama R, Sakane F. Combined inhibition/silencing of diacylglycerol kinase α and ζ simultaneously and synergistically enhances interleukin-2 production in T cells and induces cell death of melanoma cells. J Cell Biochem. 2021;122(5):494-506.
4. Arranz-Nicolás J, Martin-Salgado M, Adán-Barrientos I, Liébana R, Del Carmen Moreno-Ortíz M, Leitner J, et al. Diacylglycerol kinase α inhibition cooperates with PD-1-targeted therapies to restore the T cell activation program. Cancer Immunol Immunother. 2021.
5. Arranz-Nicolás J, Martin-Salgado M, Rodríguez-Rodríguez C, Liébana R, Moreno-Ortiz MC, Leitner J, et al. Diacylglycerol kinase ζ limits IL-2-dependent control of PD-1 expression in tumor-infiltrating T lymphocytes. J Immunother Cancer. 2020;8(2).
6. Ávila-Flores A, Arranz-Nicolás J, Andrada E, Soutar D, Mérida I. Predominant contribution of DGKζ over DGKα in the control of PKC/PDK-1-regulated functions in T cells. Immunol Cell Biol. 2017;95(6):549-63.
7. Joshi RP, Schmidt AM, Das J, Pytel D, Riese MJ, Lester M, et al. The ζ isoform of diacylglycerol kinase plays a predominant role in regulatory T cell development and TCR-mediated ras signalling. Sci Signal. 2013;6(303):ra102.
8. Chauveau A, Le Floc'h A, Bantilan NS, Koretzky GA, Huse M. Diacylglycerol kinase α establishes T cell polarity by shaping diacylglycerol accumulation at the immunological synapse. Sci Signal. 2014;7(340):ra82.
9. Howden AJM, Hukelmann JL, Brenes A, Spinelli L, Sinclair LV, Lamond AI, et al. Quantitative analysis of T cell proteomes and environmental sensors during T cell differentiation. Nat Immunol. 2019;20(11):1542-54.
10. Martínez-Moreno M, García-Liévana J, Soutar D, Torres-Ayuso P, Andrada E, Zhong XP, et al. FoxO-dependent regulation of diacylglycerol kinase α gene expression. Mol Cell Biol. 2012;32(20):4168-80.
11. Baldanzi G, Pighini A, Bettio V, Rainero E, Traini S, Chianale F, et al. SAP-mediated inhibition of diacylglycerol kinase α regulates TCR-induced diacylglycerol signalling. J Immunol. 2011;187(11):5941-51.
12. Panchal N, Booth C, Cannons JL, Schwartzberg PL. X-Linked Lymphoproliferative Disease Type 1: A Clinical and Molecular Perspective. Front Immunol. 2018;9:666.
13. Filipovich AH, Zhang K, Snow AL, Marsh RA. X-linked lymphoproliferative syndromes: brothers or distant cousins? Blood. 2010;116(18):3398-408.
14. Ruffo E, Malacarne V, Larsen SE, Das R, Patrussi L, Wülfing C, et al. Inhibition of diacylglycerol kinase α restores restimulation-induced cell death and reduces immunopathology in XLP-1. Sci Transl Med. 2016;8(321):321ra7.
15. Velnati S, Centonze S, Girivetto F, Baldanzi G. Diacylglycerol Kinase alpha in X Linked Lymphoproliferative Disease Type 1. Int J Mol Sci. 2021;22(11).
16. Katz G, Krummey SM, Larsen SE, Stinson JR, Snow AL. SAP facilitates recruitment and activation of LCK at NTB-A receptors during restimulation-induced cell death. J Immunol. 2014;192(9):4202-9.

17. Chen R, Latour S, Shi X, Veillette A. Association between SAP and FynT: Inducible SH3 domain-mediated interaction controlled by engagement of the SLAM receptor. Mol Cell Biol. 2006;26(15):5559-68.
18. Li C, Schibli D, Li SS. The XLP syndrome protein SAP interacts with SH3 proteins to regulate T cell signalling and proliferation. Cell Signal. 2009;21(1):111-9.
19. Gu C, Tangye SG, Sun X, Luo Y, Lin Z, Wu J. The X-linked lymphoproliferative disease gene product SAP associates with PAK-interacting exchange factor and participates in T cell activation. Proc Natl Acad Sci U S A. 2006;103(39):14447-52.
20. Tomasevic N, Jia Z, Russell A, Fujii T, Hartman JJ, Clancy S, et al. Differential regulation of WASP and N-WASP by Cdc42, Rac1, Nck, and PI(4,5)P2. Biochemistry. 2007;46(11):3494-502.
21. Zeng R, Cannon JL, Abraham RT, Way M, Billadeau DD, Bubeck-Wardenberg J, et al. SLP-76 coordinates Nck-dependent Wiskott-Aldrich syndrome protein recruitment with Vav-1/Cdc42-dependent Wiskott-Aldrich syndrome protein activation at the T cell-APC contact site. J Immunol. 2003;171(3):1360-8.
22. Nikolov NP, Shimizu M, Cleland S, Bailey D, Aoki J, Strom T, et al. Systemic autoimmunity and defective Fas ligand secretion in the absence of the Wiskott-Aldrich syndrome protein. Blood. 2010;116(5):740-7.
23. Sasahara Y, Rachid R, Byrne MJ, de la Fuente MA, Abraham RT, Ramesh N, et al. Mechanism of recruitment of WASP to the immunological synapse and of its activation following TCR ligation. Mol Cell. 2002;10(6):1269-81.
24. Kumari S, Depoil D, Martinelli R, Judokusumo E, Carmona G, Gertler FB, et al. Actin foci facilitate activation of the phospholipase C-γ in primary T lymphocytes via the WASP pathway. Elife. 2015;4.
25. Cianferoni A, Massaad M, Feske S, de la Fuente MA, Gallego L, Ramesh N, et al. Defective nuclear translocation of nuclear factor of activated T cells and extracellular signal-regulated kinase underlies deficient IL-2 gene expression in Wiskott-Aldrich syndrome. J Allergy Clin Immunol. 2005;116(6):1364-71.
26. Sun X, Wei Y, Lee PP, Ren B, Liu C. The role of WASp in T cells and B cells. Cell Immunol. 2019;341:103919.
27. Walter JE, Ayala IA, Milojevic D. Autoimmunity as a continuum in primary immunodeficiency. Curr Opin Pediatr. 2019;31(6):851-62.
28. Rubio I, Grund S, Song SP, Biskup C, Bandemer S, Fricke M, et al. TCR-induced activation of Ras proceeds at the plasma membrane and requires palmitoylation of N-Ras. J Immunol. 2010;185(6):3536-43.
29. de la Fuente MA, Sasahara Y, Calamito M, Antón IM, Elkhal A, Gallego MD, et al. WIP is a chaperone for Wiskott-Aldrich syndrome protein (WASP). Proc Natl Acad Sci U S A. 2007;104(3):926-31.
30. Baldanzi G, Cutrupi S, Chianale F, Gnocchi V, Rainero E, Porporato P, et al. Diacylglycerol kinase-alpha phosphorylation by Src on Y335 is required for activation, membrane recruitment and Hgf-induced cell motility. Oncogene. 2008;27(7):942-56.
31. Takahashi M, Yamamoto T, Sakai H, Sakane F. Calcium negatively regulates an intramolecular interaction between the N-terminal recoverin homology and EF-hand motif domains and the C-terminal C1 and catalytic domains of diacylglycerol kinase α. Biochem Biophys Res Commun. 2012;423(3):571-6.
32. Olenchock BA, Guo R, Carpenter JH, Jordan M, Topham MK, Koretzky GA, et al. Disruption of diacylglycerol metabolism impairs the induction of T cell anergy. Nat Immunol. 2006;7(11):1174-81.

33. De Meester J, Calvez R, Valitutti S, Dupré L. The Wiskott-Aldrich syndrome protein regulates CTL cytotoxicity and is required for efficient killing of B cell lymphoma targets. J Leukoc Biol. 2010;88(5):1031-40.
34. Velnati S, Ruffo E, Massarotti A, Talmon M, Varma KSS, Gesu A, et al. Identification of a novel DGKα inhibitor for XLP-1 therapy by virtual screening. Eur J Med Chem. 2019;164:378-90.
35. Sylla BS, Murphy K, Cahir-McFarland E, Lane WS, Mosialos G, Kieff E. The X-linked lymphoproliferative syndrome gene product SH2D1A associates with p62dok (Dok1) and activates NF-kappa B. Proc Natl Acad Sci U S A. 2000;97(13):7470-5.
36. Jiang Y, Qian W, Hawes JW, Walsh JP. A domain with homology to neuronal calcium sensors is required for calcium-dependent activation of diacylglycerol kinase alpha. J Biol Chem. 2000;275(44):34092-9.
37. Baldanzi G, Mitola S, Cutrupi S, Filigheddu N, van Blitterswijk WJ, Sinigaglia F, et al. Activation of diacylglycerol kinase alpha is required for VEGF-induced angiogenic signalling in vitro. Oncogene. 2004;23(28):4828-38.
38. Cutrupi S, Baldanzi G, Gramaglia D, Maffè A, Schaap D, Giraudo E, et al. Src-mediated activation of alpha-diacylglycerol kinase is required for hepatocyte growth factor-induced cell motility. EMBO J. 2000;19(17):4614-22.
39. Quann EJ, Merino E, Furuta T, Huse M. Localized diacylglycerol drives the polarization of the microtubule-organizing center in T cells. Nat Immunol. 2009;10(6):627-35.
40. Zha Y, Marks R, Ho AW, Peterson AC, Janardhan S, Brown I, et al. T cell anergy is reversed by active Ras and is regulated by diacylglycerol kinase-alpha. Nat Immunol. 2006;7(11):1166-73.
41. Moroi AJ, Zwifelhofer NM, Riese MJ, Newman DK, Newman PJ. Diacylglycerol kinase ζ is a negative regulator of GPVI-mediated platelet activation. Blood Adv. 2019;3(7):1154-66.
42. Li C, Schibli D, Li SS. The XLP syndrome protein SAP interacts with SH3 proteins to regulate T cell signalling and proliferation. Cell Signal. 2009;21(1):111-9.
43. Panchal N, Houghton BC, Vassalou E, Thrasher AJ, Booth C. Allosteric Inhibition of SHP2 rescues functional T-cell abnormalities in SAP deficiency. J Allergy Clin Immunol. 2022.
44. Peled M, Tocheva AS, Sandigursky S, Nayak S, Philips EA, Nichols KE, et al. Affinity purification mass spectrometry analysis of PD-1 uncovers SAP as a new checkpoint inhibitor. Proc Natl Acad Sci U S A. 2018;115(3):E468-E77.
45. Jung IY, Kim YY, Yu HS, Lee M, Kim S, Lee J. CRISPR/Cas9-Mediated Knockout of DGK Improves Antitumor Activities of Human T Cells. Cancer Res. 2018;78(16):4692-703.
46. Koneru M, Schaer D, Monu N, Ayala A, Frey AB. Defective proximal TCR signalling inhibits CD8+ tumor-infiltrating lymphocyte lytic function. J Immunol. 2005;174(4):1830-40.
47. Kritikou JS, Oliveira MM, Record J, Saeed MB, Nigam SM, He M, et al. Constitutive activation of WASp leads to abnormal cytotoxic cells with increased granzyme B and degranulation response to target cells. JCI Insight. 2021;6(6).
48. Sims TN, Soos TJ, Xenias HS, Dubin-Thaler B, Hofman JM, Waite JC, et al. Opposing effects of PKCtheta and WASp on symmetry breaking and relocation of the immunological synapse. Cell. 2007;129(4):773-85.

14 Supplementary Material

Table S1: Complete list of identified DAG species in unstimulated and stimulated (OKT3+CD28 1µg/ml) Jurkat cells.
Supp. Mat. 1: DGKα immunoprecipitation is not affected by stimulation in both control shRNA and WASp shRNA Jurkat cells.
Supp. Mat. 2: No significant differences in DAG fluctuations between Jurkat cells and Jurkat WASp shRNA cells
Supp. Mat. 3: CDC42 Q61L overexpression does not inhibit DGKαSupp. Mat. 4: WASp deficiency neither effect RICD nor NUR77, FASLG or FOS expression
Supp. Mat. 5: DGKα inhibition restores IL-2 expression in WASp deficient lymphocytes
Supp. Mat. 6: NCK-1 silencing neither effect RICD nor IFNγ, NUR77 or FASLG expression
Supp. Mat. 7: ARP2/3 inhibition has no effect on IL-2 expression

15 Figure Captions

Figure 1: WASp is required for DGKα inhibition upon CD3 stimulation
Control shRNA and WASp shRNA Jurkat cells (3×10^7) were stimulated with CD3 agonist (UCHT1 10 µg/ml for 15 minutes). Post-stimulation, cells were lysed and:

- **A)** immunoprecipitated with anti-DGKα antibody followed by DGK activity assays, the lower panel is a representative assay, upper panel is the mean ± SEM of 4 experiments normalized as the % of unstimulated cells.
- **B)** Total cell lysates were analysed by western blotting with anti DGKα antibodies, the lower panel is a representative blot, upper panel is the mean ± SEM of 4 experiments normalized as the % of unstimulated cells.
- **C)** Total cell lysates were analysed by western blotting with anti-pERK antibodies, the lower panel is a representative blot, upper panel is the mean ± SEM of 4 experiments normalized as the % of unstimulated cells.
- **D)** WASp mRNA levels were measured by qRT-PCR at 3 different timings during the experiments and shown as mean ± SEM using control shRNA as reference.

Figure 2: ARP2/3 has no effect on DGKα inhibition upon CD3 stimulation
Jurkat cells were treated with ARP2/3 inhibitor (CK666 – 60 µM) or jasplakinolide (0.5 µg/ml) for 30 minutes and/or were stimulated with CD3 agonist (UCHT1 10 µg/ml for 15 minutes). Post-stimulation, cells were lysed and:

- **A)** immunoprecipitated with anti-DGKα antibody followed by DGK activity assays, the lower panel is a representative assay, and the upper panel is the mean ± SEM of at least 3 experiments normalized as the % of unstimulated cells.
- **B)** Total cell lysates were analysed by western blotting with anti DGKα antibodies, the lower panel is a representative blot, upper panel is the mean ± SEM of at least 3 experiments normalized as the % of unstimulated cells.
- **C)** Total cell lysates were analysed by western blotting with anti-pERK antibodies, the lower panel is a representative blot, upper panel is the mean ± SEM of at least 3 experiments normalized as the % of unstimulated cells.

Figure 3: WASp overexpression inhibits DGKα activity

myc-DGKα and FLAG-WASp were transfected together or with GFP control vector in 293T-cells. 48 hours post-transfection, cells were collected, homogenized, and used in:

A) DGK activity assays normalized considering DGKα overexpressed homogenates as control, the lower panel is a representative assay, upper panel is the mean ± SEM of 5 independent experiments.

B) Quantifications of DGKα total protein as % of myc-DGKα transfected cells, the lower panel is a representative assay, upper panel is the mean ± SEM of 5 independent experiments.

C) Quantifications of FLAG-WASp total protein as % of FLAG-WASp transfected cells, the lower panel is a representative assay, upper panel is the mean ± SEM of 5 independent experiments.

Figure 4: DGKα and WASp associate in a complex

A) Isolated human PBLs were seeded on poly-L-lysine coated glasses and stimulated for 15 minutes with anti-CD3 (UCHT1 10 μg/ml) and anti-CD28 (CD28.2, 5 μg/ml) antibodies, fixed and permeabilized. PLA was performed to assess DGKα and WASp proximity, representative images are shown.

B) Quantification of the spots/cell resulting from PLA of two independent experiments are shown with mean ± SEM (n = 60 negative control; n = 109 unstimulated; n = 90 CD3+CD28).

C) Myc-DGKα and FLAG-WASp were co-expressed in 293T cells. After 48 hours lysates were immunoprecipitated with either anti-FLAG (left side) or anti-myc (right side) antibodies. Immunoprecipitated proteins were analysed by western blotting with anti-FLAG antibody (upper panel) followed by anti-myc antibody after stripping (lower panel). The bands corresponding to FLAG-WASp and myc-DGKα are highlighted by black arrows.A representative experiment is shown out of three.

D) Total cell lysates from experiments shown in C.

Figure 5: DGKα binds to WASp through the recoverin homology domain

HEK 293-T cells were co-transfected with the indicated plasmids. 48 hours later, proteins were immunoprecipitated with anti-FLAG (B and D) or anti-GST antibody (C) and subsequently analysed by western blotting.

A) DGKα and DGKγ constructs used with domains and tags evidenced.

B) Interaction between FLAG-WASp and myc-DGKα WT or myc-DGKα-L360* deletion mutant and the corresponding total cell lysates.

C) Interaction between FLAG-WASp and GST-DGKα or GST-DGKα-E86* deletion mutant and the corresponding total cell lysates.

D) Interaction between FLAG-WASp and HA-DGKγ and the corresponding total cell lysates.

Figure 6: WASp interacts with DGKα through the WH1 domain while N-WASp does not bind.

HEK 293-T cells were co-transfected with the indicated plasmids. 48 hours later, proteins were immunoprecipitated with anti-FLAG antibody and subsequently analysed by western blotting.

A) WASP constructs used with domains and tags evidenced.

B) Interaction between myc-DGKα and FLAG-WASp or FLAG-WASp deletion mutants (FLAG-WASp K232* and FLAG-WASp Q297*) and the corresponding total cell lysates.

C) Interaction between FLAG-WASp or myc-FLAG N-WASp with myc-DGKα WT and the corresponding total cell lysates.

Figure 7: DGKα silencing or pharmacological inhibition rescues IL-2 defects in WASp deficient lymphocytes

A) Activated lymphocytes from healthy donors were transfected using ctrl siRNAs, WASp siRNAs and DGKα siRNAs. After 4 days, transfected cells were restimulated using both OKT3 (1 μg/ml) and CD28.2 (1 μg/ml) for 4 hours followed by quantitative rt-PCR gene expression analysis to verify IL-2 expression. Data are the mean ± SEM of 5 experiments from 5 individual healthy donors.

B) WASp and DGKα expression in a representative donor from A were evaluated by western blotting using vinculin as a normalizer.

C) WASp protein quantification (relative to ctrl) in the experiments shown in A and B.

D) DGKα protein quantification (relative to ctrl) in the experiments shown in A and B.

E) Activated lymphocytes from healthy donors were transfected using ctrl siRNAs or WASp siRNAs. After 4 days, transfected cells were restimulated using both OKT3 (1 μg/ml) and CD28.2 (1 μg/ml) for 4 hours in the presence or absence of the DGKα specific inhibitor (AMB639752 - 10 μM), followed by quantitative rt-PCR gene expression analysis to verify IL-2 expression. Data are the mean ± SEM of 10 experiments performed in triplicates from 10 individual healthy donors.

F) Quantitative rt-PCR gene expression analysis of WASp mRNA in the experiments shown in E.

Figure 8: DGKα silencing or pharmacological inhibition rescues IL-2 defects in CDC42 deficient lymphocytes

A) Activated lymphocytes from healthy donors were transfected using ctrl siRNAs, CDC42 siRNAs and DGKα siRNAs. After 4 days, transfected cells were restimulated using both OKT3 (1 μg/ml) and CD28.2 (1 μg/ml) for 4 hrs followed by quantitative rt-PCR gene expression analysis to verify IL-2 expression. Data are the mean ± SEM of 6 experiments from 3 individual healthy donors.

B) CDC42 and DGKα expression in a representative donor from A were evaluated by western blotting using actin as a normalizer.

C) CDC42 protein quantification (relative to ctrl) from the experiments shown in A and B.

D) DGKα protein quantification (relative to ctrl) from the experiments shown in A and B.

E) Activated lymphocytes from healthy donors were transfected using ctrl siRNAs or CDC42 siRNAs. After 4 days, transfected cells were restimulated using both OKT3 (1 μg/ml) and CD28.2 (1 μg/ml) for 4 hours in the presence or absence of the DGKα specific inhibitor (AMB639752 - 10 μM), followed by quantitative rt-PCR gene expression analysis to verify IL-2 expression. Data are the mean ± SEM of 8 experiments performed in triplicates from 6 individual healthy donors.

F) Quantitative rt-PCR gene expression analysis of CDC42 mRNA in the experiments shown in E.

Figure 9: DGKα silencing or pharmacological inhibition potentiates IL-2 expression in NCK-1 deficient lymphocytes

A) Activated lymphocytes from healthy donors were transfected using ctrl siRNAs, NCK-1 siRNAs and DGKα siRNAs. After 4 days, transfected cells were restimulated using both OKT3

(1 µg/ml) and CD28.2 (1 µg/ml) for 4 hrs followed by quantitative rt-PCR gene expression analysis to verify IL-2 expression. Data are the mean ± SEM of 6 experiments from 4 individual healthy donors.

B) NCK-1 and DGKα expression in a representative donor from A were evaluated by western blotting together with vinculin as a normalizer.

C) NCK-1 protein quantification (relative to ctrl) from 3 experiments shown in A and B.

D) DGKα protein quantification (relative to ctrl) from 3 experiments shown in A and B.

E) Activated lymphocytes from healthy donors were transfected using ctrl siRNAs or NCK-1 siRNAs. After 4 days, transfected cells were restimulated using both OKT3 (1 µg/ml) and CD28.2 (1 µg/ml) for 4 hours in the presence or absence of the DGKα specific inhibitor (AMB639752 - 10 µM), followed by quantitative rt-PCR gene expression analysis to verify IL-2 expression. Data are the mean ± SEM of 6 experiments from 6 individual healthy donors for gene expression analysis and all experiments were performed in triplicates.

F) NCK-1 mRNA in the experiments shown in E was measured by quantitative rt-PCR gene expression analysis.

Figure 10: Divergent signalling pathways downstream to SAP

The SAP-NCK-1/CDC42-WASp pathway controls DGKα activity and DAG cellular metabolism. This pathway tunes IL-2 and RICD responses in T cells. Other SAP interactors such as Lck and Fyn are crucial regulators of RICD onset.

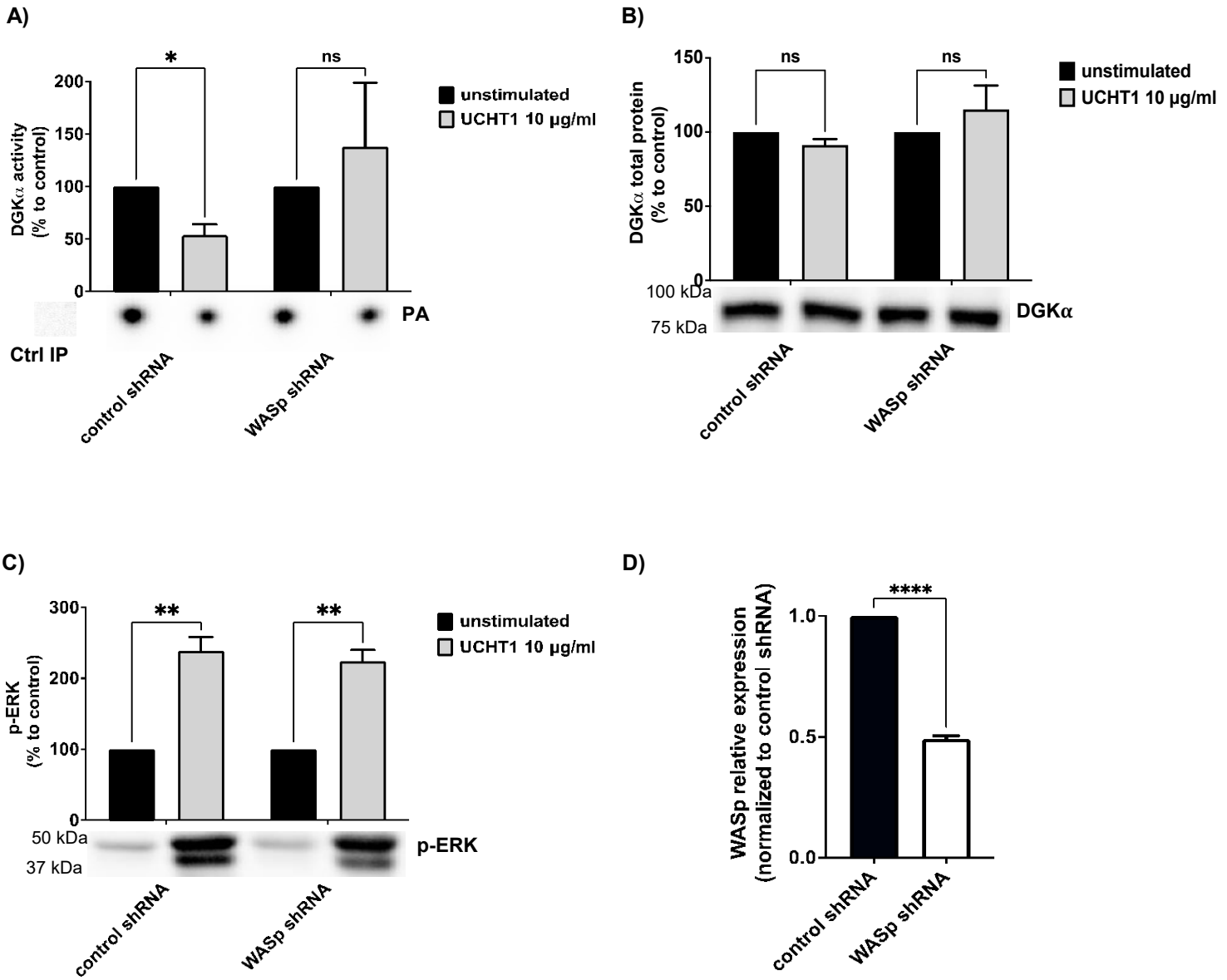
A)
*
ns
200
150
100
50
0
DGKα activity
(% to control)
unstimulated
UCHT1 10 µg/ml
PA
Ctrl IP
control shRNA
WASp shRNA
B)
150
100
50
0
ns
ns
DGKα total protein
(% to control)
unstimulated
UCHT1 10 µg/ml
100 kDa
75 kDa
DGKα
control shRNA
WASp shRNA
C)
300
200
100
0
**
**
p-ERK
(% to control)
unstimulated
UCHT1 10 µg/ml
50 kDa
37 kDa
p-ERK
control shRNA
WASp shRNA
D)
****
1.0
0.5
0.0
WASp relative expression
(normalized to control shRNA)
control shRNA
WASp shRNA

Figure 1

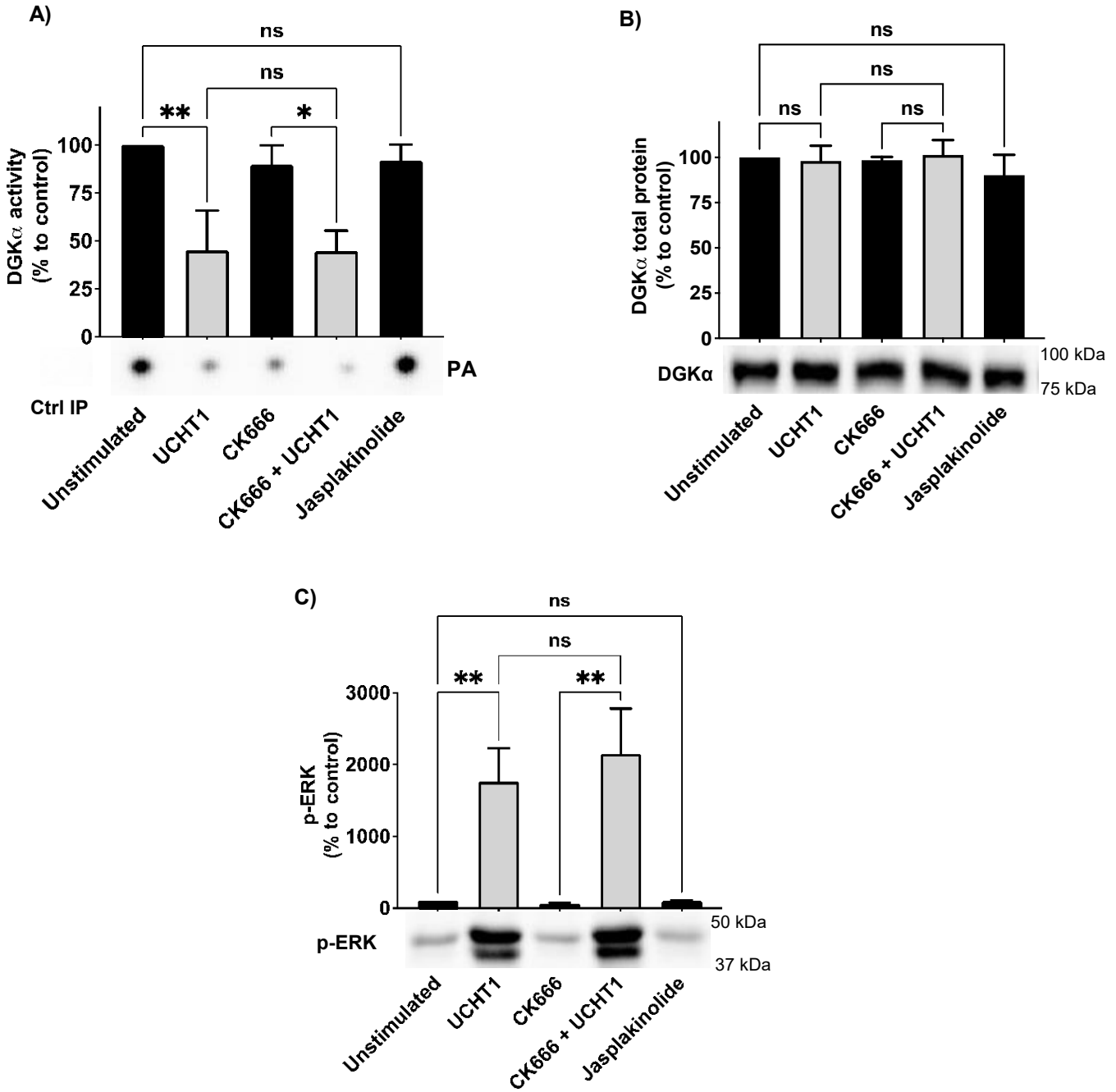
A)
ns
ns
**
*
DGKα activity
(% to control)
100
75
50
25
0
PA
Ctrl IP
Unstimulated
UCHT1
CK666
CK666 + UCHT1
Jasplakinolide
B)
ns
ns
ns
ns
DGKα total protein
(% to control)
100
75
50
25
0
DGKα
100 kDa
75 kDa
Unstimulated
UCHT1
CK666
CK666 + UCHT1
Jasplakinolide
C)
ns
ns
**
**
p-ERK
(% to control)
3000
2000
1000
0
p-ERK
50 kDa
37 kDa
Unstimulated
UCHT1
CK666
CK666 + UCHT1
Jasplakinolide

Figure 2

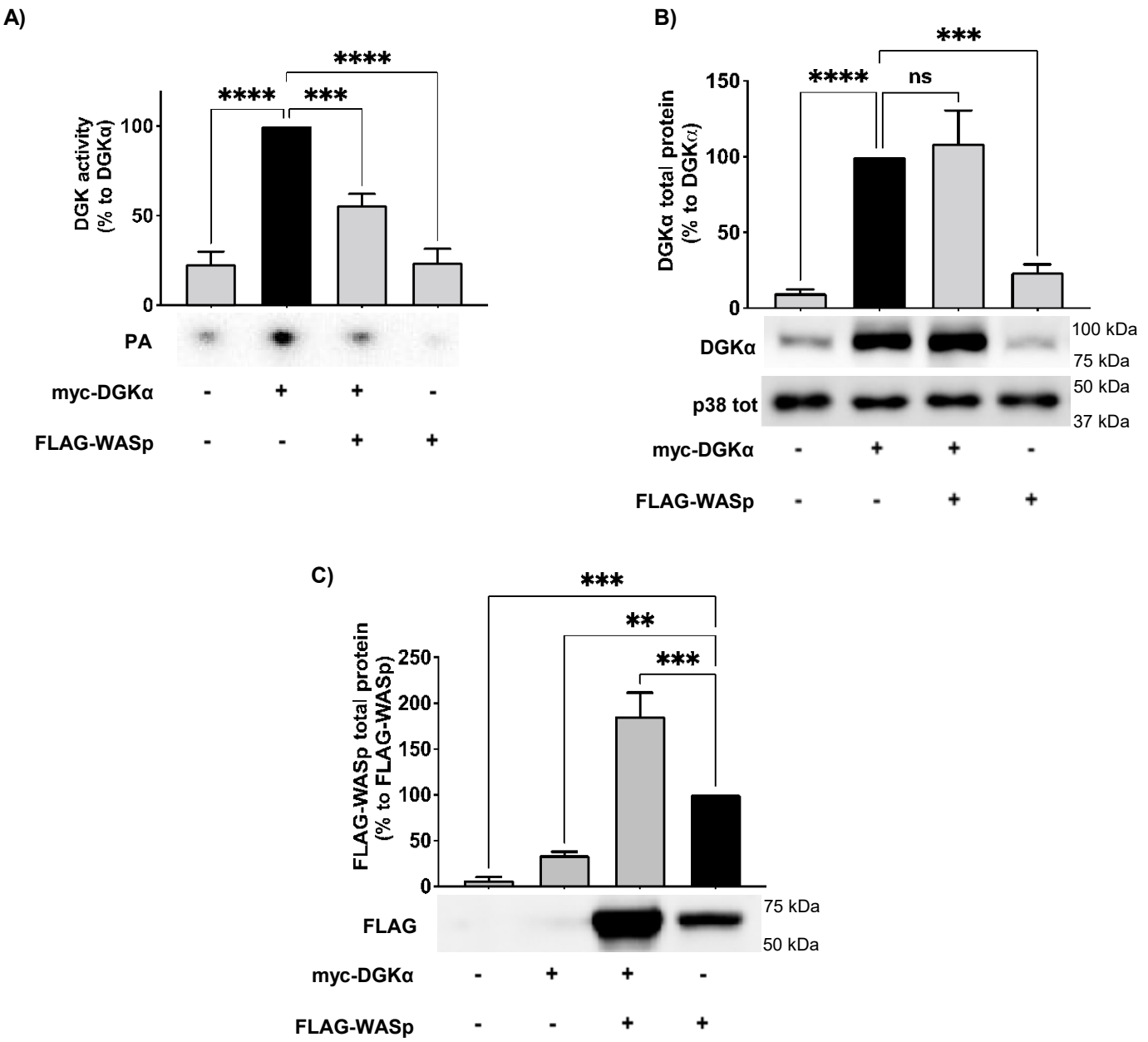
A)
DGK activity (% to DGKα)
100
50
0
****
****
***
PA
myc-DGKα - + + -
FLAG-WASp - - + +
B)
DGKα total protein (% to DGKα)
150
100
50
0
****
ns
***
DGKα
p38 tot
100 kDa
75 kDa
50 kDa
37 kDa
myc-DGKα - + + -
FLAG-WASp - - + +
C)
FLAG-WASp total protein (% to FLAG-WASp)
250
200
150
100
50
0
***
**
***
FLAG
75 kDa
50 kDa
myc-DGKα - + + -
FLAG-WASp - - + +

Figure 3

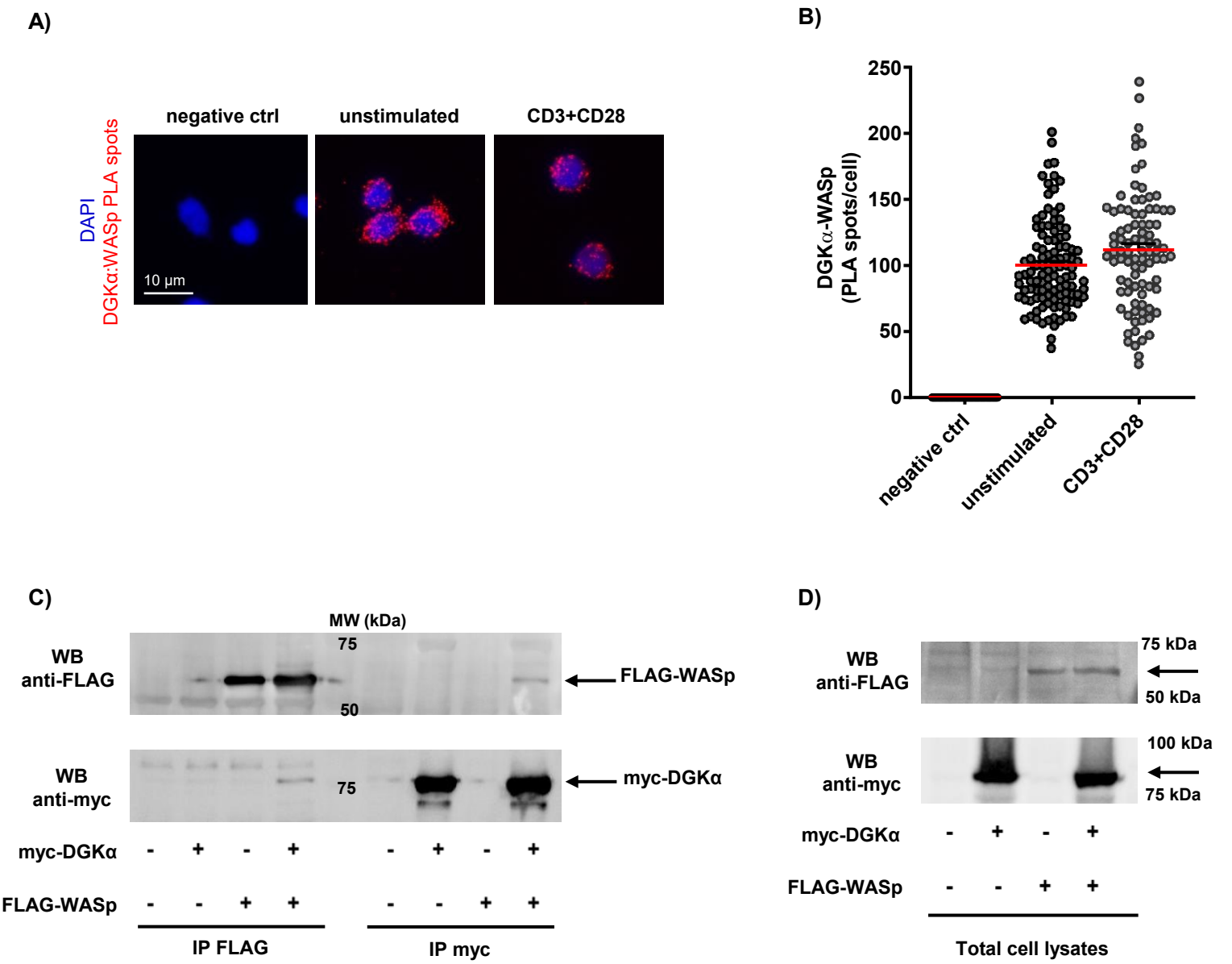
A)
negative ctrl
unstimulated
CD3+CD28
DAPI
DGKα:WASp PLA spots
10 µm
B)
DGKα-WASp
(PLA spots/cell)
250
200
150
100
50
0
negative ctrl
unstimulated
CD3+CD28
C)
MW (kDa)
WB
anti-FLAG
75
50
FLAG-WASp
WB
anti-myc
75
myc-DGKα
myc-DGKα - + - + - + - +
FLAG-WASp - - + + - - + +
IP FLAG
IP myc
D)
WB
anti-FLAG
75 kDa
50 kDa
WB
anti-myc
100 kDa
75 kDa
myc-DGKα - + - +
FLAG-WASp - - + +
Total cell lysates

Figure 4

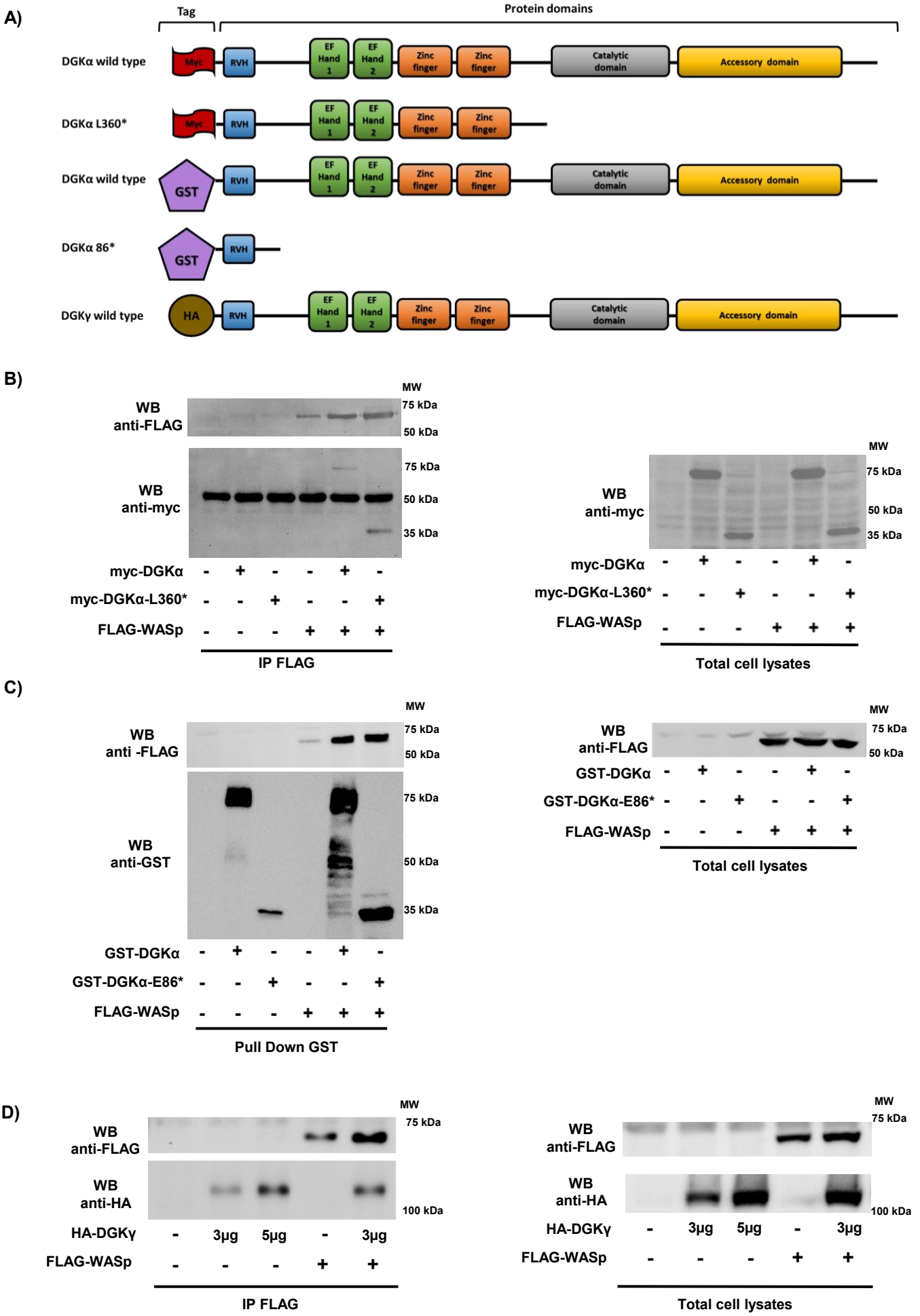
A)
Tag
Protein domains
DGKα wild type
Myc
RVH
EF Hand 1
EF Hand 2
Zinc finger
Zinc finger
Catalytic domain
Accessory domain
DGKα L360*
DGKα wild type
GST
DGKα 86*
GST
DGKγ wild type
HA
B)
WB anti-FLAG
WB anti-myc
MW
75 kDa
50 kDa
35 kDa
myc-DGKα
myc-DGKα-L360*
FLAG-WASp
IP FLAG
Total cell lysates
C)
WB anti -FLAG
WB anti-GST
GST-DGKα
GST-DGKα-E86*
FLAG-WASp
Pull Down GST
Total cell lysates
D)
WB anti-FLAG
WB anti-HA
100 kDa
HA-DGKγ
3μg
5μg
FLAG-WASp
IP FLAG
Total cell lysates

Figure 5

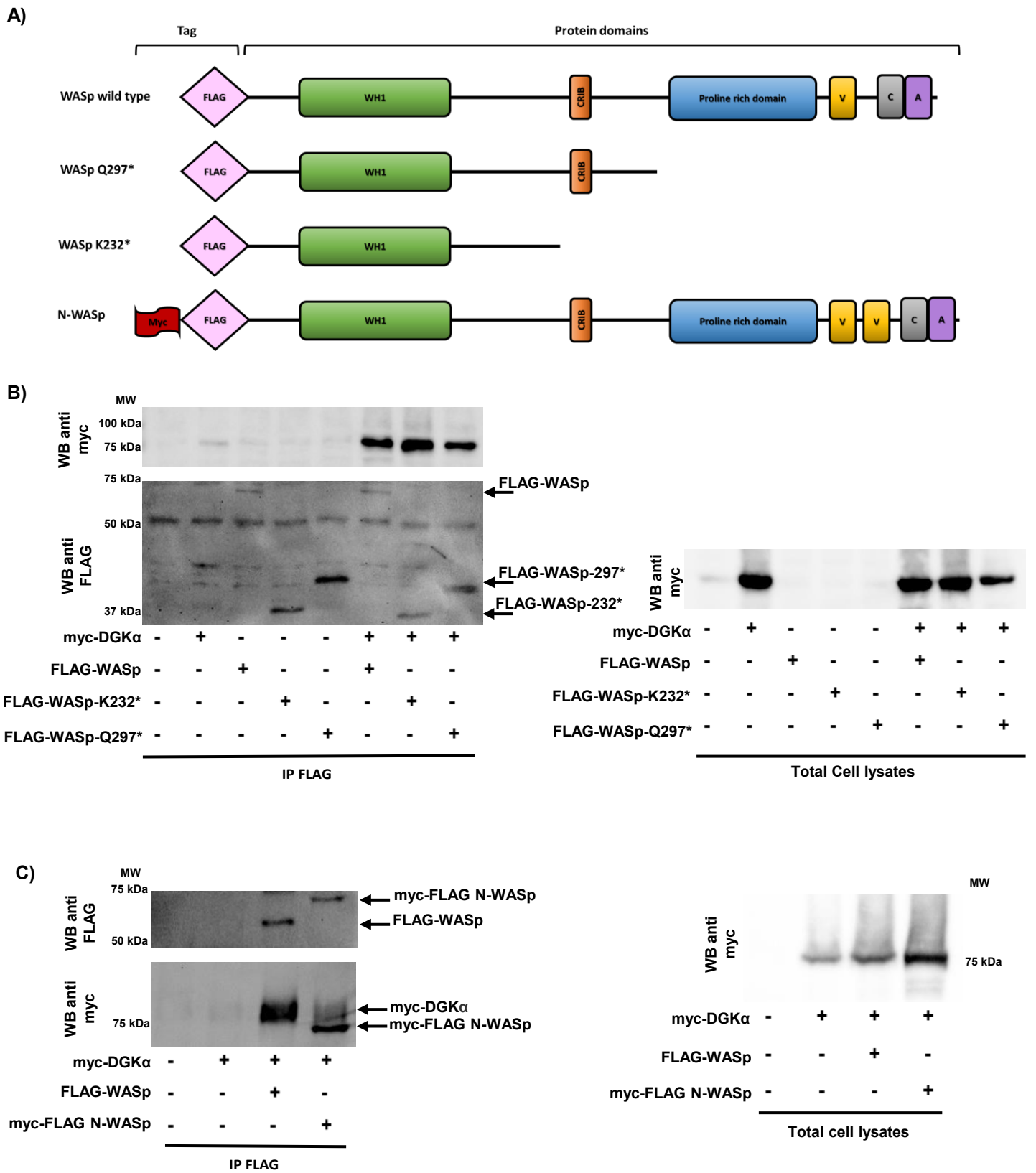
A)
Tag
Protein domains
WASp wild type
FLAG
WH1
CRIB
Proline rich domain
V
C
A
WASp Q297*
WASp K232*
N-WASp
Myc
B)
MW
WB anti myc
100 kDa
75 kDa
WB anti FLAG
50 kDa
37 kDa
FLAG-WASp
FLAG-WASp-297*
FLAG-WASp-232*
myc-DGKα
FLAG-WASp
FLAG-WASp-K232*
FLAG-WASp-Q297*
IP FLAG
Total Cell lysates
C)
myc-FLAG N-WASp
myc-DGKα
Total cell lysates

Figure 6

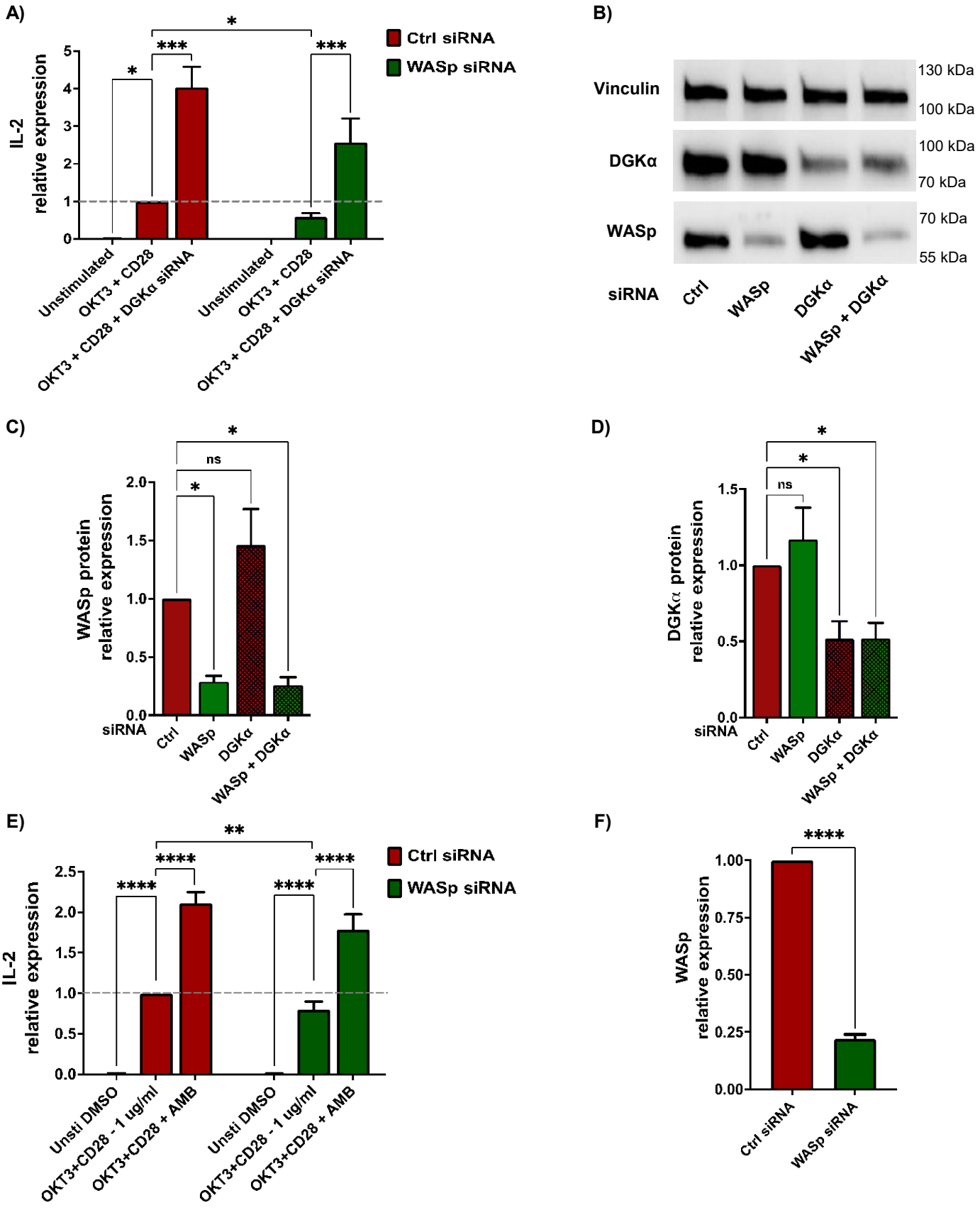
A)
IL-2
relative expression
Ctrl siRNA
WASp siRNA
Unstimulated
OKT3 + CD28
OKT3 + CD28 + DGKα siRNA
B)
Vinculin
DGKα
WASp
siRNA
Ctrl
WASp
DGKα
WASp + DGKα
130 kDa
100 kDa
70 kDa
55 kDa
C)
WASp protein
relative expression
D)
DGKα protein
relative expression
E)
IL-2
relative expression
Unsti DMSO
OKT3+CD28 - 1 ug/ml
OKT3+CD28 + AMB
F)
WASp
relative expression
Ctrl siRNA
WASp siRNA

Figure 7

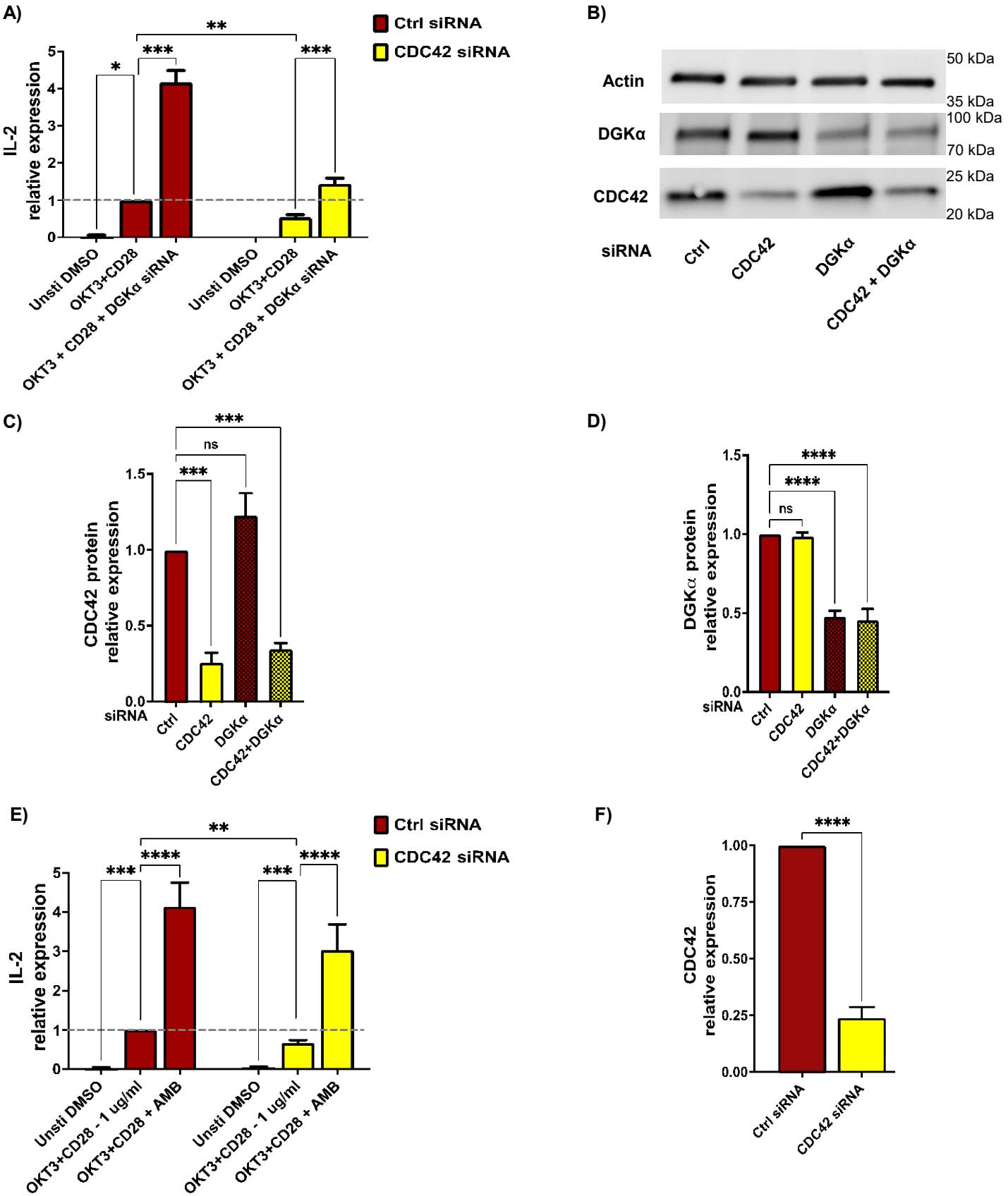
A)
Ctrl siRNA
CDC42 siRNA
IL-2 relative expression
Unsti DMSO
OKT3+CD28
OKT3 + CD28 + DGKα siRNA
B)
Actin
DGKα
CDC42
50 kDa
35 kDa
100 kDa
70 kDa
25 kDa
20 kDa
siRNA
Ctrl
CDC42
DGKα
CDC42 + DGKα
C)
CDC42 protein relative expression
ns
D)
DGKα protein relative expression
E)
OKT3+CD28 - 1 ug/ml
OKT3+CD28 + AMB
F)
CDC42 relative expression
Ctrl siRNA
CDC42 siRNA

Figure 8

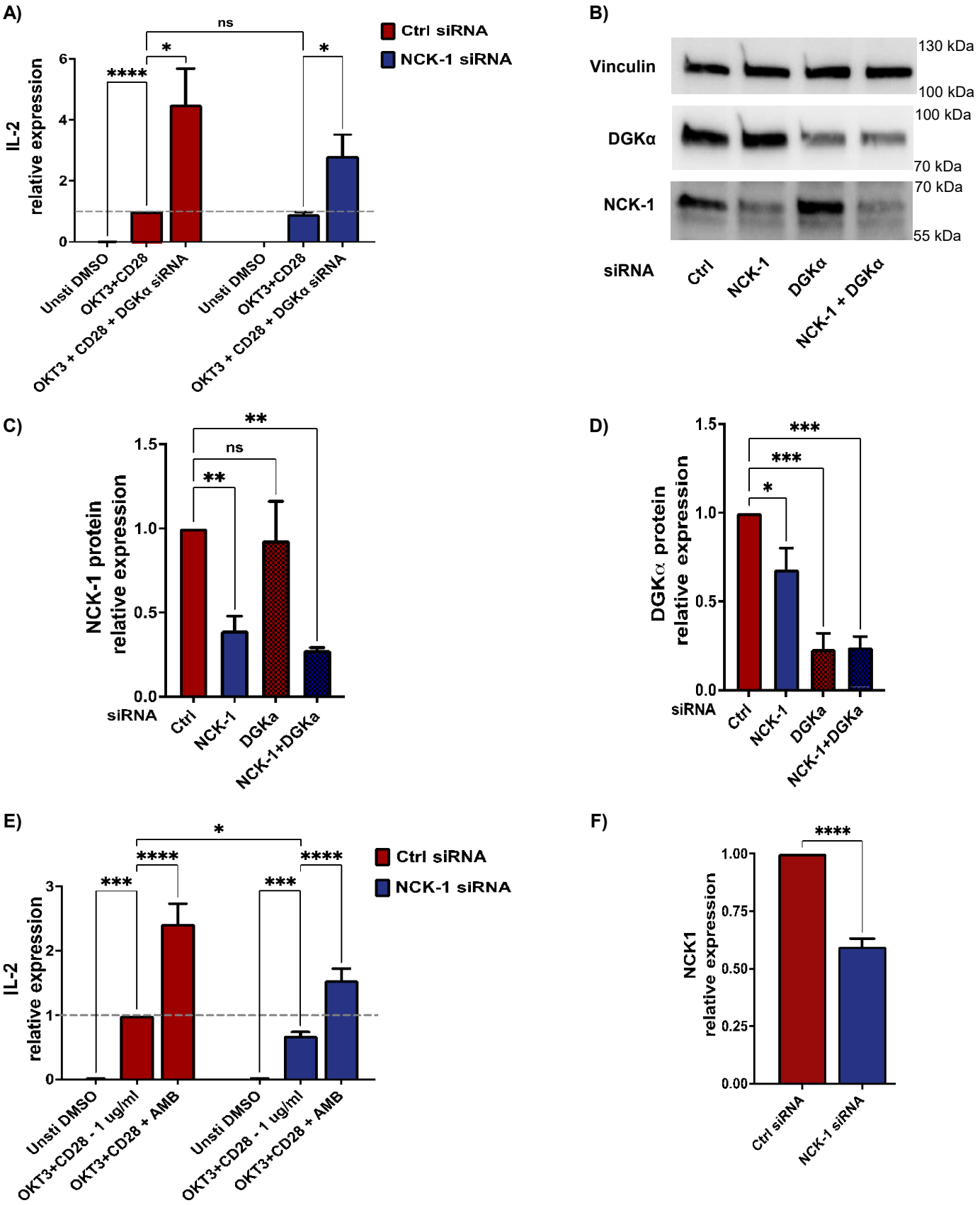
A)
ns
*
*
****
Ctrl siRNA
NCK-1 siRNA
IL-2
relative expression
6
4
2
0
Unsti DMSO
OKT3+CD28
OKT3 + CD28 + DGKα siRNA
Unsti DMSO
OKT3+CD28
OKT3 + CD28 + DGKα siRNA
B)
Vinculin
130 kDa
100 kDa
DGKα
100 kDa
70 kDa
NCK-1
70 kDa
55 kDa
siRNA
Ctrl
NCK-1
DGKα
NCK-1 + DGKα
C)
**
ns
**
NCK-1 protein
relative expression
1.5
1.0
0.5
0.0
siRNA
Ctrl
NCK-1
DGKa
NCK-1+DGKa
D)
***
***
*
DGKα protein
relative expression
1.5
1.0
0.5
0.0
siRNA
Ctrl
NCK-1
DGKa
NCK-1+DGKa
E)
*
****
***
***
****
Ctrl siRNA
NCK-1 siRNA
IL-2
relative expression
3
2
1
0
Unsti DMSO
OKT3+CD28 - 1 ug/ml
OKT3+CD28 + AMB
Unsti DMSO
OKT3+CD28 - 1 ug/ml
OKT3+CD28 + AMB
F)
****
NCK1
relative expression
1.00
0.75
0.50
0.25
0.00
Ctrl siRNA
NCK-1 siRNA

Figure 9

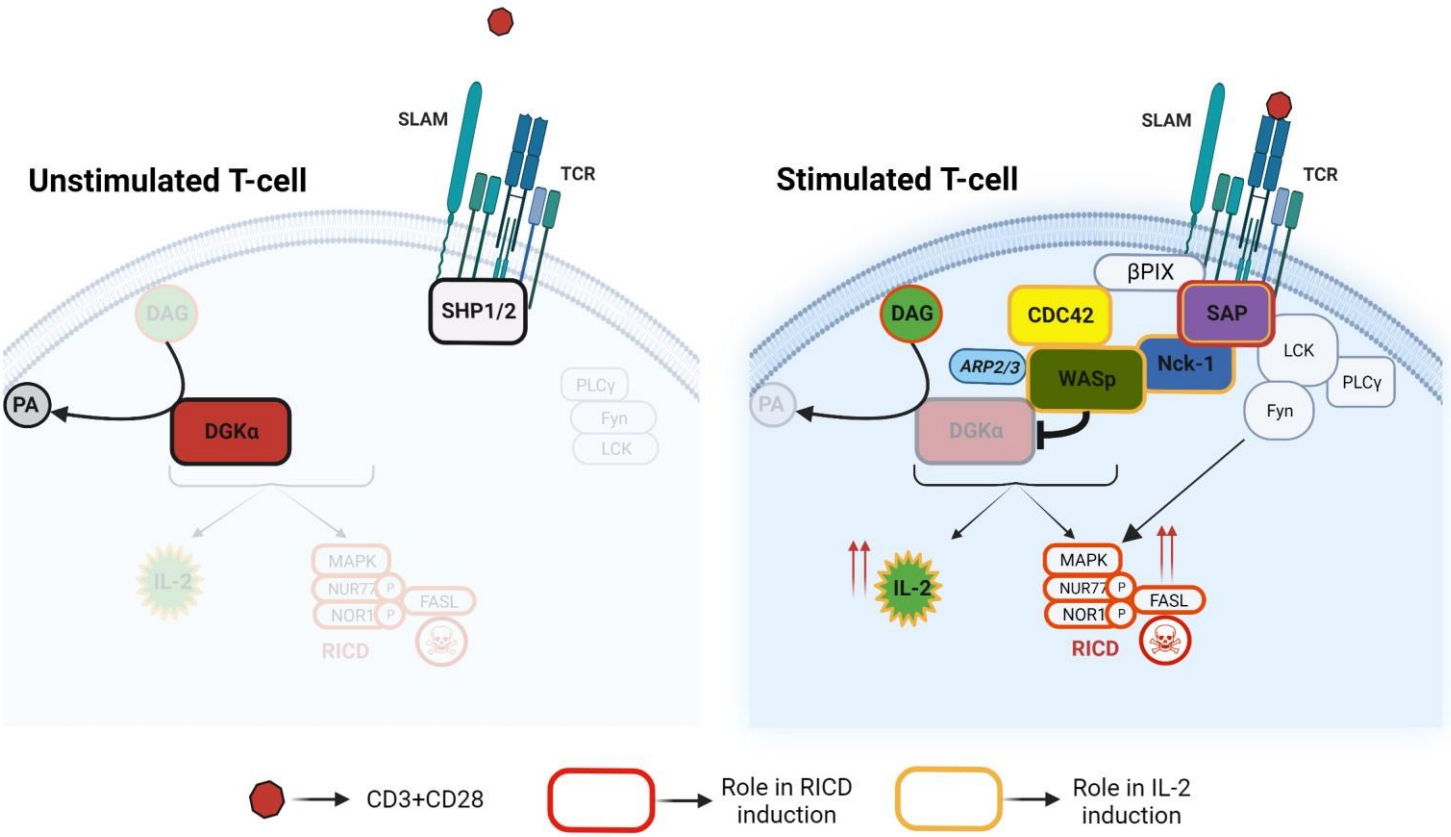
Unstimulated T-cell
SLAM
TCR
SHP1/2
DAG
PA
DGKα
PLCγ
Fyn
LCK
IL-2
MAPK
NUR77
NOR1
P
FASL
RICD
Stimulated T-cell
SLAM
TCR
βPIX
DAG
CDC42
SAP
ARP2/3
WASp
Nck-1
LCK
PLCγ
Fyn
PA
DGKα
IL-2
MAPK
NUR77
NOR1
P
FASL
RICD
CD3+CD28
Role in RICD induction
Role in IL-2 induction

Figure 10

8. ACKNOWLEDGEMENTS

"*Un dottorato di ricerca è il più alto titolo accademico rilasciato da un'università, successivo alla laurea*". Non sono d'accordo. O almeno, non del tutto. Al di là delle definizioni, non credo che il dottorato sia solo un "titolo". Per me ha rappresentato molto, molto di più. È stato un percorso di crescita sia umana che professionale, un'esperienza formativa per la mia carriera e senz'altro uno dei periodi più intensi della mia vita.
E come in tutti i percorsi, non si cresce mai davvero da soli. Pertanto, desidero ringraziare di seguito quanti hanno contribuito, in un modo o nell'altro, al raggiungimento di questo traguardo.

Vorrei ringraziare il Professor *Gianluca Baldanzi*, per avermi accolto nel suo laboratorio di Biochimica e avermi dato la possibilità di svolgere questo progetto di tesi. Lo ringrazio inoltre per avermi accordato la sua fiducia fin dall'inizio, responsabilizzandomi e lasciandomi ampia autonomia di azione e di pensiero. Lo ringrazio per la sua immancabile disponibilità a parlare di scienza, per i suoi consigli e per essere stato per me un punto di riferimento in questi anni. Grazie, professore.

Ringrazio il Dott. *Suresh Velnati*, per avermi introdotto (nel bene e nel male!) all'affascinante mondo della biochimica. Lo ringrazio per avermi aiutato in momenti critici, prima in laboratorio e poi a distanza di qualche regione. Anche se presente solo nella prima metà del dottorato, lo ringrazio soprattutto per la calma rassicurante dei suoi "don't worry", anche quando c'era molto per cui preoccuparsi.

Un grazie speciale va alla Dott.ssa *Annamaria Antona* per la logistica degli esperimenti in trasferta (e per molte altre cose meno professionali) e ai ragazzi del gruppo Biochimica di palazzo Bellini, sia chi è rimasto sia chi è partito per la sua strada:
Jacopo, Giovanni, Sandeep, Reshu, Konkonika…Grazie per tutto!

Un immenso ringraziamento va all'intero gruppo *Immunomics* del CAAD: grazie per avermi insegnato cos'è il team working senza essere il mio lab team. Siete tanto simpatici quanto molesti, ma il dottorato non sarebbe stato lo stesso senza di voi. Grazie per aver reso più leggeri questi anni di laboratorio, in mille modi e in mille occasioni…

Un grazie speciale va soprattutto alla mia famiglia, che mi ha sempre incoraggiato in questi anni, senza mai farmi mancare il proprio supporto e affetto in ogni momento o situazione di difficoltà. Ringrazio *Giorgia*, mia sorella, per aver condiviso con me gioie e disagi del dottorato, sotto ogni punto di vista, direi quasi in parallelo. Forse in famiglia è l'unica che arrivi a capire nel profondo il significato di cosa voglia dire davvero dottorarsi…Gio, ora tocca a te!!!
Grazie *mamma e papà* per il vostro sostegno e amore incondizionato. Siete dei genitori speciali e spero di avervi resi orgogliosi di me.
Alle mie due *nonne*: un grazie di cuore per essere sempre dalla mia parte, a prescindere.

In ultimo, ma non certo per importanza, un grazie a *Michaël*, mio marito. Per ricordarmi ogni giorno che se la motivazione è forte, i mezzi si trovano sempre. E che anche i sogni più grandi possono avverarsi se hai le persone giuste accanto a te. Grazie per credere in me sempre e comunque, così come sono. Grazie davvero.

Sara Centonze